The role of endogenous free radical signalling in human endometrium

Marwa Khalid Ebrahim Ali Al Sabbagh

A thesis submitted to Imperial College London
for the degree of Doctor of Philosophy

Institute of Reproductive and Developmental Biology
Department of Surgery and Cancer
Hammersmith Campus
Imperial College London

September 2011

Statement of Originality

All experiments included in this thesis were performed by myself, Marwa Al Sabbagh, unless otherwise stated in the text.

Abstract

Differentiation of human endometrial stromal cells (HESCs) into specialized decidual cells is critical for embryo implantation and maintenance of a successful pregnancy. Initiation of this differentiation process, termed decidualization, is strictly dependent on elevated cAMP levels, whereas its maintenance requires continuous progesterone signalling. Here I show that NADPH oxidase-dependent reactive oxygen species (ROS) play a critical role in initiating and maintaining the decidual process. I first show that cAMP-dependent induction of decidual marker genes can be attenuated or enhanced upon inhibition or activation of the NADPH oxidase complex, respectively. Time-course analysis demonstrated that cAMP enhances endogenous ROS production, apparent after 12 hours of stimulation, which coincides with a marked induction of differentiation markers. By a process of elimination, I identified NOX4 as the main catalytic subunit involved in decidualization. Silencing of NOX4, or its cofactor $p22^{PHOX}$, impaired the decidual process. I then show that the NOX4/$p22^{PHOX}$ complex regulates the transcriptional activity of CCAAT/enhancer binding protein β, a key regulator of HESC differentiation. Furthermore, microarray analysis revealed that the NOX4/$p22^{PHOX}$ complex functions downstream FOXO1, a multifaceted transcription factor involved in antioxidant defences, DNA repair and cell cycle regulation. In agreement, knockdown of NOX4/$p22^{PHOX}$ complex disrupted endogenous ROS production and resulted in a paradoxical prooxidant stress response further characterized by activation of the DNA repair pathway in the absence of primary DNA damage or cell death. Finally, I provide preliminary data that $p22^{PHOX}$ is downregulated at the transcript and protein level in the eutopic endometrium of patients with endometriosis. In summary, endogenous ROS signalling is critical for the differentiation and redox homeostasis of HESCs. Furthermore, deregulation of endometrial NADPH oxidase-dependent ROS production and signalling may be a hallmark of endometriosis, a prevalent and debilitating reproductive disorder.

Acknowledgement

I would first like to extend my thanks to my supervisor Prof. Jan Brosens for welcoming me into his lab, for his excellent guidance and support throughout the project, for his brilliant ideas, for his valuable advice, for pushing me to think in a critical and conceptual manner, for always being there in the ups and the downs, for teaching me to choose my battle, for all the scientific and general discussions we had and most importantly for his time and for being an amazing supervisor and a great friend. It was a real pleasure being supervised by him.

I would also like to thank Dr. Mark Christian, Dr. Aylin Hanyaloglu and Prof. Eric Lam for their guidance and support, for their valuable insights and technical advice, for their interest in my project and most importantly for taking the time to discuss my work.

My thanks also go to previous and current members of Prof. Brosens lab for all their help and support. Special thanks go to Zoe Brame for her effort and contribution to the endometriosis project. I would also like to thank Dr. Jennifer Steel, Lara Monteiro, Dr. Keiji Kudro, Madhuri Salker and Dr. Yun Lee for their technical help and contribution.

My appreciation and gratitude extends to Dr. Luca Fusi and Prof Jennifer Higham for providing us with human endometrial biopsies. My thanks and appreciation also go to all the women who participated in this study.

I would also like to extend my gratitude to HRH Prince Salman bin Hamad Al-Khalifa for giving me the privilege of pursuing my PhD degree through his international scholarship programme. My thanks also go to the CPISP staff and to Dorothy and Dr. Roger Baxter for all their encouragement and support. I would also like to acknowledge Imperial College's International Office for awarding me the Overseas Research Student scholarship, which funded a significant part of my PhD course.

Special thanks, appreciation and gratitude go to my family for always being there, for believing in me and supporting me all the way through. I would also like to thank my close network of friends for always being there, for cheering me along the way and for pushing me to reach the finish line. Thank you.

Table of Contents

Statement of Originality…….. 2
Abstract…….. 3
Acknowledgement……... 4
List of Figures…… 11
List of Tables…… 14
Abbreviations…… 15

CHAPTER 1: INTRODUCTION…… 20

1.1 Decidualization of the human endometrial stroma…… 21
1.1.1 The endometrium…… 21
1.1.2 The decidual process…….. 24
1.1.3 Morphological differentiation of stromal cells…….. 25
1.1.4 Biochemical differentiation of HESCs…….. 25
1.1.5 Functions of decidual HESCs……... 26
a. Embryo selection and implantation…… 26
b. Trophoblast invasion…… 28
c. Haemostasis…….. 28
d. Immunomodulation…….. 28
e. Oxidative stress defences…….. 29
1.1.6 Cyclic adenosine monophosphate (cAMP) signalling in HESCs…. 30
1.1.7 Progesterone signalling in HESCs…… 34
1.1.8 Transcription factors involved in decidualization…… 35
1.1.9 Cross-talk of cAMP and progesterone signalling in HESCs……. 36
1.1.10 Summary…… 38
1.2 Reactive oxygen species (ROS)…… 38
1.2.1 Effects of ROS…….. 38
1.2.2 Cellular oxidative defence mechanism…… 39
1.2.3 Redox homeostasis…… 39
1.2.4 ROS as signalling molecules…… 40
1.2.5 Measurements of intracellular ROS…….. 41
1.2.6 Sources of ROS production in the mammalian cell…… 42
1.3 The NADPH oxidase complex…… 44
1.3.1 The phagocytic NADPH oxidase complex…… 44
1.3.2 Structure of the phagocytic NADPH oxidase complex…….. 44

1.3.3 Non-phagocytic NADPH oxidase complex…….. 47
1.3.4 Phagocytic vs non-phagocytic NADPH oxidase complex…… 50
1.3.5 Activators and inhibitors of the NADPH oxidase complex…… 50
a. Diphenylene iodonium (DPI)…….. 50
b. Apocynin…… 51
c. AEBSF…… 54
1.3.6 Non-phagocytic NADPH oxidase complex: biology and disease…. 54
1.4 Endometriosis…… 54
1.4.1 Endometriosis: definition and diagnosis……... 54
1.4.2 The pathogenesis of endometriosis…….. 55
1.4.3 The immune system and endometriosis……. 55
1.4.4 Progesterone resistance and endometriosis……... 56
1.4.5 Oxidative stress and endometriosis…….. 57
1.5 Hypothesis and Aims……... 58

CHAPTER 2: MATERIALS AND METHODS……. 59

2.1 Materials……. 60
2.1.1 Primary antibodies……... 60
2.1.2 Secondary antibodies…….. 61
2.1.3 Plasmids…… 62
2.1.4 siRNA…… 62
2.1.5 Cell lines…… 62
2.1.6 Culture materials and media…….. 62
2.1.7 Chemicals and reagents…… 63
2.1.8 Kits…… 65
2.2 Methods…… 65
2.2.1 Cell Culture…… 65
2.2.1.1 Human endometrial tissue sample……... 65
2.2.1.2 Dextran coated charcoal (DCC) stripped serum preparation. 65
2.2.1.3 Primary cell culture…….. 66
2.2.1.4 Immortalized cells…… 67
2.2.2 Transient transfections…… 67
2.2.2.1 Transfection of primary HESCs using the calcium phosphate co-precipitation method…… 67
2.2.2.2 Reporter Assay…… 68
2.2.2.3 Small interfering RNA (siRNA)…….. 69

2.2.3 Western blotting…….. 70
2.2.3.1 Protein extraction…… 70
2.2.3.2 Measurement of protein concentration…… 71
2.2.3.3 SDS-PAGE and western blot analysis……. 71
2.2.3.4 Densitometry…… 72
2.2.4 Reverse transcription polymerase chain reaction (PCR)…….. 73
2.2.4.1 RNA Extraction…… 73
2.2.4.2 cDNA synthesis…… 73
2.2.4.3 Real-time quantitative PCR (RTQ-PCR)……. 74
2.2.4.4 Primer design and testing for real-time quantitative PCR……. 75
2.2.5 Electron mobility shift assay (EMSA)…… 76
2.2.6 Immunofluorescence analysis and confocal microscopy imaging... 76
2.2.7 Measurement of cellular reactive oxygen species (ROS)……. 77
2.2.8 Measurement of cell proliferation and viability…… 78
2.2.8.1 CellTiter 96® Aqueous One Solution Cell Proliferation Assay 78
2.2.8.2 Apo Tox-Glo™ Triplex Assay……. 79
2.2.9 Comet assay…… 79
2.2.10 Bacterial propagation of plasmids……... 80
2.2.10.1 Transformation of competent bacteria by heat shock……. 80
2.2.10.2 Large-scale preparation of plasmid DNA (maxiprep)…….. 81
2.2.10.3 Preparation of glycerol stocks…… 81
2.2.11 Statistical analysis…… 81
2.2.12 Gene expression analysis using Affymetrix microarrays…… 81
2.2.12.1 Sample preparation and selection…… 82
2.2.12.2 RNA quality control……... 82
2.2.12.3 Laboratory methodologies employed by Almac Diagnostics. 82
a. Eukaryotic target preparation…… 82
b. Amplification of total RNA…….. 82
c. Exon Processing…….. 83
d. Fragmentation and labelling of amplified single-stranded cDNA 83
e. Hybridization, washing, staining and scanning of 7abelled cDNA…… 83
f. Quality control of the generated data…… 83
g. Data normalization, differential gene selection and data analysis…… 84

CHAPTER 3: RESULTS 1 – NADPH OXIDASE-DEPENDENT ROS SIGNALLING IS CRITICAL FOR INITIATING THR DECIDUAL PROCESS… **85**

Introduction…….. 86

3.1 Measuring intracellular ROS in HESCs…… 87

3.2 Modulation of the NADPH oxidase activity in HESCs by apocynin and DPI…… 90

3.3 NADPH oxidase-dependent ROS play a role in HESC differentiation…. 92

3.4 The kinetics of the NADPH oxidase-dependent ROS production…… 99

3.5 Characterization of the NADPH oxidase complex in HESCs…… 103

3.6 NADPH oxidase-dependent ROS signalling in HESCs…… 111

Summary of results…… 117

CHAPTER 4: RESULTS 2 – ROLE OF NADPH OXIDASE PRODUCED ROS SIGNALLING IN PROLONGED DECIDUALIZATION…… **119**

Introduction…….. 120

4.1 The role of NADPH oxidase-dependent ROS in prolonged decidualization…… 121

4.2 Characterization of NOX4/p22^{PHOX}-dependet genes in decidualizing HESCs…….. 127

4.3 Characterizing the interaction between the NOX4/p22^{PHOX} complex and FOXO1…….. 132

4.4 The effects of NOX4/p22^{PHOX} knockdown in decidualizing HESCs……. 138

4.5 Lack of endogenous ROS signalling disrupts redox homeostasis in decidualizing HESCs…… 144

Summary of results…… 149

CHAPTER 5: RESULTS 3 – CHARACTERIZATION OF THE NOX4/P22^{PHOX} COMPLEX IN PATIENTS WITH ENDOMETRIOSIS…… **152**

Introduction…….. 153

5.1 Endometrial p22^{PHOX} and NOX4 expression in patients with or without endometriosis…….. 155

5.2 Regulation of the NOX4/p22^{PHOX} complex in the secretory phase of the menstrual cycle…… 159

5.3 Characterization of the NOX4/p22^{PHOX} complex in the proliferative phase of the menstrual cycle…… 163

5.4 NOX4/p22^{PHOX} expression profiling in eutopic HESCs from patients with and without endometriosis…… 165

5.5 FOXO1 expression in patients with endometriosis……. 169
Summary of Results…… 172

CHAPTER 6: DISCUSSION…….. 174

6.1 Endogenous ROS production is critical for initiating the decidual response…… 176
…
6.2 Continuous NOX4/P22^{PHOX}-dependent ROS signalling in decidualizing HESCs…….. 178
6.3 Deregulation of the NADPH oxidase complex in endometriosis…….. 181
6.4 Endometrial hormesis and endometriosis…… 182

APPENDICES…….. 187

Appendix 1 – RTQ-PCR primer sequences……. 188
Appendix 2 – NOX4/p22^{PHOX}-repressed genes…….. 189
Appendix 3 – NOX4/p22^{PHOX}-induced genes…….. 197
Appendix4 – The top five associated networks resulted from the *in silico* analysis of the NOX4/p22^{PHOX}-dependent genes…….. 200
REFERENCES…….. 207
PUBLICATIONS…… 231

List of Figures

CHAPTER 1

Fig 1.1 The endometrium…… 22
Fig 1.2 The menstrual cycle…… 23
Fig 1.3 Functions of decidualizing HESCs……... 27
Fig 1.4 Initiation of the decidual process is primarily dependent on cAMP. 32
Fig 1.5 The decidual-specific transcription complex……... 37
Fig 1.6 The Mechanism of action of the oxidant-sensing probe DCFH-DA 43
Fig 1.7 The phagocytic NADPH oxidase complex…….. 46
Fig 1.8 Non-phagocytic NADPH oxidase…….. 49
Fig 1.9 DPI is not a specific inhibitor of the NADPH oxidase complex…… 52
Fig 1.10 Apocynin and DPI modulate the activity of the NADPH oxidase complex…..... 53

CHAPTER 3

Fig 3.1 Comparing the efficacy of DCFH-DA and DHR 123 in measuring ROS in HESCs. …… 88
Fig 3.2 Apocynin activates the NADPH oxidase complex in HESCs……... 91
Fig 3.3 NADPH oxidase-dependent ROS play a critical role in the differentiation of HESCs into decidual cells…… 94
Fig 3.4 The NADPH oxidase complex is the main source of ROS involved in the decidual process……... 96
Fig 3.5 Effects of apocynin on decidualization…… 97
Fig 3.6 Overexpression of catalase attenuates the cAMP-dependent induction of IGFBP1 and PRL…… 98
Fig 3.7 The kinetics of cAMP-dependent induction of PRL and IGFBP1 transcripts…….. 100
Fig 3.8 Kinetics of cAMP-dependent ROS production in decidualizing HESCs…… 102
Fig 3.9 The NADPH oxidase profile in HESCs…… 104
Fig 3.10 RAC1 is not required for the induction of the decidual markers… 105
Fig 3.11 $p22^{PHOX}$ and NOX4 protein expression in HESCs……... 107
Fig 3.12 Knockdown of NOX4 and $p22^{PHOX}$ attenuates the cAMP-dependent induction of PRL and IGFBP1…… 108

Fig 3.13 The NOX4/p22^{PHOX} complex underpins the burst in ROS observed in HESCs…….. 110
Fig 3.14 NADPH oxidase-dependent ROS enriches the 8-br-cAMP-dependent protein expression of C/EBPβ…… 112
Fig 3.15 NADPH oxidase-dependent ROS enriches the 8-br-cAMP-dependent DNA binding activity of C/EBPβ in HESCs…….. 113
Fig 3.16 Knockdown of the NOX4/p22^{PHOX} complex attenuates the 8-br-cAMP-dependent enrichment of C/EBPβ DNA binding activity…… 115
Fig 3.17 NADPH-oxidase ROS enhances C/EBPβ-dependent transcription in HESCs……. 116

CHAPTER 4

Fig 4.1 The NOX4/p22^{PHOX} complex is upregulated at the transcript level upon prolonged decidualization.…… 122
Fig 4.2 The NOX4/p22^{PHOX} complex is upregulated at the protein level upon prolonged decidualization.…… 123
Fig 4.3 Silencing of the NOX4/p22^{PHOX} complex perturbs prolonged decidualization…….. 124
Fig 4.4 Perpetual endogenous ROS signalling is required for maintenance of the decidual process…….. 125
Fig 4.5 The regulation pattern of NOX4/p22^{PHOX} and decidual-dependent genes…….. 128
Fig 4.6 Validation of the NOX4/p22^{PHOX}-dependent gene expression……. 129
Fig 4.7 NOX4/p22^{PHOX}-dependent genes overlap with FOXO1-dependnet genes…….. 133
Fig 4.8 The NOX4/p22^{PHOX} complex is not upstream FOXO1…….. 134
Fig 4.9 FOXO1 is upstream NOX4 and p22^{PHOX}…… 136
Fig 4.10 NOX4/p22^{PHOX}-dependent genes are regulated in a similar manner by FOXO1……... 137
Fig 4.11 Silencing of the NOX4/p22^{PHOX} complex induces phosphorylation of H2A.X in decidualizing HESCs.…… 139
Fig 4.12 Silencing of the NOX4/p22^{PHOX} complex activates the DNA damage and repair pathway in decidualizing HESCs.…… 140
Fig 4.13 Silencing of the NOX4/p22^{PHOX} complex does not induce cell death in decidualizing HESCs……... 142

Fig 4.14 Knockdown of the NOX4/p22^{PHOX} complex does not induce DNA damage in HESCs…… 143
Fig 4.15 Knockdown of the NOX4/p22^{PHOX} complex alters the redox status of decidualizing HESCs……... 145
Fig 4.16 Knockdown of the NOX4/p22^{PHOX} complex induces stress signals in decidualizing HESCs…….. 146
Fig 4.17 Antioxidant enzymes are attenuated upon knockdown of the NOX4/p22^{PHOX} complex in decidualizing HESCs…….. 148

CHAPTER 5

Fig 5.1 NOX4 and p22^{PHOX} transcript levels in patients with endometriosis…… 157
Fig 5.2 NOX4 and p22^{PHOX} protein expression levels in endometriosis….. 158
Fig 5.3 Immunohistochemistry analysis for p22^{PHOX} in patients with and without endometriosis…….. 161
Fig 5.4 Immunohistochemistry analysis for NOX4 in patients with and without endometriosis……. 162
Fig 5.5 NOX4 and p22^{PHOX} protein expression in the proliferative phase of the menstrual cycle. …… 164
Fig 5.6 Basal transcript expression of NOX4/p22^{PHOX} complex in primary HESCs……. 167
Fig 5.7 The oxidative status of eutopic HESCs with endometriosis……. 168
Fig 5.8 FOXO1 mRNA expression in patients with endometriosis……... 170
Fig 5.9 Immunohistochemistry analysis for FOXO1 in patients with and without endometriosis…….. 171

CHAPTER 6

Fig 6.1 Similarities between endometriosis and endometrial cancer…….. 186

APPENDECIES

Appendix 4

Network 1: Cell Cycle, Cancer, Skeletal and Muscular Disorders…….. 200
Network 2: Cell Cycle, Cellular Assembly and Organization, DNA Replication, Recombination, and Repair …… 201
Network 3: Cell-To-Cell Signalling and Interaction, Cell Cycle, DNA Replication, Recombination, and Repair…… 202

Network 4: Cellular Assembly and Organization, Cellular Growth and Proliferation, Haematological Disease……. 203
Network 5: DNA Replication, Recombination and Repair, Gene Expression, Cell Cycle……. 204

List of Tables

CHAPTER 4

Table 4.1 The top five associated network functions of the microarray data analysis (Ingenuity Pathways Analysis)……..... 131

Table 4.2 The top five molecular and cellular functions of the microarray data analysis (Ingenuity Pathways Analysis)…….. 131

Table 4.3 The top five canonical pathways of the microarray data analysis (Ingenuity Pathways Analysis)…… 131

Appendices

Appendix 1 - RTQ-PCR primer pairs…… 188

Appendix 2 - NOX4/p22^{PHOX}-repressed genes…… 189

Appendix 3 - NOX4/p22^{PHOX}-induced genes…… 197

Abbreviations

%	percent
°C	centigrade
8-br-cAMP	8-bromoadenosine-3', 5'-cyclic monophosphate
AEBSF	4-(2-Aminoethyl)benzenesulfonylfluoride
AMP	adenosine monophosphate
AP1	activating protein1
Apo	apocynin
APS	ammonium persulphate
ATM	ataxia telangiectasia mutated
ATP	adenosine triphosphate
ATR	ataxia telangiectasia and Rad3 related
BIRC5	baculoviral IAP repeat containing 5
BLAST	basic local alignment search tool
bp	base pair
BRCA	breast cancer
BSA	bovine serum albumin
c-Myc	myelocytomatosis oncogene
C/EBPβ	CCAAT/enhancer binding protein beta
Ca^{2+}	calcium
$CaCl_2$	calcium chloride
cAMP	cyclic adenosine monophosphate
$CaPO_4$	calcium phosphate
CARM1	co-activator associated methyltransferases
CGD	chronic granulomatous disease
CHK	checkpoint
cm^2	centimeter squared
CO_2	carbon dioxide
COLEC10	collectin sub-family member 10
CRE	cAMP response elements
CREB	cAMP response element binding protein
CREM	cAMP response element modulators
CRH	corticotropin-releasing hormone
Ct	threshold cycle
DBD	DNA binding domain

DBS	DNA binding site
DCC	dextran coated charcoal
DCF	2′,7′-dichlorofluorescein
DCFH-DA	2′,7′-dichlorofluorescein-diacetate
DEPC	diethylpyrocarbonate
dH_2O	distilled water
DHR 123	dihydrorhodamine 123
DMEM	dulbecco's Modified Eagles Medium
DMSO	dimethyl sulfoxide
DNA	deoxyribonucleic acid
DNMT	maintenance of DNA methylation
DPI	diphenylen iodonium
DTT	dithiothreitol
E+	with evidence of endometriosis
E_2	estradiol
ECM	extracellular matrix
EDTA	ethylenediamine tetraacetic acid
Em	emission
EMSA	electrophoresis mobility shift assay
EMT	epithelial-mesenchymal-transition
ER	estrogen receptor
ESE	early secretory
Ex	excitation
FAD	flavin adenine dinucleotide
FBS	fetal bovine serum
Fe	iron
FOXO	forkhead box transcription factor class O
g	gram
g	gravity force
GADD45	growth arrest and DNA damage
GDP	guanosine diphosphate
GEFs	guanine nucleotide exchange factor
GO	gene ontology
GPx	glutathione peroxidase
GTP	guanosine-5'-triphosphate
H2A.X	H2A histone family, member X

H_2O	water
H_2O_2	hydrogen peroxide
hCG	Human chorionic gonadotrophin
HCl	hydrochloric acid
HEPES	4-(2-hydroxyethyl)-1-piperazineethanesulfonic acid
HESCs	human endometrial stromal cells
HOXA	homeobox A
HRP	horse radish peroxidase
IAP	inhibitor of apoptosis
ICAM1	intercellular adhesion molecule 1
ICER	inducible early repressor (ICER)
IDO	indole-amine 2,3-dioxygenase
IF	immunofluorescence
IGFBP1	insulin-like growth factor binding protein
IgG	immunoglobulin G
IHC	immunohistochemistry
IPA	ingenuity pathway analysis
iPSCs	induced pluripotent stem cells
JNK	c-Jun-N-terminal kinase
KCl	potassium chloride
KLF4	Krüppel-like factor
L	litre
L-NAME	*N*-omega-Nitro-L-arginine methyl ester
LMA	low melting agar
LSE	late secretory
M	molar
MET	mesenchymal-epithelial-transition
mg	miligram
$MgCl_2$	magnecium chloride
ml	millilitre
mm Hg	millimetre of mercury
MMPs	matrix metalloproteinases
MPA	medroxyprogesterone acetate
mRNA	mesenger RNA
MS	menstrual shedding
MSE	mid secretory

NaCl	sodium chloride
NADPH	nicotinamide dinucleotide phosphate
NE	without evidence of endometriosis
NK	natural killer cells
nM	nanomolar
nm	nanometer
NMA	normal melting agar
NO	nitric oxide
NOS	nitric oxide synthase
NOX	NADPH oxidase
NP-40	nonidet P-40
NT	non-targeting
O_2	molecular oxygen
O_2^-	superoxide anion
OCT4	octamer-binding transcription factor 4
p-ATM	phospho-ATM
p-ATR	phospho-ATR
p-BRCA1	phospho-BRCA1
p-CHK	phospho-CHK
p-H2A.X	phospho-H2A.X
PBS	phosphate buffered saline
PCR	polymerase chain reaction
PDE_2	phosphodiesterase
PE E+	proliferative with evidence of endometriosis
PE NE	proliferative without evidence of endometriosis
PES	phenazine ethosulfate
PFA	paraformaldehyde
PGE_2	prostaglandin E_2
PHOX	phagocyte oxidase
PKA	protein kinase A
PKB	protein kinase B
PMSF	phenylmethylsulfonyl floride
PR	progesterone receptor
PRL	prolactin
PVDF	polyvinylidene fluoride
RLX	relaxin

RNA	ribonucleic acid
RNS	reactive nitric species
ROS	reactive oxygen species
RTQ-PCR	real time quantitative PCR
SCGE	single cell gel electrophoresis
SDS	sodium dodecylsulphate
SDS-PAGE	SDS-polyacrylamide gel electrophoresis
SE E+	secretory with evidence of endometriosis
SE NE	secretory without evidence of endometriosis
SGK1	serum- and glucocorticoid-induced protein kinase
siRNA	small interfering RNA
SOD2	superoxide dismutase 2
SOX2	SRY (sex determining region Y)-box 2
SRC	steroid receptor coactivator
STAT	signal transducer and activator of transcription
SUMO	small ubiquitin-like modifier
TBS	tris buffered saline
TBS-T	TBS-Tween
TEMED	tetramethylethylenediamine
TF	tissue factor
TGFβ	transforming growth factor β
TNF	tumour necrosis factor
Tris	trishydroxymethylaminomethane
TXN	thioredoxin
U	unit
uNK	uterine natural killer cells
v/v	volume/volume
w/v	weight/volume
WB	western blot
XO	xanthine oxide
μg	micro gram

Chapter 1: Introduction

1. Introduction

1.1 Decidualization of the human endometrial stroma

1.1.1 The endometrium

The endometrium is the mucosal layer that lines the lumen of the uterus. It is comprised of a single layer of luminal epithelial cells resting on a layer of stromal and glandular cells. During the reproductive phase, two layers can be distinguished in the endometrium, a basal layer that lies beneath a superficial layer (Figure 1.1). The superficial layer of the endometrium acts as the functional layer and is under extensive hormonal regulation (1). The basal layer of the endometrium contains progenitor cells that are critical for endometrial regeneration, which takes place after menstrual shedding of the superficial endometrial layer (2-4).

The fluctuations in circulating levels of ovarian estrogen and progesterone induce profound changes in the endometrium, giving rise to the menstrual cycle, which averages 28 days. The first half of the cycle is referred to as the proliferative phase. This phase is characterized by increased estrogen levels, which induce the ordered growth of the endometrium (5). The second half of the cycle, day 14 - 28, is referred to as the secretory phase of the menstrual cycle. The secretory phase is characterized by a post-ovulatory rise in circulating progesterone levels, which inhibit the proliferation of the estrogen-primed endometrium and trigger its differentiation process, which is also termed as “decidualization” (5).

Interestingly, as illustrated in figure 1.2, whole-genome molecular phenotyping of endometrial tissue biopsy samples taken across the menstrual cycle, revealed that the secretory phase can be classified into three functionally distinct stages: the early secretory phase (ESE), the mid-secretory phase (MSE) and the late secretory phase (LSE) (6).

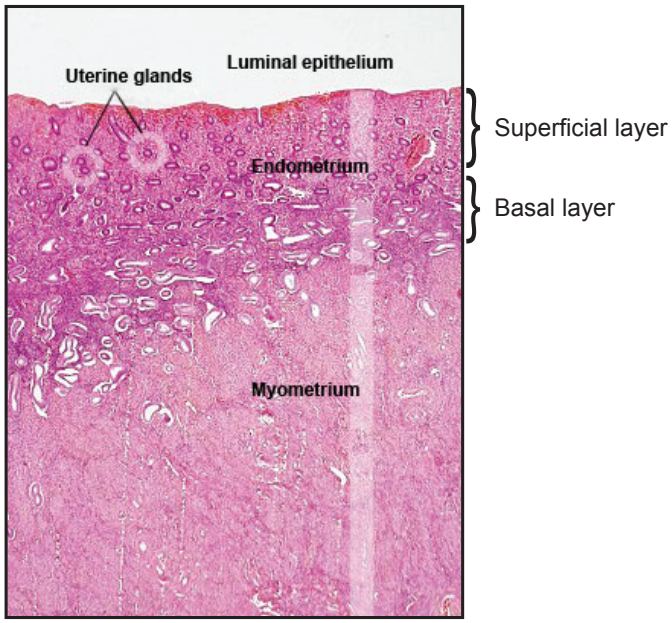


Fig 1.1 The endometrium. During the reproductive years, two layers in the endometrium can be distinguished. The superficial layer, which represents the functional layer that responds to fluctuations in the levels of the circulating ovarian hormones estrogen and progesterone. The basal layer is more of a dormant layer that does not respond to hormonal stimuli, shows minimal proliferative activity and is deficient in mounting a predecidual reaction in the LSE phase of the cycle. (The illustration is adopted from www.lab.anhb.uwa.edu.au/mb140).

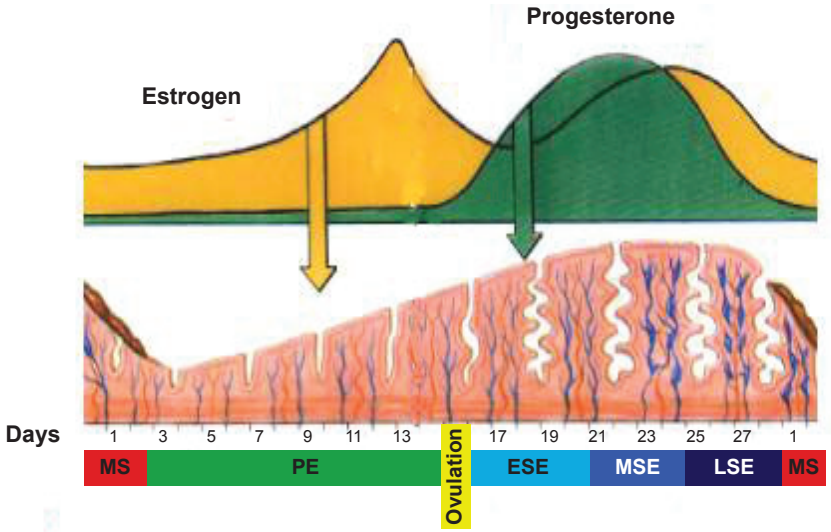


Fig 1.2 The menstrual cycle. The schematic diagram illustrates the different phases of the menstrual cycle. The proliferative phase is initiated after menstrual shedding (MS) of the superficial endometrial layer. This phase harbours the growth and proliferation of the endometrium. Some of the molecular functions enriched in this phase are DNA synthesis, cell cycle regulation and extracellular matrix structural constituents, all of which are consistent with the tissue growth and extracellular modeling that occurs in this phase. The secretory phase can be divided into ESE, MSE and LSE. The ESE phase is known for robust glycogen synthesis, high-energy demands and an increase in mitochondrial size and number. The genes enriched in this phase are involved in metabolism and biosynthesis of macromolecules such as cholesterol, amino acids and lipids. The MSE is the phase in which decidualization is initiated. Hence, the genes enriched in this phase are involved in cell communication, intracellular signalling cascades and negative regulation of cell proliferation to name but a few. The LSE phase in the absence of pregnancy is enriched for cell motility and communication, apoptosis and cell cycle regulation in favour of cell cycle arrest. Genes enriched in this phase are involved in endocytosis, phagocytosis, immune response as well as response to inflammation, pathogens and chemicals.

1.1.2 The decidual process

Decidualization refers to the progesterone-dependent morphological and biochemical differentiation of the endometrial stromal fibroblasts into secretory, epithelioid-like decidual cells (7, 8). It occurs in all species in which embryo implantation necessitates breaching of the luminal epithelium (1, 8). In most organisms, decidualization is reliant on the presence of a blastocyst (5). However, in humans and very few other species, decidualization is a maternally driven process and occurs in each cycle, independently of pregnancy (1, 8).

Decidualization in pre-menopausal women is initiated in the MSE phase of the menstrual cycle i.e. day 23 in an ideal 28-day cycle. Histologically, the commencement of the decidual process signals the end of the period of receptivity, also known as the "implantation window". During this period embryo implantation can take place (5). Conversely however, it is widely believed that decidualization is required for endometrial receptivity. In fact, decidual marker genes such as prolactin (*PRL*) and insulin-like growth factor binding protein 1 (*IGFBP1*) are enhanced *in vivo* prior to the morphological changes (5, 9). In the absence of pregnancy, the fall of progesterone levels, in the LSE phase of the menstrual cycle, induces shedding of the decidualized superficial endometrial layer leading to menstruation (7). Hence, in their reproductive phase, women in developed countries undergo cyclic decidualization and menstrual shedding on average 400 times (5, 10).

Due to the extensive trophoblast invasion which encompasses the endometrium as well as the uterine junctional zone, which refers to the inner third of the myometrium, decidualization in humans is very pronounced and includes all the various compartments of the uterus: the junctional zone myocytes, spiral arteries, local immune cells, the endometrial, epithelial and stromal compartments (1, 8). It should be pointed out that this is a broader definition of decidualization as it entails all the different changes that occur in all cellular compartments associated with pregnancy.

The decidual process is a progressive event. Its onset is first apparent in stromal cells around the spiral arteries of the superficial endometrial layer. In the presence of pregnancy, the endometrium is under extensive regulation and influence from steroid hormones as well as maternally- and blastocyst-derived signals (5, 9). Consequently, the decidual process progressively continues to ultimately involve the endometrium as a whole (8).

1.1.3 Morphological differentiation of stromal cells

Undifferentiated human endometrial stromal cells (HESCs) are mesenchymal cells with an elongated spindle-shaped fibroblastic appearance (7, 8, 10). Upon decidualization, HESCs are characterized by a marked enlargement in their size, rounding of the nucleus and expansion of the secretory machinery, which encompasses the rough endoplasmic reticulum and the Golgi complex, and finally cytoplasmic accumulation of glycogen and lipid droplets (10). Decidualizing HESCs are further morphologically characterized by the appearance of multiple club-shaped processes on their surface that extend to the extracelullar matrix (ECM) (8, 11).

1.1.4 Biochemical differentiation of HESCs

The morphological adaptations of decidualizing HESCs are underpinned by extensive molecular and biochemical changes that accompany the decidual process. Genome-wide microarray profiling studies, whether applied on endometrial biopsies taken during or post the window of implantation, or applied on HESCs subjected to decidual stimuli *in vitro*, have been instrumental in shedding light on the extensive gene networks that are regulated during the decidual process (6, 12-19). Based on these studies, decidualization can be defined as the sequential reprogramming of functionally related families of genes involved in extracellular and cytoskeletal organization, cell adhesion, signal transduction, steroid metabolism, differentiation and apoptosis (10, 20). Hence, upon decidualization, HESCs adopt new biochemical functions that are critical for embryo implantation and successful pregnancy. For instance, decidualizing HESCs acquire a secretory phenotype releasing various proteins and a myriad of cytokines and growth factors that are critical for maintaining and augmenting the decidual phenotype and regulating trophoblast invasion and placental formation (1, 20). Two major secreted proteins, PRL and IGBP1 are commonly used as markers of decidualization (8, 21-23). Interestingly, decidualizing HESCs appear to adopt a myofibroblastic phenotype as they express α-smooth muscle actin, desmin and vimentin (10, 21, 24-26).

Decidual transformation of HESCs is an interesting example of mesenchymal-epithelial transition (MET). MET is an important process that is involved in various developmental events like kidney organogenesis and somitogenesis (27, 28). It is the reverse of the epithelial-mesenchymal transition (EMT). The interconversion between the epithelial and mesenchymal phenotype through EMT and MET processes is essential for embryogenesis, organ development and most importantly for wound

healing like in liver injury and for cellular remodeling during differentiation (29-31). Epithelial cells are adherent cells that bestow cell-to-cell cohesion and integrity of multicellular organs, and form barriers separating external from internal environments (29, 31). Mesenchymal cells, in contrast, are highly mobile and have invasive properties (29, 31, 32). Upon decidualization, HESCs express a myriad of genes that are a characteristic of epithelial cells (8). MET has also been implicated in the generation of induced pluripotent stem cells (iPSCs) from mouse fibroblasts upon exogenous expression of octamer-binding transcription factor 4 (Oct4), SRY (sex determining region Y)-box 2 (Sox2), Krüppel-like factor (Klf4) and myelocytomatosis oncogene (c-Myc) (33). Interestingly, microarray analysis revealed that OCT4, KLF and MYC are upregulated upon decidualizing HESCs (18, 34).

1.1.5 Functions of decidual HESCs

Decidualization not only bestows cellular plasticity on endometrial cells but also other seemingly conflicting properties. For instance, decidual cells are capable of resisting cell death upon oxidative stress at the same time they possess the ability to undergo apoptosis in response to progesterone withdrawal (18, 35). Decidual cells are also able to regulate local immune responses, haemostasis and acquire invasive properties. Interestingly, those properties are also observed in ectopic implants that occur upon retrograde menstruation leading to the gynecological disorder endometriosis (36-38). Figure 1.3 illustrates the different functions of decidual HESCs.

a. Embryo selection and implantation

Recently, it has been reported that decidual HESCs act as biosensors capable of recognizing compromised embryos and subsequently preventing their implantation (39-41). Therefore, decidualization is not only critical for embryo implantation and placental formation, but may also play a role in maternal recognition and rejection of developmentally compromised human embryos.

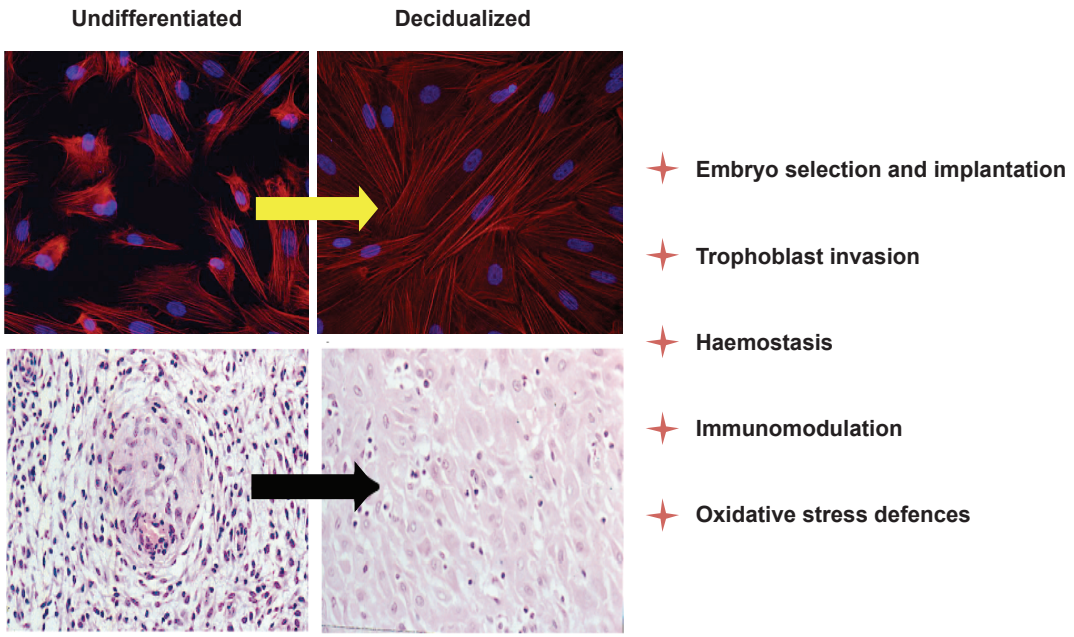


Fig 1.3 Functions of decidualizing HESCs. Decidualization can be recapitulated *in vitro* by administering 8-bromoadenosine-3', 5'-cyclic monophosphate (8-br-cAMP) and medroxyprogesterone acetate (MPA). Decidual HESCs acquire a secretory phenotype and become specialized epithelioid cells that can regulate various biological functions that are cardinal for ensuring a successful pregnancy like embryo selection and implantation, trophoblast invasion, haemostasis, immunomodulation and oxidative stress defence mechanisms.

b. Trophoblast invasion

Trophoblast invasion refers to the breaching of the luminal endometrial epithelial cells and forms the basis of implantation and placenta formation (8). This process is critical for remodeling the uterine spiral arteries in order to increase the maternal blood flow to the placenta and consequently supports fetal growth (9, 42). Decidualization can be viewed as the maternal defence mechanism that regulates trophoblast invasion and promotes attachment of the latter (9, 43). Trophoblast invasion is a tightly regulated process that involves the secretion of decidual-specific factors like transforming growth factor β (TGFβ) as well as the expression of matrix metalloproteinases (MMPs) and adhesive molecules on the trophoblasts (8, 43, 44).

c. Haemostasis

Decidualization involves remodeling of the spiral arteries, which entails endothelial swelling, vacuolation and disorganization of the smooth muscle media (34). Decidualizing HESCs secrete several factors that promote haemostasis before and during trophoblast invasion (34). An example of a secreted factor involved in haemostasis is tissue factor (TF), a membrane-bound glycoprotein that acts as a receptor for coagulation factor VII/VIIa (45, 46). Interestingly, during the decidual process, an influx of innate immune cells like macrophages and uterine natural killer cells (uNK) infiltrate the decidua (47, 48). These cells tolerate the semi-allogenic trophoblasts and are known to possess angiogenic properties due to their expression of several molecules that regulate trophoblast invasion and vascular remodeling such as angiogenic factors, endothelial cell mitogens and chemokines (34, 49, 50).

d. Immunomodulation

Pregnancy is an inflammatory-related process, which requires complex immuno-regulation to prevent the fetal antigens being recognized by cytotoxic T-cells and to protect the feto-maternal interface (34). As mentioned before, decidualization is associated with an influx of uNK cells as a response to decidual-specific secreted chemoatractants (51). Interestingly, microarray studies revealed that uNK cells express immunomodulatory molecules that inhibit T-cell proliferation and survival and therefore protect the fetus from being recognized (34, 49). Further, decidual cells also express factors that attenuate T-cell dependent inflammatory responses. For example, decidual cells express tryptophan-catabolizing enzyme indole-amine 2,3-dioxygenase (IDO), which has been suggested to have an important role in pregnancy by preventing inflammatory responses and protecting the fetus (52-55). Another factor decidual cells highly express is Fas ligand, which is a member of the

tumour necrosis factor (TNF) superfamily and acts as a death signal for activated T-cells (34, 56).

e. Oxidative stress defences

In the course of a normal pregnancy, major fluctuations in oxygen (O_2) concentrations take place at the feto-maternal interface. At the early stages of pregnancy, the invasion of the spiral arteries in the endovascular trophoblast protects the conceptus from exposure to reactive oxygen species (ROS) (57-59). As the pregnancy progresses, dislocation of the trophoblast occurs, which enables further transformation of the spiral arteries and the perfusion of the placental intervillous space (8). This results in a major increase in the partial O_2 pressure within the placenta. For instance, at weeks 7 and 10 post gestation, the O_2 partial pressure is less than 20 mm Hg. However, between weeks 11 and 14, which is when the maternal perfusion of the placenta is initiated, the partial O_2 pressure increases to 50 mm Hg resulting in a burst of ROS (8, 60).

The significance of the decidual process in protecting the fetus is illustrated by the contrasting responses of undifferentiated and decidualizing HESCs to ROS. Undifferentiated HESCs are readily susceptible to oxidative cell death whereas decidualizing cells are remarkably resistant (35). The resistance of the decidual cells is attributed to several mechanisms that work in concert, to maintain the integrity of the decidua, during the extensive remodeling that takes place as a requirement for a functional feto-maternal interface. For example to prevent oxidative stress and subsequent damage that might occur at the feto-maternal interface, decidualized HESCs switch on the oxidative defence mechanisms that enable them to neutralize the effects of ROS and repair any damages caused by them (61, 62). For instance, decidualizing HESCs highly express antioxidant enzymes like superoxide dismutase 2 (SOD2), thioredoxin (TXN), and glutathione peroxidase 3 (GPx3), all of which are free radical scavengers (6, 14, 17, 18, 35, 63, 64). In addition, oxidative stress signalling and activation of the stress-responsive c-Jun N-terminal kinase (JNK) pathway is attenuated in decidualizing HESCs (65). Moreover, differentiated HESCs highly express GADD45α (growth arrest and DNA damage alpha), a stress response gene involved in cell cycle arrest, chromatin remodeling and DNA repair (66, 67). Interestingly, decidualizing HESCs downregulate the proapoptotic member of the Forkhead family of transcription factors, FOXO3a, which is normally activated in undifferentiated HESCs subjected to a source of ROS like hydrogen peroxide (H_2O_2) (35).

Taken together, decidualization is not only critical for embryo implantation and placental formation, but also play a vital role in protection of the offspring as well as in maternal recognition and rejection of developmentally compromised human embryos. Hence, it goes without saying that perturbed decidualization can manifest in a range of reproductive disorders, including recurrent pregnancy loss and disorders associated with impaired placental formation, such as pre-eclampsia, fetal growth restriction, and preterm delivery. In fact a recent study suggested a role for the homeobox gene *HOXA10* in maintenance of pregnancy (68). *HOXA10* encodes for a transcription factor that plays a critical role in decidualization. Loss of HOXA10 has been suggested to contribute to progestin resistance in preterm labour (68), indicating that preterm labour is not strictly a disease of the myometrium only.

1.1.6 Cyclic adenosine monophosphate (cAMP) signalling in HESCs

Although decidualization is known to be primarily progesterone-dependent, a plethora of evidence suggests that progesterone is not the primary trigger of the decidual process (25, 26, 69, 70). Progesterone, on the other hand, plays a pivotal role in maintaining and augmenting the decidual phenotype (25, 26). *In vivo*, PRL, a phenotypic marker of decidualization, and other decidual-specific genes, are only detectable in the superficial endometrial layer 10 days after the post-ovulatory rise of circulating progesterone levels (69, 71). This observation suggests that decidual-specific genes are not under direct transcriptional control of activated progesterone receptor (PR). Activation by steroid hormone receptors is generally rapid and occurs usually within 1 - 4 hours post ligand stimulation (72). Furthermore, *In vitro*, progesterone alone or in combination with estradiol (E_2) or relaxin can only induce decidualization of HESCs after at least 8 - 10 days of stimulation (7, 23, 72, 73).

Overwhelming evidence suggests that initiation of the decidual process is dependent on increased cAMP signalling and sustained activation of the protein kinase A (PKA) pathway (7, 73, 74). cAMP is a ubiquitous second messenger that is formed from adenosine triphosphate (ATP). Binding of ligand to members of G-protein-coupled receptors activates adenylate cyclase, which consequently converts ATP to cAMP and pyrophosphate as a byproduct (74, 75). Several lines of evidence strongly support the notion that elevated cAMP levels sensitize HESCs to progesterone signalling. First, it has been reported that the cAMP content in endometrial biopsies obtained from patients in the secretory phase of the menstrual cycle is higher than the proliferative phase (76). Second, basal adenylate cyclase activity peaks in the

MSE phase of the menstrual cycle (76). Moreover, prostaglandin-stimulated adenylate cyclase activity is higher in secretory than proliferative endometrial biopsies (76). Fourth, *in vitro* studies investigating the effect of progesterone on cultured HESCs revealed that progesterone treatment elevates intracellular cAMP levels (71). Finally, *in vitro* studies comparing the independent and combined effects of cAMP and progesterone on the induction of the decidual marker gene *PRL* and its promoter activity revealed that cAMP is a potent inducer of the decidual phenotype. Progesterone, in comparison, is a much weaker stimulus, and its effects are apparent after a lag period of 10 or more days, as mentioned before (Figure 1.4) (25, 26, 69, 77, 78).

Various studies indicated that elevated cAMP levels during the secretory phase of the menstrual cycle is a response to the post-ovulatory exposure of the endometrium to local factors capable of inducing cAMP induction such as relaxin, corticotrophin-releasing hormone, pituitary gonadotrophins and prostaglandin E_2 (PGE_2) (10, 79-85). During pregnancy, maintenance of cAMP signalling in the decidua is speculated to occur due to the exposure to the massively secreted human chorionic gonadotrophin (hCG) (86). Intracellular cAMP concentrations are not only regulated by stimuli inducing its production, but again by intracellular phosphodiesterases (PDEs), which mediate its degradation and hydrolysis (83, 84).

A major downstream effector of cAMP is PKA, a cytoplasmic holoenzyme, which in its inactive state is comprised of two regulatory and two catalytic subunits (7). The regulatory subunits inhibit the activity of the catalytic subunits when the holoenzyme is in its tetramer state. Upon binding of cAMP to the regulatory subunits, the catalytic subunits are released and consequently phosphorylate downstream targets of the PKA pathway leading to modulation in the activity of the modified proteins (73). Since cAMP is a ubiquitous second messenger, several mechanisms exist to control its signalling. In most cell systems, those mechanisms evolved to attenuate cellular responses to an ongoing external stimulus rendering cAMP signalling a transient event. Interestingly, decidualizing HESCs represent an exception to this rule. In other words, maintenance of the decidual phenotype requires sustained cAMP signalling and consequently, sustained activation of the PKA pathway (7, 74, 87).

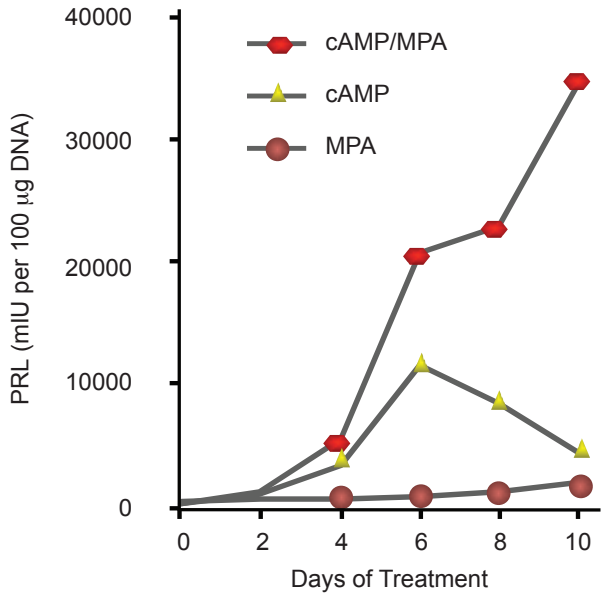


Fig 1.4 Initiation of the decidual process is primarily dependent on cAMP. Treatment with cAMP alone markedly induces the decidual marker PRL, but is incapable of maintaining the decidual phenotype. Treatment with MPA alone induces PRL after a lag period of 8 to 10 days. However, treatment with cAMP in combination with MPA has a synergistic effect on PRL production characterized by a marked induction and maintenance of the decidual phenotype. (Adapted from (69)).

Major nuclear targets of the holoenzyme PKA are the cAMP response element binding protein (CREB) and the cAMP response element modulators (CREMs). CREB and CREM are transcription factors that exert their effects by binding to cAMP response elements (CREs) in promoters of target genes (87). Alternative splicing, translation initiation and promoter usage give rise to various CREM isoforms (87). Depending on the presence or absence of a transactivation domain, those CREM isoforms can act as transcriptional activators or repressors (88-90). Furthermore, the use of an alternative cAMP-inducible intronic promoter termed (P2), which is found on the CREM DNA binding domains (DBDs), generates the inducible early repressor (ICER) (89, 90). ICER is a powerful repressor of cAMP-induced transcription and negatively autoregulates its own transcription (88, 89, 91).

Interestingly, cAMP signalling in decidualizing HESCs forms an exception to the above model. ICER transcripts were found to be strongly upregulated in decidualizing HESCs and their level was parallel to the induction of the decidual *PRL* (87). In other words, the induction of ICER is not transient but sustained, and the negative autoregulatory feedback loop is not established upon activation of the PKA pathway resulting in sustained cAMP signalling (87).

Promoter studies revealed that cAMP activation of the decidual PRL promoter in HESC is a biphasic response characterized by an initial weak but rapid induction followed by a secondary, much more enhanced induction apparent after 12 hours of stimulation (73). Interestingly, further analysis of the decidual PRL promoter showed that the initial and delayed cAMP-dependent responses are dependent on distinct cAMP response elements (CREs). In fact, the initial rapid response is dependent on a non-palindromic CRE at position -12, whereas, the major but rather delayed activation of the decidual PRL promoter is dependent on a regulatory region that lies between position -332 and -270 (73). At this stage, it is noteworthy to point out that the decidual PRL transcript is initiated at an alternative start-site to that of the pituitary PRL (73, 77, 92, 93). The decidual PRL startsite is 6 kb upstream of the pituitary start-site, resulting in an elongated 5'-untranslated region within the decidual transcript, but gives rise to a decidual PRL protein that is identical to the pituitary PRL (73, 77, 92, 93).

1.1.7 Progesterone signalling in HESCs

Progesterone is a steroid hormone that plays a critical role in the female reproductive system (94-98). It governs key events such as mammary gland development, ovulation, decidualization, implantation, menstruation and maintenance of pregnancy (99). Progesterone exerts its effects primarily through activation of PR. PR knockout mice show various reproduction defects including sexual behaviour, ovulation and implantation, supporting the notion that progesterone act as a pleiotropic regulator of diverse reproduction events (100, 101).

PR belongs to the nuclear receptor superfamily of transcription factors (102). Two isoforms of PR exist, PR-A and PR-B. They arise from the same gene but are the result of alternative promoter usage and translation at two distinct start-sites (94, 103). PR-A lacks an N-terminal stretch of 165 amino acids, which harbours a transactivation function that is specific to PR-B and is critical for activation of PR-B specific targets. PR-A also acts as a negative regulator of PR-B and other steroid receptors like the estrogen receptor (ER), and therefore, it is regarded as an important modulator of hormone receptor action (95, 104, 105). Interestingly, PR-A knockout mice are infertile, exhibit perturbed ovulation and cannot undergo decidualization, suggesting that the two isoforms are not functionally redundant in so far that PR-B on its own is incapable of maintaining normal reproductive events (103) (106, 107). In agreement with this notion, both PR isoforms are expressed in the endometrium, however, PR-A was the predominant isoform in the stromal compartment (108).

Upon binding of ligand, PR undergoes a conformational change, which consequently leads to its phosphorylation and dissociation from heat shock proteins. Subsequently, PR dimerizes and binds to specific response elements in the promoter region of target genes. The latter event requires interaction with steroid receptor co-activators (SRCs), which in turn recruit SRC-associated histone acetyltransferases (CBP and pCAF) and co-activator associated methyltransferases (CARM1) that are responsible for modifying the chromatin landscape to enable transcription initiation (7, 109-112).

An increasing body of evidence has indicated that post-translational modifications play a critical role in regulating steroid receptor activity. PR is not an exception and its ligand-dependent and ligand-independent activity is regulated by post-translational modifications such as phosphorylation, ubiquitination, methylation, acetylation and

sumoylation (70, 113-117). Unlike ubiquitination, sumoylation of transcription factors does not lead to their degradation but has a significance effects on their stability, cellular localization, protein-protein interaction and transcriptional activity (118-120). Sumoylation is a dynamic and reversal post-translational modification. Generally, sumoylation of transcription factors, including PR, results in stabilization of the protein and repression of its transcriptional activity (113). Interestingly, upon decidualization, cAMP signalling attenuates PR sumoylation leading to increased transcription activity of the receptor and enhanced turnover (70). In other words, a decrease in PR sumoylation is, at least in part, responsible for sensitizing HESCs to progesterone signalling (70).

1.1.8 Transcription factors involved in decidualization

An Increasing body of experimental evidence has implicated a number of transcription factors in the decidual process. In addition to PR, Forkhead transcription factor (FOXO1), signal transducers and activators of transcription (STATs), CCAAT/enhancer binding protein beta (C/EBPβ), activating protein 1 (AP1), Ets transcription factors, Sp1, HOXA10, HOXA11 and the tumour suppressor p53 have all been shown to play a role in the differentiation of HESCs into decidual cells (121-135).

Multiple experiments have demonstrated that PR interacts with various transcription factors that play a critical role in mediating the decidual response. For instance, PR interacts C/EBPβ, and this interaction is responsible for enhancing C/EBPβ-dependent induction of the decidual promoter (121, 136).

In addition to C/EBPβ, PR also interacts with STAT5, which is a cAMP-induced transcription factor that plays a vital role in decidualization (121, 125, 137). STAT5 have been show to enhance the activity of the decidual PRL promoter (121, 125).

Another transcription factor that interacts with PR and has been shown to enhance the activity of the decidual PRL promoter is FOXO1 (121, 125). FOXO proteins belong to the Forkhead family of transcription factors, which are characterized by a conserved DNA-binding domain known as “Forkhead box” or “FOX” (138). The members of the FOX family are further classified into subgroups that range from FOXA to FOXR according to sequence similarity (138). Members of the FOXO class include FOXO1, FOXO3 and FOXO4 and are regulated by the protein kinase B

(PKB)/AKT signalling pathway (139). Upon phosphorylation by PKB/AKT, FOXO proteins are translocated to the cytoplasm, repressing their transcriptional activity (140, 141). Another factor that regulates FOXO proteins is the serum glucocorticoid kinase (SGK1), which is closely related to PKB/AKT (139). FOXO transcription factors are critical regulators of cardinal cellular processes such as cell fate and apoptosis, cell cycle progression, differentiation and oxidative stress resistance (138, 139).

Interestingly, genome-wide microarray studies comparing decidualizing HESCs subjected to siRNA-mediated knockdown of FOXO1 to those containing the endogenous transcription factor revealed that FOXO1 in HESCs has an anti-proliferative effects and is involved in important cellular processes such as cell cycle regulation, cellular assembly and organization as well as DNA replication, recombination and repair (18).

1.1.9 Cross-talk of cAMP and progesterone signalling in HESCs

PR interactions with FOXO1, C/EBPβ and STAT5 led to the hypothesis that PR provides a platform for the formation of the decidual-specific transcription complex, which is responsible for regulating the expression of decidual-specific genes (Figure 1.5) (7). Further evidence suggests that cAMP sensitizes HESCs to progesterone signalling. First, cAMP signalling and activation of the PKA pathway dissociates PR from it co-repressors N-CoR and SMRT and facilitates the recruitment of its co-activator SRC-1 (142, 143). Second, the expression and/or activation of FOXO1, C/EBPβ and STAT5, is known to be induced by cAMP signalling (121, 122, 125, 136, 144, 145).

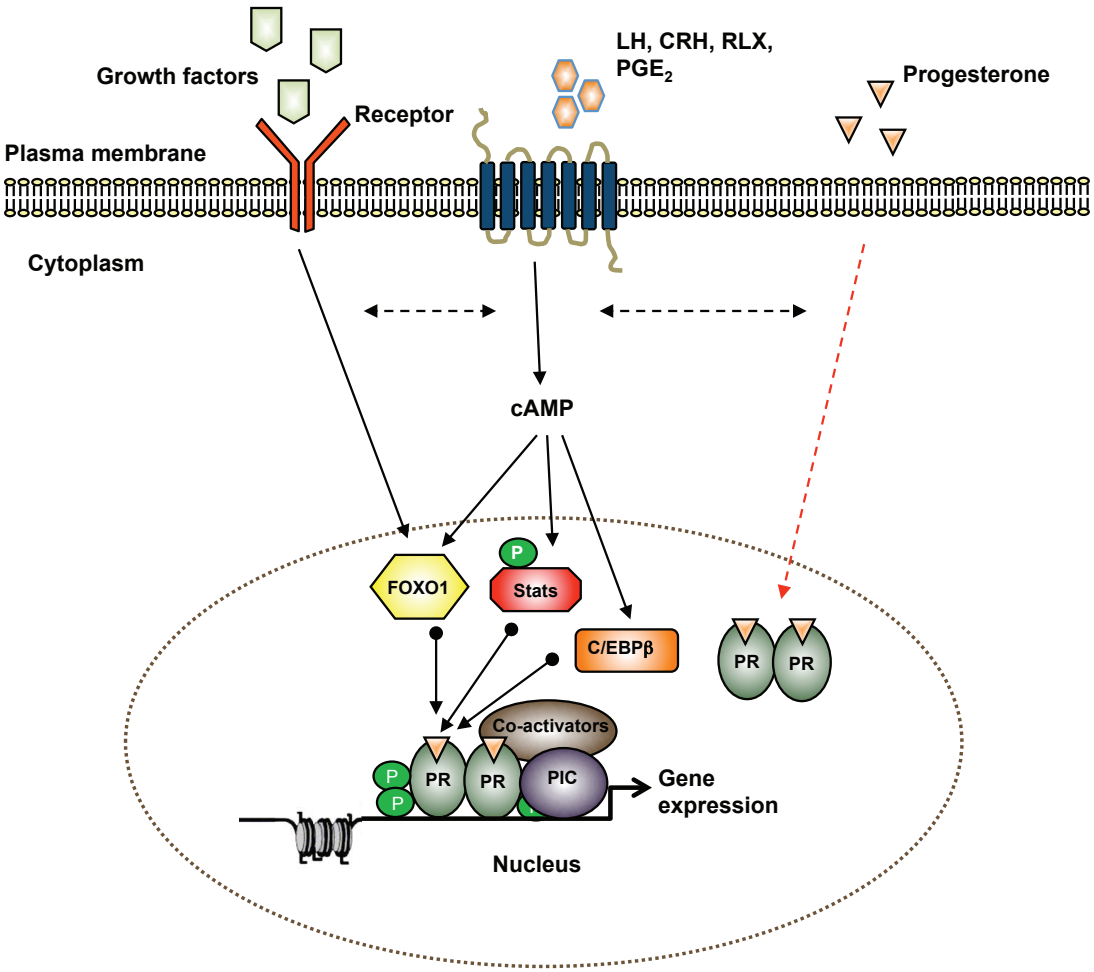


Fig 1.5 The decidual-specific transcription complex. PR forms a platform for the interaction of the different transcription factors, co-activators and the pre-initiation complex involved in the decidual-specific transcription machinery. (Adapted from Al Sabbagh et al, Mol Cell Endocrinol, Submitted).

1.1.10 Summary

Decidualization is a highly regulated event and is cardinal for the maintenance of a successful pregnancy. It encompasses various morphological responses underpinned by extensive biochemical changes. The signalling cascades involved in this differentiation process are complex and intertwined and rely heavily on the synergy and crosstalk between cAMP and progesterone signalling which in turn triggers a cascade of events and regulates a number of transcription factors. Decidualization also confers resistance of HESCs to environmental cues rendering them robust for embryo implantation and further trophoblast invasion and placental formation.

Taken together, failure to mount an adequate decidual response perturbs a cascade of events which can manifest in various reproductive and pregnancy disorders like recurrent miscarriages, pre-eclampsia, pre-term labour and fetal growth restriction.

1.2 Reactive oxygen species (ROS)

1.2.1 Effects of ROS

ROS, such as superoxide anion (O_2^-), hydroxyl radical (-OH) and H_2O_2, are highly reactive and relatively unstable small molecules that are the natural by-products of aerobic metabolism (146, 147). Those free radicals are the metabolite of molecular O_2, which are formed during various electron transfer reactions (62). Electron transfer reactions, also known as “redox” reactions, refer to the process by which one or more electrons move from one molecule to another. For instance, O_2^- and H_2O_2 are partially reduced to molecular O_2 through one- and two-electron reduction reactions (62, 148). Other reactive metabolites require the presence of transition metal ions, such as iron (Fe), to be formed. An example of which is -OH (62, 148).

Denham Harman, in 1956, described ROS as a “Pandora’s box of evil” as they can induce cellular damage, mutagenesis, cancer, degenerative processes and aging (147, 149-152). Since then, ROS were predominantly known for their toxic cellular effects that can damage macromolecules like DNA, proteins and lipids, disrupting cellular functions and leading to a wide spectrum of human diseases (62, 147, 153, 154).

More recently however, a large body of evidence has emerged implicating ROS in physiological cellular processes and signalling, including cell cycle progression, the immune response against infectious agents, differentiation and apoptosis (153, 155, 156).

The term “redox signalling” is used to describe the cascade of events in which ROS mediate signal transductions and protein modifications that are essential for various physiological functions (149). Beneficial redox signalling occurs at low/moderate but measurable concentrations of ROS in the cell (149, 153, 157, 158). Pathological disorders, however, are associated with higher, persistent and deregulated concentrations of ROS (149, 157, 158). Interestingly, a shift in the oxidative status of the cell towards a higher concentration of ROS may not necessarily lead to a pathological disorder but reflect a natural cellular progression like aging (149, 157-159).

1.2.2 Cellular oxidative defence mechanisms

To protect against the potential detrimental effects of ROS, unicellular and multicellular organisms have evolved multiple levels of defence mechanisms (160). Antioxidant enzymes, like SOD, which dismutase O_2^- to O_2 and H_2O_2, and catalase, which decomposes H_2O_2 to water (H_2O) and O_2, form the main line of defence in multicellular organisms together with GPx and TXN (153, 160). Those enzymes squelch highly reactive ROS, thereby protecting the cell from potential damages (62). Other non-enzymatic antioxidants include α-tocopherol (vitamin E), β-carotene, ascorbic acid (vitamin C) and glutathione (149, 160).

1.2.3 Redox homeostasis

Since ROS are involved in various physiological processes, their complete ablation could hinder and perturb ROS-dependent physiological functions (158). Therefore, in a normally functioning cell, there is always a delicate balance between ROS production and the various antioxidant enzymes, indicative of the dual role of antioxidants defense enzymes in protecting the cells from damage and facilitating the beneficial use of free radicals in physiological functions (153). It follows then, that an imbalance between the antioxidant capacity of the cell and the amount of oxidants produced leads to oxidative stress (62). In other words, oxidative stress could be defined as the disturbance in the equilibrium status of prooxidant and antioxidant molecules in favour of prooxidants, in a biological system (153, 160, 161). Oxidative

stress has been implicated in various pathological disorders such as cardiovascular diseases, atherosclerosis, rheumatoid arthritis, cancer, inflammatory diseases, diabetes, neurodegenerative diseases like Alzheimer's and Parkinson's disease (148, 153, 162-171). Oxidative stress is also implicated in several reproductive disorders, ranging from endometriosis to infertility, early pregnancy loss and preeclampsia (57, 60, 172-175).

The maintenance of the oxidative equilibrium status, also known as "redox homeostasis" is an important feature of biological systems and is achieved through a mechanism called "redox regulation" (149, 153). Spatial and temporal regulation of the redox homeostasis may occur. For instance, different amount of antioxidant enzymes exist at different subcellular locations (160). Moreover, different cell types possess different types and concentrations of antioxidants (160). The redox status of a cell will vary when it goes through different processes, such as proliferation, differentiation, aging and senescence (176), reflecting changes in antioxidant capacity and/or ROS production.

1.2.4 ROS as signalling molecules

There are several characteristics that define a signalling molecule. First, its production should be a response to a stimulus. Second, it has to exert an effect either in the cell in which it was produced or on adjacent cells. Third, its production and signalling can be switched off upon another stimulus or a change of cellular condition (146).

In the case of ROS, which act as second messengers in signalling cascades, the second condition is the hardest to comply with, as most of the free radicals are highly reactive with very short half-lives (154, 160). Exceptions are O_2^- and H_2O_2, as various reports have implicated them in signalling cascades (157, 177-181). H_2O_2 is relatively more stable than O_2^- and it has been suggested in various reports that although in a cell O_2^- is the primary source of ROS, it is rapidly further reduced/dismutated by SOD to H_2O_2, which is regarded as a secondary source of ROS that acts as a signalling molecule (147, 149, 154, 157, 178). Interestingly, the relative stability (relatively long half-life compared to other free radicals) of H_2O_2 enables it to diffuse through the cell plasma membrane to adjacent cells, where it can act as a signalling intermediate (149, 154, 169).

Regardless of their harmful effects in cells, it is now well established that endogenously generated ROS act as a second messenger relaying various signals involved in cell cycle progression, apoptosis, and differentiation (147, 153, 156, 158, 159, 181, 182). Various cytokines and growth factors have been implicated in triggering the production of intracellular ROS (147, 157).

1.2.5 Measurement of intracellular ROS

Due to their high reactivity and relative instability, it is difficult to measure intracellular ROS concentrations (62, 183). All current methods are indirect and depend on measuring the end products that results from DNA, lipid or protein interactions with ROS. The most commonly used methods depend on the reaction of ROS with an oxidant-sensing detector molecule that emit fluorescence or light upon oxidation (62, 183).

Lucigenin is an aromatic compound with chemiluminescent properties. It is used as a detector molecule for O_2^- (183). Upon oxidation, lucigenin is reduced, rendering its electrons in an excited state and consequently emitting light, which can be detected by a luminometer (184). Lucigenin has been used to detect O_2^- produced from various intracellular free radical sources in various biological systems, including phagocytic cells, fibroblasts and smooth muscle cells (62, 183-187). However, one major limitation of lucigenin is its ability to auto-oxidize and generate O_2^- upon interaction with molecular O_2 (62, 183, 188). Another minor limitation is reflected in its specificity of measuring O_2^- and not H_2O_2. In most biological systems, not only does H_2O_2 represent the prime free radical signalling molecule, but, as mentioned earlier, O_2^- is rapidly dismutated to O_2 and H_2O_2. To measure the oxidative status of the cell, it is better therefore to select a detector that is sensitive to both O_2^- and H_2O_2.

A second detector molecule for measuring intracellular ROS is dihydrorhodamine 123 (DHR 123). DHR 123 is an uncharged and non-fluorescent membrane permeable oxidant-sensing probe. Upon oxidation by ROS, DHR 123 is oxidized to the fluorescent compound rhodamine 123, which in turn exhibits green fluorescence (189, 190).

A third and commonly used detector molecule is dihydrofluroscein diacetate (DCFH-DA) (191). DCFH-DA is a membrane permeable non-fluorescent molecule. Once it is in the cytosol, it gets cleaved by cellular estrases converting it to the membrane

impermeable molecule DCFH. Upon interaction with ROS, DCFH is converted to the fluorescent probe DCF, which emits fluorescent signal that can be measured and monitored over time by a fluorometer (192). Figure 1.6 illustrates the mechanism of action of DCFH-DA. The amount of fluorescence emitted is proportional to the amount of ROS produced in the cell.

1.2.6 Sources of ROS production in the mammalian cell

Although it is widely assumed that the main source of ROS in the cell is their production as byproducts from the mitochondrial electron transport chain, a plethora of evidence points to the nicotinamide adenine dinucleotide phosphate (NADPH) oxidase complex as the prime source of ROS (147, 148, 153, 167, 193). Superoxide generation is not the prime purpose of the mitochondria, but a byproduct of the electron transport chain, a mechanism by which several electrons are transferred between molecules in order to produce chemical energy (167). The NADPH oxidase complex, on the contrary, has evolved for the prime reason of ROS production (147, 194). Other sources of free radicals in the cell are the nitric oxide synthase (NOS) and the xanthine oxidase (XO). NOS is the prime source for nitric oxide (NO) in cells. NO is rapidly oxidized, and consequently, derives the production of other reactive nitric species (RNS) (147, 195). XO is another source of ROS in cells. It catalyses the oxidation of hypoxanthine to xanthine as well as the oxidation of xanthine to uric acid, generating H_2O_2 as a by-product in both reactions (167, 193, 196). A large body of experimental evidence has implicated the NADPH oxidase complex in physiological functions such as proliferation and differentiation as well as pathological disorders like cardiovascular diseases (197-202).

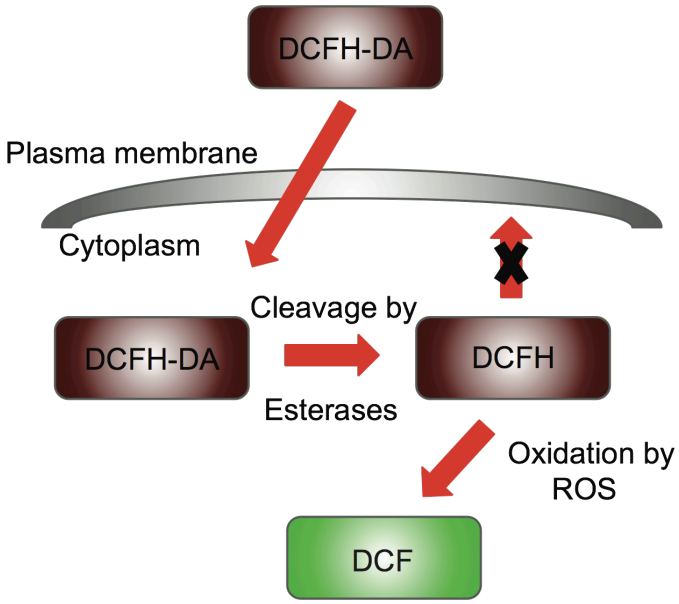


Fig 1.6 The Mechanism of action of the oxidant-sensing probe DCFH-DA. DCFH-DA is a non-fluorescent membrane permeable probe. Once it diffuses through the cell, DCFH-DA gets cleaved to DCFH by cellular esterases, rendering it membrane impermeable. Upon interaction with ROS, DCFH gets oxidized to the fluorescent probe DCF. The amount of fluorescence emitted is proportional to the amount of ROS in the cell.

1.3 The NADPH oxidase complex

The NADPH oxidase complex was first discovered in phagocytes as an enzymatic system with the prime function of generating O_2^- (147, 203, 204). The later discovery of homologues of the catalytic subunit NOX2 (NOX: *N*ADPH *ox*idase) of the NADPH oxidase complex in various other cell types like fibroblats, demonstrated that endogenous ROS production is not limited to phagocytic cells (147, 203, 205).

1.3.1 The phagocytic NADPH oxidase complex

The NADPH oxidase complex is responsible for the respiratory burst in phagocytic cells (147, 204). The respiratory burst refers to the rapid release of ROS (O_2^- and H_2O_2) from cells such as monocytes, leukocytes and neutrophils, as part of the immune response against pathogenic agents and antigens, such as bacteria and fungi. In other words, the respiratory bursts functions as a bactericidal capacity in phagocytic cells (147, 206).

Clinically, a diminished capacity to generate a respiratory burst in phagocytic cells is associated with recurrent infections. This condition is known as chronic granulomatous disease (CGD), a hereditary disease in which innate immunity is impaired due to an inability to produce a respiratory burst in response to pathogens (147, 194, 203, 206, 207). Interestingly, other functions of the immune cells, like phagocytosis, chemotaxix and degranulation, appear not to be affected in patients with CGD (147). In many affected patients, the catalytic subunit NOX2 or its cofactor $p22^{PHOX}$ is mutated in leukocytes, leading to inactivation of the NADPH oxidase complex (147, 194, 203).

1.3.2 Structure of the phagocytic NADPH oxidase complex

The phagocytic NADPH oxidase complex produces superoxide through catalyzing the one-electron reaction of molecular O_2, using NADPH oxidase as an electron donor (194, 203). As illustrated in Figure 1.7, the NADPH oxidase complex is composed of two transmembrane proteins, three cytosolic regulatory proteins and the Rho family member RAC. The transmembrane proteins are NOX2, previously known as $gp91^{PHOX}$, and $p22^{PHOX}$, encoded by *CYBA* (208, 209). The PHOX superscript originally referred to *Ph*agocyte *OX*idase (203). The three cytosolic components of the complex are $p47^{PHOX}$, $p67^{PHOX}$ and $p40^{PHOX}$.

The transmembrane components of the NADPH oxidase complex NOX2 and $p22^{PHOX}$ form a heterodimeric flavohemoprotein known as cytochrome b_{558} (203, 209). The formation of the heterodimer is essential for the stability and activity of the NADPH oxidase complex (203, 210, 211). This heterodimer contains one flavin adenine dinucleotide (FAD)-binding domain, two heme domains and an NADPH-binding region (194, 203, 212).

In the inactive state, the cytosolic regulatory proteins dissociate from the phagocytic cytochrome b_{558} and remain in the cytoplasm. Upon activation of the complex through cellular interactions with chemoattractants, chemokines and pathogenic particles, the cytosolic components $p47^{PHOX}$, $p67^{PHOX}$, $p40^{PHOX}$ and RAC translocate to the membrane to assemble the enzyme in its active state (Figure 1.7) (194, 203, 213). The translocation of the cytosolic components is triggered by phosphorylation of $p47^{PHOX}$, which occurs when the phagocytic cell is exposed to an activating stimulus (147, 203). Furthermore, in the inactive state, RAC resides in the cytoplasm bound to guanine nucleotide-dissociation inhibitor (GDI). Once the cell is stimulated, the guanine exchange factors (GEFs) enable the disassociation of RAC from GDI and interact with guanine triphosphate GTP. It has been reported that activation of RAC is involved in translocating the NADPH oxidase cytosolic components to the membrane of the stimulated cell (203, 213, 214).

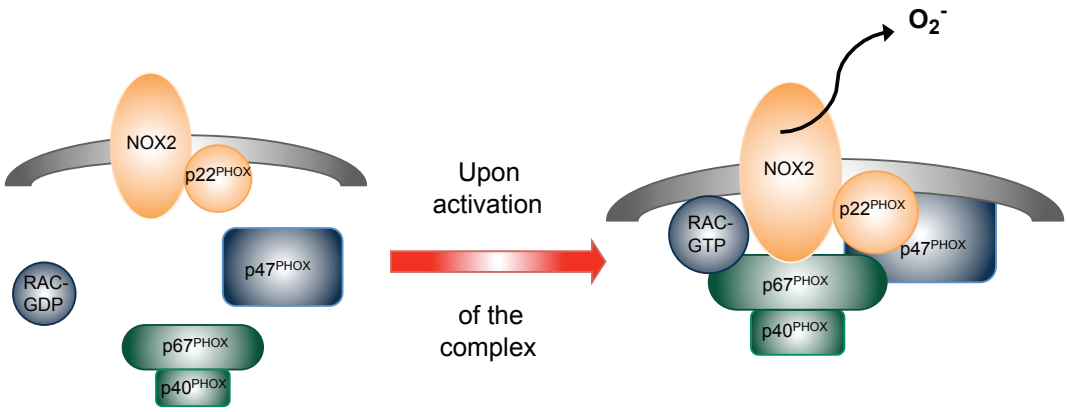


Fig 1.7 The phagocytic NADPH oxidase complex. In the absence of a stimulus, the complex dissociates and the regulatory subunits RAC, $p47^{PHOX}$, $p67^{PHOX}$ and $p40^{PHOX}$ reside in the cytoplasm. Upon activation of the complex, the cytosolic components are translocated to the membrane assembling the enzyme in its active state.

1.3.3 Non-phagocytic NADPH oxidase complexes

After its initial discovery in immune cells, several lines of evidence indicated the presence of an NADPH oxidase complex in non-phagocytic cells. First, various observations reported the ability of non-phagocytic cells to produce moderate amounts of endogenous ROS. Second, $p22^{PHOX}$ is found ubiquitously in almost all cells (194). Third, the discovery of homologues of the NOX2 in various different non-phagocytic cells like fibroblasts, smooth muscle cells and endothelial cells has indicated the presence of alternative NADPH oxidase complexes (168, 185, 194, 203, 212, 215-217).

To date, there are 7 known NOX homologues in non-phagocytic cells. The phagocytic NOX2 is the prototypic NOX subunit. The other homologues are named NOX1, NOX3, NOX4, NOX5, DUOX1 and DUOX2. Each homologue is encoded by a designated gene, and the degree of homology with the prototypic NOX2 differ between the various homologues (218, 219). The numbering of the NOX homologues reflects the order of discovery (147).

The NOX2 homologues can be categorized into three different subgroups. The first group consists of NOX1, NOX3 and NOX4. Members of this group closely resemble NOX2 in terms of structure, consisting of a FAD domain, two heme domains, an NADPH-binding region and 6 transmembrane domains. The second group has only a single member, NOX5. This homologue has two additional calcium (Ca^{2+})-binding EF hand motifs in its N-terminal. The third group consists of DUOX1 and DUOX2. Those homologues are larger than the others as they contain a peroxidase domain in their N-terminal in addition to the two Ca^{2+}-binding EF hand motifs. Further, the DUOX enzymes contain an additional transmembrane domain separating the peroxidase region from the dual EF hand motifs (194).

Another method of categorizing the NOX homologues is based on their dependency on the various cytosolic regulatory components. As illustrated in the schematic diagram (Fig 1.8), NOX1, NOX2, NOX3 and NOX4 are $p22^{PHOX}$-dependent whereas NOX5 is not. Instead, NOX5 and the dual DUOX subunits are Ca^{2+}-dependent, reflecting the presence of the dual EF hand motifs present in their structures (147, 208). Moreover, only NOX1, NOX2 and, to a lesser extent, NOX3 are RAC1-dependent. NOX4 represents an exception as its activation only requires $p22^{PHOX}$ and it does not interact with any other regulatory components of the oxidase (208,

220). Interestingly, these characteristics render NOX4 constitutively active, generating ROS continuously at a very moderate level (218, 220). However, the capacity of NOX4 to generate ROS can be stimulated by various compounds and signals (191, 217, 221).

The expression of the NOX homologues in non-phagocytic cells is not necessarily restricted to one homologue per cell type (217, 222). The relative ratios of the NOX homologues also vary. For instance, in vascular smooth muscle cells, NOX4 expression is 40-fold higher than NOX1 (218, 222). Moreover, the cellular location of each NOX homologue can be distinct within one cell, differ between an undifferentiated and differentiated cell, as well as between different cell types (218, 222). For example, NOX4, in vascular smooth muscle cells co-localizes with vinculin, an actin-binding protein used as a marker for focal adhesion plaques that links integrin adhesion molecules to the actin cytoskeleton (218, 222, 223). In endothelial cells however, NOX4 was found to localize to the endoplasmic reticulum (218, 224). Interestingly, the distinct subcellular localization of the NOX homologues fits nicely with the observation that endogenous ROS production is highly compartmentalized and often restricted to the subcellular location at which free radicals exert their physiological signalling effects (222, 225). It also fits with some experimental evidence demonstrating that different NOX homologues mediate their effects through distinct signalling pathways (221). In fact, various cytokines, growth factors and signalling cascades have different impact on distinct NOX homologues (222, 224). This indicates that ROS generation from different NOX homologues trigger distinct signalling cascades in a highly cell-specific and environmentally specific context (222, 224, 225). Moreover, there is evidence to suggest that different NOX homologues may produce different species of ROS. For instance, it has been reported that NOX4 generates H_2O_2 instead of O_2^- (217, 220).

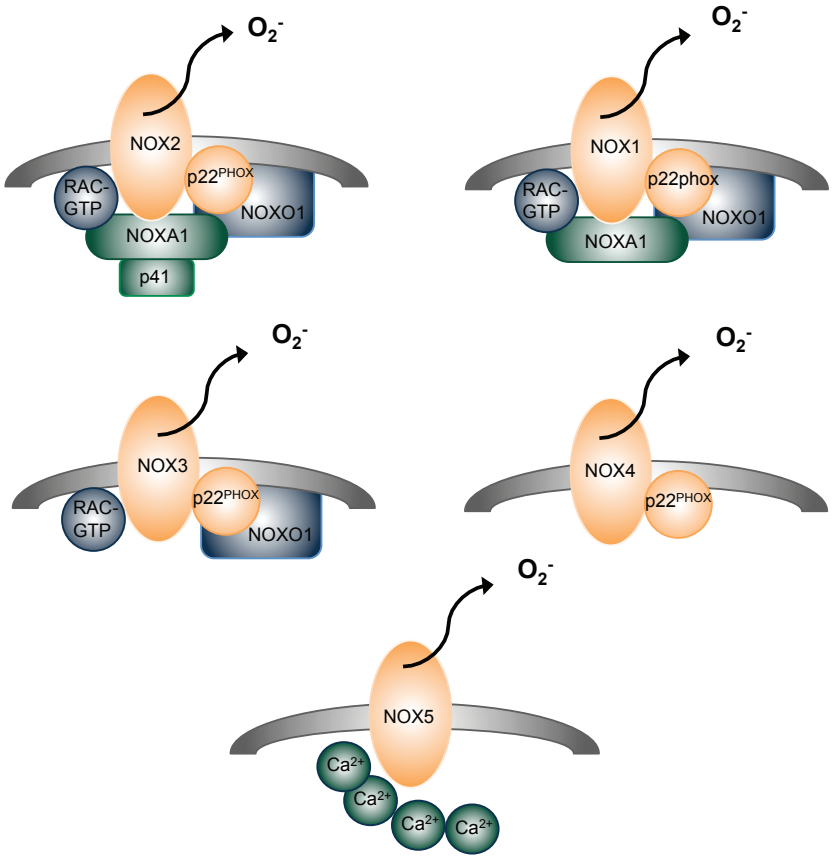


Fig 1.8 Non-phagocytic NADPH oxidase. The different NOX homologues differ in their requirement of the cytosolic regulatory components. NOXA1, NOXO1 and p41 are the homologues for $p67^{PHOX}$, $p47^{PHOX}$ and $p40^{PHOX}$ respectively, in non-phagocytic cells.

1.3.4 Phagocytic vs non-phagocytic NADPH oxidase complex

The phagocytic and non-phagocytic NADPH oxidase complexes share similarities in their structure and function; however, they differ in their biochemical characteristics (185). The first difference manifests in the amount of O_2^- produced. The phagocytic NADPH oxidase produces a relatively high amount of O_2^- but only during the respiratory burst. The non-phagocytic NADPH oxidase, on the other hand, generates O_2^-, sometimes constitutively, at low levels (185, 226). A second difference lies in the kinetics of the complex. The phagocytic complex generates O_2^- instantaneously upon stimulation by a pathogenic particle or a chemokine signal, whereas there is a lag period that can span minutes to hours between the stimulation of the non-phagocytic NADPH oxidase and subsequent ROS generation (185-187, 227).

1.3.5 Activators and inhibitors of the NADPH oxidase complex

The activity of the NADPH oxidase complex can be modulated using various chemicals that can stimulate or abolish the activity of the phagocytic and non-phagocytic NADPH oxidase complex. Manipulation of the complex is important to determine the physiological and pathophysiological role of NADPH oxidase-dependent ROS signalling in various cell types. One limitation of the NADPH oxidase inhibitors is their lack of specificity (147). Most inhibitors can block ROS production from other sources in the cell, like the XO or NOS. However, this limitation can be circumvented by using inhibitors for other sources of ROS in the cell, and comparing their effect with that of the NADPH oxidase inhibitor. Alternatively, NADPH oxidase-dependent ROS production can be disabled using siRNA-mediated knockdown of one or more of the complex subunits (220, 224).

The following are some of the most commonly used inhibitors and or activators of the complex:

a. Diphenylene iodonium (DPI)

DPI is the most commonly used inhibitor of the NADPH oxidase complex. DPI acts by removing an electron from an electron transporter and forming a radical, which covalently binds to the FAD-binding domain of the cytochrome b_{558} (147, 218, 228). The mechanism of action of DPI renders it not only an inhibitor for all NOX homologues but also for other flavin-containing enzymatic sources of ROS, such as the XO, the mitochondrial electron transport chain and NOS (228, 229). As mentioned, lack of specificity of DPI can be circumvented by carrying out well-

controlled experiments that involve all the appropriate controls and specific inhibitors for other sources of ROS (Figure 1.9) (147, 228). Moreover, DPI, at efficient concentrations, does not confer cell toxicity and has no oxidant scavenging potential (228).

b. Apocynin

Apocynin is a phenol compound *4-hydroxy-3-methoxyacetophenone* extracted from the roots of the medicinal plant *Picrorhiza kurroa* (147, 230). It has the ability of inhibiting the respiratory burst in phagocytic cells (230). The mechanism of action of apocynin depends on preventing the translocation of the regulatory components of the NADPH oxidase complex to the plasma membrane and therefore blocking the assembly of the complex in stimulated cells (147, 231, 232).

Although apocynin is a selective NADPH oxidase inhibitor, there is strong evidence that it can also activate the complex in certain cell types (228, 230). For instance, apocynin induces superoxide production in vascular fibroblasts (Figure 1.10) (233). The reason behind apocynin's dual function in different biological systems lies in its mechanism of action. It has been reported that in the presence of H_2O_2 or myeloperoxidase, apocynin forms a dimer, which inhibits the NADPH oxidase complex (232, 234). This dimerization occurs after a lag period. Accordingly, exposure of phagocytes to apocynin transiently increases ROS production followed by a decrease in ROS concentrations below basal levels (232, 234). The initial short period of ROS production that precedes the inhibition of the NADPH oxidase complex represents the effect of apocynin as a monomer (232). Therefore, in cells that lack myeloperoxidases such as vascular fibroblasts, apocynin as a monomer activates the NADPH oxidase complex. However, pretreatment of apocynin with H_2O_2 or horseradish peroxidase (HRP), prior to incubating it with vascular fibroblasts, inhibited superoxide production (233). Like DPI, it has been reported that apocynin does not have cytotoxic effects (228).

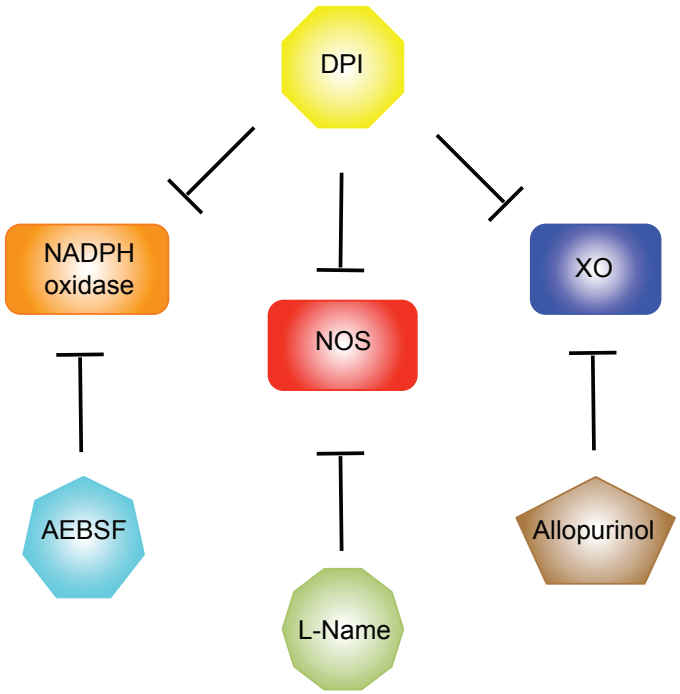


Fig 1.9 DPI is not a specific inhibitor of the NADPH oxidase complex. Lack of specific NADPH oxidase complex inhibitors, can be circumvented by inhibiting other sources of ROS, using specific compounds. Allopurinol specifically inhibits O_2^- production from the XO and L-Name is a specific inhibitor of NOS. AEBSF is an alternative inhibitor of the NADPH oxidase but, as a serine protease, it can affect a wide spectrum of other proteins.

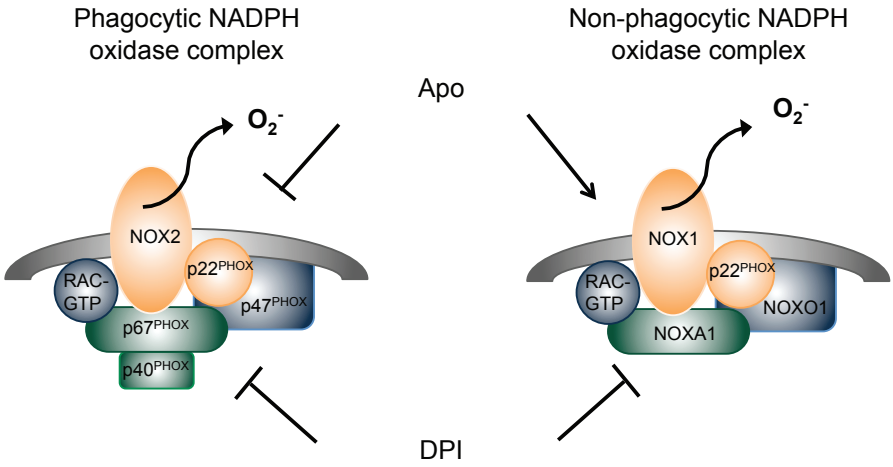


Fig 1.10 Apocynin and DPI modulate the activity of the NADPH oxidase complex. DPI is a potent inhibitor of the phagocytic and non-phagocytic NADPH oxidase complex. On the contrary, the effect of apocynin (Apo) differs between cell types. Generally, it acts as an inhibitor of the phagocytic NADPH oxidase but an activator of the non-phagocytic complex.

c. AEBSF

AEBSF, 4-(2-Aminoethyl)benzenesulfonylfluoride, is another NADPH oxidase inhibitor. It is a serine protease inhibitor that interferes with the translocation of the cytosolic components of the NADPH oxidase and consequently perturbs the assembly of the enzyme (147). The exact mechanism of action of the compound is not yet elucidated. Further, since it is a serine protease inhibitor, it can affect various other proteins unrelated to the NADPH oxidase complex (147).

1.3.6 Non-phagocytic NADPH oxidase complex: biology and disease

An increasing body of evidence implicates NADPH oxidase-dependent ROS signalling in a spectrum of physiological functions. For instance, NADPH oxidase activity is important for endothelial activation, a process that is pivotal to inflammatory responses and enables endothelial-leukocyte interactions and permeability (208, 235). NADPH-dependent ROS signalling also play a role in angiogenesis, proliferation and differentiation (156, 217). Conversely, perturbation in the NADPH oxidase complex expression or activity, either through genetic mutations or in response to an adverse cellular environment, leads to pathological disorders and diseases. For example, aberrant NADPH-dependent ROS production is widely implicated in cardiovascular diseases and cancer (185, 211, 218).

1.4 Endometriosis

1.4.1 Endometriosis: definition and diagnosis

Endometriosis is a common, benign, estrogen-dependent inflammatory disease characterized by the presence of endometrium-like tissue outside the uterus, primarily on the pelvic peritoneum and ovaries (236, 237). Endometriosis is a chronic systemic disease that affects 6 -10 % of women of reproductive age (236, 238). It is a complex disease that may be asymptomatic or present as pelvic pain and/or subfertility. Overall, the symptoms associated with pelvic endometriosis are non-specific and surgical assessment, by laparoscopy or laparotomy, is still viewed as the gold standard for diagnosis (237, 239).

1.4.2 The pathogenesis of endometriosis

The exact cause of endometriosis is unknown, but there are a number of theories, including retrograde menstruation, immune dysfunction, genetic predisposition, endometrial cells spreading through the bloodstream or lymphatic system, environmental causes, and metaplasia (239-242). Although retrograde transport of viable endometrial debris at the time of menstruation, and subsequent implantation of endometrial cells at ectopic sites, is widely viewed as the most common cause of endometriosis (243), this phenomenon occurs in 90% of women. Hence, it appears likely that multiple factors contribute to the pathogenesis of endometriosis as a chronic disease. For example, environmental factors, toxins like dioxin and phytoestrogens, have been implicated in the pathogenesis of endometriosis (236, 242, 244), although the evidence remains controversial. Genetic inheritance has also been recognized as a feature of the disease and several genome wide association studies demonstrated linkage between SNPs and specific loci with risk of endometriosis (245, 246). The risk for women whose first-degree relatives suffer from severe endometriosis has also been reported to be six times higher than women with unaffected female relatives (237).

Further, several molecular defects and/or immunologic abnormalities have been associated with endometriosis (236, 247, 248), which may account for the defective immunoclearance of endometrial cells in the peritoneal cavity and subsequent implantation and progression of the ectopic lesions (249). Further, various studies have associated the endometrium of patients with endometriosis with molecular defects like activation of oncogenic pathways and increased production of hormones and cytokines (236, 250-252). In addition, some epigenetic markers like methylation as well as the enzymes involved in maintenance of DNA methylation (DNMTs) are deregulated in the eutopic endometrium from patients with endometriosis compared to healthy individuals (248, 253).

1.4.3 The immune system and endometriosis

As mentioned briefly above, defective immune response and immunosurveillance of menstrual tissue in the peritoneal area has been associated with endometriosis. Natural killer (NK) cells have been implicated in clearing the peritoneal cavity from any ectopic tissue that ends there as a result of retrograde menstruation (249). NK cells can recognize and destroy tumour cells, pathogen-infected cells and foreign cells that have been transplanted in the body (249). One explanation for how NK

cells in healthy women can recognize autologous cells and respond to normal self-antigens depends on endometrial cells in the peritoneal area secreting different cytokines to which the natural killer cells can respond to (244). In women with endometriosis however, NK cells have reduced activity and cytotoxicity against such foreign bodies (249, 254-256). Interestingly, this reduction in activity was correlated with the severity of the disease (254).

Another mechanism that may be responsible for the defective immunosurveillance in women with endometriosis is the release of factors, like intercellular adhesion molecule 1 (ICAM1), from the ectopic endometriotic implants that prevent their recognition by the NK cells (249).

1.4.4 Progesterone resistance and endometriosis

Another characteristic of the eutopic endometrium of patients with endometriosis is resistance to progesterone signalling. There is an increasing body of evidence suggesting that the postovulatory rise in progesterone does not trigger profound gene regulation in the eutopic endometrium as it is seen with healthy individuals (257). Genome wide microarray analysis comparing biopsies taken in the MSE phase of the menstrual cycle from women with and without endometriosis revealed that over 200 genes were aberrantly regulated in endometriosis samples (258). A subsequent study comparing global gene expression and regulation through the different phases of the menstrual cycle between eutopic endometrial cells from women with and without endometriois not only confirmed the attenuated progesterone response but also indicated that endometriosis cells show perturbation in the proliferative-to-secretory transition, which is a hallmark of decidualization (257). Moreover, this study also showed that endometriosis cells possess enhanced cellular survival and continual expression of genes involved in DNA synthesis and mitogenic pathway (257). Another study applying genome wide microarray analysis in comparing the response of eutopic HESCs from women with and without endometriosis to 8-br-cAMP, revealed that cAMP downregulates genes involved in cell cycle progression and upregulates genes involved in cytoskeletal changes (238). However, this response was deregulated in samples from women with endometriosis, confirming the observation that endometriosis cells possess persistent proliferative phenotype regardless of exposure to decidual stimuli (238).

The deregulation of a subset of progesterone-dependent genes in the endometrium of patients with endometriosis has been termed as “progesterone resistance”. However, one should interpret this concept with caution. Progesterone controls a myriad of reproductive events including ovulation, embryo implantation, decidualization and menstruation, which is associated with influx of uNK cells and controlled inflammatory response. A recent microarray study comparing purified eutopic HESCs from patients with and without endometriosis upon progesterone stimulation revealed that aberrant gene expression is not confined to progesterone response but is also evident in unstimulated cultures (259). This observation, in addition to the aberrant gene expression level upon cAMP stimulation indicate that the basal transcriptome in endometriosis samples is perturbed and might suggest aberrant epigenetic regulation that affect the chromatin landscape.

1.4.5 Oxidative stress and endometriosis

Oxidative stress is associated with various pathological disorders including endometriosis (260). It is yet not clear how ROS may contribute to the pathogenesis of endometriosis; however, several studies suggested that higher concentrations of ROS might induce proliferation and adhesiveness of eutopic endometrial cells in the peritoneal cavity (261-263). Some studies have attributed enhanced ROS concentrations in the peritoneal cavity to the increase in infiltrating macrophages (264-266). However, the findings of these studies are controversial with others that did not find association with oxidative stress (261, 264, 267, 268). The controversy in the findings has been attributed to differences in the biomarkers used to assess oxidative stress and the methods of investigation utilized in these studies (260, 261, 264). Regardless of such controversy, emerging evidence is increasingly linking high ROS concentrations in eutopic endometriosis HESCs with the disease (172).

1.5 Hypothesis and Aims

Recently, endogenous ROS signalling has been implicated in different physiological functions like proliferation and differentiation in various biological systems. I hypothesize that endogenous ROS production and signalling play an integral role in the differentiation of HESCs into decidualized cells. Conversely, aberrant endogenous ROS production may play an important role in chronic inflammatory disorders of the female reproductive tract, such as pelvic endometriosis.

The specific aims of this project are:

- To determine the main source of endogenous ROS production in HESCs.
- To investigate the role and mechanism of endogenous ROS signalling in initiating and maintaining the decidual process.
- To investigate whether aberrant ROS production and signalling in eutopic endometrium play a role in the pathogenesis of endometriosis.

Chapter 2

Materials and Methods

2. Materials and Methods

2.1 Materials

2.1.1 Primary antibodies

Catalase	Rabbit anti-Catalase (ab76024; Abcam). Used for western blot (WB) at 1:10000 in phosphate buffered saline (PBS)
C/EPBβ	Rabbit anti-C/EPBβ (Sc-150 X; Santa Cruz Biotechnology Inc.). Used for WB at 1:400 dilution in 5% non-fat dry milk weight/volume (w/v) in 1% Tris buffered saline-Tween TBS-T volume/volume (v/v) (5% non-fat dry milk in TBS-T) and for supershift analysis at 2 μg per 5 μg of nuclear protein extract
FOXO1	Rabbit anti-FOXO1 (C29H4; Cell Signalling Technology). Used for WB at 1:1000 dilution in 5% BSA (w/v) in 1% TBS-T (v/v) (5% BSA in TBS-T)
JNK	Rabbit anti-JNK (56G8; Cell Signalling Technology). Used for WB at 1:1000 dilution in 5% BSA in TBS-T
Lamin B	Mouse anti-Lamin B (N412; Calbiochem). Used for WB at 1:5000 dilution in 5% non-fat dry milk in TBS-T
MKP1	Rabbit anti-MKP1 (c-370; Santa Cruz Biotechnology). Used for WB at 1:1000 dilution in 5% non-fat dry milk in TBS-T
NOX4	Rabbit anti-NOX4 (Kind gift from Prof. D. Lambeth, Emory University, Atlanta, GA). Used for WB at 1:1000 dilution in 5% non-fat dry milk (w/v) in 1% TBS-T (v/v)
p-ATM	Rabbit anti-p-ATM (5883; Cell Signalling Technology). Used for WB at 1:1000 dilution in 5% BSA in TBS-T
p-ATR	Rabbit anti-p-ATR (2853; Cell Signalling Technology). Used for WB at 1:1000 dilution in 5% BSA in TBS-T
p-BRCA1	Rabbit antil-p-BRCA1 (9009; Cell Signalling Technology). Used for WB at 1:1000 dilution in 5% BSA in TBS-T
p-CHK1	Rabbit antii-p-CHK1 (2349; Cell Signalling Technology). Used for WB at 1:1000 dilution in 5% BSA in TBS-T
p-CHK2	Rabbit antil-p-CHK2 (2661; Cell Signalling Technology). Used for WB at 1:1000 dilution in 5% non-fat dry milk in TBS-T

p-H2A.X	Rabbit anti-p-Histone H2A.X (9718; Cell Signalling Technology). Used for WB at 1:1000 dilution in 5% BSA in 1% TBS-T and for immunofluorescence (IF) 1:120 in 5% normal goat serum in PBS
p-JNK	Rabbit anti-phospho-JNK (98F2; Cell Signalling Technology). Used for WB at 1:1000 dilution in 5% BSA in TBS-T
PR	Mouse anti-PR (NCL-L-PGR-312; Novocastra Laboratories). Used for WB at 1/1667 in PBS
$p22^{PHOX}$	Rabbit anti-$p22^{PHOX}$ (FL-195; Santa Cruz Biotechnology Inc.). Used for WB at 1:200 in 5% non-fat dry milk in 1% TBS-T
RAC1	Mouse anti-RAC1 (MAB3735; Chemicon/Merck KGaA). Used for WB at 1:1000 in PBS
STAT-5	Rabbit anti-STAT5 (Upstate/ Merck KGaA). Used for WB at 1:1000 dilution in 5% non-fat dry milk in TBS-T
SUMO	Rabbit anti-SUMO1 (Zymed, Burlingame). Used for WB at 1:1000 dilution in 5% non-fat dry milk in TBS-T
SRC	Mouse anti-SRC (L4A1; Cell Signalling Technology). Used for WB at 1:1000 in 5% non-fat dry milk in 1% TBS-T
α-tubulin	Mouse anti-α-tubulin (sc-8035; Santa Cruz Biotechnology Inc.). Used for WB at 1:1000 dilution in 5% non-fat dry milk in TBS-T
β-actin	Mouse anti-β-actin (A1978; Sigma Aldrich). Used for WB at 1:1000000 dilution in 5% non-fat dry milk in TBS-T

2.1.2 Secondary antibodies

HRP-conjugated anti-rabbit	Goat anti-rabbit IgG HRP (P0448; Dako UK Ltd.). Used for WB at 1:2000 dilution in 5% non-fat dry milk in TBS-T
HRP-conjugated anti-mouse	Goat anti-mouse IgG HRP (P0447; Dako UK Ltd). Used for WB at 1:2000 dilution in 5% non-fat dry milk in TBS-T
FITC-conjugated anti-rabbit	Goat anti-rabbit IgG FITC (H17101; Invitrogen). Used for IF at 1:500 dilution in 5% goat serum in PBS

2.1.3 Plasmids

(C/EBP)-pGL4	(C/EBP)-pGL4 reporter construct (a kind gift from Prof. P. Bennett, Imperial College London, London UK)
(FOXO)-PGL4	(FOXO1)-pGL4 reporter construct previously described in (121)
pcDNA3-catalase	Catalase overexpression vector (a kind gift from Dr. S. Grimm, Imperial College London)
pcDNA3-FOXO1	FOXO1 overexpression vector has been previously described in (121)
pcH110	Control vector used for constitutive β-galactosidase expression (a kind gift from Prof. M. parker, Imperial College London)
pSG-C/EBP	C/EBP selective expression vector has been previously described in (126)

2.1.4 siRNA

Non-targeting siRNA	siGENOME Non-targeting siRNA #2, D-001210-02-20; Dharmacon
FOXO1 siRNA	siGENOME SMART pool M-003006-03, Human FOXO1, NM_002015; Dharmacon
NOX4 siRNA	siGENOME SMART pool M-010194-00, Human NOX4, NM_016931; Dharmacon
$p22^{PHOX}$ siRNA	siGENOME SMART pool M-011020-01, Human CYBA, NM_000101; Dharmacon
RAC1 siRNA	siGENOME SMART pool M-003560-02-0005, Human RAC1, NM_018890; Dharmacon

2.1.5 Cell lines

HESC	Human endometrial stromal cells (HESCs - Primary culture)
Hela	Immortalised cell line derived from cervical cancer cells

2.1.6 Cell culture materials and media

Antibiotic/Antimycotic solution, Invitrogen

Charcoal, Sigma

Collagenase type A1, Sigma

Dextran, Sigma

DNaseI, Roche

Dulbecco's Modified Eagles Medium (DMEM):F-12, Invitrogen

Fetal Bovine Serum (FBS), Sigma

Insulin, Sigma

L-glutamine, Invitrogen

Trypsin/EDTA, Invitrogen

2.1.7 Chemicals and reagents

17α-Medroxyprogesterone acetate (MPA), Sigma

2′,7′-dichlorofluorescein-diacetate (DCFH-DA), Molecular Probes, Invitrogen

2-Butanol, Sigma

30% Acrylamide/bis-acrylamide (37.5:1), Bio-Rad

30% Hydrogen peroxide (H_2O_2), Fluka

4-(2-Aminoethyl)benzenesulfonylfluoride (AEBSF), Sigma

4-(2-hydroxyethyl)-1-piperazineethanesulfonic acid (HEPES), Sigma

Acetone, BDH

Allopurinol, Sigma

Ammonium persulphate (APS), Sigma

Ampicillin, Sigma

Apocynin, Sigma

Bovine serum albumin (BSA), Sigma

Bradford assay reagent, Bio-Rad

Bromophenol blue, Sigma

Calcium chloride ($CaCl_2$), Sigma

Charcoal, Sigma

Chloroform, Sigma

Complete protease inhibitor, Roche

Diethylpyrocarbonate (DEPC)-treated water, Ambion

Dihydrorhodamine 123 (DHR 123), Invitrogen

Dimethyl suloxide (DMSO), Sigma

Diphenyleneiodonium (DPI), Invitrogen

Dithiothreitol (DTT), Bio-Rad

DNase I, amplification grade, Invitrogen

Estradiol, Sigma

Ethanol, BDH

Ethylenediamine tetraacetic acid (EDTA), Sigma

Glycerol, Sigma

Glycine, Sigma

Hydroxyureas, Sigma

Imidazole, BDH

Insulin, Sigma

Isopropanol, Sigma

Kanamycin, SIgma

Low melting point agarose (LMA), Promega

Luciferase assay reagent, Promega

Magnesium chloride ($MgCl_2$), Sigma

Methanol, BDH

N-omega-Nitro-L-arginine methyl ester

Nonidet P-40 (NP-40), BDH

Normal goat serum, Dako

Normal melting agarose (NMA), Promega

Paraformaldehyde (PFA), Sigma

Polyvinylidene fluoride (PVDF), GE Healthcare

Potasium cloride (KCL), Sigma

Phenylmethylsulfonyl floride (PMSF), Sigma

Reporter assay lysis buffer, Promega

RNA STAT-60 reagent, AMS Biotechnology

Skimmed milk powder, Fulka

Sodium Chloride (NaCl), BDH

Sodium dodecylsulphate (SDS), BDH

STAT-60, AMS Biotechnology

SYBR green PCR master mix, Applied Biosystem

Tetramethylethylenediamine (TEMED), Sigma

Trishydroxymethylaminomethane (Tris), BDH

Triton-X, Sigma

β-mercaptoethanol, Sigma

2.1.8 Kits

Amersham™ ECL™ Plus Chemiluminescence, Amersham

ApoTox-Glo™ Triplex Assay, Promega

CellTiter 96® AQ_{ueous} One Solution Cell Proliferation Assay, Promega

DNA Damage Antibody Sampler Kit, Cell Signalling Technology

Galacto-Light Plus™ System, Applied Biosystems

HiSpeed Plasmid Maxi Kit, Qiagen

ProFection® Mammalian Transfection System - Calcium Phosphate, Promega

RNeasy MinElute Cleanup Kit, Qiagen

SuperScript® First-Strand Synthesis System for RT-PCR, Invitrogen

2.2 Methods

2.2.1 Cell Culture

2.2.1.1 Human endometrial tissue samples

Endometrial samples were obtained from premenopausal women without uterine pathology. All the women were not on hormonal treatment and had regular menstrual cycles. Where the tissue was directly used for measuring basal levels of proteins and mRNA transcripts of interest, the samples were classified as “proliferative” if taken within the first 14 days of the last menstrual period, and as “secretory” if taken on day 15 or later. For establishing primary cultures, biopsies from both phases of the menstrual cycles were used. Written informed consent was obtained from all participating subjects before tissue collection. The study was approved by the Research Ethics Committee of Hammersmith and Queen Charlotte's Hospital NHS Trust.

2.2.1.2 Dextran coated charcoal (DCC) stripped serum preparation

Fetal bovine serum (FBS) normally added to cell medium contains endogenous steroid hormones that may mask the effect of exogenously added ligands. Therefore, FBS used for cell culture is stripped of small molecules. This is achieved by adding 1.25 g charcoal and 125 mg dextran to 500 ml of FBS. The mixture was then incubated in a waterbath for two hours at 56°C, inverting at regular intervals. Subsequently, the mixture was centrifuged at 4000 *g* for 30 minutes. The resulting

supernatant was sterilized by passing it through a 0.2 μm bottle-neck filter using suction, aliquoted and stored at -20°C.

2.2.1.3 Primary cell culture

Endometrial biopsies from independent patients were transferred to a Petri dish and cut finely using scalpels. Subsequently, the finely cut tissue was transferred into a 25 cm^2 flask with digestion media. The digestion media consisted of 10 ml of additive-free Dulbecco's Modified Eagles Medium (DMEM) F-12 with phenol red supplemented with 0.5 mg/ml collagenase type 1A and 0.1 mg/ml DNase 1. The collagenase was used in order to breakdown the extracellular matrix whereas the DNase was used to remove the viscous DNA released during the digestion process as a result of a small percentage of cell death. Digestion was allowed to proceed for one hour at 37°C in a humid atmosphere with 5% v/v carbon dioxide (CO_2) with vigorous shaking every 20 minutes. Following the one-hour incubation period, 10 ml of 10% v/v DCC/DMEM with phenol red was added to the digestion media in order to stop the action of the collagenase and the mix was centrifuged at 180 *g* for 5 minutes. The pellet which contained stromal, epithelial and blood cells was resuspended in 12 ml of 10% DCC/DMEM with phenol red supplemented with 2 mM L-glutamine, antibiotic/antimycotic solution, 1 nM estradiol and 2 mg/ml insulin, and transferred into a flask, the size of which depends on the size of the digested biopsy, and maintained in a humidified cell culture incubator at 37°C with 5% v/v CO_2. Stromal endometrial cells attach to the culture flask earlier than the epithelial cells. This allowes for the separation of the two types of cells by transferring the media, which largely contains blood and epithelial cells, after one hour of incubation into a new flask. The initial flask, which contains mostly stromal cells, is washed and incubated with 10% DCC/DMEM with phenol red supplemented with all the above. The 10% DCC/DMEM with phenol red supplemented with 2 mM L-glutamine, antibiotic/antimycotic solution, 1 nM estradiol and 2 mg/ml insulin, will be referred to as 10% DCC/DMEM medium. This 10% DCC/DMEM medium was used to propagate the HESCs and was changed every other day.

Once the cultures reach confluency they were passaged. This was carried out by aspirating the media and washing the cells with 3 ml of trypsin-EDTA (Invitrogen). Subsequently, cultures were incubated with 5 ml trypsin-EDTA for five minutes at 37°C. Following incubation, the flat was tapped genetly to dislodge the cells and 5 ml of 10% DCC/DMEM was added to the cultures to stop the action of the trypsin. Cells

were pelleted by centrifugation at 180 *g* for five minutes and the pellet was resuspended in 10% DCC/DMEM. HESCs suspension was cultured at a suitable dilution, normally 1:2.

To investigate the early events involved in the differentiation of HESCs into decidual cells, confluent cultures were treated with 0.5 mM 8-bromoadenosine-3', 5'-cyclic monophosphate in 2% DCC/DMEM without phenol red and supplemented with antibiotic/antimycotic solution. The 2% DMEM without phenol red and supplemented with antibiotic/antimycotic solution will be referred to as 2% DCC/DMEM medium. Prolonged decidualization was achieved by treating HESCs with 0.5 mM 8-br-cAMP and 1 μM 17α-Medroxyprogesterone acetate (MPA) in 2% DCC/DMEM. MPA was made up in ethanol whereas 8-br-cAMP was made in DMEM without additives. Therefore, ethanol was used as vehicle for MPA in control samples.

To activate and inhibit the NADPH oxidase complex, HESCs were treated with 1.5 mM apocynin and 10 μM diphenyleneiodonium (DPI) respectively. AEBSF (4-(2-Aminoethyl)benzenesulfonylfluoride), an alternative NADPH oxidase inhibitor was used at 250 μM. The xanthine oxidase (XO) activity was inhibited using allopurinol at 100 μM and the nitric oxide synthase (NOS) activity was inhibited using *N*-omega-Nitro-L-arginine methyl ester (L-Name) at 500 μM. Dimethyl sulfoxide (DMSO) was used to dilute apocynin, DPI and allopurinol whereas L-NAME and AEBSF were diluted in distilled water (dH_2O). All treatments were carried out in 2% DCC/DMEM.

2.2.1.4 Immortalized cells

Hela cells were propagated in 10% FBS/DMEM and maintained and treated in 2% FBS/DMEM. Hela cell line was only used as a control for DNA damage induction by hydroxyurea.

2.2.2 Transient transfections

2.2.2.1 Transfection of primary HESCs using the calcium phosphate co-precipitation method

Primary HESCs were transiently transfected using the ProFection® Mammalian Transfection System, which is based on the calcium phosphate ($CaPO_4$) co-precipitation method. Calcium phosphate-mediated transfection facilitates the binding

of Deoxyribonucleic acid (DNA) or oligonucleotides to the cell membrane and the entry of the DNA or oligonucleotides into the cell by endocytosis. This method entails mixing the DNA directly with calcium cloride ($CaCl_2$) and a phosphate buffer to form a fine precipitate, which is dispersed over the cultured cells. Prior to transfecting the cells, primary HESCs were seeded into 6-, 24- or 96-well plates and propagated with 10% DCC/DMEM until the cultures reach 80% confluency. The day before the transfection was carried out, the cells were serum-starved by replacing the 10% DCC/DMEM with 2% DCC/ DMEM. Serum-starving the cells enhances the uptake of DNA or oligonucleotides into the cells and therefore, increases the transfection efficiency. The following day, one hour before the transfection, the 2% DCC/DMEM was replaced with 5% DCC/DMEM in half the normal volume: 1 ml, 250 μl or 100 μl in a well of a 6-, 24- or 96-well plate respectively. The transfection mix was prepared as follows: solution A was made by adding the required amount of DNA or oligonucleotides to sterile, deionized water and mixing well by vortexing before adding $CaCl_2$ to the mix at a concentration of 245 mM, then vortexing again and incubating the mix for five minutes at room temperature. Solution B is prepared by adding 2x HEPES-buffered saline in equal volume to solution A. Solution A was then added drop-wise to solution B while the latter was being vortexed. The transfection mix was then incubated at room temperature for 30 minutes to allow formation of $CaPO_4$ precipitate. The transfection mix is then vortexed and dispersed on the cells in the following volumes 480 μl, 120 μl or 48 μl in a well of 6-well plate, 24-well plate or 96 well plates respectively. The cells were incubated with the transfection mix for six to nine hours and subsequently washed and left untreated overnight. Treatments were carried out the following day.

2.2.2.2 Reporter Assay

Luciferase reporter assays were performed on primary HESCs transfected in 24-well plates using the ProFection® Mammalian Transfection System. The final concentration of the luciferase reporter constructs and expression vectors added to the cells was 500 and 125 ng respectively. PCH110, an expression vector encoding for β-galactosidase, which leads to constitutive β-galactosidase expression, was used to compare transfection efficiency between samples and was transfected at a final concentration of 50 ng. Before harvesting, the media was aspirated and cells were washed with 1 ml PBS prior to adding 50 μl of reporter lysis buffer to each well. The plate was then placed on an orbital shaker on a low setting for 15 minutes at 4°C and then frozen at -80°C for at least 30 minutes. Following thawing at room

temperature, the lysates were transferred to eppendorfs and centrifuged at 16000 *g* for two minutes to pellet the cellular debris. Subsequently, 10 μl of the lysate was transferred in duplicate into a 96-well opaque plate and 50 μl of luciferase assay reagent containing substrate and assay buffer was added. Luminescence was measured using a Victor II plate reader (PerkinElmer).

β-galactosidase activity was measured using the Galacto-Light Plus™ System, a chemiluminescent reporter assay system designed for rapid and sensitive detection of β-galactosidase reporter enzyme in cell lysates. Galacton-Plus substrate in the reaction buffer is cleaved by β-galactosidase enzyme. The Accelerator-II reagent is added to the samples in the reaction buffer to terminate the enzyme activity and to trigger light emission from the cleaved substrate. Galacton-Plus chemiluminescent substrate emits light at a near constant level with a half-life of approximately 180 minutes after the addition of Accelerator-II, rendering it ideal for use with instruments without reagent injectors.

To carry out the assay, protein lysates were first heated for 50 - 60 minutes at 48°C to inactivate endogenous β-galactosidase that can be present in cells. Endogenous β-galactosidase activity can result in high background reading and decrease the sensitivity of the assay. Following the inactivation step, 10 μl of the lysate was transferred to an optically clear flat-bottom 96-well plate and 70 μl of Reactiion Buffer, which consists of Dilute Galacton-Plus substrate diluted 1:100 with Reaction Buffer Diluent, was added to each well. Following incubation of the plate for 30 minutes at room temperature, 100 μl of Accelerator-II was added to each well and luminescence was read using a Victor II plate reader (PerkinElmer). This protocol is according to the manufacturer's instructions.

2.2.2.3 Small interfering RNA (siRNA)

siRNA technology was used to knockdown expression of genes of interest in primary HESCs. The ProFection® Mammalian Transfection System was used to transfect siRNA into HESCs. All targeting and non-targeting (NT) siRNA were siGENOME SMART pool duplexes purchased from Dharmacon and were used at a 100 nm concentration.

2.2.3 Western blot analysis

2.2.3.1 Protein extraction

For protein extraction, primary HESCs were cultured and treated in 6-well plates. Whole cell lysates were harvested using Laemmeli buffer (0.5 M Tris-HCL, pH 6.8, 0.5 M Imidazole, pH 6.8, 10% SDS, 10% glycerol, 2% β-mercatoethanol, 0.5% Bromophenol blue). To harvest whole cell lysates, the media was aspirated and 60 μl of Laemmili buffer, boiled to 100°C, was added to each well. Cells were scraped using cell scraper and the viscous lysate was transferred into eppendorfs using a 200 μl pipette tip with a snipped tip. The samples were then boiled to 100°C, centrifuged at 16000 *g* for 1 minute and stored at -80°C.

For cytosolic/nuclear extraction, primary HESCs were cultured and treated in 6-well plates. To harvest, the media was aspirated and 70 μl of Cytosolic Buffer A (10 mM HEPES, 10 mM KCl, 0.1 mM EDTA, 0.1 mM EGTA, 2 mM DTT, 1% v/v NP-40 and complete protease inhibitor tablets) was added to each well and cells were scraped using a cell scraper. Subsequently, lysates were transferred to an eppendorf and incubated for 5 - 20 minutes on ice. Following vortexing of the lysates for 10 minutes at full speed, samples were then centrifuged at 16,000 *g* for 30 seconds at 4°C. The supernatants, resembling the cytosolic extracts, were transferred to an eppendorf and stored at -80°C. The remaining pellets were resuspended in 20 μl of Nuclear Buffer B (10 mM HEPES, 10 mM KCl, 0.1 mM EDTA, 0.1 mM EGTA, 2 mM DTT, 400 mM NaCl, 1% v/v NP-40 and complete protease inhibitor tablets). The samples were then stored on ice with minimal shaking for 15 minutes and subsequently centrifuged at 16,000 *g* for 5 minutes at 4°C. The supernatants, resembling the nuclear extract, were transferred to a new eppendorf and stored at -80°C.

To extract protein from tissue biopsies, High Salt Homogenisation Buffer (0.4M KCl, 20 mM HEPES pH 7.4, 20% v/v glycerol, 1 mM DTT, 1 mM PMSF, 1x mini complete protease inhibitor cocktail) was used. To each tissue biopsy, 1 ml of High Salt buffer was added and homogenised mechanically. Lysates were then centrifuged at maximum speed to pellet the debri, and the supernatent was transferred to a new eppendorf. Samples were then stored at -80°C.

2.2.3.2 Measurement of protein concentration

Protein concentration of lysates was quantified using the Bradford assay. The Bradford assay is a colorimetric protein assay, which is based on the absorbance shift of the dye Coommassie Blue. Upon binding to arginine and hydrophobic amino acid residues present in proteins, the Commassie Blue dye found in the Bradford Reagent (Bio-Rad) is converted from red to blue. The binding of the protein stabilizes the blue form of the dye. The bound form of the dye has an absorption spectrum maximum at 595 nm. The increase in absorbance is proportional to the amount of bound dye and therefore is proportional to the concentration of protein in the sample.
To carry out the assay, a set of standards in a volume of 800 μl was prepared using bovine serum albumin (BSA) dissolved in and diluted with dH_2O to the following concentration: 0, 0.005, 0.01, 0.02, 0.04, 0.06, 0.08 and 0.1 μg. The protein samples to be quantified were diluted 1:400 in 800 μl of distilled water. To each sample and standards, 200 μl of Bradford reagent was added and mixed well by vortexing. Samples and standards were incubated for 15 minutes at room temperature. Following vortexing, 200 μl of each standard and sample was transferred in duplicate into a flat-bottom, optically clear 96-well plate and the absorbance at 595 nm was measured. The protein concentration in the samples was quantified by reference to the standards.

2.2.3.3 SDS-PAGE and western blot analysis

SDS-polyacrylamide gel electrophoresis (SDS-PAGE) was used to resolve proteins on a discontinuous polyacrylamide gel using the Invitrogen XCell SureLock Mini-Cell. Gels were prepared in disposable plastic cassettes (invitorgen) from two solutions to form the lower resolving gel (375 mM Tris-HCl pH 8.9, 1% w/v SDS, 10 or 7.5% v/v acrylamide/bis-acrylamide (37.5:1), 0.03% w/v APS, TEMED added 1/500) and the upper stacking gel (80 mM Tris-HCl, pH 6.8, 80 mM Imidazol, pH 6.8, 0.06% w/v SDS, 5% acrylamide/bis-acrylamide (37.5:1), 0.11% w/v APS, TEMED added 1/500). The lower resolving gel solution is first poured into the disposable cassette until it reaches within 1 cm from the base of the prospective wells and overlaid with dH_2O butanol and was left for one hour to polymerize. When polymerization was complete, the butanol was rinsed off with dH_2O and the upper stacking gel solution was poured on top of the polymerized resolving gel and a comb with the appropriate number of wells was inserted. The gel was left to polymerize for 30 minutes. Once the stacking gel had set, the cassette was fitted in the electrophoresis tank and running buffer (25 mM Tris, 190 mM glycine, 0.1% w/v SDS) was loaded. Protein lysates in loading

buffer, with equal volume and concentration, were loaded into the wells alongside prestained molecular weight markers. The gels were first run at 80 V for 30 minutes to allow slower, even entry of the loaded samples into the stacking gel. The difference in density and pH of the two gels allowes compaction of the samples at their border and provides crisp resolution on the resolving gel. The gels were further run at 135 V for approximately one hour and 15 minutes or until the prestained molecular weight marker reaches the desired resolving state.

When SDS-PAGE was completed, the cassette was opened and the resolving gel removed for western blotting. Protein samples resolved on the stacking gel were transferred to a PVDF membrane for immunoblotting using the semidry blotting method. A sandwich was assembled consisting of two sheets of Mini Trans-blot filter paper (Invitrogen) pre-equilibrated in transfer buffer (11.66 g Tris, 5.8 g glycine, 20% methanol v/v, and 7.5 ml 10% SDS for a 2 L stock made up with dH_2O), followed by the PVDF membrane activated in methanol and pre-equilibrated in dH_2O then transfer buffer, followed by the resolving gel and finally two sheets of Mini Trans-blot filter papers pre-equilibrated in transfer buffer. Every sheet of filter paper and the PVDF membrane was rolled to eliminate any bubbles. Semidry transfer was performed with a constant voltage at 25 V for one hour and five minutes. When the transfer was completed, the PVDF membrane was allowed to air-dry, then it was activated in methanol and washed briefly in 1x TBS (130 mM NaCl, 20 mM Tris, pH 7.6). The membrane was then blocked with 5% non-fat dry milk for one hour at room temperature while rotating on an orbital shaker. Following washing of the membrane with 1x TBS, the desired primary antibody in the appropriate dilution was added to the membrane and left rotating overnight at 4°C. The following day, the membrane was subjected to three washes of 10 minutes each in 1x TBS-T (0.1% Tween-20 in TBS). The appropriate secondary antibody was then added to the membrane and the membrane was incubated for one hour at room temperature. The membrane was then washed three times for 10 minutes per wash with 1x TBS-T, and detergent was rinsed of with 1x TBS. Chemiluminescent signals were visualized by using the ECL Plus Western Blotting Detection System according to instructions provided by the manufacturer.

2.2.3.4 Densitometry

Densitometry was carried out to quantify the protein bands in a Western blot. The software ImageJ was used for this purpose (www.rsb.info.nih.gov/ij/index.html).

2.2.4 Reverse transcription polymerase chain reaction (PCR)

2.2.4.1 RNA Extraction

Total RNA was extracted from primary HESCs cultured in 6-well plates using the RNA STAT-60 reagent, which is composed of a phenol and guanidinium thiocyanate in a mono phase solution. Following aspiration of the culture media, 500 μl of RNA STAT-60 reagent was added to each well, spread over the whole culture surface using a cell scraper and incubated at room temperature for five minutes. The lysate was then transferred to RNase-free 1.5 ml centrifuge tubes and then pipetted repetitively to ensure the complete dissociation of nucleoprotein complexes. Next, to each tube, prechilled chloroform was added in fifth the volume of the STAT-60 reagent, mixed well by vortexing for 15 seconds, incubated at room temperature for two minutes and centrifuged at 12000 *g* for 30 minutes at 4°C. This allows the separation of the solution into an upper colourless aqueous phase and a lower red phenol organic phase. RNA remains exclusively in the aqueous phase whereas DNA and proteins are in the interphase and organic phase. The aqueous phase is then transferred to a fresh 1.5 ml centrifuge tube, pre-chilled isopropanol in half the volume of STAT-60 was added to each tube, and samples were incubated at room temperature for five minutes in order to precipitate the RNA. Subsequently the RNA was pelleted by centrifugation at 12000 *g* for 20 minutes at 4°C, washed with 70% v/v prechilled ethanol. The final pellet was left to air-dry and was dissolved in a suitable volume of DEPC-treated RNase free dH_2O.

RNA concentration was measured using the Nanodrop 1000 spectrophotometer (Thermoscientific), and RNA purity was assessed by determining the ratio of absorbance at 260/280 nm. Satisfactory values were considered equal or greater to 1.8, indicative of highly purified RNA free from contaminating protein. RNA samples were stored at -80°C.

2.2.4.2 cDNA synthesis

Prior to cDNA synthesis, total RNA harvested from primary HESCs was subjected to deoxyribonuclease I (DNase) treatment in order to remove any contaminating genomic DNA, which could be amplified along with the targeted mRNA during Real-time quantitative PCR. To 1 μg of total RNA, 1 U of amplification grade DNase I was added to each sample, in the presence of 1x DNase I reaction buffer in a total

volume of 10 μl made up with DEPC-treated water. Following incubation of samples for 15 minutes at room temperature, DNase I was inactivated by the addition of 1 μl of 25 mM EDTA and heating to 65°C for 10 minutes.

cDNA synthesis was carried out using the superscript First-Strand Synthesis for RT-PCR. To each 8 μl of DNase treated RNA sample (about 800 ng in total), 1 μl of 500 ng/μl oligo(dTs) primers and 1 μl dNTP mix (added to a final concentration of 1 mM) was added. Samples were incubated at 65°C for five minutes to remove the secondary structure within the RNA template. Following incubation, samples were immediately incubated on ice for at least one minutes to prevent secondary structure from reforming. For each sample, a master reaction mixture was prepared with the following components: 2 μl 10x RT buffer, 4 μl 25 mM $MgCl_2$, 2 μl 0.1 M DTT and 1 μl RNase OUT (40 U/μl), a recombinant RNase Inhibitor. To each sample, 9 μl of the master reaction mixture was added, mixed gently and incubated at 42°C for 2 minutes. Subsequently, 50 U of SuperScript II reverse transcriptase were added to each sample and reincubated at 42°C for 50 minutes to allow cDNA synthesis. The reaction was then terminated by incubating the samples at 70°C for 15 minutes, and subsequently chilling them on ice. To remove the RNA template from samples and to increase the sensitivity of subsequent PCRs, 2 U of RNase H were added to each sample an the mixture was incubated at 37°C for 20 minutes. Prior to storing samples at -20°C, an aliquote of each sample was used to create a pooled cDNA sample, which was used for setting up a set of standards for RTQ-PCR and was also stored at -20°C.

2.2.4.3 Real-time quantitative PCR (RTQ-PCR)

RTQ-PCR was performed to measure mRNA transcript of genes of interest as an indication of gene expression. Specific primers to the gene of interest were used and RTQ-PCR was performed using the Applied Biosystems StepOne™ Real Time PCR System. The PCR reactions were performed in a 96-well plate thermal cycler and the amplified products were detected by the presence of fluorescence resulting from the intercalating fluorescent dye SYBR Green I. SYBR Green in its free form is non-fluorescent, however, once incorporated into double stranded DNA it fluoresces. Therefore, as the PCR progresses, more double-stranded DNA products of the gene of interest accumulate. Consequently, more SYBR Green is intercalated within the DNA strengthening the fluorescence signal. Background fluorescence is determined between PCR cycles 3 and 15 and provides a baseline measurement from which the

software can then calculate a change in fluorescence intensity (ΔRn) during each cylce. An amplification plot of ΔRn versus the cycle number is generated and a threshold is chosen to coincide with the exponential phase of the reaction. The cycle number at which the increasing ΔRn crosses this threshold is defined as the threshold cycle (Ct) and is used as a measurement of mRNA abundance. Therefore the lower the Ct value, the more highly expressed a gene is. This real time monitoring of exponential nucleic acid amplification is more accurate and sensitive than the assessment of the final product in the conventional PCR method.

The RTQ-PCR reaction was performed in a total volume of 15 μl in a MicroAmp® Fast Optical 96-Well Reaction Plate (Applied Biosystems). The reaction mixture composed of: 7.5 μl of SYBR Green PCR Master Mix (Applied Biosystem), optimized primer pairs and the reaction was made up to a total of 12 μl using DEPC-treated water. In each well, 3 μl of cDNA diluted 6 X with DEPC-treated water was added to 12 μl of the Master Mix. Each sample was run in triplicate. A serial five-fold dilution of pooled cDNA was set up as standards. In three reactions, no cDNA template was added to control for the formation of primer dimmers and to act as negative controls. The RTQ-PCR was carried out under the following conditions: an initial denaturing step at 95°C for 10 minutes, 40 cycles of denaturation at 95°C for 15 seconds, and 60°C for 1 minute for annealing and extension.

Quantification of amplified products was carried out by the relative standard curve method. Arbitrary units were assigned to the Ct values of the serially diluted standards to generate a standard curve whereby the Ct values of the known samples were referenced. The universally expressed ribosomal protein *L19* represented a non-regulated gene and its expression served as an internal control and was used for data normalisation. Primer sequences used in this thesis can be found in Appendix 1.

2.2.4.4 Primer design and testing for real-time quantitative PCR

Primers were designed with the Primer3 software (Whitehead Institute for Biomedical Research, MIT, US), using sequences from the Ensembl genome database (www.ensembl.org). The following design criteria were used: amplicon size of 90 - 120 bp, GC content 40 - 50% and melting temperature 58 - 62°C. In order to reduce the possibility of amplifying genomic DNA that has not been completely eliminated from the sample, the primer pairs were designed within a short sequence of DNA crossing an intron-exon boundary. Prior to ordering the primer set from Invitrogen,

using the Basic Local Alignmet Sequence Tool (BLAST), primers were compared with all human sequences in the gene database of the National Centre for Biotechnology Information (NCBI) to confirm there is no significant homology with other genes. Primers were dissolved to a storage concentration of 100 pmol/μl, and the appropriate working concentration was used to reach the optimized final concentration of primers.

2.2.5 Electron mobility shift assay (EMSA)

EMSA is a common affinity electrophoresis technique that was used to study protein-DNA interactions. Briefly, 5 μg of nuclear protein extracts was incubated for one hour with non-radiolabeled non-specific and specific oligonucleotides in binding buffer (20% v/v glycerol; 5 mM $MgCl_2$, 2 mM EDTA; 50 mM Tris-HCl, pH 7.5; 250 mM NaCl; and 2 mM DTT), followed by a 45-minute incubation with 0.035 pmol [γ-^{32}P] ATP ended-labeled oligonucleotide probes. The non-specific oligonucleotides would not be competing with the radiolabeled specific oligonucleotides and therefore a slower migrating band would be visualized by autoradiography as a result of labeled oligonucleotides forming specific DNA-protein complexes with the target protein. On the other hand, excess non-labeled oligonucleotides to the nuclear protein and labeled specific oligonucleotides mix would be competing with the labeled oligonucleotides forming specific DNA-protein complexes and therefore, no band will be visualized. To check for the specificity of the protein, supershift analysis was carried out, where samples were incubated with 2 μg with antibody against the protein of interest for one hour on ice prior to incubation with the probe. DNA-protein complexes were separated from unbound DNA probe on a 4% nondenaturing acrylamide gel in 0.25x TBE running buffer (9 mM Tris-borate and 0.2 mM EDTA, pH 8.0). Gels were vacuum dried and exposed to Amersham MP films at -80°C for 16-48 hours. The consensus oligonucleotides for OCT1 were purchased from Promega Life Science (E 3241), and from Santa Cruz Biotechnology for CEBP (sc-2525).

2.2.6 Immunofluorescence analysis and confocal microscopy imaging

Primary HESCs were cultured on 4-chamber culture slides. For fixing the cells, the media was removed, the cells were washed once with 1x PBS and 1 ml of 4% paraformaldehyde (PFA) was added to each well and the slide was incubated for 15 minutes at room temperature. PFA was then removed and the cells were washed 3x with PBS, permeabilized with 0.1% v/v Triton X-100 in filtered PBS for 30 minutes and finally the slide was washed 3x with PBS. Cells were blocked with 250 μl of 5%

normal goat serum in PBS for 45 minutes at room temperature. Following incubation, primary antibody against the protein of interest is diluted to the appropriate concentration in 0.01% v/v normal goat serum in PBS and 250 μl of the antibody was added to each well. As a negative control, one well had 250 μl of 0.01% v/v normal goat serum in PBS added without the primary antibody. The culture slide was incubated overnight at 4°C. The following day, the slide was washed 3x with PBS and secondary antibody diluted 1:500 in 0.01% v/v normal goat serum in PBS and was added to each well and incubated for one hour at room temperature in the dark. The slide was then washed 3x with PBS, the chambers were detached from the slide using the apparatus provided by the manufacturer and the slide was left to air-dry. A coverslip was then mounted on the slide using Vectashield with DAPI. The staining was visualized under the SP5 Leica confocal microscope.

2.2.7 Measurement of cellular reactive oxygen species (ROS)

2',7'-dichlorodihydrofluoresein diacetate (DCFH-DA) was used to measure intracellular ROS in primary HESCs. DCFH-DA is membrane permeable, colourless and non-fluorescent until the acetate group is cleaved by intracellular esterases rendering it membrane impermeable. Oxidation of the compound, yields the fluorescent fluorophore, 5-(and-6)-carboxy-2',7'-dichlorofluorescein (DCF). The amount of fluorescence is proportional to the oxidation of the compound, which is proportional to the amount of ROS in the cell.

To carry out the assay, cultured HESCs were seeded in 96-well black plates with clear bases and maintained in 10% DCC/DMEM until they become confluent. Cells where either decidualized or left untreated. Thirty minutes before terminating the treatments, cultured HESCs were loaded with (DCFH-DA) at a final concentration of 30 μM and incubated at 37°C in a cell culture incubator in a humid condition with 5% v/v CO_2 for 30 minutes. The cells were then washed twice with PBS and the appropriate media with or without the treatment was added to the cells. Hydrogen peroxide (H_2O_2) was used as a positive control, to ensure the validity of the DCFH-DA probe. Measurement was then taken using the fluorometer at an excitation and emission wavelengths of λ = 485 and λ = 535, respectively, every two minutes for a 30 minute period. To control for the amount of cells in each well, the media was aspirated and the cells were washed twice with PBS. Consequently, the cells were stained with propodium iodide (PI) prepared in a 1% NP40-PI 10 μg per ml solution. The plate was placed on an orbital shaker for 15 minutes at room temperature.

Measurement was then taken using the flourometer at an excitation wavelength λ = 535, and emission wavelength λ = 600.

When DCF fluorescence was measured using flow cytometry, HESCs were cultured and treated in 6-well plates. The cells were then stained with DCF-DA/PI (30 μM/10 μg) in suspension for 30 minute, washed and resuspended in PBS. Subsequently DCF and PI fluorescence were measured using the following flow cytometer detectors respectively FL-H1 and RL-3H.

The same protocol was used to assess the alternative oxidant-sensing probe DHR 123, which was also used at a final concentration of 30 μM.

2.2.8 Measurement of cell proliferation and viability

2.2.8.1 CellTiter 96® AQ_{ueous} One Solution Cell Proliferation Assay

The CellTiter 96® AQ_{ueous} One Solution Cell Proliferation Assay is a colorimetric assay used to determine the number of viable cells in proliferation or cytotoxicity studies. The CellTiter 96® AQ_{ueous} One Solution Reagent contains a novel tetrazolium compound [3-(4,5-dimethylthiazol-2-yl)-5-(3-carboxymethoxyphenyl)- 2-(4-sulfophenyl)-2H-tetrazolium, inner salt; MTS] and an electron coupling reagent phenazine ethosulfate (PES). PES has enhanced chemical stability, which allows it to be combined with MTS to form a stable solution. The MTS tetrazolium compound is bioreduced by cells into a coloured formazan product that is soluble in tissue culture medium, and has an absorbance spectrum of 490 nm. The quantity of formazan product, therefore, measured by the absorbance at 490 nm is directly proportional to the number of living cells in culture.

To carry out the assay, primary cultures were seeded in optically clear flat-bottom 96-well plates and treated as desired. When the treatment period is completed, 20 μl of CellTiter 96® AQ_{ueous} One Solution Reagent was pipetted into each well of the 96-well assay plate containing the samples in 200 μl of culture medium. The plate was incubated for three hours in a humid condition with 5% CO_2 v/v at 37°C. Following the incubation period, absorbance was measured at 490 nm using a spectrophotometer.

2.2.8.2 Apo Tox-Glo™ Triplex Assay

The Apo Tox-Glo™ is an alternative method of assessing cell viability. The assay measures a marker of cell viability and another marker for cytotoxicity. The cell viability marker is a cell protease that is restricted to viable cells and is measured by a cell-permeable probe that fluoresces once it is cleaved by the protease. The cell cytotoxicity marker is a dead-cell protease that is released from cells once they lose their membrane integrity. It is measured by a cell-impermeable probe that fluoresces once it gets cleaved by the dead-cell protease. The two probes have different excitation and emission wavelengths allowing their simultaneous addition to the cells. To carry out the assay, cells were seeded in 96-well black plates and treated as desired. When the treatment period was completed, 20 μl of the Viability/Cytotoxicity reagents were added to each well and the plate was briefly mixed by an orbital shaker. Subsequently, the cells were incubated for one hour at 37°C with 5% v/v CO_2 in a humidified incubator. Viability was quantified by measuring the fluorescence signal at $400_{Ex}/505_{Em}$ and cytotoxicity was quantified by measuring the fluorescence signal at $485_{Ex}/520_{Em}$. H_2O_2 was used as a positive control.

2.2.9 Comet assay

The comet assay, also known as single cell gel electrophoresis (SCGE) is a technique for analyzing DNA damage in individual cells. A cell with DNA damage would resemble a “comet” shape with distinct head and tail, the head of the comet represents the intact DNA whereas the tail consists of damaged DNA. TO carry out the assay, HESCs were cultured in 6-well plates and once they reached 80% confluency they were transfected with NT siRNA or siRNA targeting NOX4 and $p22^{PHOX}$. Two days post transfection, cultures were either left untreated or treated with 8-br-cAMP and MPA for 72 hours. As a positive control for DNA damage, cells were treated with 1 μM of epirubicin overnight. The following day, microscopy slides were coated with thin agarose gel (1% NMA w/v in dH_2O). HESCs from each well were pelleted and resuspended in 100 μl of 1x PBS, and between 2 - 10 μl of cell suspension was added to each agarose coated slide and 85 μl of 0.7% LMA in PBS was poured on top of the cells and a coverslip was placed on top in order to separate the cells. The slide was stored at 4°C for 10 minutes. Following incubation, the coverslip was removed another 85 μl of 0.7% LMA in PBS was poured. The slide was incubated for another 10 minutes. Subsequently, the cells were lysed by removing the coverslips and placed the slide containg the cells in a slide merging flask containg the lysis buffer (146.1 g NaCl, 37.2 g NaEDTA, 1.2 g Tris-HCl, 25.88

ml N-lausarcosylsarcosinte, 10 g NaOH, 1% Triton-X and 10% DMSO) which was kept at 4°C. The slide was incubated in the slide merging flask for one hour at 4°C in the dark. Following incubation, the slide was dried by placing it on an absorbing material. Subsequently, the slide was inserted in an electrophorsis tank with the electrophoresis buffer (0.555 g NaEDTA and 10 g NaOH in dH_2O), which was placed on ice and covered with foil for 20 minutes. Electrophoresis was carried out on ice for 15 minutes at 300 mA. To stop the electrophoresis process, the slides were neutralized by adding 2x neutralization buffer (48% Tris HCl in dH_2O). To mount the coverslips, 30 µl of Vectashield with DAPI was added and the slides were stored in a humid and dark environment until the slides were analyzed under a fluorescence microscope.

2.2.10 Bacterial propagation of plasmids

The *Escherichia coli* strain DH5α was used to propagate plasmids. Bacteria were streaked out on L-agar plates (1% w/v bactotryptone, 0.5% w/v yeast extract, 0.5% w/v NaCl, 0.1% w/v glucose, 1.5% w/v bactoagar) and incubated at 37°C overnight. A single colony was used to inoculate 5 ml of L-agar with the appropriate antibiotic which was then incubated for eight hours at 37°C with continuous shaking. Subsequently, 50 µl of the culture was transferred to 200 ml L-agar with the appropriate antibiotic and incubated overnight at 37°C with continuous shaking. The following day, the bacteria were harvested by centrifugation at 3300 *g*, at 4°C for 15 minutes. The final pellet was resuspended in 2.5 ml ice-cold sterile solution consisting of 20% v/v glycerol and 0.1 M $CaCl_2$. The cell suspension was aliquoted into 100 µl, snap frozen on dry ice and stored at -80°C.

2.2.10.1 Transformation of competent bacteria by heat shock

Escherichia coli strain DH5α was used to propagate plasmids. A 100 µl aliquot of DH5α supercompetent cells was thawed on ice and subsequently 5 µl of plasmid solution, containing 2-10 ng/µl DNA was added to the cell suspension, mixed gently and incubated on ice for 30 minutes. Heat shock was performed by incubation in a waterbath at 42°C for 45 seconds and the bacteria were then placed on ice for two minutes. Subsequently, 680 µl of L-agar medium (1% w/v bactotryptone, 0.5% w/v yeast extract, 0.5% w/v NaCl, 0.1% w/v glucose, 1.5% w/v bactoagar) were added to the cell suspension which was then incubated in a waterbath at 37°C for one hour. All expression vectors used carried either an ampicillin or kanamycin resistance gene. Consequently, the cells were spread for selection on L-agar plates (1% w/v

bactotryptone, 0.5% w/v yeast extract, 0.5% w/v NaCl, 0.1% w/v glucose, 1.5% w/v bactoagar) with 100 µg/ml ampicillin or 30 µg/ml kanamyacin and incubated at 37°C overnight.

2.2.10.2 Large-scale preparation of plasmid DNA (maxiprep)

The Qiagen HiSpeed Maxi Kit was used to prepare up to 500 µg of high-copy plasmid DNA. A single colony was used to inoculate 5 ml of L-agar containing 100 µg/ml ampicillin or 30 µg/ml kanamyacin and incubated for eight hours at 37°C with continuous shaking. Subsequently, 50 µl of the culture was transferred to 200 ml L-agar with the appropriate antibiotic and incubated overnight at 37°C with continuous shaking. The following day, the bacteria were harvested by centrifugation at 4300 *g*, at 4°C for 15 minutes. The final pellet was resuspended in 2.5 ml ice-cold sterile solution consisting of 20% v/v glycerol and 0.1 M $CaCl_2$. The cell suspension was aliquoted into 100 µl, snap frozen on dry ice and stored at -80°C. The pellet was then stored at -20°C for a 1 week maximum or processed using the Qiagen HiSpeed Plasmid Maxi Kit and according to manufacturer instructions.

2.2.10.3 Preparation of glycerol stocks

Bacterial transformants were grown in L-broth containing 100 µg/ml ampicillin or 30 µg/ml kanamyacin. A 300 µl aliquot was mixed with an equal volume of 40% v/v glycerol in L-agar autoclaved solution, snap frozen on dry ice and stored at -80°C.

2.2.11 Statistical analysis

Statisitcal analysis was performed on quantitative data categorized in two groups. Students *t*-test was applied and values were considered significant if $p < 0.05$.

2.2.12 Gene expression analysis using Affymetrix microarrays

Microarray analysis was employed to address the following question:

Which genes are regulated by the NOX4/$p22^{PHOX}$ complex in decidualizing HESCs?

Three independent primary HESC cultures were set up from biopsies obtained from three different patients. From each biopsy, passage 2 was plated in 4 6-well plates. Upon reaching 80% confluency, the cells were transfected with non-targeting siRNA or siRNA targeting NOX4/$p22^{PHOX}$. HESCs were treated two days post transfection with 8-br-cAMP and MPA for 72 hours. Total RNA was harvested using the STAT-60

reagent. RNA quality and integrity was checked using the Nanodrop and the Agilent 2100 Bioanalyzer respectively. The RNA was then cleaned up using the RNeasy MinElute Cleanup Kit. Subsequent sample manipulation and data analysis was outsourced to Almac Diagnostics. The methodologies employed are briefly described below.

2.2.12.1 Sample preparation and selection

RNA extraction was performed using the standard protocol mentioned above and stored at -80°C. To ensure that cultures responded adequately to treatment, aliquots were used for first-strand synthesis followed by RTQ-PCR to determine the transcript levels of both decidual markers *PRL* and *IGFBP1* as well as to determine the efficiency of *NOX4* and $p22^{PHOX}$ silencing on the mRNA level. All three samples used for the microarray analysis responded well to the decidual stimuli and showed efficient knockdown at the mRNA level.

2.2.12.2 RNA quality control

The purity of the total RNA was assessed using the Nanodrop, where the samples generated a 260/280 nm absorbance ration range of 2.02 – 2.07. The RNA integrity was inspected qualitatively with an Agilent 2100 bioanalyzer. All samples displayed distinct 18S/28S peaks indicative of non-fragmented RNA.

2.2.12.3 Laboratory methodologies employed by Almac Diagnostics

a. Eukaryotic target preparation

All eukaryotic target preparations using the project-appropriate NuGEN™ RNA Amplification System in combination with the FL-Ovation™ cDNA Biotin Module V2 were performed in accordance with the NuGEN™ protocol.

b. Amplification of total RNA

Total RNA was amplified using the NuGEN™ WT-Ovation™ Pico System. First-strand synthesis of cDNA was performed using a unique first-strand DNA/RNA chimeric primer mix, resulting in cDNA/mRNA hybrid molecules. Following fragmentation of the mRNA component of the cDNA/mRNA molecules, second-strand synthesis was performed and double-stranded cDNA was formed with a unique DNA/RNA heteroduplex at one end. In the final amplification step, RNA within the heteroduplex was degraded using RNaseH, and replication of the resultant

single-stranded cDNA was achieved through DNA/RNA chimeric primer binding and DNA polymerase enzymatic activity. The amplified single-stranded cDNA was purified for accurate quantitation of the cDNA and to ensure optimal performance during the fragmentation and labelling process. The single stranded cDNA was assessed using spectrophotometric methods in combination with the Agilent Bioanalyzer.

c. Exon Processing

The NuGEN WT-Ovation™ Exon Module is used to enable global gene expression analysis of RNA samples on Affymetrix GeneChip® Exon arrays. For this system, total RNA was amplified first with the WT-Ovation™ FFPE System, and then the Exon Module was used to generate sense-strand cDNA targets ready for fragmentation and labelling with NuGEN's FL-Ovation™ cDNA Biotin Module V2.

d. Fragmentation and labelling of amplified single-stranded cDNA

The appropriate amount of amplified single-stranded cDNA was fragmented and labeled using the FL-Ovation™ cDNA Biotin Module V2. The enzymatically and chemically fragmented product (50-100 nt) was labeled via the attachment of biotinylated nucleotides onto the 3'-end of the fragmented cDNA.

e. Hybridization, washing, staining and scanning of labeled cDNA

The resultant fragmented and labeled cDNA was added to the hybridization cocktail in accordance with the NuGEN™ guidelines for hybridization onto Affymetrix GeneChip® arrays. Following the hybridization for 16-18 hours at 45°C in an Affymetrix GeneChip® Hybridization Oven 640, the array was washed and stained on the GeneChip® Fluidics Station 450 using the appropriate fluidics script, before being inserted into the Affymetrix autoloader carousel and scanned using the GeneChip® Scanner 3000.

f. Quality control of the generated data

Following raw data generation and scan assessment, GeneChip® quality metric assessment and data integrity assessment was performed. The GeneChip® quality metrics allow for the evaluation of assay and hybridisation performance, whereas the data integrity assessment ensures the suitability of the data for analysis and that there are no underlying variables causing unexpected patterns in the data.

g. Data normalization, differential gene selection and data analysis

Raw data was normalized by applying the Robust Multichip Average (RMA) algorithm to generate the processed data. Differentially expressed transcripts were selected using a number of fold change and hypothesis testing filters. An ANOVA with post-hoc testing (Partek) was performed to generate the statistical p-values for the pairwise comparison. The data was first filtered on p-value and then on fold change.

Chapter 3: Results 1

NADPH oxidase-dependent ROS signalling is critical for initiating the decidual process

Introduction

Decidualization is critical for embryo implantation and placental formation. In humans, the signals that trigger this differentiation process are entirely maternal, and therefore decidualization of the stromal compartment is a spontaneous autonomous maternally driven process that occurs even in the absence of pregnancy. There is overwhelming evidence that initiation of the decidual process is dependent upon increased cellular cAMP levels and sustained activation of the PKA pathway (7). Progesterone, on the other hand, is not the primary trigger of the decidual process, but is essential to maintain and enhance the differentiated phenotype (69). Upon decidualization HESCs acquire a secretory phenotype, characterized by the expression of various marker genes such as *PRL* and *IGFBP1*.

Conventionally, ROS were known for their cytotoxic effects in biological systems, which manifest in damage to macromolecules such as DNA, proteins and lipids (62). More recently however, accumulating evidence has implicated redox signalling in a variety of physiological and cellular processes such as cell proliferation, differentiation and migration, apoptosis, angiogenesis and tissue repair (155, 156).

One of the main sources of ROS in non-phagocytic cells is the NADPH oxidase complex, a multi-component enzyme that transfers electron to molecular oxygen using NADPH as an electron donor to generate O_2^- by one-electron reduction reaction (207). The NADPH oxidase complex and the mechanisms by which it gets activated are more extensively studied in phagocytic than in non-phagocytic cells. The phagocytic NADPH complex comprises of two membrane associated proteins, gp91phox (NOX2) and $p22p^{PHOX}$, three cytosolic components, $p47^{PHOX}$, $p67^{PHOX}$ and $p40^{PHOX}$, in addition to the small GTPase molecule RAC1 (214). Homologues of the catalytic subunit NOX2 have been identified in non-phagocytic cells: NOX1, NOX3, NOX4, NOX5, DOUX1 and DOUX2. As alluded to previously in chapter 1, NADPH oxidase-produced ROS has been implicated in various cellular processes like proliferation, cell cycle regulation and differentiation (200, 201).

In this chapter, I look at the main source of endogenous ROS in HESCs. I also investigate the role of endogenous ROS signalling in initiating the decidual process. I further look at the mechanism by which ROS exert their signalling effects in decidualizing HESCs.

3.1 Measuring intracellular ROS in HESCs

ROS are difficult to measure due to their high reactivity and relative instability. As mentioned previously in chapter 1, current approaches for assessing the amount of endogenous ROS are all indirect. One of the most commonly applied method is based on the use of oxidant-sensing detector molecules that react with ROS and result in emission of light or fluorescence. DCFH-DA and DHR 123 are two examples of fluorescent oxidant-sensing detector molecules.

DCFH-DA is a colourless membrane permeable non-fluorescent probe. Once DCFH-DA permeates the cell membrane, it is subjected to deacetylation by intracellular estrases forming the now membrane-impermeable DCFH. Subsequent interaction with ROS oxidizes the non-fluorescent DCFH probe into the highly fluorescent product DCF. Therefore, the amount of fluorescent signals emitted is proportional to the concentration of ROS in the cell (62, 192). Fluorescence of DCF can be monitored using a fluorometer or microplate reader at excitation of λ = 485 nm and emission at λ = 535 nm.

DHR 123 is another cell-permeable fluorogenic probe that is used to detect ROS. Upon oxidization, DHR 123 is converted to the fluorescent compound Rhodamine 123. Unlike DCFH-DA, DHR 123 is not subjected to any biochemical reaction such as deacetylation. Therefore, DHR 123 does not require loading into the cell prior to measuring ROS and can be converted to Rhodamine 123 by interacting with O_2^- that is generated on the plasma membrane to be exteriorly released. Similar to DCF, fluorescence of Rhodamine 123 can be monitored using a fluorometer or microplate reader at excitation of λ = 500 nm and emission at λ = 536 nm.

To investigate the role of endogenous ROS in differentiation of HESCs, I first had to establish a reliable method of measuring endogenous ROS in our cell system. To do so, I compared the efficacy of DCFH-DA and DHR 123 in measuring the oxidative status of HESCs. Undifferentiated and decidualizing primary cultures were therefore loaded with DCFH-DA or DHR 123 for 25 minutes, pulsed with an increasing concentration of H_2O_2, and fluorescence was measured every 2 minutes over a 30-minute period using a fluorometric plate-reader. As shown in Figure 3.1, although both probes showed increased fluorescence in undifferentiated HESCs with higher

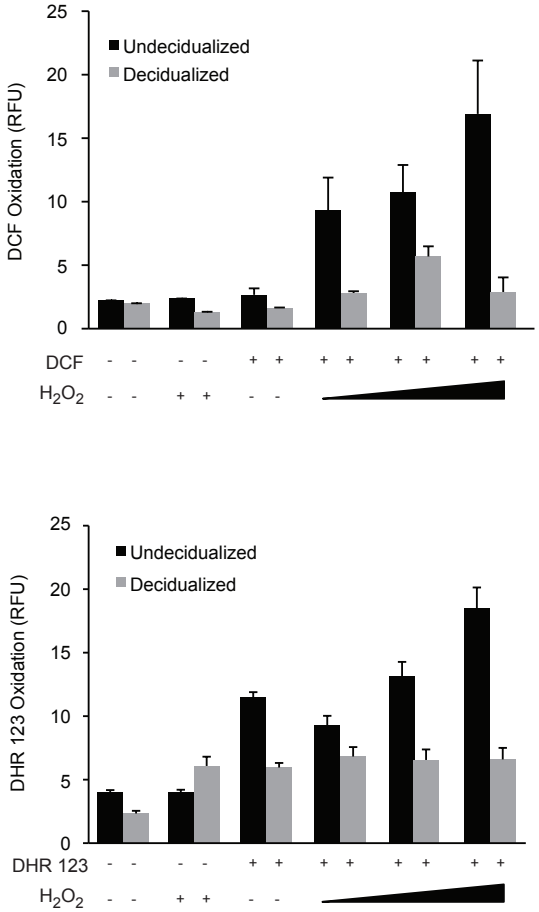


Fig 3.1 Comparing the efficacy of DCFH-DA and DHR 123 in measuring ROS in HESCs. Undifferentiated HESCs or decidualized with 8-br-cAMP and MPA for 72 hours were loaded with DHR123 or DCFH-DA for 25 minutes, washed twice with PBS and pulsed with an increasing concentration of H_2O_2 (250 μM, 500 μM and 1 mM). H_2O was used as a vehicle. The fluorescence was measured every 2 minutes over a 30-minute period using a fluorometric plate reader. Data are normalized to PI reading and represent the mean DCF or DHR 123 oxidation level (± SEM) at each interval. This experiment is a representative of three biological samples.

H_2O_2 concentrations, DCFH-DA yielded tighter fluorescent reading when cells were not stimulated with H_2O_2. Interestingly, with both fluorescent probes, there was no increase in fluorescence when decidualizing HESCs were stimulated with increasing concentrations of H_2O_2, which may point to the high resistance of decidualizing HESCs to oxidative stress.

Based on these observations, I decided to use the detector probe DCFH-DA for detecting endogenous ROS in HESCs. There were a number of additional considerations for favouring the DCFH-DA as an oxidant-sensing molecule over DHR123. First, it has been claimed that in some cell systems, DHR 123 is less sensitive to O_2^- and is oxidized to the fluorescent product Rhodamine 123 mainly by H_2O_2 (189, 190, 269). Moreover, the conversion of DHR 123 to Rhodamine 123 is a slow reaction unless catalyzed by peroxidase (190). It has also been reported that DHR 123 is not a suitable probe for distinguishing between intracellular and extracellular ROS (190). This may be attributed to what I mentioned before about DHR 123 not being subjected to any biochemical modification and therefore it can be converted to the fluorescent product Rhodamine 123 without diffusing into the cell. DCFH-DA on the other hand is sensitive to H_2O_2 as well as O_2^-, and is also specific to intracellular ROS, as the cleavage by esterases traps the fluorescent probe within the cell rendering it inaccessible to H_2O_2 or O_2^- generated at the plasma membrane to be released exteriorly (62, 190, 192).

3.2 Modulation of the NADPH oxidase activity in HESCs by apocynin and DPI

The activity of the NADPH oxidase complex can be modulated using chemical inhibitors or activators. DPI, for instance, is the most commonly used inhibitor of the NADPH oxidase complex. DPI works by removing an electron from an electron donor and forming a radical, which in turn would inhibit the activity of the respective electron donor through a covalent interaction (147). The mechanism of action of DPI forms the basis of its major limitation, rendering it a nonspecific inhibitor of various electron transporters such as NOS and XO.

Apocynin effects, on the other hand, are cell-type specific. For example, apocynin acts as an inhibitor of the NADPH oxidase complex in phagocytes such as neutrophils and macrophages but stimulates ROS production in other non-phagocytic cells, including vascular fibroblasts (147, 231, 233).

To determine whether apocynin acts as an activator or inhibitor of the NADPH oxidase complex in HESCs, undifferentiated primary cultures were loaded with DCFH-DA for 25 minutes, then pulsed with apocynin, DPI or DMSO as a vehicle, and ROS measurement were taken every 2 minutes over a 30-minute period. As shown in Figure 3.2, apocynin strongly induced intracellular ROS production in undifferentiated HESCs, whereas DPI had no discernible effects. These observations suggest two things: first, HESCs contain functional NADPH oxidase complexes and the activity of which can be stimulated by apocyinin; second, basal NADPH oxidase-dependent ROS production appears low in undifferentiated HESCs cells.

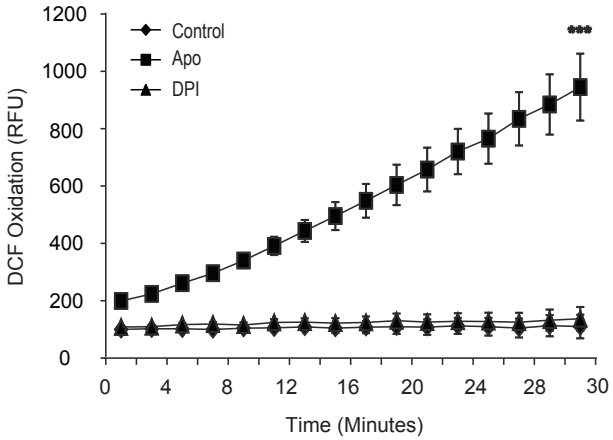


Fig 3.2 Apocynin activates the NADPH oxidase complex in HESCs. Undifferentiated primary HESCs were loaded with DCFH-DA for 25 minutes and then pulsed with apocynin (Apo) or DPI. DCF fluorescence was measured every 2 minutes over a 30-minute period. The data represent the mean DCF oxidation level of sextuplicate determinations (± SEM) at each interval. N = 3, ***, $P < 0.001$.

3.3 NADPH oxidase-dependent ROS play a role in HESC differentiation

Once I established that the NADPH oxidase complex can be activated in HESCs using the chemical apocynin; and based on the well-established inhibitory effects of DPI (185, 191), I had identified the tools to examine if NADPH oxidase-dependent ROS signalling plays a role in decidualization.

As mentioned previously, there is a plethora of evidence suggesting that initiation of the decidual process is dependent upon increased cellular cAMP levels and sustained activation of the PKA pathway (7, 73, 74). Progesterone on the other hand, is essential for maintaining and enhancing the decidual process (69, 70, 270). To study the role of the NADPH oxidase-dependent ROS signalling in decidualization, I first examined if endogenous ROS play a role in the early stages of the decidual process.

To test this hypothesis, primary cultures were treated with 8-br-cAMP for 24 hours, in the presence or absence of apocynin or DPI, total RNA was harvested and RTQ-PCR analysis was carried out to look at the transcript levels of the two decidual marker genes, *IGFBP1* and *PRL*. As shown in Figure 3.3, the synergistic effect of apocynin and 8-br-cAMP on the induction of both decidual marker genes was very striking. The transcript level of IGFBP1 and PRL was increased over 8000 fold and ~ 200 fold respectively, when cultures were treated with 8-br-cAMP in the presence of apocynin. DPI on the other hand exerted an inhibitory effect on the induction of PRL and IGFBP1 transcript levels.

As mentioned previously, a major limitation of using DPI as an inhibitor of the NADPH oxidase complex is its lack of specificity to the complex. However, this limitation can be circumvented by using specific inhibitors to other sources of ROS in the cell, such as NOS and XO. Specific inhibitors for NOS and XO exist. Therefore, to determine the mechanism of the inhibitory effect of DPI on the decidual process and test whether the ROS involved in the differentiation of HESCs are NADPH oxidase-specific, HESCs were treated with 8-br-cAMP for 24 hours in the presence or absence of a XO inhibitor allopurinol, the NOS inhibitor L-NAME, an alternative NADPH oxidase inhibitor AEBSF and apocynin. As illustrated in Figure 3.4, allopurinol and L-Name failed to antagonize IGFBP1 and PRL expression, whereas

treatment with AEBSF, mimicked the effects of DPI, indicating that the production of ROS involved in decidualization is NADPH-specific.

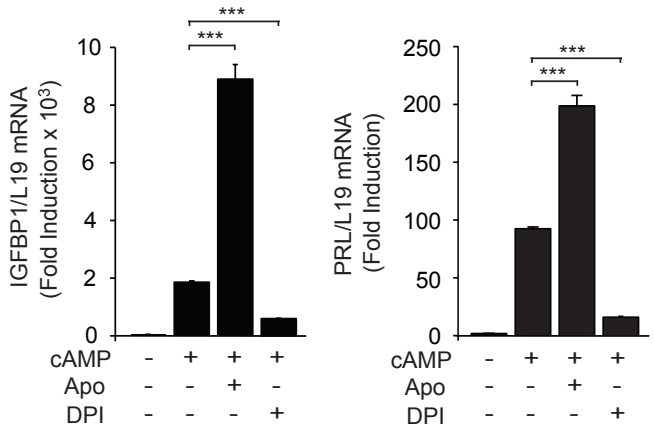


Fig 3.3 NADPH oxidase-dependent ROS play a critical role in the differentiation of HESCs into decidual cells. HESCs were maintained untreated or treated with 8-br-cAMP in the presence or absence of apocynin (Apo) or DPI for 24 hours. RTQ-PCR analysis was carried out for PRL and IGFBP1 mRNA levels normalized to L19 mRNA. Data are depicted as fold induction relative to transcript levels of untreated samples and represent means (± SD) of triplicate determinations from three different biological samples. ***, $P < 0.001$.

In view of the potent effects of apocynin on cAMP-dependent induction of PRL and IGFBP1 expression in HESCs, I tested if activation of the NADPH oxidase complex, either alone or in combination with MPA treatment, would be sufficient to trigger decidualization. To test this conjecture, primary cultures were treated with 8-br-cAMP or MPA in the presence or absence of apocynin or with apocynin alone. All the treatments were carried out for a period of 24 hours. Subsequently, RTQ-PCR was carried out to measure the transcript levels of PRL and IGFBP1. However, as shown in Figure 3.5, treatment with apocynin, alone or in combination with MPA, was insufficient to induce either IGFBP1 or PRL mRNA expression, indicating that the effect of endogenous ROS signalling on HESC differentiation is dependent on simultaneous activation of the cAMP pathway. I therefore concluded that treatment with apocynin does not sensitize the cells to progesterone signalling.

Although the activated NADPH oxidase generates O_2^- from molecular oxygen, this can be rapidly dismutated to H_2O_2 and both radicals have been implicated in cellular signal transduction. To further validate that endogenous ROS play a critical role in the initial decidual process, HESCs were transfected with a vector encoding catalase, a highly efficient enzyme that converts H_2O_2 to H_2O and O_2. Subsequently, total RNA was harvested and the transcript level of the decidual markers was measured using RTQ-PCR. Interestingly, overexpression of catalase also attenuated the cAMP-dependent induction of PRL and IGFBP1, as shown in Figure 3.6, providing further evidence that endogenous ROS signalling plays an integral role in initiating the decidual response.

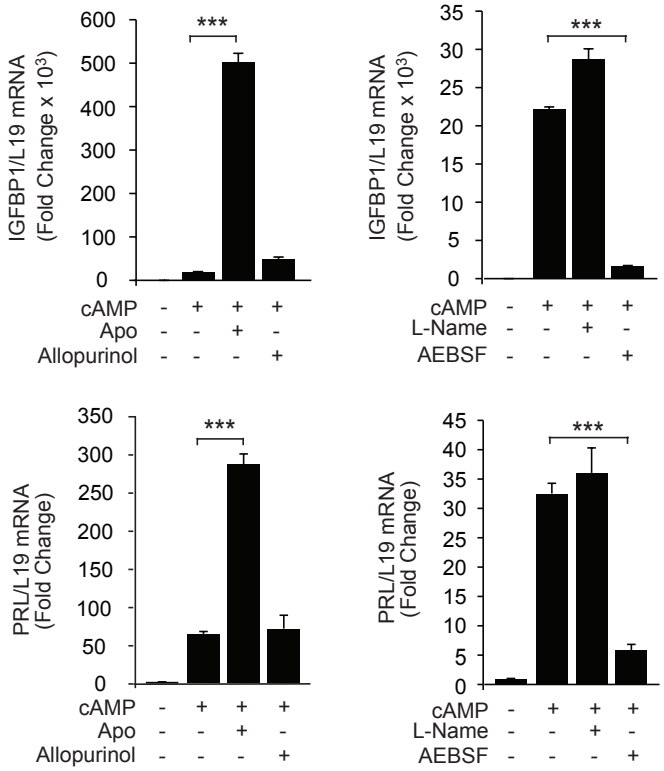


Fig 3.4 The NADPH oxidase complex is the main source of ROS involved in the decidual process. Primary HESCs were maintained untreated or treated with 8-br-cAMP in the presence or absence of apocynin (Apo), allopurinol, L-Name or AEBSF. RTQ-PCR analysis was carried out for PRL and IGFBP1 mRNA levels normalized to L19 mRNA. Data are depicted as fold induction relative to transcript levels of undifferentiated samples and represent means (± SD) of triplicate determinations from three different biological samples. ***, $P < 0.001$.

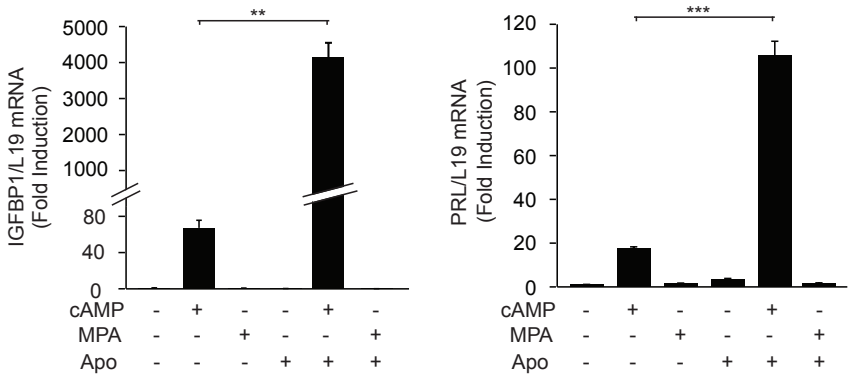


Fig 3.5 Effects of apocynin on decidualization. HESCs were either maintained untreated or treated with 8-br-cAMP or MPA in the presence or absence of apocynin (Apo), or with apocynin alone for 24 hours. Total RNA was harvested and RTQ-PCR analysis was carried out for IGFBP1 and PRL, normalized to L19 transcript levels. Data are depicted as fold induction relative to transcript levels of untreated samples and represent means (± SD) of triplicate determinations from three different biological samples. **, $P < 0.01$, ***, $P < 0.001$.

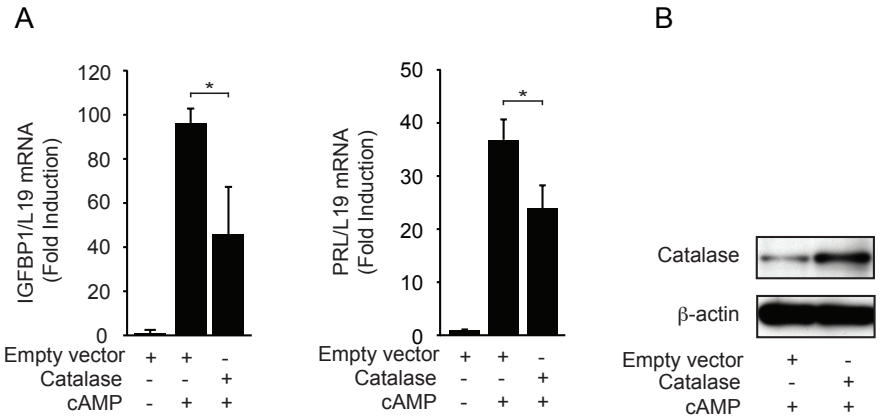


Fig 3.6 Overexpression of catalase attenuates the cAMP-dependent induction of IGFBP1 and PRL. A, Primary cultures were transfected with a catalase expression vector or empty vector. The cells were treated two days later with 8-br-cAMP for 24 hours. Total mRNA was harvested and PRL and IGFBP1 transcript levels were measured using RTQ-PCR analysis. Data are depicted as fold induction relative to transcript levels of undifferentiated samples and represent means (± SD) of triplicate determinations from three different biological samples. B, Western blot analysis on whole cell lysates was carried out to validate catalase overexpression. *, $P < 0.05$.

3.4 The kinetics of the NADPH oxidase-dependent ROS production.

Based on reporter assay studies investigating the kinetics of cAMP-dependent induction of the decidual PRL (dPRL) promoter activity, initiation of the decidual process has been described as a biphasic response characterized by an initial rapid but modest induction followed by a sharp rise in promoter activity apparent after 12 hours of stimulation (73). To shed light on the role of endogenous ROS signalling on the kinetics of this initial differentiation response, time-course studies were carried out in primary cultures treated with 8-br-cAMP alone or in combination with apocynin, and the transcript levels of both decidual markers PRL and IGFBP1 were measured using RTQ-PCR. As illustrated in Figure 3.7, *PRL* and *IGBP1* transcript levels rose by 8- and 48-fold, respectively, after 3 hours of 8-br-cAMP treatment and the levels remained relatively unchanged at 6 hours, before rising sharply after 12 hours of treatment. Intriguingly, cotreatment with apocynin somewhat attenuated the early response before markedly increasing PRL and IGFBP1 mRNA expression during the second phase of this initial cAMP response, starting approximately after 12 hours of stimulation.

This observation suggests that apocynin acts as an antagonist to cAMP signalling in the first phase of the biphasic response and switches to an agonist in the second phase enhancing the magnitude of cAMP-dependent induction of PRL and IGFBP1 transcript levels. I postulated that the temporal switching of apocynin from acting as an antagonist to an agonist might be a result of alteration in the oxidative status of the cell. To test this hypothesis, I set out to investigate the kinetics of changes in cellular ROS production upon initiation of the decidual process. Primary cultures were, therefore, treated with 8-br-cAMP for 3, 6, 12 and 24 hours, loaded with the oxidant-sensing fluorescent DCFH-DA probe and the fluorescent signal was measured and normalized to that of parallel untreated cultures. Interestingly, a triphasic response was observed in all primary cultures tested (n = 4) as illustrated in Figure 3.8A. This response was characterized by a modest increase in DCF fluorescence upon 3 hours of 8-br-cAMP treatment, followed by a gradual decline by 12 hours and a subsequent sharp increase between 12 and 24 hours of 8-br-cAMP stimulation. The decline in DCF fluorescence observed indicates that the level of ROS in 8-br-cAMP stimulated cells is below that of untreated cells. Therefore the sharp rise in DCF fluorescence elucidates a burst in cellular ROS between 12 and 24 hours of 8-br-cAMP stimulation. Interestingly, this burst in ROS coincided with the

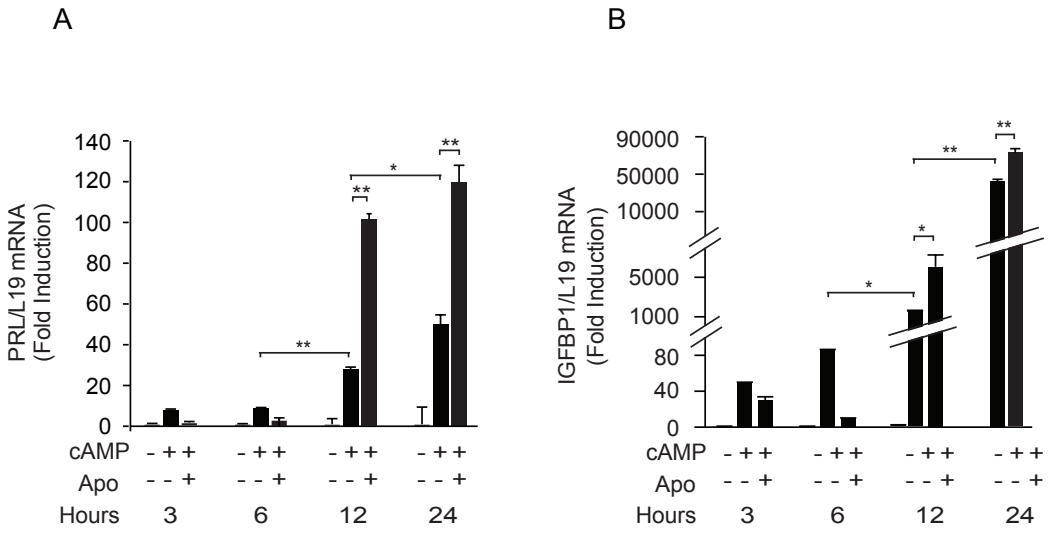


Fig 3.7 The kinetics of cAMP-dependent induction of PRL and IGFBP1 transcripts. Cultured HESCs were treated or left untreated with 8-br-cAMPin the presence or absence of apocynin (Apo) for 3, 6, 12 and 24 hours. Total RNA was harvested and RTQ-PCR was carried out to measure PRL (A) and IGFBP1 (B) mRNA expression. Transcript levels were normalized to L19 mRNA. Data are depicted as fold induction relative to transcript levels of untreated samples and represent means (± SD) of triplicate determinations from three different biological samples. *, $P < 0.01$; **, $P < 0.001$.

induction of the transcript levels of both decidual marker genes *PRL* and *IGFBP1* in response to 8-br-cAMP alone or in combination with apocynin.

To confirm that the burst in cellular ROS observed earlier is NADPH oxidase-dependent, primary cultures were treated with 8-br-cAMP alone or in the presence of the NADPH oxidase inhibitor DPI or the NADPH oxidase activator apocynin for 24 hours. Prior to terminating the treatments, the cultures were loaded with DCFH-DA for 25 minutes and the fluorescent signal was measured using a flow cytometer. The baseline represents the level of fluorescence of untreated cultures. As expected, 8-br-cAMP alone, induced cellular oxidation by 24 hours of stimulation and this response was further enhanced by cotreatment with apocynin, however, cotreatment with DPI abolished the induction of ROS (Fig 3.8B). This finding further confirmed that the burst in ROS observed between 12 and 24 hours of 8-br-cAMP treatment is NADPH oxidase dependent.

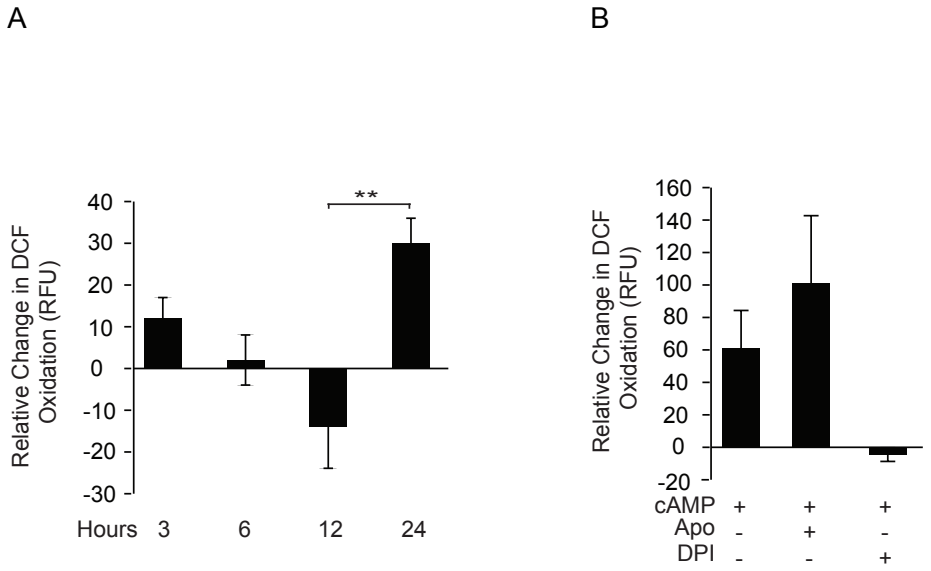


Fig 3.8 Kinetics of cAMP-dependent ROS production in decidualizing HESCs. A, Primary cultures were treated or left untreated with 8-br-cAMP for 3, 6, 12 and 24 hours. Cultures were loaded with DCFH-DA for 25 minutes prior to terminating the treatments. DCF fluorescence was measured every 2 minutes over a 30-minute period using a fluorometer. Data are depicted as the difference in ROS production between 8-br-cAMP treated and untreated cultures and represent means (± SEM) of sextuplicate determinations from four different biological samples. B, HESCs from three different biological samples were untreated or treated with 8-br-cAMP for 24 hours then pulsed with apocynin (Apo) or DPI for 30 minutes. Subsequently, the cells were loaded with DCHF-DA for 25 minutes and DCF fluorescence was measured using flow cytometry. **, $P < 0.001$.

3.5 Characterization of the NADPH oxidase complex in HESCs

The catalytic component of the NADPH oxidase complex is the NOX subunit. As mentioned in chapter 1, there are four homologues to NOX2, the prototypic NOX catalytic subunit of the NADPH oxidase complex, excluding DUOX1 and DUOX2 (147). As illustrated in Figure 1.8, each catalytic subunit requires different regulatory proteins. Further, more than one NOX homologue can be expressed in one cell type (147, 221).

To further elucidate the role and mechanism of NADPH oxidase-dependent ROS signalling in HESCs, it was important to determine the NOX homologue that is most critical in the decidual process. Previous microarray analysis carried out in our laboratory comparing gene networks in undifferentiated and decidualizing HESCs, identified three different NOX homologues in HESCs: NOX1, NOX4 and NOX5 and the NOX cofactor $p22^{PHOX}$ (Fig 3.9) (18). This makes the other two NOXs, NOX2 and NOX3, unlikely to be critical for mounting the decidual response.

RAC GTPases are known to activate the catalytic subunits NOX1, NOX2 and to a lesser extent NOX3 (147). Moreover, RAC1 is expressed in HESCs where it plays a critical role in regulating embryo implantation (271). A process of elimination was utilized to determine if NOX1, NOX2 and NOX3 are critical for the initiation of HESCs decidualization. To this end, I first examined RAC1 expression by Western blot analysis using whole cell lysates from primary cultures left untreated or treated with 8-br-cAMP for 24 hours. As shown in Figure 3.10A, RAC1 levels were comparable in undifferentiating cultures with those treated with 8-br-cAMP for 6, 8, 10, 16 and 24 hours. Next, primary cultures were first transfected with NT siRNA or siRNA targeting RAC1. Two days post transfection, cultures were treated with 8-br-cAMP for the various time points. Western blot and RTQ-PCR analysis were carried out to validate the efficiency of the knockdown. As illustrated in figure 3.10B, the efficiency of RAC1 knockdown was high at the mRNA and protein level (B), yet there was no attenuation of the induction of PRL and IGFBP1 mRNA expression in response to 8-br-cAMP stimulation (C). This indicates that the decidual process at least in the first 24 hours is not RAC1-dependent, and therefore it is highly unlikely that NOX1, NOX2 and NOX3 are the primary source of ROS production in decidualizing HESCs.

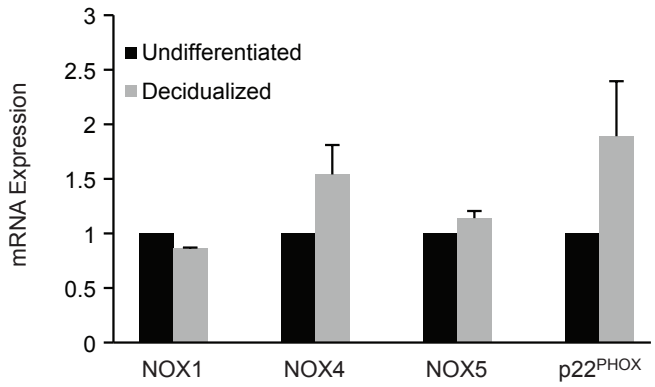


Fig 3.9 The NADPH oxidase profile in HESCs. Primary cultures were left untreated or stimulated with 8-br-cAMP and MPA for 72 hours and subjected to microarray analysis. Data represents components of the NADPH oxidase complex that were identified by the array and represent means (± SD) of triplicate determinations from three different biological samples. (Disclaimer: This experiment has been carried out by previous members of the laboratory (18), however, the mining of the data was carried out by myself).

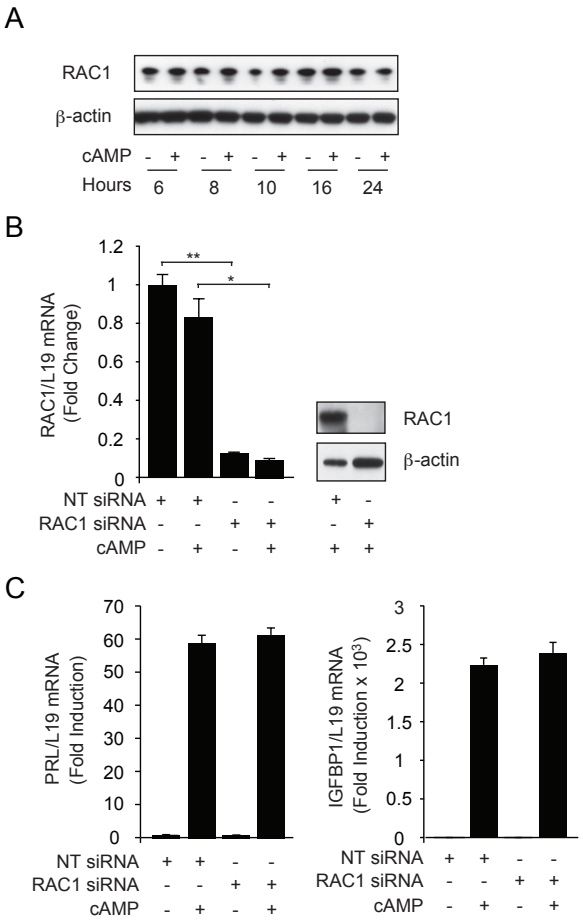


Fig 3.10 RAC1 is not required for the induction of the decidual markers. A, Cultured HESCs were untreated or treated with 8-br-cAMP for 6, 8, 10, 16 and 24 hours. Whole cell lysates were extracted and blotted for RAC1 expression. β-actin served as a loading control. B, The Left panel shows RTQ-PCR analysis of RAC1 transcript levels, normalized to L19 mRNA, in cells transfected with NT or RAC1 siRNAs and treated 2 days later with 8-br-cAMP for 24 hours. Data are depicted as fold change relative to transcript levels of undifferentiated samples and represent means (± SD) of triplicate determinations from three different biological samples. The right panel shows Western blot analysis of RAC1 expression in protein lysates from parallel cultures. β-actin served as a loading control. C, RTQ-PCR analysis for PRL and IGFBP1 levels, normalized to L19 mRNA, upon RAC1 silencing. The results are fold change relative to transcript levels of undifferentiated samples transfected with NT siRNA and represent means (± SD) of triplicate determinations from three different biological samples. *, $P < 0.01$; **, $P < 0.001$.

Having eliminated NOX1, NOX2 and NOX3 indirectly, I focused on the remaining NOX4 and NOX5. As mentioned earlier, NOX4 is $p22^{PHOX}$ dependent, whereas NOX5 does not require any coregulatory proteins, since its mechanism of action is Ca^{2+}-dependent (203, 207). $p22^{PHOX}$ is ubiquitously expressed in different cell types and forms a heterodimer with NOX1 - 4. The formation of the heterodimer is critical for the activity and stability of the NOX complex. In addition to NOX5, DOUX1 and 2 are also $p22^{PHOX}$-independent in their stability and activity (147, 207, 214).

Manual mining of existing genome-wide gene expression profiling of HESCs treated with 8-br-cAMP and MPA for 72 hours, revealed that $p22^{PHOX}$ was significantly upregulated upon decidualization (Fig 3.9) (18). Moreover, NOX4 was the only upregulated NOX homologue at the transcript level in decidualizing HESCs (Fig 3.9)

These observations, in addition to the fact that NOX5 transcript level is not significantly upregulated in decidualizing HESCs (Fig 3.9), led us to postulate that NOX4 is the most critical catalytic subunit of the NADPH oxidase complex. Consequently, I focused on examining the role of NOX4 and its regulatory component $p22^{PHOX}$ in decidualizing HESCs.

To test whether the hypothesis that NOX4 and $p22^{PHOX}$ are required for the initiation of the decidual process, I first set out to examine the expression of $p22^{PHOX}$ and NOX4 at the protein level in a short time course study. HESCs cells were treated with 8-br-cAMP for 6, 8, 10, 16 and 24 hours, whole cell lysates were collected and blotted for NOX4 and $p22^{PHOX}$. Interestingly, as shown in Figure 3.11, $p22^{PHOX}$ expression at the protein level increased when cells were treated for 16 hours or longer with 8-br-cAMP. NOX4 protein expression, on the other hand, did not appear to change over this time course. However, this observation was not enough to rule out the involvement of NOX4 in the decidual process as an increase in $p22^{PHOX}$ protein expression might enhance NOX4 activity. Therefore, to determine if NOX4 and $p22^{PHOX}$ are critical for the decidual process, siRNA-mediated knockdown of those two subunits was carried out independently in HESCs. As shown in Figure 3.12, the knockdown of both NOX4 and $p22^{PHOX}$ was sufficient to attenuate the induction of PRL and IGFBP1 transcripts in cultures treated with 8-br-cAMP for 24 hours. In fact, siRNA-mediated knockdown of $p22^{PHOX}$ resulted in a reduction of cAMP-dependent induction of PRL and IGFBP1 transcripts by 38 and 62%, respectively. Similarly, NOX4 knockdown was as effective as $p22^{PHOX}$ silencing in attenuating the induction of decidual PRL and IGFBP1 transcripts.

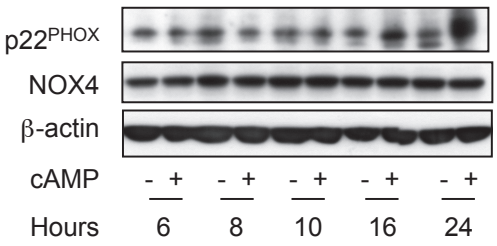


Fig 3.11 p22^{PHOX} and NOX4 protein expression in HESCs. Cultured HESCs were left untreated or treated with 8-br-cAMP for 6, 8, 10, 16 and 24 hours. Whole cell lysates were extracted and blotted for p22^{PHOX} and NOX4 expression. β-actin served as a loading control.

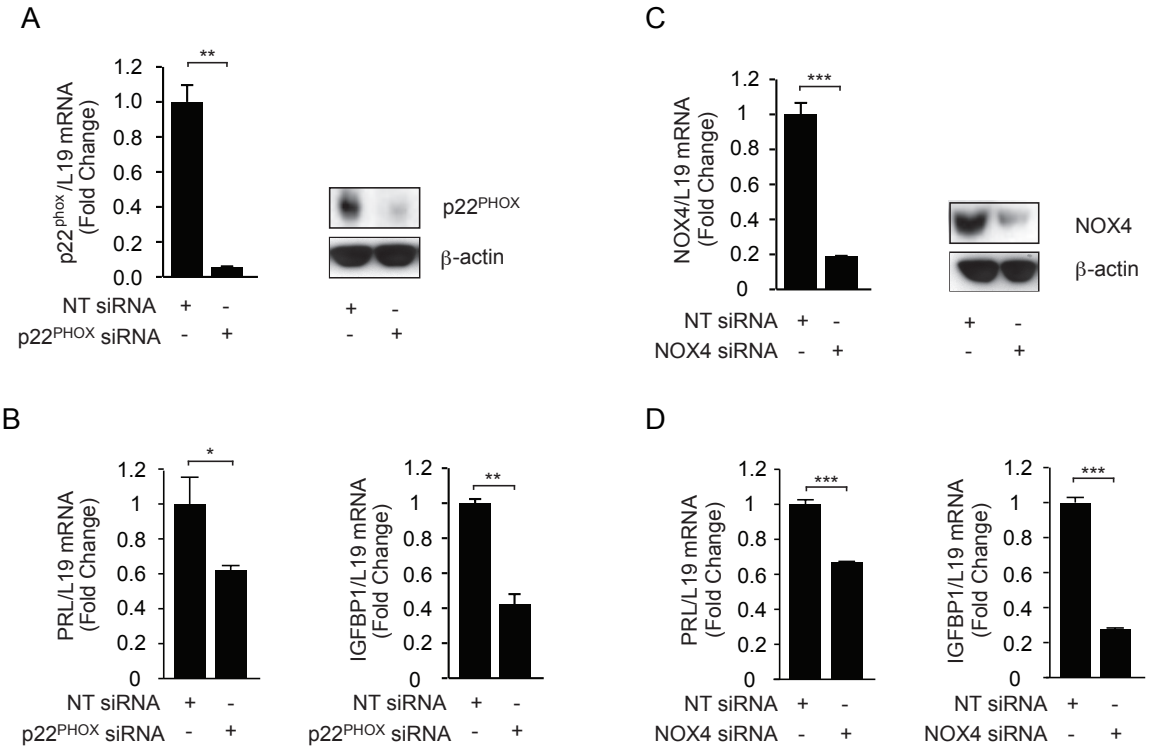


Fig 3.12 Knockdown of NOX4 and p22^{PHOX} attenuates the cAMP-dependent induction of *PRL* and *IGFBP1*. A, Validation of p22^{PHOX} knockdown at mRNA (left) and protein level (right) in HESCs transfected with NT or p22^{PHOX} siRNA. B, RTQ-PCR analysis for both PRL and IGFBP1 levels, normalized to L19 mRNA upon p22^{PHOX} silencing. C, Validation of NOX4 knockdown at mRNA (left) and protein level (right) in HESCs transfected with NT or NOX4 siRNA. D, RTQ-PCR analysis for both PRL and IGFBP1 levels, normalized to L19 mRNA upon NOX4 silencing. Data in B and D are depicted as fold change relative to transcript levels of samples transfected with NT siRNA and represent means (± SD) of triplicate determinations from three different biological samples. *, $P < 0.05$; **, $P < 0.01$; ***, $P < 0.001$.

To further implicate the involvement of NOX4/p22^{PHOX} complex in the production of ROS in decidualizing HESCs, I set out to determine if NOX4/p22^{PHOX} activation underpins the burst in ROS observed in HESCs treated with 8-br-cAMP for longer than 12 hours. To this end, primary cultures were transfected with either NT siRNA or siRNA targeting NOX4 and p22^{PHOX}, and two days later, cultures were left untreated or treated with 8-br-cAMP for 24 hours. Prior to terminating the treatments by 25 minutes, cultures were loaded with the oxidant-sensing DCFH-DA probe, and fluorescence was measured every 2 minutes over a 30-minute period. As illustrated in Figure 3.13, siRNA-mediated knockdown of NOX4 and p22^{PHOX} abolished the burst in ROS previously observed in HESCs treated with 8-br-cAMP for 24 hours, indicating that the NOX4/p22^{PHOX} complex is a primary source of ROS involved in decidualization.

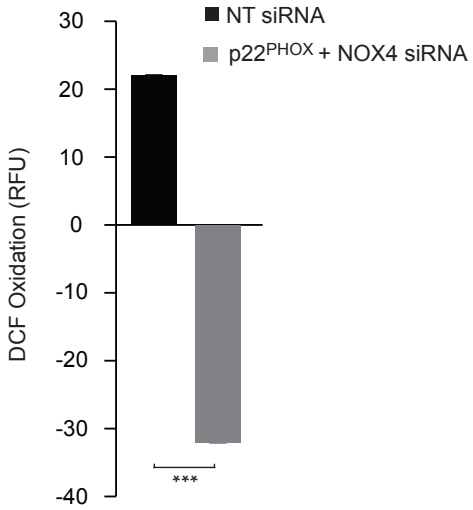


Fig 3.13 The NOX4/p22^{PHOX} complex underpins the burst in ROS observed in HESCs. Primary cultures were transfected with NT siRNA or siRNA targeting p22^{PHOX} and NOX4 and treated two days later with 8-br-cAMP for 24 hours. The cells were then loaded with DCFH-DA for 25 minutes and DCF fluorescence was measured over a 30-minute period. Data are depicted as the difference in ROS production between 8-br-cAMP treated and untreated cultures and represent means (± SEM) of sextuplicate determinations from three different biological samples. ***, $P < 0.001$.

3.6 NADPH oxidase-dependent ROS signalling in HESCs

Amongst the transcription factors and kinases implicated in decidual transformation of HESCs, there are some known to be either redox-sensitive or interact with the NADPH oxidase complex in other cell systems. This category of transcription factors and kinases include FOXO1, STAT5, C/EBPβ and SRC kinase (18, 125, 136, 272). I speculated that changes in the redox state of HESCs due to activation or inhibition of the NADPH oxidase complex might alter the activity or expression of some key signalling intermediates or transcription factors implicated in mounting the decidual response, leading to changes in their cellular localization. To test this hypothesis, Western blot analysis on cytosolic and nuclear extracts derived from HESCs treated with 8-br-cAMP in the presence or absence of apocynin for 24 hours was carried out to examine the expression level and cellular localization of FOXO1, STAT5, C/EBPβ and SRC kinase. As shown in Figure 3.14, there was no change observed in the expression level in either the cytoplasmic or nuclear compartment of FOXO1, STAT5 and SRC kinase when HESCs were treated with 8-br-cAMP alone or in the presence of apocynin. Notably, activation of these signal intermediates in response to decidual stimuli tended to be a delayed response, apparent only after 2 or more days of differentiation (7). C/EBPβ expression levels, on the other hand, were enriched when HESCs were treated with 8-br-cAMP for 24 hours, a response further enhanced by apocynin. Interestingly, unlike FOXO1, STAT5 and SRC, C/EBPβ is induced in HESCs between 8 to 24 hours of 8-br-cAMP treatment (126).

Next, to validate the notion that endogenous ROS signalling in HESCs impacts on C/EBPβ DNA binding activity, electron mobility shift assay (EMSA) was carried out on nuclear extracts derived from HESCs treated with 8-br-cAMP alone or in combination with apocynin for 24 hours. As represented in Figure 3.15, compared to untreated cells, C/EBPβ binding activity is enriched with 8-br-cAMP treatment, a response further enhanced when samples were treated with 8-br-cAMP in the presence of apocynin.

To further substantiate that C/EBPβ DNA binding activity is specifically regulated by the NOX4/$p22^{PHOX}$ complex, I combined siRNA-mediated knockdown with EMSA. Thus, HESCs were transfected with siRNA targeting NOX4 and $p22^{PHOX}$ and two days post transfection, cells were treated with 8-br-cAMP for 24 hours. EMSA was

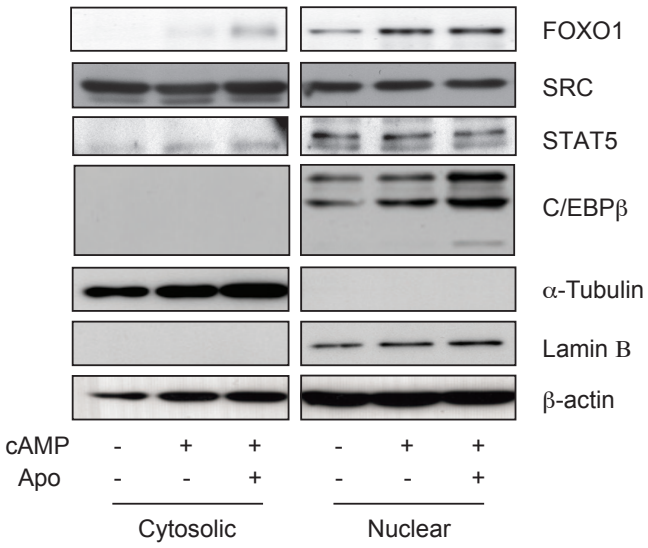


Fig 3.14 NADPH oxidase-dependent ROS enriches the 8-br-cAMP-dependent protein expression of C/EBPβ. Cultured HESCs were left untreated or treated for 24 hours with 8-br-cAMP in the presence or absence of apocynin (Apo). Cytosolic/nuclear extracts were prepared and blotted for SRC, STAT5, FOXO1 and C/EBPβ. The expression of Lamin B and α-Tubulin was assessed to confirm the integrity of the cell fractionation. As a loading control, samples were blotted for β-actin.

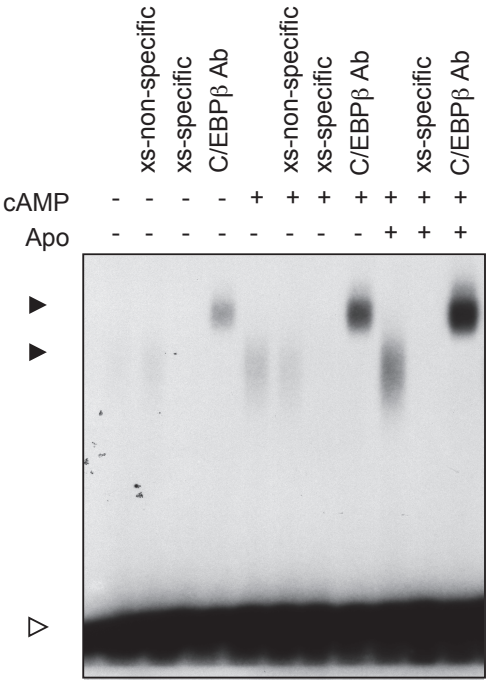


Fig 3.15 NADPH oxidase-dependent ROS enriches the 8-br-cAMP-dependent DNA binding activity of C/EBPβ in HESCs. HESCs were treated for 24 hours with 8-br-cAMP alone or in combination with apocynin (Apo) and DNA binding activity of C/EBPβ contained in the nuclear extracts was analyzed by EMSA. Nuclear lysates were incubated with excess of [^{32}P]-labeled C/EBP, OCT1 (xs-non-specific) and unlabeled C/EBP (xs-specific) oligonucleotides. Both OCT1 and unlabeled C/EBP oligonucleotides served as DNA binding competitors to verify binding specificity. For supershift analysis, nuclear extracts were incubated with an antibody against C/EBPβ prior to addition of the hot probe. Solid arrowhead indicate position of specific complexes, open arrowhead marks the position of uncomplexed DNA probe. (Disclaimer: The radioactivity work was handled by Dr. Yun Lee).

then carried out on nuclear extracts form the transfected cultures. As shown in Figure 3.16, silencing of the NOX4/p22^{PHOX} complex decreased the 8-br-cAMP-dependent enrichment of C/EBPβ DNA binding activity, the opposite of what was observed when the NADPH oxidase complex in HESCs was activated with apocynin.

To provide further evidence that NADPH oxidase-dependent ROS regulate the activity of C/EBPβ in HESCs, primary cultures were transfected with a luciferase reporter under the control of two cognate response elements. The cells were then treated with 8-br-cAMP and/or apocynin for 24 hours and the luciferase activity was measured. As illustrated in Figure 3.17, treatment with apocynin alone induced the C/EBP-dependent transcription to a similar degree to what is achieved with 8-br-cAMP treatment. Interestingly, the combined treatment of apocynin and 8-br-cAMP yielded a synergistic response.

Taken together, the result demonstrate that modulating the activity of the NADPH oxidase complex affects C/EBPβ expression levels as well as its DNA binding activity, indicating that C/EBPβ is a mediator of endogenous NOX4/p22^{PHOX}-produced ROS signalling in HESCs upon 8-br-cAMP treatment.

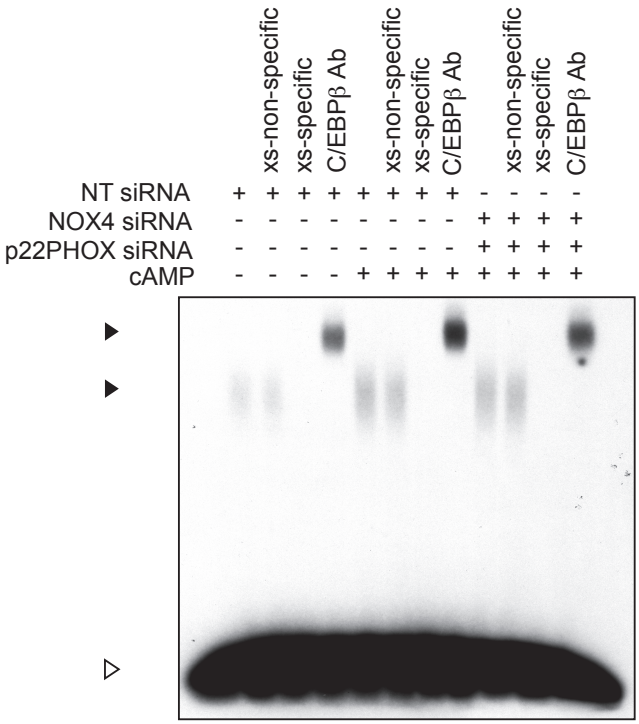


Fig 3.16 Knockdown of the NOX4/p22^{PHOX} complex attenuates the 8-br-cAMP-dependent enrichment of C/EBPβ DNA binding activity. Undifferentiated HESCs were transfected with NT siRNA or siRNA targeting p22^{PHOX} and NOX4 and treated two days later with 8-br-cAMP. DNA binding of C/EBPβ contained in nuclear extracts was analysed by EMSA. To verify DNA binding, bindng specificity and for supershift analysis, nuclear lysates were incubated with excess [^{32}P]-labeled C/EBP, OCT1 and unlabeled C/EBP oligonucleotides. For supershift analysis, nuclear extracts were incubated with an antibody against C/EBPβ prior to addition of the hot probe. Solid arrowhead indicate position of specific complexes, open arrowhead marks the position of uncomplexed DNA probe. (Disclaimer: The radioactivity work was handled by Dr. Yun Lee).

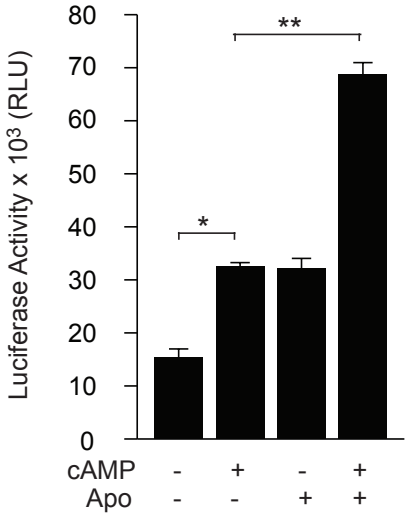


Fig 3.17 NADPH-oxidase ROS enhances C/EBPβ-dependent transcription in HESCs. Primary cultures were transfected with C/EBP-pGL4, pSG5-C/EBPβ and pCH110 (encoding for β-galactosidase). The cells were left untreated or treated with 8-br-cAMP in the presence or absence of apocynin (Apo) or with apocynin alone for 24 hours. Subsequently, firefly luciferase activity was measured (N = three different biological samples). * = $P < 0.05$, ** = $P < 0.01$.

Summary of results

Decidualization denotes the morphological and biochemical differentiation of HESCs into decidual cells. Decidualization is critical for a successful pregnancy since decidual cells play a critical role in embryo implantation. For instance, decidual cells control subsequent trophoblast invasion and placenta formation, regulate the recruitment of specialized immune cells, such as uNK cells to the feto-maternal interface, protect the early conceptus from environmental stress signals and more recently, it has been reported that decidual cells act as biosensors of embryo quality, capable of recognizing and responding selectively to developmentally compromised blastocysts (8, 18, 40).

Overwhelming evidence suggests that cAMP is the main stimulus for triggering the decidual process. It is well established that *in vivo*, the initiation of the decidual process coincides with enrichment in the levels of cAMP as a result of enhanced expression of local factors that activate adenylate cyclase in stromal cells such as relaxin, corticotrophin releasing hormone and PGE_2 (10, 79-85). Furthermore, increased *in vivo* levels of cAMP coincide with the downregulation of PDE4, the phosphodiesterase family member that converts cAMP back to AMP (83, 84).

In this chapter, I provide evidence that NADPH oxidase-produced ROS are required for the differentiation of HESCs into decidual cells. First, I show that activating the NADPH oxidase complex using a chemical activator apocynin, enhances the expression level of the decidual markers *PRL* and *IGFBP1*. Conversely, DPI, the NADPH oxidase inhibitor, attenuates the transcript levels of both decidual markers. Next, I validate that the endogenous ROS involved in initiating the decidual process are mainly NADPH oxidase-dependent. This was carried out by using inhibitors to other sources of endogenous ROS that exist in various cell systems such as NOS and XO. It is worth pointing out that activating the NADPH complex alone in HESCs is not sufficient to induce the transcript levels of PRL and IGFBP1, indicating that endogenous ROS have a synergistic effect with cAMP in triggering the decidual phenotype.

Most importantly, I show, by measuring the cellular oxidative status of HESCs treated with 8-br-cAMP for various time points, that there is a burst in ROS that occurs between 12 and 24 hours of treatment. Interestingly, this burst in ROS not only coincides with the induction of the transcript levels of PRL and IGFBP1, but also, with previously published studies about the timed activation of the dPRL promoter as well as with the activation of the transcription factor C/EBPβ (73, 126).

I then provide evidence that the decidual process, at least in the first 24 hours is not RAC1-dependent, therefore ruling out NOX1, NOX2 and NOX3 as the prime source of endogenous ROS involved in differentiation of HESCs. Further, from time course studies, I show that $p22^{PHOX}$ is induced upon decidualization or treating the cells with 8-br-cAMP for 16 hours or longer. Although NOX4 is not induced at this time point, it should not be ruled out as a source of endogenous ROS in HESCs. In fact, Edderkaoui et al (2011) recently reported that in pancreatic cancer cells, upregulation of $p22^{PHOX}$ increases NOX4/$p22^{PHOX}$ complex formation and subsequent activation of the oxidase (211). Therefore, my results point towards NOX4 being the most important NOX homologue in the decidual phenotype. I next confirmed this notion by carrying out siRNA-mediated knockdown of NOX4 and $p22^{PHOX}$, which in turn attenuated the transcript levels of PRL and IGFBP1.

Examination of the protein expression of redox-sensitive decidual-dependent transcription factors and kinases in cytosolic and nuclear extracts of HESCs treated with 8-br-cAMP for 24 hours showed that NADPH oxidase-dependent ROS increased the cAMP-dependent expression of the C/EBPβ. Furthermore, EMSA carried out on nuclear extracts of HESCs treated with 8-br-cAMP alone or in combination with apocynin showed that NADPH oxidase-dependent ROS increased the DNA binding activity of C/EBPβ. The same analysis carried out on nuclear extracts derived from HESCs with silenced NOX4/$p22^{PHOX}$ complex revealed that abolishing of the NADPH oxidase-dependent ROS reduces the DNA binding activity of C/EBPβ to basal levels.

Taken together, our data suggests that in addition to the decidual phenotype being cAMP-dependent in its initiation, endogenous ROS production primarily produced from the NADPH oxidase complex are indispensible for mounting the decidual phenotype.

Chapter 4: Results 2

Role of NADPH oxidase-produced ROS signalling in prolonged decidualization

Introduction

Various microarray studies have yielded insight into the extent and magnitude of the changes in the transcriptome that underpins the morphological and biochemical reprogramming associated with decidualization. It is now well established that decidualization denotes the sequential reprogramming of distinct but functionally related gene networks involved in cell cycle progression, extracellular matrix organization, cell adhesion, cytoskeletal organization, metabolism, signal transduction, differentiation and apoptosis (18).

Compared to undifferentiated HESCs, decidual cells acquire a remarkable resistance to oxidative cell death (35). This resistance upon decidualization is partly characterized by induction of various free radical scavengers, most notably SOD2, TXN and GPx3, and partly due to the downregulation of the proapoptotic gene FOXO3a (18). Furthermore, decidualization is associated with a global hyposumoylation, which plays a role in sensitizing HESCs to progesterone signalling by attenuating the ligand-dependent SUMO-modification of PR-A (70).

In the previous chapter, we have provided unequivocal evidence that endogenous NADPH oxidase-produced ROS signalling is critical for triggering the decidual response. We have also illustrated that in the initial stages of decidualization, NADPH oxidase-produced ROS exert their effects through affecting the protein expression levels and DNA binding activity of the transcription factor C/EBPβ.

In this chapter, we investigate the role of endogenous ROS signalling in mounting a prolonged decidual response. We also elucidate the gene networks that are sensitive to endogenous ROS signalling in decidualizing HESCs and delineate the effects of silencing the NOX4/$p22^{PHOX}$ complex on the decidual response.

4.1 The role of NADPH oxidase-dependent ROS in prolonged decidualization

I have previously shown that activation and expression of the NOX4/p22^{PHOX} complex is a cardinal step in the initiation of the decidual process in HESCs. However, whether perpetual activation of this complex is required for the maintenance of decidualization is yet unknown. To investigate this conjecture, I first carried out time course studies where primary cultures were either left untreated or treated with 8-br-cAMP and MPA for 1, 3 and 8 days, and looked at the expression of both NOX4 and p22^{PHOX} at the transcript level. As shown in figure 4.1, both NOX4 and p22^{PHOX} transcript levels were induced with the decidual stimuli and increased by 7 and 2.25 fold respectively, by day 8 (Fig 4.1A and B).

Similarly, primary cultures were treated with 8-br-cAMP and MPA for the same time-course, and Western blot analysis was carried out for NOX4 and p22^{PHOX} on whole cell lysates. As shown in figure 4.2, there was a remarkable increase in NOX4 and p22^{PHOX} protein levels throughout the time course.

The increased expression of NOX4 and p22^{PHOX} at the transcript and protein level reaffirmed our hypothesis that perpetual activation of the NOX4/p22^{PHOX} complex may be essential throughout the decidual process. Thus, I set out to determine if silencing of the NOX4/p22^{PHOX} complex would perturb the decidual phenotype beyond the 24-hour time point. As mentioned previously, progesterone is required for maintaining and enhancing the decidual process. Therefore, primary cultures were transfected with NT siRNA or siRNA targeting NOX4 and p22^{PHOX} and treated with 8-br-cAMP and MPA for 72 hours. Subsequently, total RNA was collected and the transcript levels of both decidual markers PRL and IGFBP1 were measured using RTQ-PCR. As shown in figure 4.3, knockdown of the NOX4/p22^{PHOX} complex was effective at the protein level and resulted in a marked decrease (> 60%) in the expression of both decidual marker genes. However, the perturbation in the induction of PRL and IGFBP1 observed here could be a consequence of the impaired initiation of the decidual process as, shown in chapter 3. Therefore, to investigate whether inhibiting the NOX4/p22^{PHOX} complex in the course of decidualization would impair further differentiation, I treated HESCs with 8-br-cAMP and MPA for 48 hours and

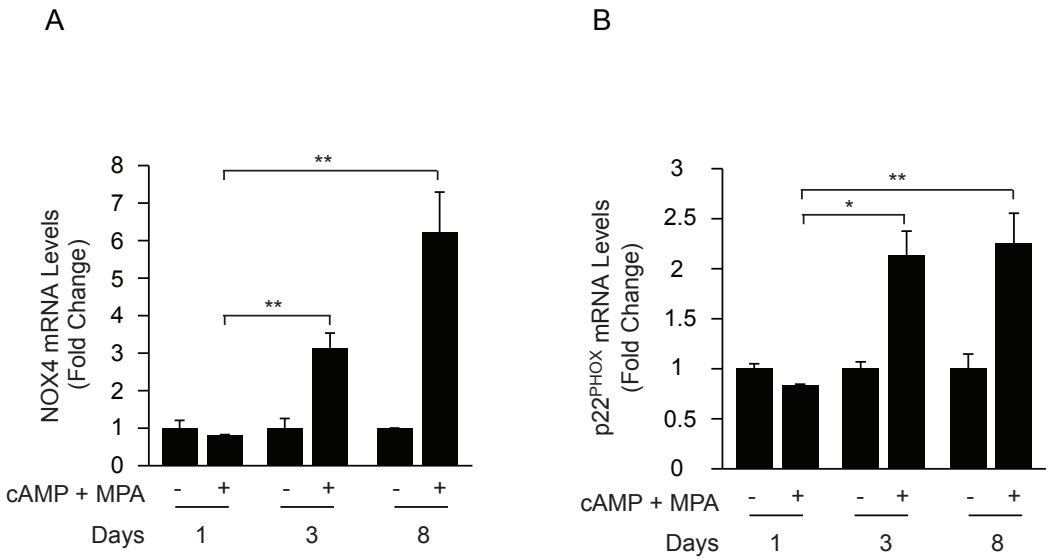


Fig 4.1 The NOX4/p22^{PHOX} complex is upregulated at the transcript level upon prolonged decidualization. A and B, Cultured HESCs were untreated or treated with 8-br-cAMP and MPA for 1, 3 and 8 days. Total RNA was harvested and RTQ-PCR analysis was carried out for NOX4 and p22^{PHOX}. Transcript levels were normalized to L19 mRNA. Data are depicted as fold induction relative to transcript levels of untreated samples and represent means (± SD) of triplicate determinations from three different biological samples. * = $P < 0.05$, ** = $P < 0.01$.

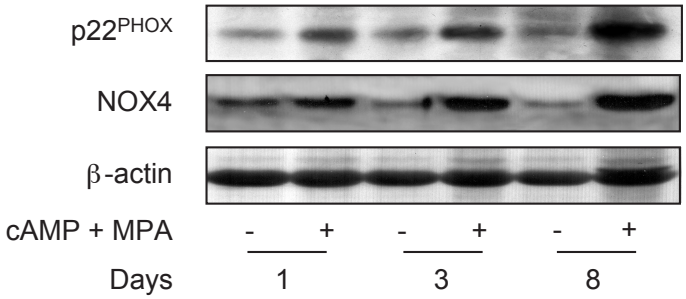


Fig 4.2 The NOX4/p22^{PHOX} complex is upregulated at the protein level upon prolonged decidualization. Cultured HESCs were untreated or treated with 8-br-cAMP and MPA for 1, 3 and 8 days. Whole-cell lysates were extracted and blotted for NOX4 and p22^{PHOX} expression. β-actin served as a loading control.

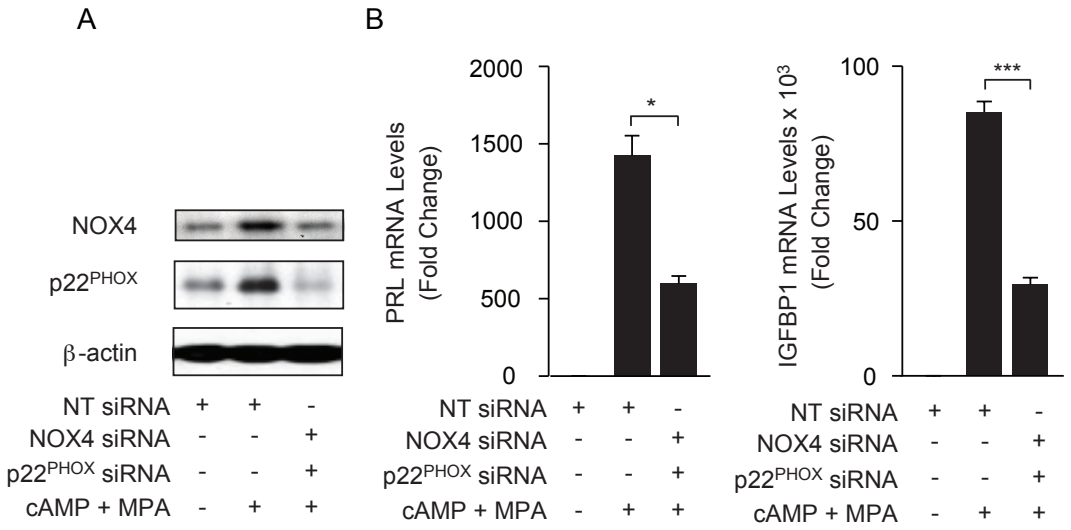


Fig 4.3 Silencing of the NOX4/p22^{PHOX} complex perturbs prolonged decidualization. A, Validation of the NOX4 and p22^{PHOX} knockdown at the protein level in HESCs transfected with NT or siRNA targeting NOX4 and p22^{PHOX} and maintained untreated or treated with 8-br-cAMP and MPA for 72 hours. B, RTQ-PCR analysis for both PRL (right) and IGFBP1 (left) levels, normalized to L19 mRNA upon NOX4/p22^{PHOX} silencing in HESCs. Data are depicted as fold induction relative to transcript levels of untreated samples transfected with NT siRNA and represent means (± SD) of triplicate determinations from three different biological samples. * = $P < 0.05$, *** = $P < 0.001$.

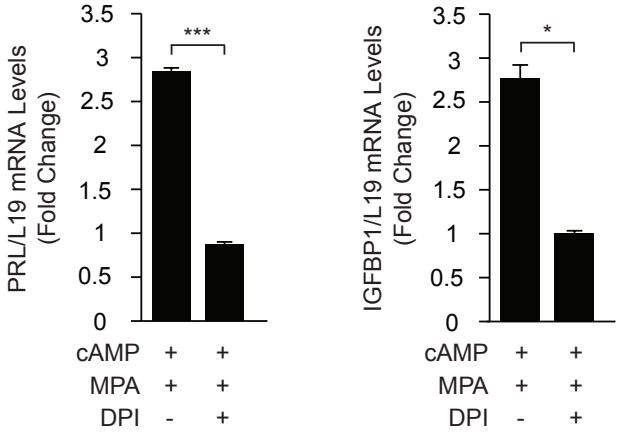


Fig 4.4 Perpetual endogenous ROS signalling is required for maintenance of the decidual process. Cultured HESCs were treated with 8-br-cAMP and MPA for 48 hours. Subsequently, cells were treated with 8-br-cAMP and MPA in the presence or absence of DPI for another 24 hours. RTQ-PCR analysis was carried out for PRL (right) and IGFBP1 (left) mRNA levels normalized to L19 mRNA. Data are depicted as normalized transcript levels to those of L19 and represent means (± SD) of triplicate determinations from three different biological samples. * = $P < 0.05$, *** = $P < 0.001$.

then refreshed the treatments in the presence or absence of the NADPH oxidase inhibitor, DPI. Total RNA was then harvested, and RTQ-PCR analysis was carried out for *PRL* and *IGFBP1*. As shown in figure 4.4, inhibition of the NOX4/p22^{PHOX} complex when the cells already express a decidual phenotype disrupts further differentiation, as exemplified by a marked reduction in *PRL* and *IGFBP1* expression. Interestingly, the level of inhibition was approximately 60%, a level comparable to the reduction attained by disabling the NADPH oxidase complex through siRNA-mediated knockdown prior to decidualizing the cells.

Taken together, I provide further evidence that activation of the NOX4/p22^{PHOX} complex and subsequent endogenous ROS signalling are critical factors for the maintenance of the decidual process.

4.2 Characterization of NOX4/p22^{PHOX}-dependent genes in decidualizing HESCs

To determine the genes that are regulated by the ROS-producing enzyme, I combined siRNA-mediated knockdown of the NOX4/p22^{PHOX} complex with microarray analysis. HESCs were either transfected with NT siRNA or siRNA targeting NOX4 and p22^{PHOX} and two days post-transfection treated with 8-br-cAMP and MPA for 72 hours. Total RNA was harvested and subjected to microarray analysis using the Affymetrix Gene 1.0 ST arrays (28,926 transcripts, Almac Diagnostics). The microarray analysis yielded 400 genes that were regulated in a NOX4/p22^{PHOX} manner (Cut off > 1.3 fold, Appendix 2 and 3). Interestingly, the majority of those genes (76%) were NOX4/p22^{PHOX} induced genes and therefore were downregulated upon the NOX4/p22^{PHOX} silencing. To elucidate the relationship between endogenous ROS signalling and decidualization, I mined and cross-referenced the NOX4/p22^{PHOX}-dependent gene list with genes known to be regulated in response to the decidual stimuli 8-br-cAMP and MPA (35). Out of the 400 NOX4/p22^{PHOX}-dependent genes, 29% were regulated upon decidualization. Interestingly, the direction of regulation of 90% of genes responsive to endogenous ROS was concordant with decidualization. For instance, 69% of the NOX4/p22^{PHOX}- and decidual-dependent genes are NOX4/p22^{PHOX} and decidual repressed genes (Fig 4.5). Similarly, 21% of the NOX4/p22^{PHOX}- and decidual-dependent genes are NOX4/p22^{PHOX} and decidual induced genes. Interestingly, cross referencing the microarray data with the data of Talbi et al (2006) revealed 30% of the NOX4/p22^{PHOX}-repressed genes were downregulated and 34% of NOX4/p22^{PHOX}-induced genes were upregulated in the secretory phase of the menstrual cycle. Therefore, the gene expression profile in response to endogenous ROS signalling appears to follow the pattern observed upon decidualization.

I used RTQ-PCR analysis to validate novel NOX4/p22^{PHOX}-dependent genes. Primary cultures were transfected with NT siRNA or siRNA targeting NOX4/p22^{PHOX} and treated with 8-br-cAMP and MPA for 72 hours. Total RNA was harvested and the mRNA expression levels of genes of interest were validated using RTQ-PCR. As shown in figure 4.6, *BIRC5*, a member of the inhibitor of apoptosis (IAP) gene family, *BRCA2*, a tumour suppressor gene involved in maintenance of gene stability, and *COLEC10*, a member of the C-lectin family, followed the regulation pattern yielded by the microarray.

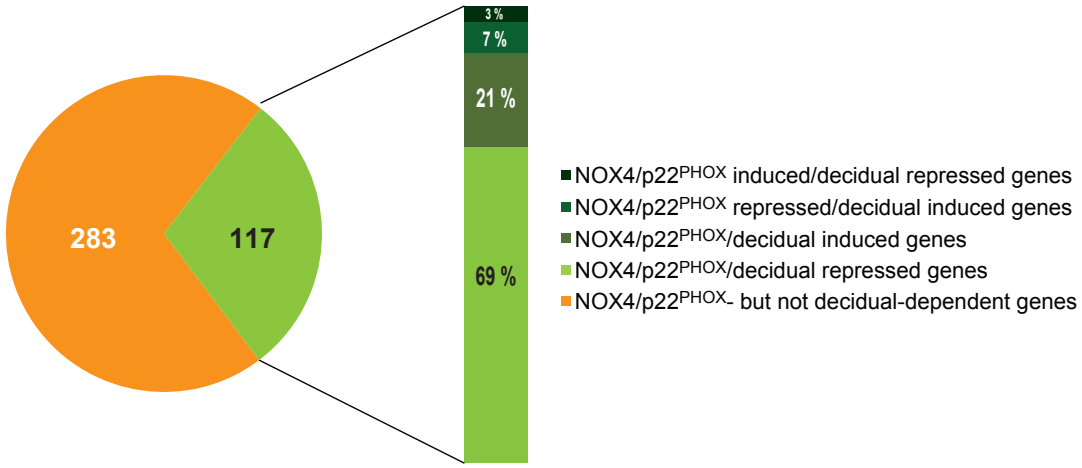


Fig 4.5 The regulation pattern of NOX4/p22^{PHOX} and decidual-dependent genes. HESCs were transfected with either NT siRNA or siRNA targeting NOX4 and p22^{PHOX}, treated with 8-br-cAMP and MPA for 72 hours and subjected to genome-wide expression profiling. The Pie of Bar chart represents the cross-referencing with known decidual-dependent genes yielded from previous microarray studies.

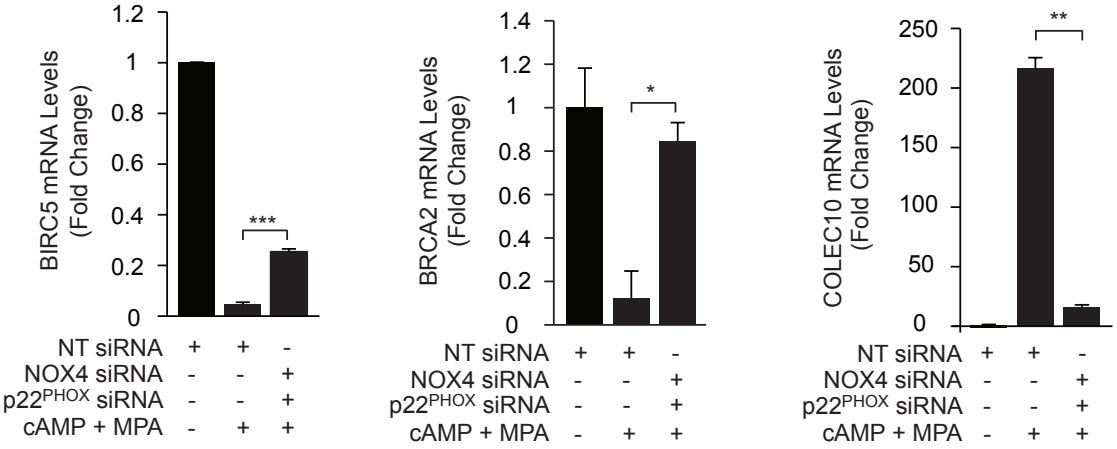


Fig 4.6 Validation of the NOX4/p22^{PHOX}-dependent gene expression. HESCs were transfected with NT siRNA or siRNA targeting NOX4 and p22^{PHOX}, two days post transfection cultures were maintained untreated or treated with 8-br-cAMP and MPA for 72 hours. RTQ-PCR analysis was carried out for BIRC5 (left), BRCA2 (middle) and COLEC10 (right) mRNA levels normalized to L19 mRNA. Data are depicted as fold induction relative to transcript levels of untreated samples and represent means (± SD) of triplicate determinations from three different biological samples. * = $P < 0.05$, ** = $P < 0.01$, *** = $P < 0.001$.

The NOX4/p22^{PHOX}-dependent genes were further annotated *in silico* using gene ontology and Ingenuity Pathways Analysis (IPA) (IPA; Ingenuity Systems, Redwood City, CA). This analysis revealed that NOX4/p22^{PHOX}-dependent genes are mainly involved in cell cycle progression, cellular assembly and organization, DNA replication, recombination and repair, signal transduction and cellular growth and proliferation (Table 1-3).

	Top 5 Associated Network Functions
1	Cell Cycle, Cancer, Skeletal and Muscular Disorders
2	Cell Cycle, Cellular Assembly and Organization, DNA Replication, Recombination, and Repair
3	Cell-To-Cell Signalling and Interaction, Cell Cycle, DNA Replication, Recombination, and Repair
4	Cellular Assembly and Organization, Cellular Growth and Proliferation, Haematological Disease
5	DNA Replication, Recombination, and Repair, Gene Expression, Cell Cycle

Table 4.1 The top five associated network functions resulted from the Ingenuity Pathways Analysis

	Top 5 Molecular and Cellular Function
1	Cell Cycle
2	Cellular Assembly and Organization
3	DNA Replication, Recombination, and Repair
4	Cellular Movement
5	Cellular Compromise

Table 4.2 The top five molecular and cellular functions resulted from the Ingenuity Pathways Analysis

	Top 5 Canonical Pathways
1	Mitotic Roles of Polo-Like Kinase
2	One Carbon Pool by Folate
3	Aryl Hydrocarbon Receptor Signalling
4	Role of BRCA1 in DNA Damage Response
5	Cell Cycle: G2/M DNA Damage Checkpoint Regulation

Table 4.3 The top five canonical pathways resulted from the Ingenuity Pathways Analysis

Tables 1 - 3 *In silico* analysis of the microarray data. The above three tables represent the top five Associated Network Functions, Molecular and Cellular Function and Canonical Pathways that resulted from the *in silico* analysis of the NOX4/p22^{PHOX}-dependent genes. Appendices 4 display the schematic diagrams of the top five Associated Network Functions.

4.3 Characterizing the interaction between the NOX4/p22^{PHOX} complex and FOXO1

Strikingly, the functional networks resulting from the *in silico* analysis of NOX4/p22^{PHOX}-dependent genes were similar to the functional networks previously shown to be under FOXO1 control in decidualizing HESCs (18). To further analyze the microarray, I mined and cross-referenced the gene list with FOXO1-dependent genes in decidualizing HESCs. I noticed that 59% of the NOX4/p22^{PHOX}- and decidual-dependent genes are known to be FOXO1-dependent (Fig 4.7). Surprisingly, none of the NOX4/p22^{PHOX}-dependent genes that are not decidual dependent cross-referenced with FOXO1-dependent genes.

Clearly, from the *in silico* analysis and the manual mining of the NOX4/p22^{PHOX}-dependent genes, there seem to be a strong interaction between FOXO1 and the NOX4/p22^{PHOX} complex in decidualizing HESCs. To investigate the interplay between the NOX4/p22^{PHOX} complex and FOXO1, I first set out to determine if silencing of the NOX4/p22^{PHOX} complex affects FOXO1 expression on the protein level. HESCs were therefore transfected with NT siRNA or siRNA targeting NOX4 and p22^{PHOX} and two days later treated with 8-br-cAMP and MPA for 72 hours. As shown in Figure 4.8A, Western blot analysis on whole cell lysate revealed that silencing of the NOX4/p22^{PHOX} complex does not perturb the induction of FOXO1 in decidualizing HESCs.

Next, I set out to examine if activating the NOX4/p22^{PHOX} complex regulates the DNA binding activity of FOXO1 in decidualizing HESCs. Thus, HESCs were transfected with a luciferase reporter under the control of 6 cognate DNA binding sites (DBS) (FOXO1-pGL4) and treated with 8-br-cAMP and/or apocynin for 24 hours. Subsequently, firefly luciferase was measured using a luminometer. As illustrated in Figure 4.8B, although statistically significant, cotreatment with apocynin only marginally enhanced the ability of FOXO1 to transactivate the 6x DBS, suggesting that NADPH oxidase-dependent ROS does not regulate the activity of FOXO1 in HESCs.

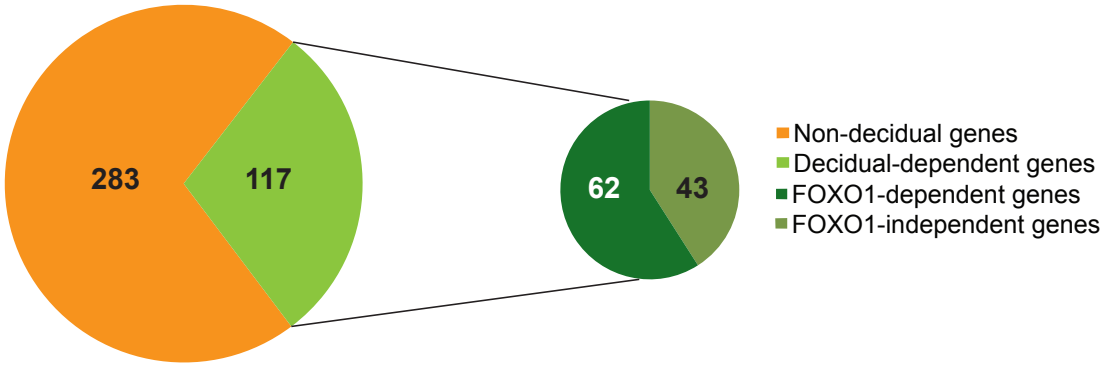


Fig 4.7 NOX4/p22^{PHOX}-dependent genes overlap with FOXO1-dependent genes. The Pie of Pie chart represents the *in silico* analysis and manual mining of the NOX4/p22^{PHOX}-dependent genes with known FOXO-1 dependent genes that resulted from previous microarray studies.

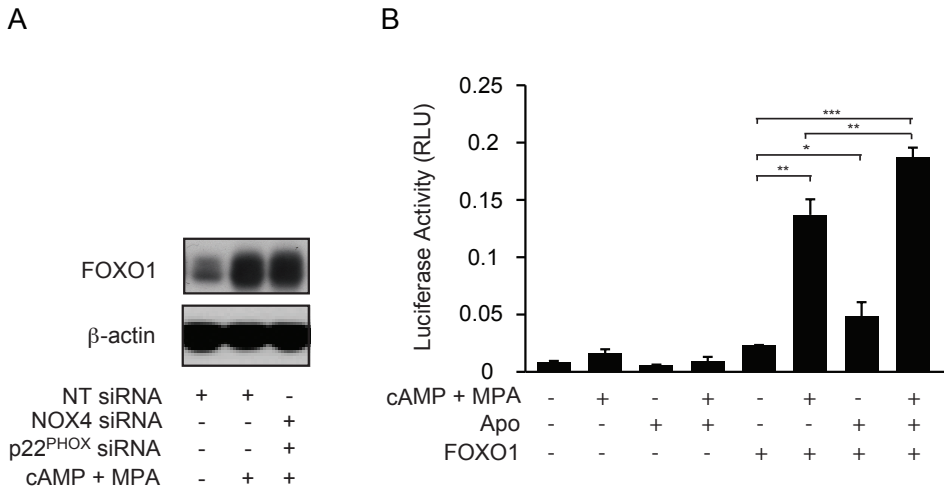


Fig 4.8 The NOX4/p22^{PHOX} complex is not upstream FOXO1. A, HESC cultures were transfected with NT siRNA or siRNA targeting NOX4 and p22^{PHOX} and two days post transfection, cells were maintained untreated or treated with 8-br-cAMP and MPA for 72 hours. Whole-cell lysates were extracted and blotted for FOXO1 expression. β-actin served as a loading control. B, Primary cultures were transfected with (FOXO1-pGL4, PSG5-FOXO1, and PCH110 (encoding for β-galactosidase). The cells were left untreated or treated with 8-br-cAMP and MPA and/or apocynin for 24 hours. Subsequently, firefly luciferase activity was measured. N = 3, * = P , 0.05, ** = P < 0.01, *** = P < 0.001.

Since our data so far indicate that the NOX4/p22^{PHOX} complex is not upstream FOXO1, I decided to investigate if FOXO1 was upstream the NOX4/p22^{PHOX} complex. To do so, I transfected HESCs with NT siRNA or FOXO1 siRNA and two days later treated the cells with 8-br-cAMP and MPA for 72 hours. Interestingly, as shown in Figure 4.9, silencing of FOXO1 in decidualizing HESCs inhibited the protein induction of both components of the NOX4/p22^{PHOX} complex.

To further validate that FOXO1 is upstream the NOX4/p22^{PHOX} complex, I examined transcript levels of selected NOX4/p22^{PHOX}-dependent genes upon siRNA-mediated knockdown of FOXO1 in HESCs decidualized for 72 hours. The NOX4/p22^{PHOX}-dependent genes *BIRC5* and *BRCA2* are known to be FOXO1-dependent, *COLEC10* on the other hand is not. Since FOXO1 is upstream the NOX4/p22^{PHOX} complex, I reasoned that the regulation pattern of BIRC5, BRCA2 and COLEC10 transcripts in FOXO1-depleted cultures would be similar to that observed upon NOX4/p22^{PHOX} knockdown. As expected, RTQ-PCR analysis confirmed that the pattern of regulation of these transcripts upon FOXO1 depletion resembles that in response to knockdown of NOX4/p22^{PHOX} in HESCs. (Fig 4.10).

Taken together, I have provided unequivocal data that the NOX4/p22^{PHOX} complex is downstream FOXO1, and does not negatively or positively feedback onto FOXO1.

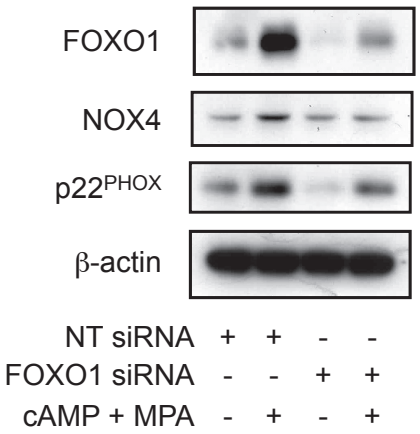


Fig 4.9 FOXO1 is upstream NOX4 and p22^{PHOX}. HESCs were transfected with NT or FOXO1 siRNA and two days post transfection, cells were maintained untreated or treated with 8-br-cAMP and MPA for 72 hours. Whole-cell lysates were extracted and blotted for FOXO1, NOX4 and p22^{PHOX} expression. β-Actin served as a loading control.

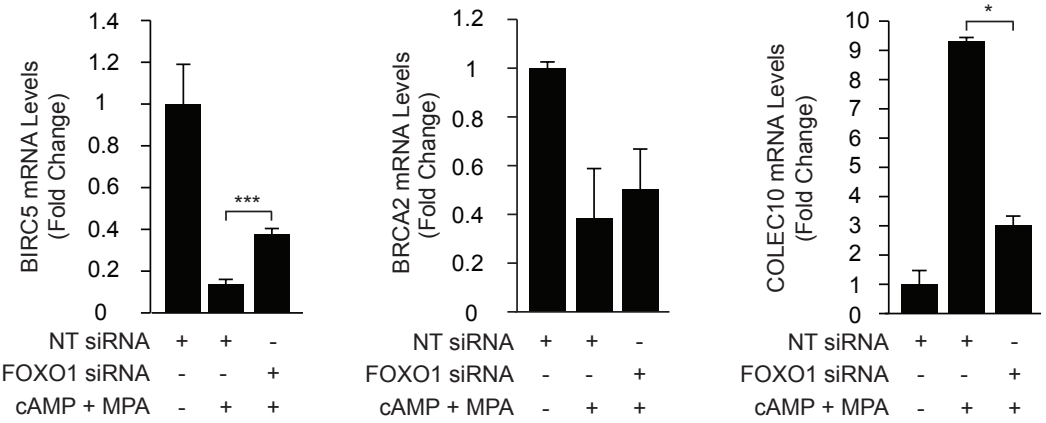


Fig 4.10 NOX4/p22^{PHOX}-dependent genes are regulated in a similar manner by FOXO1. HESCs were transfected with NT siRNA or FOXO1 siRNA, two days post transfection cultures were maintained untreated or treated with 8-br-cAMP and MPA for 72 hours. RTQ-PCR analysis was carried out for BIRC5 (left), BRCA2 (middle) and COLEC10 (right) mRNA levels normalized to L19 mRNA. Data are depicted as fold induction relative to transcript levels of untreated samples and represent means (± SD) of triplicate determinations from three different biological samples. * = $P < 0.05$, *** = $P < 0.001$.

4.4 The effects of NOX4/p22^{PHOX} knockdown in decidualizing HESCs

The *in silico* analysis of the microarray data indicated that NOX4/p22^{PHOX} knockdown perturbs gene networks involved in cell cycle regulation and genome stability. Four of the top five associated network functions implicated NOX4/p22^{PHOX}-dependent genes in cell cycle and/or genome stability. Further, the cell cycle and DNA replication, recombination and repair were in the top three molecular and cellular functions that were altered by NOX4/p22^{PHOX} knockdown in decidualizing HESCs as well as in the top five canonical pathways. I therefore hypothesized that NOX4/p22^{PHOX} silencing in HESCs might alter the activation status of the DNA damage and repair pathway. To investigate this conjecture, I monitored H2A.X phosphorylation by immunofluorescence in NOX4/p22^{PHOX}-knockeddown and decidualized HESCs. Phospho-H2A.X is a marker of checkpoint-mediated arrest of cell cycle progression and is required for efficient repair of DNA double strand breaks. As shown in Figure 4.11, confocal images of NOX4/p22^{PHOX}-silenced HESCs clearly show an enhanced level of p-H2A.X compared to cells transfected with NT siRNA, indicative of DNA repair activity.

The analysis of H2A.X phosphorylation, prompted a close examination of the DNA damage and repair pathway in decidualized HESCs upon disabling the NOX4/p22^{PHOX} complex. To this end, primary cultures were transfected with NT siRNA or siRNA targeting NOX4 and p22^{PHOX}, and two days post transfection, cultures were left untreated or treated with 8-br-cAMP and MPA for 3 and 8 days. Western blot analysis was carried out on whole cell lysates and blotted for p-ATM, p-ATR, p-CHK1, p-CHK2, p-H2A.X and p-BRCA1. As shown in Figure 4.12, decidualization seems to be associated with increased p-BRCA1, p-ATM and p-ATR and the level of activation appears transient peaking around 4 days of treatment. Surprisingly, knockdown of the NOX4/p22^{PHOX} complex modestly attenuated this biphasic phosphorylation, most evident in p-BRCA1 levels. Interestingly, CHK1, CHK2 and H2A.X, all of which are downstream of ATM/ATR, were clearly phosphorylated upon silencing of the complex in decidualizing cultures, indicating an ongoing activation of the DNA damage and repair pathway.

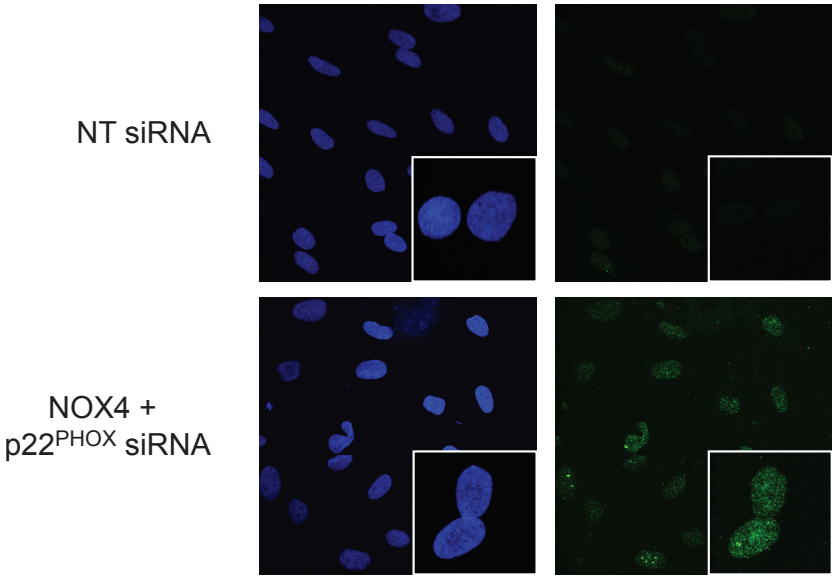


Fig 4.11 Silencing of the NOX4/p22^{PHOX} complex induces phosphorylation of H2A.X in decidualizing HESCs. Cultures were transfected with NT siRNA or siRNA targeting NOX4/p22^{PHOX} and two days later, cells were maintained untreated or treated with 8-br-cAMP and MPA for 72 hours. Subsequently, cells were fixed, permeabilized, blocked and stained with DAPI and anti-p-H2A.X antibody. Subsequently, cells were imaged using confocal microscopy.

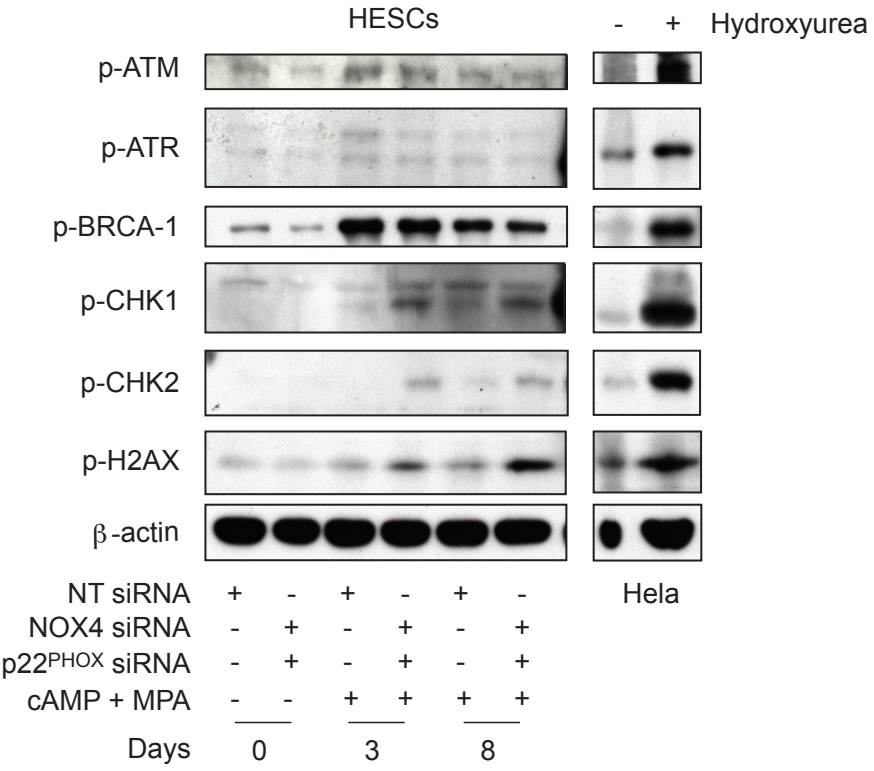


Fig 4.12 Silencing of the NOX4/p22^{PHOX} complex activates the DNA damage and repair pathway in decidualizing HESCs. HESCs were transfected with NT siRNA or siRNA targeting NOX4 and p22^{PHOX}, and two days post transfection, cultures were maintained untreated or treated with 8-br-cAMP and MPA for 3 and 8 days. Whole-cell lysates were extracted and blotted for p-ATM, p-ATR, p-BRCA-1, p-CHK1, p-CHK2 and p-H2A.X expression. β-Actin served as a loading control.

These observations are in agreement with the functional *in silico* analysis of the NOX4/p22^{PHOX}-dependent genes. However, as I mentioned previously, the outcome of the activation of this pathway could be apoptosis or enhanced repair of DNA damage and consequently cell survival. To investigate what might be happening in decidualizing HESCs, I first measured cell viability upon NOX4/p22^{PHOX} knockdown. To this end, primary cultures were transfected with NT siRNA or siRNA targeting NOX4/p22^{PHOX}, and two days post transfection, cultures were treated with 8-br-cAMP and MPA for 3 and 8 days. Cell viability was measured using the MTS assay. As shown in Figure 4.13A, silencing of the NOX4/p22^{PHOX} complex resulted in a non-significant decrease in cellular viability. To validate this observation, I used an alternative method, which assesses cell viability and cytotoxicity by measuring two protease activities, one is a marker of cell viability and is retained within the viable cell. It is measured using a fluorogenic, cell-permeant, peptide substrate (glycylphenylalanyl-aminofluorocoumarin). The other protease is a marker of cytotoxicity or dead cells, and is released from the cell that has lost membrane integrity. This protease is measured using a second, fluorogenic cell-impermeant peptide substrate. Primary cultures were therefore transfected with NT siRNA or siRNA targeting NOX4 and p22^{PHOX}, and two days post transfection, cells were left untreated or treated with 8-br-cAMP and MPA for 72 hours. Subsequently, cell viability and cytotoxicity were measured. H_2O_2 was used as a positive control. As illustrated in Figure 4.13B, there was no significant change in cell viability or increase in cell cytotoxicity in undifferentiated and decidualizing HESCs with disabled NOX4/p22^{PHOX} complex compared to HESCs with intact complex, confirming the previous observation that silencing of the NOX4/p22^{PHOX} complex does not lead to cell death in decidualizing HESCs.

These observations suggested that disabling of the NOX4/p22^{PHOX} complex might lead to illicit activation of the DNA repair pathway. In other words, it appeared possible that lack of coordinated endogenous ROS signalling perturbs cellular homeostasis in such a way that the DNA repair pathway is activated in the absence of activated DNA damage. To test this hypothesis, I carried out the Comet assay on HESCs transfected with NT siRNA or siRNA targeting NOX4 and p22^{PHOX} and treated with 8-br-cAMP and MPA for 3 days. Interestingly, as shown in Figure 4.14, there was no visible DNA damage in HESCs with disabled NOX4/p22^{PHOX} complex, further indicating that activation of the DNA repair pathway is a result of imbalance in the cellular and redox homeostasis of decidualizing HESCs rather than actual DNA damage.

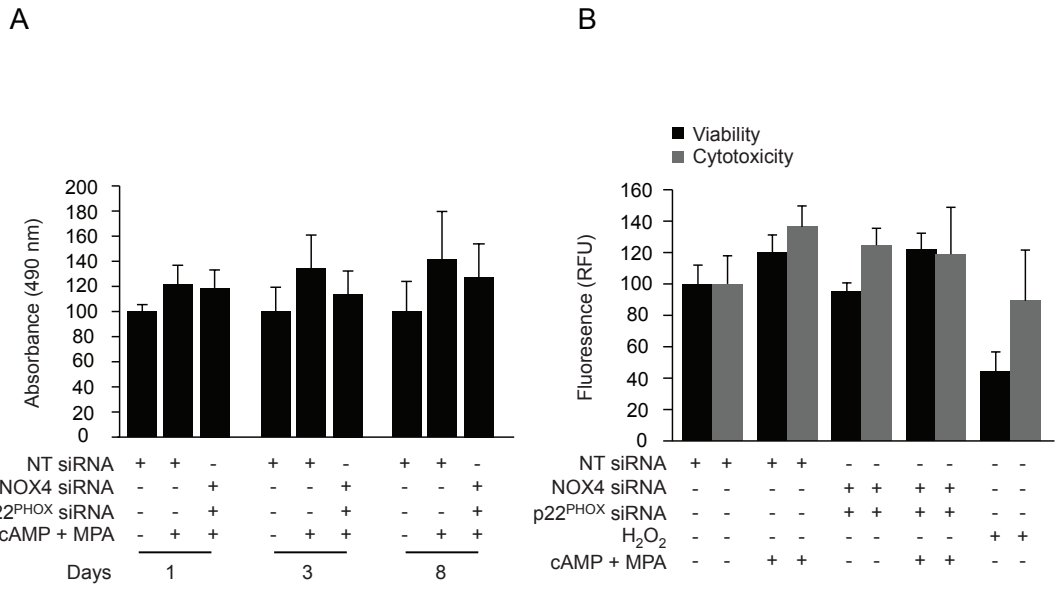


Fig 4.13 Silencing of the NOX4/p22^{PHOX} complex does not induce cell death in decidualizing HESCs. A, HESCs were transfected with NT siRNA or siRNA targeting NOX4 and p22^{PHOX} and two days post transfection, cells were left untreated or treated with 8-br-cAMP and MPA for 1, 3 and 8 days. Cell viability was measured using the CellTiter 96® AQ$_{ueous}$ One Solution Cell Proliferation Assay (Promega) and according to manufacturer protocol. Data are depicted as means (± SD) of sextuplicate measurements (N = 3). B, HESCs were transfected with NT siRNA or siRNA targeting NOX4/p22^{PHOX} and two days post transfection, the cells were maintained untreated or treated with 8-br-cAMP and MPA for 72 hours. Cell viability and cytotoxicity was then measured using the Apo Tox-Glo^{TM} Triplex Assay (Promega) according to manufacturer protocol (N = 3).

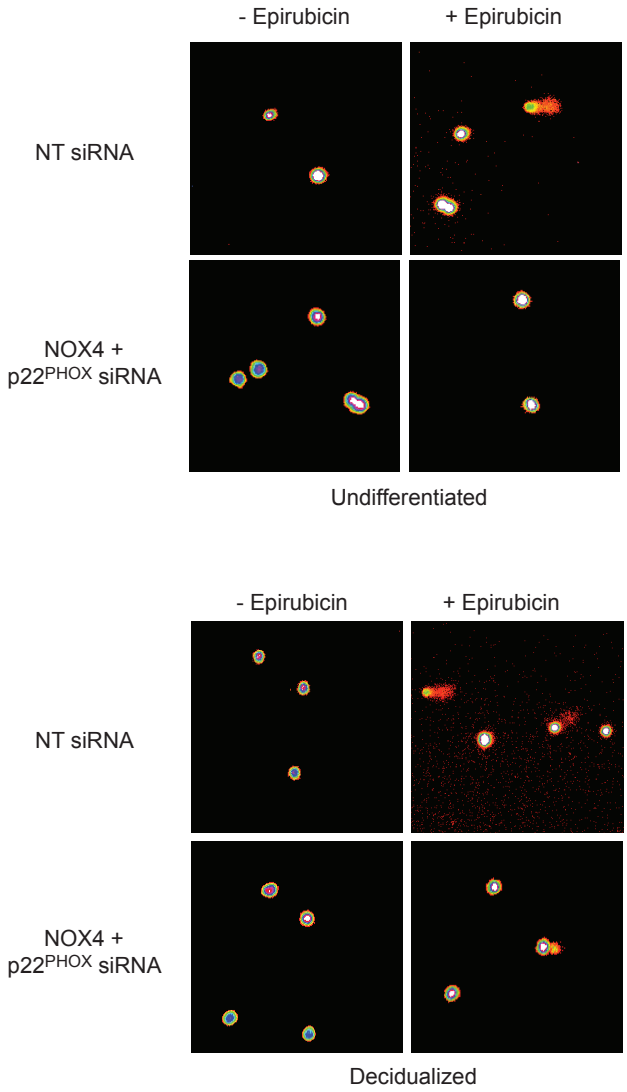


Fig 4.14 Knockdown of the NOX4/p22^{PHOX} complex does not induce DNA damage in HESCs. HESCs were transfected with NT siRNA or siRNA targeting NOX4 and p22^{PHOX}, and two days post transfection, cultures were maintained untreated or treated with 8-br-cAMP and MPA for 3 days. Subsequently, the comet assay was carried out. Epirubicin was used to induce DNA damage in HESCs. (Note: the comet assay was carried out in collaboration with Dr. Keiji Kudro, Lara Monteiro and Prof. Eric Lam).

4.5 Lack of endogenous ROS signalling disrupts redox homeostasis in decidualizing HESCs

Although our data confirms the absence of DNA damage upon knockdown of the NOX4/p22^{PHOX} complex in primary HESCs, I decided to first look at the oxidative status of the decidualizing HESCs upon abolishing endogenous ROS production. Thus, HESCs were transfected with NT siRNA or siRNA targeting NOX4 and p22^{PHOX} and treated with 8-br-cAMP for 1, 3 and 8 days. Prior to terminating the treatments, cells were loaded with DCFH-DA for 25 minutes. Subsequently, ROS measurement was taken every 2 minutes over a 30-minute period. As shown in Figure 4.15, decidualizing HESCs with functional NOX4/p22^{PHOX} complex, as I have previously published, show an initial burst in ROS at the 1-day time point, which then recedes during the decidual process. Upon disabling the NOX4/p22^{PHOX} complex, however, the initial burst in ROS is eliminated but there is a gradual increase of ROS as the cells decidualize (Fig 4.15).

I postulated that the paradoxical but gradual increase of endogenous ROS upon disabling the NOX4/p22^{PHOX} complex post the 1 day time-point, might be responsible for disrupting the redox homeostasis of decidualizing HESCs and consequently inducing cellular stress signals, which might lead to activation of the DNA damage pathway. To test this hypothesis, I decided to look at some markers of stress and hallmarks of decidualization such as the status of global sumoylation, PR level, MKP1 and p-JNK in HESCs with disabled NOX4/p22^{PHOX} complex. To this end, primary cultures were transfected with NT siRNA or siRNA targeting NOX4 and p22^{PHOX} and two days post transfection treated with 8-br-cAMP and MPA for 72 hours. Western blot analysis was carried out on whole cell lysates and blotted for global SUMO, PR, MKP1, p-JNK and t-JNK. As illustrated in Figure 4.16, silencing of the NOX4/p22^{PHOX} complex in decidualizing HESCs induced a hypersumoylation response, which is the reverse of the well-established hyposumoylation normally observed upon decidualization (70). The effect of this hypersumoylation response was reflected in the striking stability of PR, which is known to be downregulated upon decidualization. Activation of p-JNK, which is normally switched off in decidualizing HESCs, was another consequence of the silencing of the complex. MKP1, another stress-related marker, was induced and serves as another indicator that all the changes observed upon knockdown of NOX4 and p22^{PHOX} are due to HESCs subjected to redox imbalance and stress conditions.

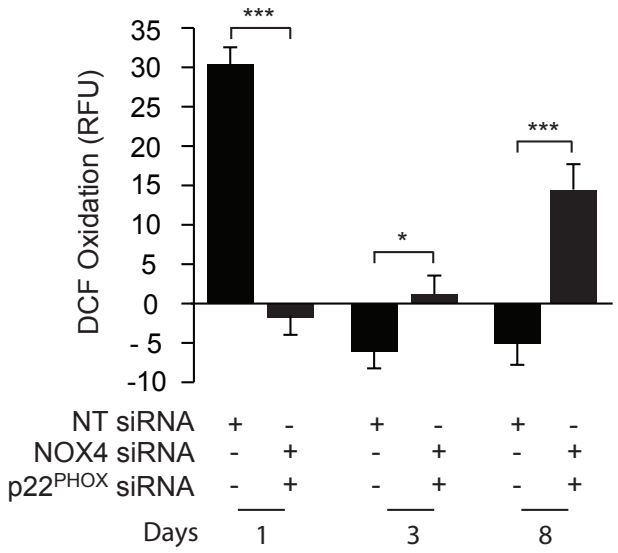


Fig 4.15 Knockdown of the NOX4/p22^{PHOX} complex alters the redox status of decidualizing HESCs. HESCs were transfected with NT siRNA or siRNA targeting NOX4 and p22^{PHOX}. Two days post transfection, Cultures were maintained untreated or treated with 8-br-cAMP and MPA for 1, 3, and 8 days. Cultures were loaded with DCFH-DA 25 minutes before terminating the treatments. DCF fluorescence measurements were taken every 2 minutes over a 30-minute period using a fluorometer. The baseline represents untreated cells. Data are depicted as the difference in ROS production between treated and untreated cultures and represent means (± SEM) of sextuplicate determinations. N = 3, * = $P < 0.05$, *** = $P < 0.001$.

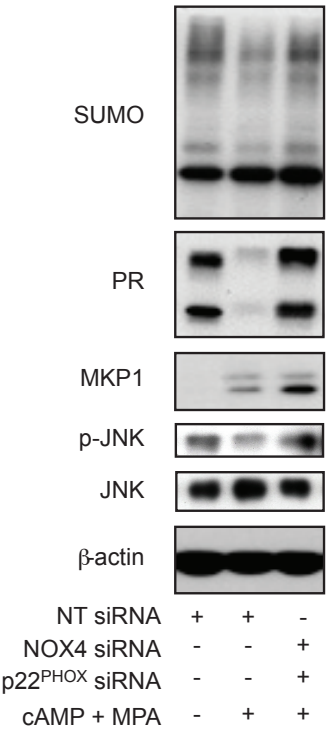


Fig 4.16 Knockdown of the NOX4/p22^{PHOX} complex induces stress signals in decidualizing HESCs. HESCs were transfected with NT siRNA or siRNA targeting NOX4 and p22^{PHOX}, and two days post transfection cultures were maintained untreated or treated with 8-br-cAMP and MPA for 72 hours. Whole-cell lysates were extracted and blotted for SUMO, PR, MKP1, p-JNK and JNK expression. β-actin served as a loading control.

Oxidative stress and alteration in the oxidative status of the cells may point towards an imbalance between the amount of endogenous ROS, and the antioxidant enzymes that are part of the cellular defence mechanism. It is well established that decidualization is associated with increased expression of antioxidant enzymes such as SOD2, TXN and GPx. To test if the induction of those antioxidant enzymes is perturbed in decidualizing HESCs with a disabled ROS-producing complex, primary cultures were transfected with NT siRNA or siRNA targeting NOX4 and $p22^{PHOX}$. Two days post transfection, cells were treated with 8-br-cAMP and MPA for 72 hours. Total RNA was harvested and RTQ-PCR analysis was carried out to look at the transcript levels of SOD2, TXN and GPx. As shown in Figure 4.17, all the antioxidant enzymes showed a significant increase upon decidualization. Interestingly, silencing of the NOX4/$p22^{PHOX}$ complex in decidualizing cells significantly attenuated the induction of SOD2, TXN and GPx. This observation suggests that silencing of the NOX4/$p22^{PHOX}$ complex upon decidualization perturbs the oxidative status of HESCs disrupting the homeostasis between endogenous ROS and the antioxidant defence enzymes.

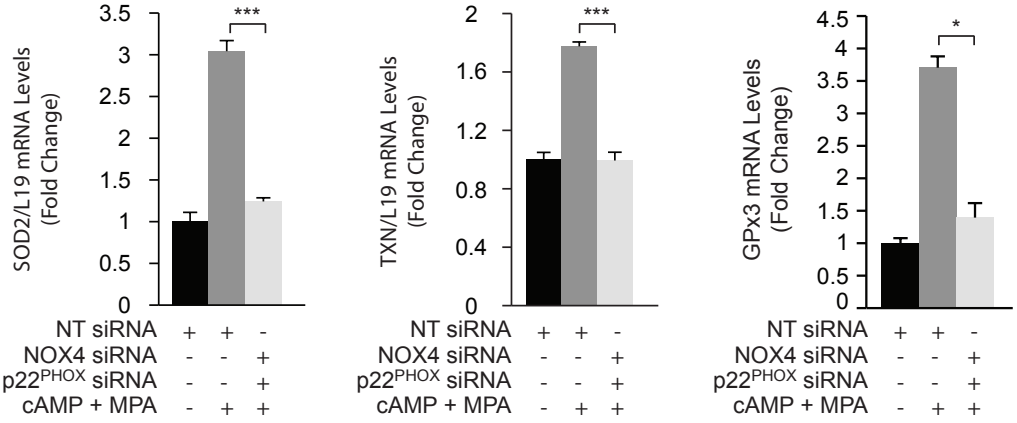


Fig 4.17 Antioxidant enzymes are attenuated upon knockdown of the NOX4/p22^{PHOX} complex in decidualizing HESCs. HESCs were transfected with NT siRNA or siRNA targeting NOX4 and p22^{PHOX} and two days post transfection cultures were maintained untreated or treated with 8-br-cAMP and MPA for 72 hours. RTQ-PCR analysis was carried out for SOD2 (left), TXN (middle) and GPx3 (right) mRNA levels normalized to L19 mRNA. Data are depicted as fold induction relative to transcript levels of untreated samples and represent means (± SD) of triplicate determinations. * = $P < 0.05$, *** = $P < 0.001$.

Summary of results

I have previously shown in chapter 3 that the NADPH oxidase complex is the main source of ROS in HESCs and that the NOX4/p22^{PHOX} complex, specifically, is required for initiation of the decidual response.

In this chapter, I provide further evidence that implicate the NOX4/p22^{PHOX} complex in maintenance of the decidual process. Several lines of evidence led to this conclusion. First, both transmembrane components of the NOX4/p22^{PHOX} complex are upregulated at the transcript and protein level upon decidualizing HESCs for 8 days. Second, siRNA-mediated knockdown of NOX4 and p22^{PHOX} resulted in a marked attenuation of the decidual markers *PRL* and *IGFBP1* at the transcript level. Third, inhibiting the activity of the NADPH oxidase complex by administering DPI, the NADPH oxidase inhibitor in the midst of decidualization, also resulted in a marked attenuation of PRL and IGFBP1 transcript levels. Interestingly, the attenuation in the induction of PRL and IGFBP1 transcripts as a result of siRNA-mediated knockdown of the complex was comparable to that achieved by inhibiting the complex using DPI (~ 60%). Therefore, this data strongly implicate NOX4/p22^{PHOX}-dependent ROS signalling in prolonged decidualization and maintenance of this differentiation process.

Microarray analysis comparing decidualizing HESCs with and without siRNA-mediated knockdown of the NOX4/p22^{PHOX} revealed that ~ 29% of the NOX4/p22^{PHOX} dependent genes are decidual dependent. Interestingly, the pattern of regulation in response to the NOX4/p22^{PHOX}-dependent ROS, of ~ 90% of those genes is in the same direction as that observed in response to decidual stimuli. It is not surprising therefore that disabling the NOX4/p22^{PHOX} complex perturbs the decidual process.

One of the most striking findings of this chapter is the overlap between the NOX4/p22^{PHOX}-dependent and the FOXO1-dependent genes. This observation led to the finding that FOXO1 is upstream of the NOX4/p22^{PHOX} complex. Several lines of evidence confirmed this observation. First, the *in silico* analysis of the NOX4/p22^{PHOX}-dependent genes revealed similar network, molecular and cellular functions to that attained by *in silico* analysis of the FOXO1-dependent gene list. Second, 62% of the NOX4/p22^{PHOX}- and decidual-dependent genes are also FOXO1-dependent and share the same pattern of regulation. Third, siRNA-mediated knockdown of the

NOX4/p22^{PHOX} complex does not alter FOXO1 expression at the protein level, whereas knockdown of FOXO1 attenuates the induction of NOX4 and p22^{PHOX} observed upon decidualizing HESCs. Fourth, based on reporter studies, NOX4/p22^{PHOX}-dependent ROS production upon stimulation with apocynin, alone or in combination with 8-br-cAMP, only marginally enhance the DNA binding activity of FOXO1. One should interpret this finding with caution. Although the marginal increase is statistically significant, it is very low and therefore negligible when put in context of reporter studies and artificial systems. Therefore, although one might be inclined to interpret the result as NADPH oxidase-produced ROS might feedback on FOXO1, further experimental work is required to investigate this angle.

Several lines of evidence strongly suggested that disrupting the NOX4/p22^{PHOX}-dependent ROS signalling perturbs the redox homeostasis of decidualizing HESCs. First, siRNA-mediated knockdown of the NOX4/p22^{PHOX} complex activates the DNA repair pathway in decidualizing HESCs without apparent DNA damage or apoptosis. This suggests that activation of the DNA repair pathway is not a response to DNA damage but a consequence of an imbalance of the redox homeostasis in decidualizing HESCs.

Second line of evidence is paradoxical. Disabling the NOX4/p22^{PHOX} complex led to a shift in the amount of endogenous ROS in decidualizing HESCs in favour of prooxidant. One might have expected a decrease in the amount of endogenous ROS production upon disabling the NOX4/p22^{PHOX} complex. However, the increase in ROS production over time might be a result of attenuation of the induction of the anti-oxidant enzymes upon knockdown of NOX4 and p22^{PHOX}. Normally, antioxidant enzymes like SOD2, TXN and GPx are markedly upregulated in decidualizing HESCs with fully-active NADPH oxidase complex.

Third, disrupting the NOX4/p22^{PHOX}-dependent ROS signalling induces stress signals in decidualizing HESCs characterized by a hypersumoylation response, induction of MKP1 and activation of p-JNK. Interestingly, the hypersumoylation response goes hand in hand with the increase stability of PR. It is known that sumoylation of steroid hormone receptors decrease their turnover and increase their stability and is associated with attenuated activity and response to ligand (113, 118-120).

Interestingly, the hypersumoylation response, the PR stability and the activation of p-JNK are not only characteristics of stress signals but also characteristics of

undifferentiated HESCs. It is not surprising therefore, that disabling the NOX4/$p22^{PHOX}$ complex disrupts the decidual phenotype and perturbs genes involved in DNA repair and cell cycle regulation as the *in silico* analysis of the microarray revealed.

Chapter 5: Results 3

Characterization of the NOX4/p22^{PHOX} complex in patients with endometriosis

Introduction

Endometriosis is a condition in which endometrium-like tissue is found primarily on the pelvic peritoneum and ovaries. It occurs in 6 – 10% of women of reproductive age and is believed to be mainly the result of retrograde menstruation and subsequent transplantation of eutopic endometrial tissue fragments and cells to the peritoneum. (237, 238). 50% of women with pelvic pain and/or infertility have endometriosis. Infertility in this context may be due to several factors, one of which is abnormal eutopic endometrium with compromised embryonic implantation (238, 258).

Several studies utilizing microarray analysis and comparing endometrial tissue from women with and without endometriosis revealed abnormalities in the proliferative-to-secretory phase transition normally observed in the menstrual cycle. Other studies revealed that the most profound perturbation is observed in the secretory phase of the cycle in patients with endometriosis but not confined to it. Aberrant gene expression has also been observed in the proliferative phase in diseased patients.

Moreover, as mentioned previously in the introduction, eutopic endometrium from patients with endometriosis is associated with the “progesterone resistance” theory, which is attributed to the observation that a subset of progesterone-dependent genes are perturbed in eutopic endometrium from diseased patients (257). It is noteworthy to mention that “progesterone resistance’ not only refers to perturbation in progesterone-dependent gene expression but encompasses signal transduction and the expression of downstream target genes. Importantly, increasing amount of evidence suggests that progesterone-resistance *in vivo* is recapitulated *in vitro* in primary HESCs obtained from the eutopic endometrium of patients with endometriosis. For instance, Aghajanova et *al*. (2010) revealed that primary cultures of eutopic endometrium from diseased patients compared to control groups almost fail to induce progesterone-dependent genes upon being stimulated with the steroid hormone (273).

Although the “progesterone resistance” theory may hold true, progesterone signalling is not the only perturbation observed in the endometrium of patients with endometriosis. In fact, as mentioned previously in chapter 1, emerging evidence suggests that basal gene expression in undifferentiated HESCs from diseased patients, responsiveness to hCG and cAMP signalling are also perturbed in endometriosis.

Endometriosis is also associated with chronic inflammation. Reactive oxygen species (ROS) are key players in inflammation and are known to be proinflammatory mediators that modulate cell proliferation. A recent study demonstrated that cellular redox status is impaired in endometriotic cells characterized by higher endogenous oxidative stress with an increase in ROS production, alterations in ROS detoxification pathways, a drop in catalase levels in addition to increased cellular proliferation and activation of ERK1/2 (172).

As outlined in the previous chapters, the NOX4/$p22^{PHOX}$ complex not only critically regulates redox signalling in HESCs but also determines cellular responses to differentiation signals. Hence, I postulated that impaired cycle-dependent expression of NOX4 or $p22^{PHOX}$ in eutopic endometrium of patients with endometriosis might contribute to the pathogenesis of the disease.

5.1 Endometrial $p22^{PHOX}$ and NOX4 expression in patients with or without endometriosis

Endometriosis is associated with chronic inflammation. ROS are key players in inflammation and are known to be proinflammatory mediators that modulate cell proliferation. I therefore postulated that the NOX4/$p22^{PHOX}$ complex might be deregulated in the eutopic endometrium from patients with endometriosis.

I focused on examining the expression of $p22^{PHOX}$ and NOX4, in the secretory phase of the menstrual cycle. Several considerations underpin this decision. First, decidualization occurs in the secretory phase of the cycle. Second, I showed in Figures 4.1 and 4.2, that NOX4 and $p22^{PHOX}$ expression at the protein and transcript level is upregulated in decidualizing HESCs. Third, disabling the activity of the complex by siRNA-mediated knockdown of NOX4 and $p22^{PHOX}$ or by administering chemical inhibitors to decidualizing HESCs perturbs the decidual process and attenuates the induction of PRL and IGFBP1 transcripts. Fourth, HESCs from eutopic endometrium of patients with endometriosis fail to fully decidualize and show blunted response to decidual stimuli (236).

The biological samples used for this study came from two different sources. The 23 cDNA samples I used to look at the transcript levels of NOX4, $p22^{PHOX}$ and FOXO1; and the tissue sections used for immunohistochemistry were a kind gift from Dr. Matti Poutanen (University of Turku, Finland). This group of sample consisted of 11 control samples and 12 samples of eutopic endometrium obtained from patients with endometriosis. The endometriosis patients and the control groups were aged between 22 and 46 years of age. Endometrial histology confirmed that each biopsy taken was normal secretory.

The 39 tissue biopsies that were used to extract proteins were received locally. This group of sample consisted of proliferative and secretory eutopic endometrial tissue. The proliferative group of samples consisted of 7 tissue biopsies of eutopic endometrium from patients with the disease and an equal number of biopsies from control patients. The secretory group consisted of 13 samples from patients with endometriosis and 12 samples from control patients. All samples were taken at the time of laparoscopy for either pelvic pain or infertility exploration. The endometriosis patients and the control groups were aged between 20 and 44 years of age.

To characterize the NOX4/$p22^{PHOX}$ complex in patients with endometriosis, I first compared the transcript levels of NOX4 and $p22^{PHOX}$ in samples from diseased patients with those from a control cohort. As shown in Figure 5.1, both $p22^{PHOX}$ and NOX4 transcript levels appeared to be lower in diseased patients compared to the control group. However, $p22^{PHOX}$ alone proved to be significantly lower.

Next, I carried out Western blot analysis for NOX4 and $p22^{PHOX}$ on protein samples prepared from eutopic secretory endometrial tissue biopsies obtained from patients with proven endometriosis and patients without evidence of pelvic endometriosis. As shown in Figure 5.2A, there is a striking downregulation of $p22^{PHOX}$ protein levels in patients with endometriosis compared to the control group. NOX4 protein expression, on the other hand, does not seem to be deregulated in diseased patients. Furthermore, densitometry analysis carried out on the Western blot results for both $p22^{PHOX}$ and NOX4, confirmed that $p22^{PHOX}$ was significantly lower in eutopic endometrial tissue biopsies from patients with endometriosis compared to the control group, whereas NOX4 showed consistent protein levels in control and diseased patients (Fig 5.2B).

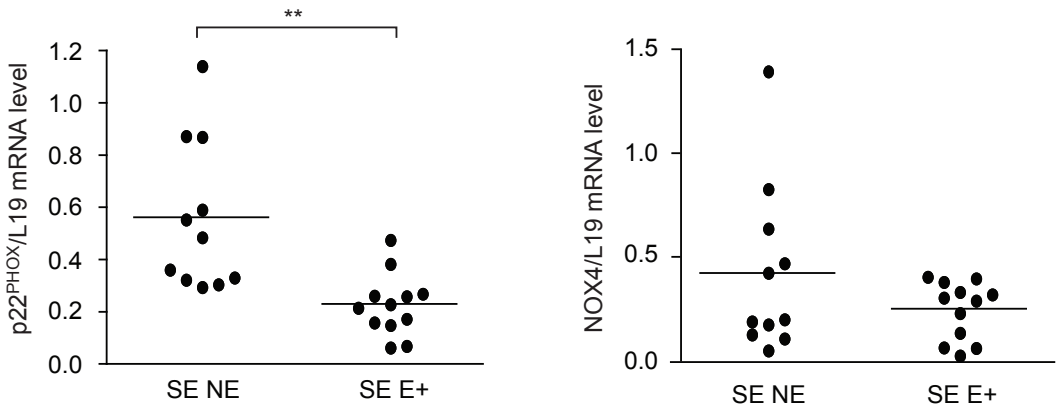


Fig 5.1 NOX4 and p22^{PHOX} transcript levels in patients with endometriosis. RTQ-PCR analysis was carried out to compare the transcript level of NOX4 and p22^{PHOX} in secretory phase eutopic endometrium from patients without laparoscopic evidence of pelvic endometriosis (SE NE) to secretory eutopic endometrial samples from patients with proven endometriosis (SE E+). **, $P < 0.01$.

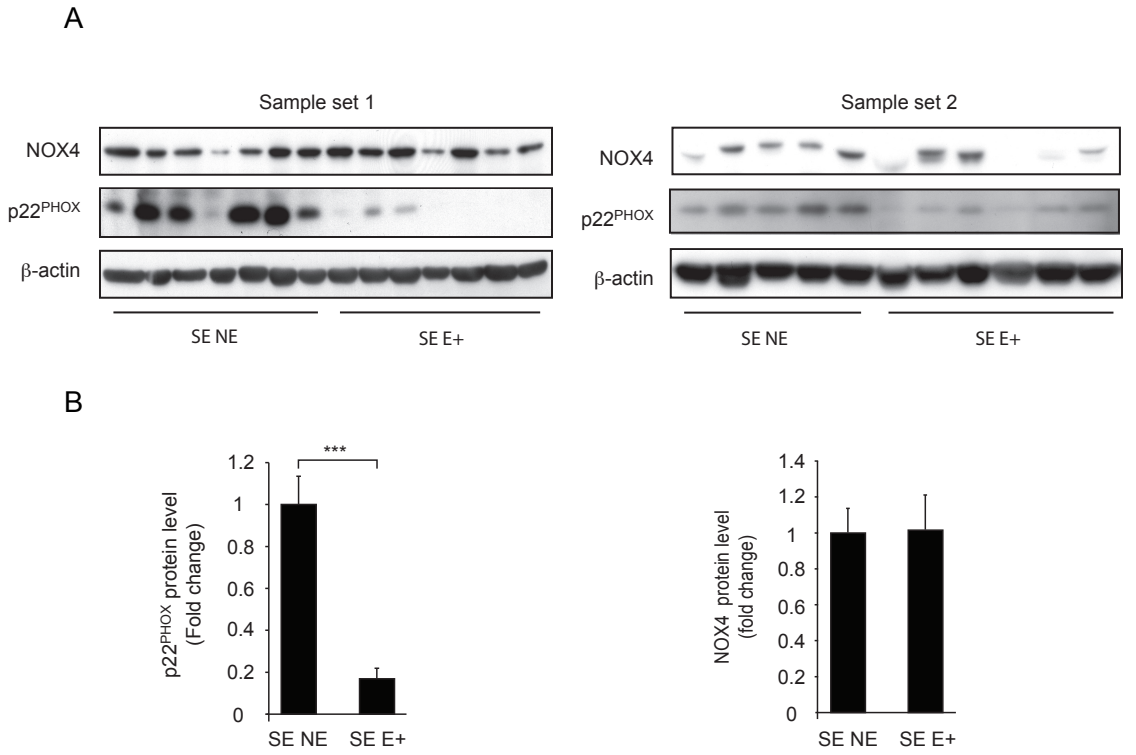


Fig 5.2 NOX4 and p22^{PHOX} protein expression levels in endometriosis. A, Western blot analysis for NOX4 and p22^{PHOX} protein expression in SE NE and SE E+ samples. B, Densitometry analysis comparing and quantifying the protein expression level of NOX4 and p22^{PHOX} in SE NE and SE E+ samples. ***, $P < 0.001$.

5.2 Regulation of the NOX4/p22^{PHOX} complex in the secretory phase of the menstrual cycle

The observation that p22^{PHOX} is downregulated in the secretory phase of the menstrual cycle in samples from patients with endometriosis was very striking. The onset of the secretory phase is on day 14 of the menstrual cycle, and is not a homogenous phase. As mentioned previously in the introduction, the secretory phase can be segregated into three functionally distinct stages: ESE, MSE and LSE.

Therefore, I decided to examine if p22^{PHOX} cellular distribution is regulated throughout the different phases of the menstrual cycle. In other words, I wondered if p22^{PHOX} was subjected to temporal and spatial regulation through the ESE, MSE and LSE phases of the menstrual cycle. To do so, I carried out immunohistochemistry staining for p22^{PHOX} on eutopic endometrial tissue sections from patients with and without endometriosis taken in ESE, MSE and LSE phases of the menstrual cycle. Interestingly, as illustrated in Figure 5.3, in patients without the disease, p22^{PHOX} levels in the ESE phase are low and restricted to the stroma, as it is completely absent from the glands. In the MSE phase of the cycle, p22^{PHOX} staining increases in the stromal compartment and starts to appear in the uterine glands as well. By the LSE phase of the menstrual cycle, p22^{PHOX} staining levels are markedly increased in the stroma, glands and the epithelial compartments.

Surprisingly, the mirror effect was observed in patients with endometriosis. p22^{PHOX} staining is at its highest levels in the ESE phase of the menstrual cycle and is found in the stromal compartments, uterine glands as well as the epithelial cells. By the MSE phase of the cycle, however, p22^{PHOX} staining levels are markedly decreased and where it is expressed, it appears to coagulate. A similar pattern of p22^{PHOX} staining in the MSE phase was observed in LSE phase tissue sections of diseased patients (Fig 5.3).

Next, I carried out the same immunohistochemistry analysis for NOX4. Although NOX4 was highly present in eutopic endometrial tissue sections from patients with and without endometriosis, it does not appear to be regulated throughout the different stages of the secretory phase (Fig 5.4). Moreover, there does not seem to be any differences in NOX4 staining between tissue sections from control and diseased patients throughout the secretory phase of the menstrual cycle.

The observation that $p22^{PHOX}$, but not NOX4, is misregulated in patients with endometriosis compared to the control group further validates our findings that $p22^{PHOX}$ alone is downregulated at the transcript and protein level in the secretory phase of the menstrual cycle in diseased patients.

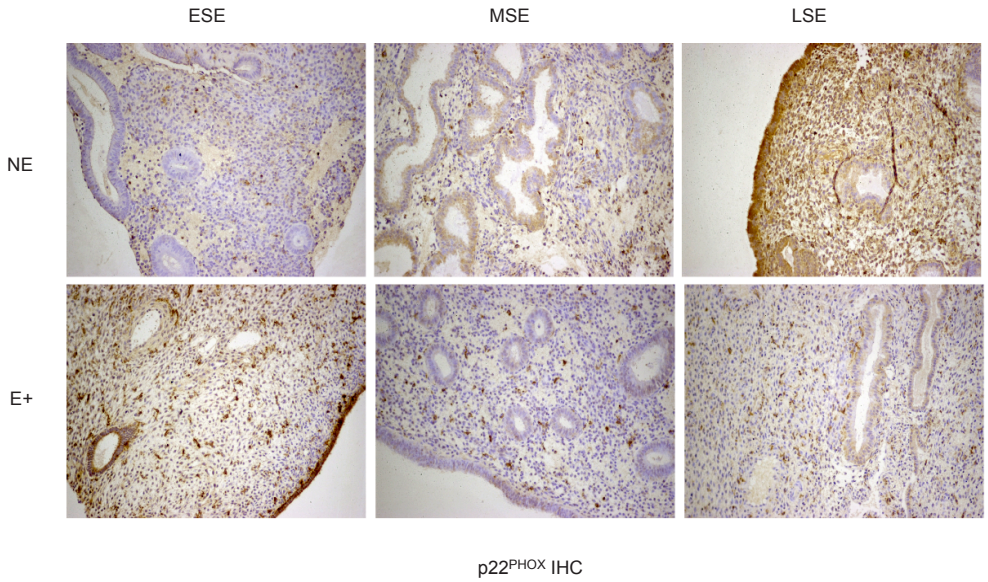


Fig 5.3 Immunohistochemistry analysis for p22^{PHOX} in patients with and without endometriosis. Immunohistochemistry staining for p22^{PHOX} carried out on SE NE and SE E+ eutopic endometrial tissue sections taken at the three different stages of the menstrual cycle: ESE, MSE and LSE. (Immunohistochemistry was carried out in collaboration with Dr. Jenny Steel).

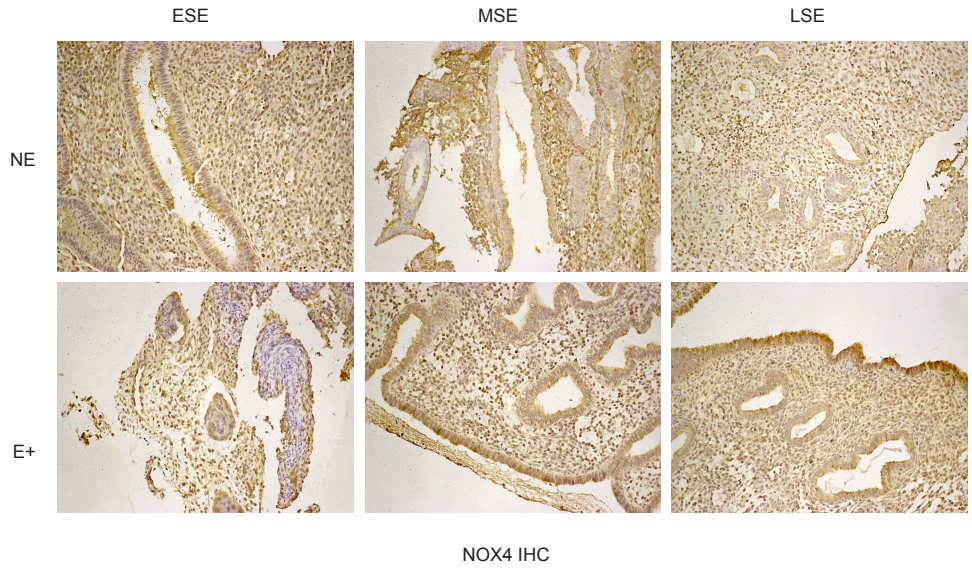


Fig 5.4 Immunohistochemistry analysis for NOX4 in patients with and without endometriosis. Immunohistochemistry staining for NOX4 carried out on SE NE and SE E+ eutopic endometrial tissue sections taken at the three different stages of the menstrual cycle: ESE, MSE and LSE. (Immunohistochemistry was carried out in collaboration with Dr. Jenny Steel).

5.3 Characterization of the NOX4/p22^{PHOX} complex in the proliferative phase of the menstrual cycle

So far, I have strong data suggesting that p22^{PHOX} alone is downregulated in the secretory phase of diseased patients compared to individuals without the disease. NOX4 expression, on the other hand, was consistent at the protein and transcript levels. This hypothesis led me to postulate that p22^{PHOX} protein levels might be generally downregulated throughout the menstrual cycle in patients with endometriosis.

To test this hypothesis, I carried out Western blot analysis to look at the expression levels of both NOX4 and p22^{PHOX} in samples taken from patients with and without endometriosis. Interestingly, as illustrated in figure 5.5, p22^{PHOX} protein levels proved to be lower in diseased patients compared to the control group, suggesting that p22^{PHOX} protein expression is generally lower in patients with endometriosis. On the contrary, NOX4 protein levels remained unchanged between the two groups, further confirming my previous observation that p22^{PHOX} alone is downregulated in eutopic endometrium of patients with the disease.

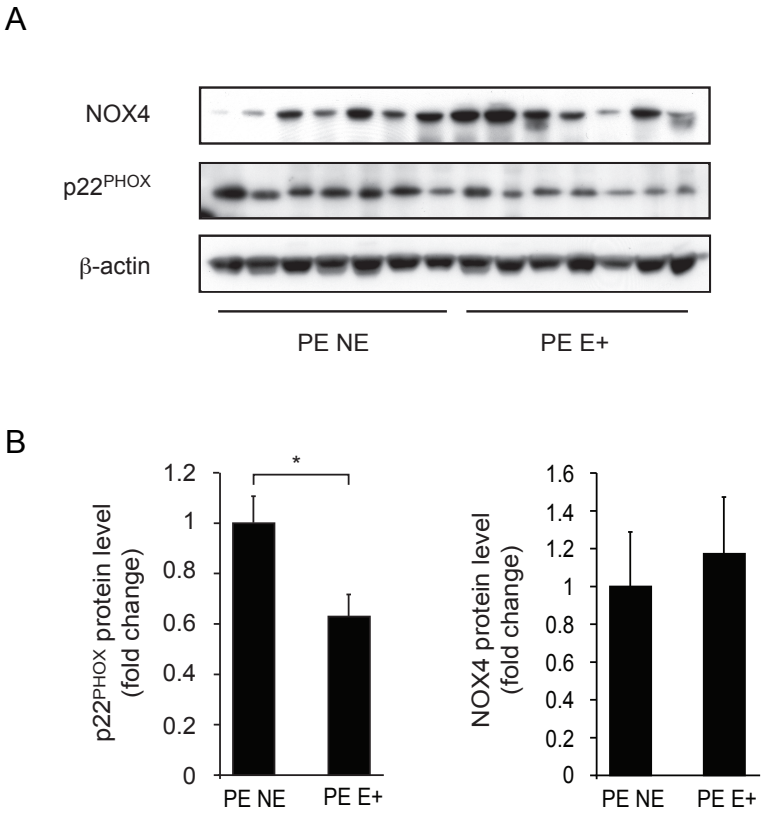


Fig 5.5 NOX4 and p22^{PHOX} protein expression in the proliferative phase of the menstrual cycle. A, Western blot analysis for NOX4 and p22^{PHOX} on proliferative eutopic endometrium form patients without endometriosis (PE NE) and with the disease (PE E+). B, Densitometry analysis comparing and quantifying the protein expression level of NOX4 and p22^{PHOX} between diseased patients and the control group. *, $P < 0.05$.

5.4 NOX4/p22^{PHOX} expression profiling in eutopic HESCs from patients with and without endometriosis

I have shown that p22^{PHOX} is downregulated in tissue samples obtained from patients with endometriosis. I hypothesized that this observation might be recapitulated *in vitro* in cultured HESCs taken from diseased patients.

To test this conjecture, HESCs from diseased and control patients were put in culture until they reach confluency. Subsequently, the medium was changed from 10% DCC to 2% DCC and cells were left in culture for 24 hours. Subsequently, total mRNA was harvested and RTQ-PCR analysis was carried out for p22^{PHOX} and NOX4. As shown in Figure 5.6, p22^{PHOX} transcript levels continued to be significantly lower in patients with endometriosis compared to control group. On the other hand, there was no significant difference in the mRNA expression of NOX4 between the two groups.

I have shown in the previous two chapters that cAMP induces a burst in ROS between 12 and 24 hours of treatment, which coincides with the induction of the decidual markers PRL and IGFBP1 as well as with the activation of the transcription factor C/EBPβ. I further went to show that this burst in ROS is not only cAMP-dependent, but also NOX4/p22^{PHOX} dependent.

NOX4 and p22^{PHOX} are known to form a heterodimer that is essential for the stability and the activity of the complex. Therefore, my finding that p22^{PHOX} is in fact lower in tissue samples and primary cultures derived from patients with endometriosis compared to control samples, led me to postulate that the kinetics of ROS upon treatment with cAMP might also be aberrantly regulated in HESCs obtained from diseased patients.

To test this hypothesis, primary cultures from patients with endometriosis were treated with 8-br-cAMP for 6, 12 and 24 hours. Prior to ending the treatments, the oxidant sensing DCFH-DA was loaded in the cells for 25 minutes and subsequently ROS measurements were taken every 2 minutes over a 30-minute period. Interestingly, as shown in Figure 5.7, although at the 6-hour treatment there appeared to be higher amount of ROS in 8-br-cAMP treated cells,

the cAMP-dependent burst in ROS normally observed between the 12 to 24 hour time-point was abolished. This observation mimicked what I observed earlier when cellular oxidation in primary cultures with an siRNA-mediated knockdown of NOX4 and $p22^{PHOX}$ was measured, indicating that the NOX4/$p22^{PHOX}$ is misregulated in primary cultures from patients with endometriosis not only at the expression level, but also at the functional level.

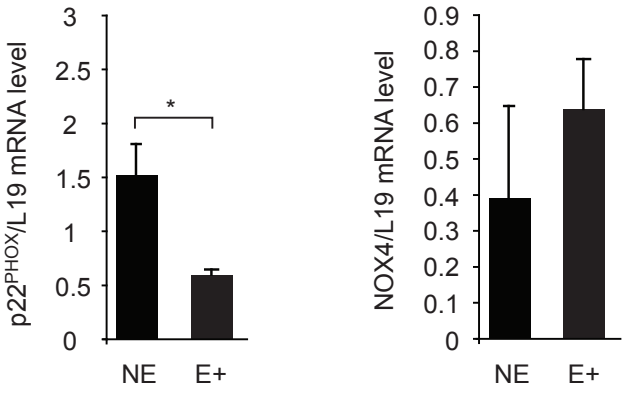


Fig 5.6 Basal transcript expression of NOX4/p22^{PHOX} complex in primary HESCs. HESCs from patients with and without endometriosis were cultured *in vitro* (N = 5). Total RNA was harvested and RTQ-PCR analysis was carried for p22^{PHOX} and NOX4 and the transcript levels were normalized to L19 mRNA. Data are depicted as normalized transcript levels and represent means (± SD) of triplicate determinations. *, $P < 0.05$.

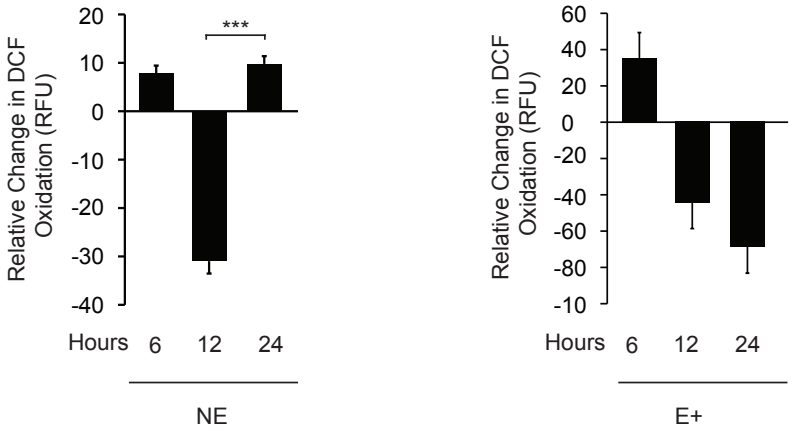


Fig 5.7 The oxidative status of eutopic HESCs with or without endometriosis. Four biologically different primary cultures from patients with and without endometriosis were left untreated or treated with 8-br-cAMP for 6, 12 and 24 hours. Cultures were loaded with DCFH-DA for 25 minutes prior to terminating the treatments. DCF fluorescence was measured every 2 minutes over a 30-minute period using a fluorometer. Data are depicted as the difference in ROS production between 8-br-cAMP treated and untreated cultures and represent means (± SEM) of sextuplicate determinations. ***, $P < 0.001$.

5.5 FOXO1 expression in patients with endometriosis

The consistent downregulation of $p22^{PHOX}$ observed in patients with endometriosis was very striking. I have provided strong evidence, in chapter 4 of this thesis, that FOXO1 is upstream the NOX4/$p22^{PHOX}$ complex. I therefore postulated that the downregulation observed in $p22^{PHOX}$ might be a consequence of downregulation in FOXO1 in patients with endometriosis.

To test this conjecture, I first compared the transcript levels of FOXO1 in samples from diseased patients with those from a control cohort. As shown in Figure 5.8, there was no difference of FOXO1 mRNA expression between patients with and without endometriosis.

Next, I carried out immunohistochemistry staining for FOXO1 on eutopic endometrial tissue sections, from the ESE, MSE and LSE phases of the menstrual cycle from patients with and without endometriosis. Interestingly, as illustrated in Figure 5.9, the expression pattern of FOXO1 appears to be similar in tissue sections from patients with and without the disease. In both patient groups, the lowest reactivity with FOXO1 is observed in the ESE phase of the cycle. By the MSE phase, FOXO1 reactivity increases and FOXO1 staining is also visible in the glands. During the LSE phase of the cycle, a marked increase in FOXO1 reactivity is observed in the stromal and glandular compartments in both groups of patients.

Taken together, I concluded that downregulation of FOXO1 is not the mechanism that underpins the aberrant regulation of $p22^{PHOX}$ in the endometrium of patients with endometriosis.

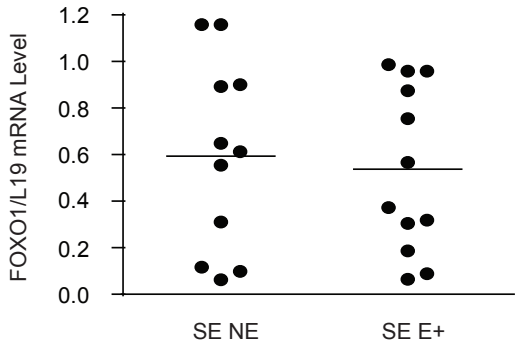


Fig 5.8 FOXO1 mRNA expression in patients with endometriosis. RTQ PCR analysis was carried out to compare the transcript level of FOXO1 in secretory phase eutopic endometrium from SE NE and SE E+ tissue samples.

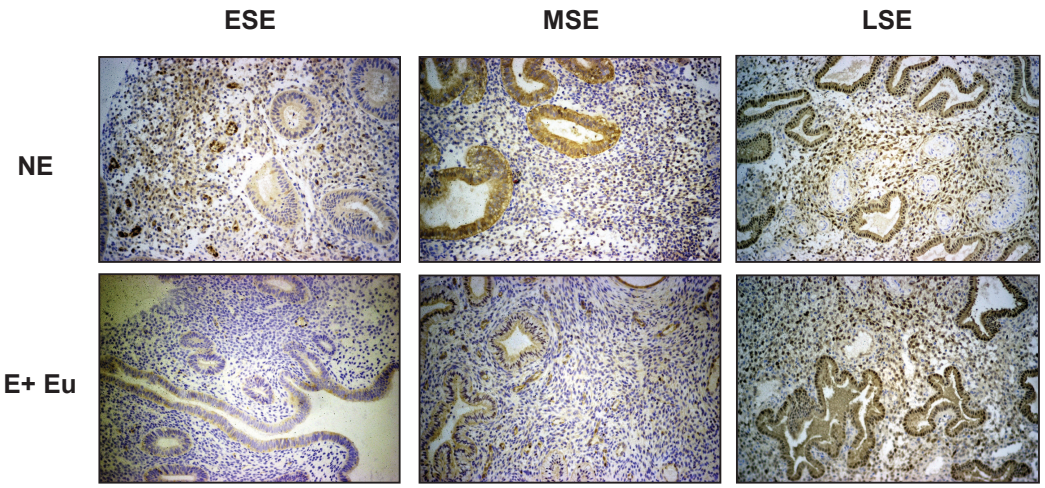


Fig 5.9 Immunohistochemistry analysis for FOXO1 in patients with and without endometriosis. Immunohistochemistry staining for NOX4 carried out on SE NE and SE E+ eutopic endometrial tissue sections taken at the three different stages of the menstrual cycle: ESE, MSE and LSE. (Immunohistochemistry was carried out in collaboration with Dr. Jenny Steel).

Summary of Results

Endometriosis is a chronic inflammatory disorder associated with resistance to progesterone signalling in the endometrium and an impaired decidual response, which normally leads to implantation failure and consequently infertility. More recent data, however, suggests that the "progesterone resistance" dogma is not entirely the prime reason for the impaired decidual response in patients with endometriosis. In fact, the general basal transcriptome in eutopic endometrium of patients with the disease might be misregulated. One underlying reason for this misregulation is aberrant epigenetic re-programming of the steroid hormone responses in the endometrium (248).

In this chapter I provide preliminary data, which shed light on a potentially different angle that may contribute to the endometriotic phenotype. I provide strong evidence that the NOX4/$p22^{PHOX}$ complex is deregulated at the expression and functional level in patients with endometriosis. My striking observation that $p22^{PHOX}$, the NOX4 cofactor, is downregulated in endometriosis is the result of four different lines of data. First, I show that $p22^{PHOX}$ is downregulated at the transcript level in secretory endometrial biopsies derived from patients with endometriosis. Second, I provide evidence that $p22^{PHOX}$ is significantly downregulated at the protein level in endometrial tissue from diseased patients. Third, the immunohistochemistry results not only show that $p22^{PHOX}$ is regulated throughout the menstrual cycle, but also that there is low immunoreactivity in tissue section from eutopic endometrium obtained from patients with endometriosis in the MSE and LSE phase of the menstrual cycle. Next, I show that $p22^{PHOX}$ is downregulated at the protein level in the proliferative phase of tissue samples with endometriosis compared to control samples, suggesting that the low expression of $p22^{PHOX}$ is a general characteristic of endometriosis.

Strangely, NOX4 does not appear to be misregulated in patients with endometriosis. My data so far cannot provide an explanation for such observation. There might be an underlying mechanism that stabilizes the expression of NOX4 regardless of the low expression of $p22^{PHOX}$ at both the protein and the mRNA level. Regardless though of NOX4 normal expression levels, I show that the cAMP-induced NOX4/$p22^{PHOX}$-dependent burst in ROS seen in control tissue between 12 and 24

hours of treatment with cAMP, is depleted in primary cultures derived from patients with endometriosis, indicating that the NOX4/$p22^{PHOX}$ complex is functionally perturbed in patients with the disease.

I further show that the downregulation observed in tissue biopsies from patients with endometriosis can be recapitulated *in vitro*. Culturing primary HESCs obtained from diseased patients and subsequently looking at the transcript levels of both NOX4 and $p22^{PHOX}$ yielded the same results as that observed when the same analysis was carried out on tissue biopsies. $p22^{PHOX}$ continued to be downregulated in endometriosis samples compared to control.

Further, I provide data indicating that downregulation of $p22^{PHOX}$ is FOXO1-independent. FOXO1 transcripts have been reported to be lower in patients with endometriosis (257, 274, 275). Despite these reports, I provide evidence suggesting that FOXO1 expression at the protein level is not aberrant in diseased patients.

Taken together, in this chapter I provided preliminary evidence that the NOX4/$p22^{PHOX}$ complex and consequently the cellular redox status are perturbed in eutopic endometrium of patients with endometriosis. However, to come up with conclusive interpretation on these data, and to understand the underlying mechanisms that stabilises NOX4, a bigger sample comprised of timed biopsies would be critical. Moreover, it might be essential to also investigate if the observation that $p22^{PHOX}$ downregulation is confined to the clinical condition endometriosis and does not hold true for other clinical conditions like recurrent miscarriages. This would confirm that downregulation of $p22^{PHOX}$ is specific to endometriosis and can potentially be a marker distinguishing eutopic endometrium from patients with endometriosis.

Chapter 6:

Discussion

Discussion

Decidualization of the endometrial stromal compartment is an essential differentiation process in all species in which implantation involves breaching of the luminal endometrial epithelium by the embryo (1, 276). Decidualized HESCs acquire specialized characteristics that enable them to act as biosensors of embryo quality and capable of rejecting developmentally compromised blastocysts (40, 41, 277). The process of endometrial decidualization is also critical for trophoblast invasion, placental formation and for protecting the early conceptus from environmental stress cues (35, 278). Importantly, decidual cells regulate the recruitment of uNK cells to the feto-maternal interface, suggesting that they play an integral part in conferring immunotolerance to the fetal semiallograft (8). Failure to mount an adequate decidual response, therefore, results either in implantation failure or contributes to a spectrum of pregnancy complications, such as early pregnancy loss, preeclampsia, preterm labour and fetal growth restriction (1).

Decidualization is a progressive process that is under extensive temporal and spatial regulation. Its onset is first apparent in stromal cells adjacent to the spiral arteries of the superficial endometrial layer and, in case of pregnancy, it progressively encompasses the whole endometrium (5, 9). Initiation of the decidual process *in vivo* coincides with elevated endometrial cAMP levels, which is thought to be a consequence of increased expression of local factors that activate adenylate cyclase in stromal cells, such as RLX, CRH, pituitary gonadotrophins and PGE_2. In addition, decidualization coincides with a downregulation of phosphodiesterase-4 expression, an enzyme that converts cAMP to AMP (10, 79-84, 279, 280). cAMP stimulation sensitizes HESCs to progesterone signalling. Once initiated, decidualizing HESCs become dependent on continuous progesterone stimulation for survival (5).

In this thesis, I provide several lines of evidence implicating NADPH oxidase-dependent ROS production in the decidual process. My observations suggest that this differentiation process is highly dependent on cross-talk involving cAMP, progesterone and endogenous ROS production and signalling. Further, I present evidence that NADPH-oxidase complex governs several cellular functions in decidualizing HESCs, including redox homeostasis. Importantly, I provide preliminary data indicating that deregulation of the NOX4/$p22^{PHOX}$ complex and attenuated

endogenous ROS production in HESCs is associated with endometriosis, a chronic inflammatory gynecological disorder.

6.1 Endogenous ROS production is critical for initiating the decidual response

As mentioned briefly in the Introduction, *PRL* in the endometrium and lymphocytes is transcribed from an alternative promoter upstream of a non-coding exon, located approximately 6 kb upstream of the pituitary-specific transcriptional start-site (281). Its expression is under control of a transposable element, termed MER20, which emerged in evolution upon divergence of eutherian (placental) from non-placental mammals (282, 283). MER20 is located at -395/-148 relative to the decidual PRL transcription start-site and contains response elements for many transcription factors indispensable for decidualization and pregnancy, including FOXO1, the homeobox protein HOXA11, ETS1, C/EBPβ, and PR (284). In fact, MER20 enhancer regions are found in the vicinity of many decidua-specific genes. Although it is not yet fully elucidated, *PRL* expression is thought to involve sequential and highly coordinated actions of specific transcription factors.

A sustained rise in intracellular cAMP levels is the primary signal for *PRL* expression in HESCs, although the transcriptional response is biphasic. The initial weak response to cAMP stimulation is attributed to the binding of CREB to a non-palindromic CRE at position -12 of the decidual PRL promoter (74), thus located outside the MER20 enhancer region. However, binding of C/EBPβ to a core sequence within MER20 triggers a more pronounced response, apparent after 12 hours of cAMP stimulation. C/EBPβ in turn has been shown to bind FOXO1 (121) and recruitment of FOXO1 to MER20, which converts HOXA11 from a repressor to a strong activator of the promoter (284).

Here, I present several lines of evidence that implicate redox signalling in the initiation of the decidual process. First, I demonstrated that apocynin, a formidable inducer of endogenous ROS production in HESCs, strongly enhances cAMP-dependent decidual *PRL* and *IGFBP1* expression in primary cultures whereas DPI, AEBSF, and catalase had the opposite effect. Notably, the effect of apocynin on *PRL* and *IGFBP1* transcription was a delayed response, apparent only after 12 hours of cAMP stimulation. Treatment with apocynin alone did not induce the expression of these decidual markers nor did it sensitize the cells to MPA; thus reinforces the fact that heightened cAMP signalling is indispensable in the decidual process.

Second, HESC differentiation in response to cAMP signalling triggered rapid but complex changes in the redox status of the cell, as measured by DCF fluorescence. Such rapid and complex changes in cellular ROS levels are not unusual. For example, Sehiah et al. (2002) reported a biphasic change in ROS production in vascular smooth muscle cells within 30 minutes of stimulation H_2O_2 (285). However, the DCF results should be interpreted with some caution. For instance, DPI had no discernible effect on DCF oxidation in undifferentiated HESCs, indicating that basal ROS production is low. However, treatment with 8-br-cAMP triggered first a reduction in DCF fluorescence prior to a marked increase between 12 and 24 hours of treatment. It is possible that rapid cAMP effects on the cytoskeleton and secretome of HESCs interfere with the uptake or retention of the probe, thereby accounting for the initial rise and decline in DCF fluorescence. On the other hand, the subsequent increase in cellular oxidation fits well with the upregulation of $p22^{PHOX}$ observed upon treating HESCs with 8-br-cAMP for 16 hours and beyond. Furthermore, siRNA-mediated knockdown of NOX4/$p22^{PHOX}$ complex had no effect on the initial transient fluctuations in DCF fluorescence but abolished the rise in cellular oxidation by 24 hours of differentiation. Interestingly, an increase in endogenous ROS concentrations has been associated with adipocytes differentiation (165).

Next, I showed that knockdown of either $p22^{PHOX}$ or NOX4 is sufficient to impair *PRL* and *IGFBP1* expression in differentiating HESCs. In contrast, RAC1 silencing had no discernible effect, rendering it unlikely that NOX1, NOX2 or NOX3 are major sources of cAMP-dependent ROS production in differentiating HESCs. However, one cannot exclude a role for these homologues in regulating other aspects of the decidual process, an angle that should be explored further.

Finally, I demonstrated that C/EBPβ is a major downstream target of the activated NOX4/$p22^{PHOX}$ complex. C/EBPβ is not only essential for reproduction in all eutherian mammals tested to date (136, 286-288), but also is a key regulator of differentiation in numerous other cell types, perhaps most prominently so in adipocytes (289). Interestingly, a recent study demonstrated that low levels of ROS trigger phosphorylation and activation of C/EBPβ in 3T3-L1 pre-adipocytes, which in turn promotes mitotic clonal expansion and terminal adipocyte differentiation (289). As reported for an increasing number of cell types, NOX4 was subsequently identified as a major source of ROS production during adipocyte and vascular smooth muscle cell differentiation (197, 198). Combined with my findings, these observations suggest

that NOX4-dependent redox regulation of C/EBPβ activity may be a highly conserved mechanism that controls differentiation of very diverse cell types.

It is noteworthy to point out that apocynin strongly activated a luciferase reporter driven by consensus C/EBP response elements in undifferentiated HESCs, yet it was insufficient to elicit endogenous *PRL* or *IGFBP1* expression. Thus, cAMP signalling must exert additional effects that couple ROS-dependent C/EBPβ activation to the expression of decidual genes.

6.2 Continuous NOX4/P22^{PHOX}-dependent ROS signalling in decidualizing HESCs

I showed that NOX4 and p22^{PHOX} are both upregulated upon prolonged decidualization of HESCs, suggesting a role for the complex beyond initiation of this differentiation process. In agreement, inhibiting the NADPH-oxidase complex before or after the cells were decidualized with cAMP and MPA was equally deleterious in terms of expression of decidual marker genes.

Knockdown experiments combined with genome-wide microarray analysis indicated that the NOX4/p22^{PHOX} complex governs a myriad of genes in differentiating HESCs, a subset of which are known decidual genes (18). Gene ontology analysis indicated that redox signalling in decidualizing HESCs impacts predominantly on DNA replication, recombination and repair, and cell cycle regulation. This is not entirely surprising as, depending on concentration and duration, ROS can either promote cell cycle progression or induce arrest, which in turn may be transient, coupled to repair processes, or permanent (158, 177, 290). Therefore, an imbalance in endogenous ROS production as a result of disabling the NOX4/p22^{PHOX} complex is bound to perturb the precise and timely regulation of the cell cycle.

Several lines of evidence indicated that NOX4/p22^{PHOX} complex in decidualizing HESCs is under the control of FOXO1. First, a comparison of available microarray data revealed that over 60% of the decidual- and NOX4/p22^{PHOX}-dependent genes are also FOXO1-dependent. Importantly, the direction of perturbation of decidual-dependent genes upon NOX4/p22^{PHOX} knockdown followed that of FOXO1 silencing. Second, siRNA-mediated knockdown of FOXO1 inhibited upregulation of NOX4 and p22^{PHOX} at the protein level in differentiating HESCs. In fact, mining of gene expression data identified *NOX4* as a bona fide FOXO1 target gene. In contrast,

expression of *CYBA*, which encodes for $p22^{PHOX}$, was not affected upon FOXO1 knockdown in decidualizing HESCs (18). In agreement, while induction of $p22^{PHOX}$ is a relatively early event in the decidual process, the kinetics of NOX4 expression follow that of FOXO1, with upregulation of both proteins apparent only after two to three days of stimulation with cAMP and MPA. The fact that FOXO1 knockdown lowers $p22^{PHOX}$ levels in differentiating HESCs may reflect increased turnover of the cofactor in response to attenuated *NOX4* expression (210, 211, 220).

Together, these lines of data indicate that induction and activation of the NOX4/$p22^{PHOX}$ complex is an important mechanism through which FOXO1 regulates the expression of specific gene networks in decidual cells. However, there was no evidence of a direct feedback mechanism that couples NOX4/$p22^{PHOX}$-dependent ROS signalling to FOXO1. For example, siRNA-mediated knockdown of the NOX4/$p22^{PHOX}$ complex did not affect FOXO1 levels in decidualizing HESCs. Further, activation of the NADPH oxidase complex with apocynin, alone or in combination with cAMP, had little effect on the ability of overexpressed FOXO1 to *trans*-activate a reporter construct. However, these results should be interpreted with caution. While endogenous ROS signalling may have little direct effect on the intrinsic transcriptional activity of FOXO1, indirectly it may have a profound impact, for example by enhancing the DNA-binding activity of C/EBPβ, a major transcriptional partner of FOXO1, or by altering the subcellular localization of FOXO1.

The effect of disabling the NOX4/$p22^{PHOX}$ complex in prolonged decidualizing HESCs by siRNA-mediated knockdown was very striking. First, disabling this source of endogenous ROS triggered activation of the DNA repair pathway without apparent DNA damage or apoptosis. Second, knockdown of the NOX4/$p22^{PHOX}$ resulted in a paradoxical increase in cellular oxidation, which was accounted for by a decrease in the expression of various antioxidant enzymes. Third, the imbalance in endogenous ROS induced a cellular stress response in decidualizing HESCs, exemplified by a global hypersumoylation response and the paradoxical induction of MKP1 together with JNK activation.

Decidualization is associated with global changes in cellular sumoylation characterized by a profound hyposumoylation response (70) and uncoupling of the SUMO pathway from environmental stress signals (65). This uncoupling was shown to be important for maintaining cellular responsiveness to progesterone under oxidative stress conditions and mediated by silencing of the JNK pathway through

induction of pathway-specific phosphatases, such as MKP1 (65). Therefore, the global hypersumoylation response, increased PR stability and enhanced JNK phosphorylation observed upon disabling the NOX4/p22^{PHOX} complex are not only characteristics of a cellular stress response but also of a more undifferentiated cellular phenotype. This observation ties in nicely with the attenuation of *PRL* and *IGFBP1* expression in decidualizing HESCs observed upon knockdown of the complex.

Interestingly, JNK activation is a feature of oxidative stress response, induced by endogenous or exogenous free radicals (65, 164, 291). The activated JNK pathway in turn facilitates the translocation of FOXO1 to the nucleus (292, 293). This ROS-JNK-FOXO axis has been widely implicated in insulin resistance and an increased lifespan in worm, fly and rodents (292, 293).

FOXO1 is associated with longevity and tumour suppression (294). Induction and increased transcriptional activity of FOXO proteins is one of the main mechanisms the cell uses to counteract oxidative stress (295). Major targets of FOXO1 in various biological systems are SOD2, catalase and GADD45 (295). When mammalian cells are exposed to oxidative stress, FOXO proteins can either induce apoptosis or trigger an adaptive recovery response, characterized by induction of antioxidant enzymes and/or DNA repair response (296-299). It is therefore not surprising, that FOXO1 acts as a regulator of the cellular homeostasis in many biological systems, ranging from osteoblasts to HESCs (295, 299). FOXO1 is also indispensable for differentiation of a variety off cell types, including osteoblasts, hepatocytes and muscle cells (299-303). Knockdown of FOXO1 in decidualizing HESCs leads to increased proliferation and perturbs the expression of differentiation markers (18, 301). Importantly, several FOXO1 target genes are intermediates in upstream regulatory pathways, including insulin receptor (*INSR*), and bone morphogenic protein and activin-membrane-bound inhibitor (*BAMBI*), suggesting the presence of complex feedback mechanisms that enables FOXO1 to fine-tune the cell's response to its microenvironment (18, 295). Interestingly, knockdown of NOX4/p22^{PHOX} in differentiating HESCs deregulated a subset of previously identified FOXO1-dependent genes resulting in concomitant shutdown and activation of two major cellular defense mechanisms: free radical scavenging and the DNA repair pathway, respectively.

In other words, my findings suggest that FOXO1 maintains the redox homeostasis of decidualizing HESCs via regulation of the NOX4/p22^{PHOX} complex. As knockdown of

FOXO1 abolishes the burst in ROS production in decidualizing cells, it seems logical to postulate that endogenous free radical signalling is responsible for the induction of antioxidant enzymes, such as SOD2, TXN and GPx. This might explain why knockdown of the NOX4/p22^{PHOX} complex triggers a paradoxical prooxidant response in decidualizing HESCs. These observations further suggest that heightened endogenous free radical production in differentiating HESCs might serve as a "hormetic" or a "preconditioning" adaptive mechanism that protects the cells from further insults by switching on the cellular defense mechanisms against oxidative stress. Hormesis is a phenomenon that occurs in various physiological processes like aging, whereby exposure to relatively low levels of stress cues protects the cells from further stronger insults (304, 305). In fact, Droge (2002) reported that elevated ROS concentrations induce the expression of genes that encode for proteins with antioxidant properties in a variety of cells and proposes that this is a mechanism, conserved in eukaryotes as well as prokaryotes, by which cells maintain redox homeostasis (149). For instance, bacterial cells possess different signalling pathways that respond to increase concentrations of ROS or a shift in the cellular redox status (149, 306-308). In *Escherichia coli*, the transcription factor OxyR responds to low levels of H_2O_2 and activates the expression of antioxidant defence genes (309, 310). It should be pointed out the OxyR is just one of many transcription factors bacterial cells posses to regulate and maintain their redox homeostasis (306-308). The budding yeast *Saccharomyces cerevisiae* also maintains its redox homeostasis through oxidative activation of the transcription factor yAP-1 which in turn induces the expression of genes that encode for proteins with antioxidant properties, including SOD, catalase and glutathione reductase (149, 311, 312). Interestingly, Droge (2002) refers to the oxidative burst as a regulatory event that leads to a temporary imbalance in the cellular redox status in order to switch on the antioxidant defence mechanism, which is critical for maintaining cellular competence (149).

6.3 Deregulation of the NADPH oxidase complex in endometriosis

Endometriosis is a condition associated with chronic inflammation and blunted response to cAMP and progesterone signalling in eutopic and ectopic endometrium. The consequences of disruption of the NOX4/p22^{PHOX} complex in decidualizing HESCs yielded a number of characteristics that are common to endometrial cells of patients with endometriosis.

First, the paradoxical increase in cellular oxidation has also been reported in the eutopic endometrium of patients with endometriosis (172). However, it should be pointed out that an increase in endogenous ROS concentration, especially in ectopic lesions, could reflect infiltration of immune cells capable of producing large amounts of ROS upon interaction with cytokines or foreign particles (165, 292). Second, endometriosis is associated with impaired immunosurveillance and affected patients have an increased incidence of atopic and autoimmune disorders (249, 254-256). The loss of either NOX4 or $p22^{PHOX}$ causes defects in the innate immune system (147, 194, 203). In fact, growing evidence implicates NADPH oxidase enzymes in signalling following pathogen recognition by toll like receptors and in the modulation of dendritic cell functions, two key aspects of innate immunity. This raises the question whether the relatively low levels of $p22^{PHOX}$ in patients with endometriosis might contribute to the chronic inflammation that characterizes the ectopic implants. Third, $p22^{PHOX}$ deficiency and the lack of the oxidative burst in differentiating HESCs fit well with the blunted response to cAMP and progesterone signalling observed in this condition (238, 257). In fact, my finding that knockdown of NOX4 and $p22^{PHOX}$ induces a hypersumoylation response, which in turn stabilizes and represses the liganded PR (65), may provide a mechanistic explanation for the apparent endometrial progesterone-resistance in affected patients.

As mentioned previously in the introduction, decidualization of HESCs is an intriguing example of MET. Combining the effects obtained upon disabling the NOX4/$p22^{PHOX}$ in decidualizing HESCs, the consistent loss of $p22^{PHOX}$ observed in endometriosis and the characteristics of endometriotic cells, my results might suggest that NOX4/$p22^{PHOX}$-dependent ROS signalling play a role in MET/EMT dynamic transition of HESCs. Endometriotic cells are motile and migrate out of the endometrium through retrograde menstruation. This might indicate that the MET is perturbed in such a condition. MET/EMT processes are dynamic; thereby the loss of the NOX4/$p22^{PHOX}$ complex may tip the balance towards EMT in endometriosis. This is similar to what has been observed in metastatic cancerous cells (27). In fact, EMT in tumourogenesis is a response to microenvironment signals and is required for cancer cell survival through acquiring motile and invasive properties (28, 313-315). Interestingly, several studies have demonstrated both direct and indirect evidence linking the role of endogenous ROS in EMT/MET (316).

6.4 Endometrial hormesis and endometriosis

The prolonged cellular stress in decidualizing HESCs as a consequence of disruption of the NOX4/p22^{PHOX} complex was associated with activation of the DNA repair pathway in the absence of discernible DNA damage or apoptosis. Since the NOX4/p22^{PHOX} complex is deregulated in eutopic endometrium from patients with endometriosis, this illicit activation of the DNA repair pathway may convey a survival advantage for HESCs at the time of menstruation by increasing resistance to environmental stressors, thereby facilitating implantation of endometrial cells at ectopic sites, such as the peritoneal cavity. In fact, activation of the DNA repair pathway is an integral part of hormesis and ischemic preconditioning (317, 318).

The concept of hormesis does not only apply to cells and organs but also to the whole organism. For example, a limited reduction of nutritional calorie uptake, so-called calorie restriction, has been shown to increase cellular ROS, stress resistance and ultimately longevity in a variety of species and model organisms (319-321). Exposure of *Ceanorabiditis elegans* to stress conditions that induces ROS concentration resulted in increased life span (322, 323). Conversely, co-treatment of nematodes with several different antioxidants, which inactivate ROS fully, abolishes the life-extending effects of calorie restriction, providing direct evidence for an essential role of increased ROS formation in extension of life span (324).

Whether or not these observations are translatable to human health has been a matter of ongoing debate. Two prospective investigations of the effects of calorie restriction on long-lived nonhuman primate species began nearly 25 years ago and are still under way. While still preliminary, prolonged calorie restriction appears to extend the lifespan of rhesus monkeys, slow the rate of muscle loss with age, and lower incidence of neoplasia, cardiovascular disease, type 2 diabetes mellitus, and apparently endometriosis (325). The latter observation, if confirmed, appears to contradict that endometrial hormesis in response to impaired NADPH-oxidase function, contributes to the formation of ectopic implants. On the other hand, increasing amount of evidence have associated low amount of endogenous ROS with physiological function and high amount of endogenous ROS with detrimental and pathological events. The amount of endogenous ROS observed upon knockdown of the NOX4/p22^{PHOX} seems beneficial on a cellular level as it confers resistance through activation of the DNA repair pathway and protection against apoptosis, yet pathological on the organism level if it manifests in a gynecological

disorder like endometriosis. Interestingly, this scenario is observed in tumourogenesis.

The consistent loss of $p22^{PHOX}$ in patients with endometriosis raises the most obvious question about the mechanism that underpins such loss. The consistent low levels of $p22^{PHOX}$ transcript rule out the option that the loss observed at the protein level is a result of a post transcription modification. Loss of $p22^{PHOX}$ could be a result of a single nucleotide polymorphism (SNP). SNPs can predispose to various diseases, however, genome-wide association studies have not implicated $p22^{PHOX}$ polymorphism with endometriosis. Polymorphism in $p22^{PHOX}$ may explain the associated defective immunosurveillance in patients with endometriosis. The other two mechanisms that can account for the loss of $p22^{PHOX}$ is misregulation by microRNA (miRNA) or aberrant epigenetics marks. Altered regulation of miRNA and miRNA-regulated pathways have been associated with ectopic and eutopic endometrium of patients with endometriosis (326, 327). Interestingly, various studies have associated aberrant methylation with endometriosis. Aberrant epigenetic regulation has been reported for PR-B, E-cadherin, HOXO10, ER-β and SRC1 (36, 37, 248). Deregulation in DNMTs, which are enzymes that incorporate a methyl group onto a 5'-carbon position of cytosine bases in CpG islands, have also been reported in endometriosis (248). This suggests that $p22^{PHOX}$ methylation state might be aberrantly regulated in endometriosis resulting in low expression at the mRNA and protein level.

Despite reports linking downregulation of FOXO1 in endometriosis, my results suggest that endometriosis is only associated with the consistent loss of $p22^{PHOX}$ (257, 274, 275). FOXO1 levels, on the contrary, appear normal. If this observation holds true, then the presence of FOXO1 might be what distinguishes endometriosis from endometrial cancer, since FOXO1 expression in the latter appears low (328, 329). There are a number of similarities in the cellular characteristics between the two clinical conditions (Figure 6.1). First, both cancerous cells and endometriotic cells are able to migrate and invade different tissues in different parts of the body (330). Second, both conditions are associated with high level of ROS (170, 172, 330). Third, cancerous cells and endometriotic cells are both associated with increased survival. Fourth, in both conditions, cellular phenotype seems in favour of EMT rather than MET. Finally, the DNA damage and repair pathway in both clinical conditions appears to be deregulated. The major difference between the two conditions though lies in the fact that endometriosis is a benign condition whereas cancer, if not

controlled, is fatal. This difference may be attributed to the presence of normal levels of FOXO1 in endometriosis but not in cancer. To elucidate the mechanism behind this, extensive experimental work is required. However, this preliminary observation and following hypothesis could be attributed to the activation of the DNA repair pathway, in endometriosis, in the absence of DNA damage. Interestingly, alterations in the DNA has been linked with cell fate regulation and reproductive disorders. Hapangama et al. reported increased in telomere length in women with reproductive failure compared to control groups (331).

In conclusion, here I present conclusive evidence that NOX4/$p22^{PHOX}$ dependent ROS signalling introduces a different level of cross-talk in decidualization. Endogenous ROS signalling is not only critical for initiating the decidual process but also plays a role in maintaining this differentiation and may contribute to the MET process. Further, knockdown of the NOX4/$p22^{PHOX}$ complex disturbs the redox homeostasis of the cell but confers resistance to DNA damage by activating the DNA repair pathway. Linking these observations with the loss of $p22^{PHOX}$ in endometriosis, I hypothesize that downregulation of the NOX4/$p22^{PHOX}$ complex tips the redox balance in favour of prooxidants which leads to activation of the DNA damage pathway in the absence of DNA damage, reversal of the epithelial phenotype to mesenchymal characteristics with increased cell motility and invasiveness and induction of inappropriate survival of stressed cells, which in turn can manifest in reproductive system disorders like endometriosis.

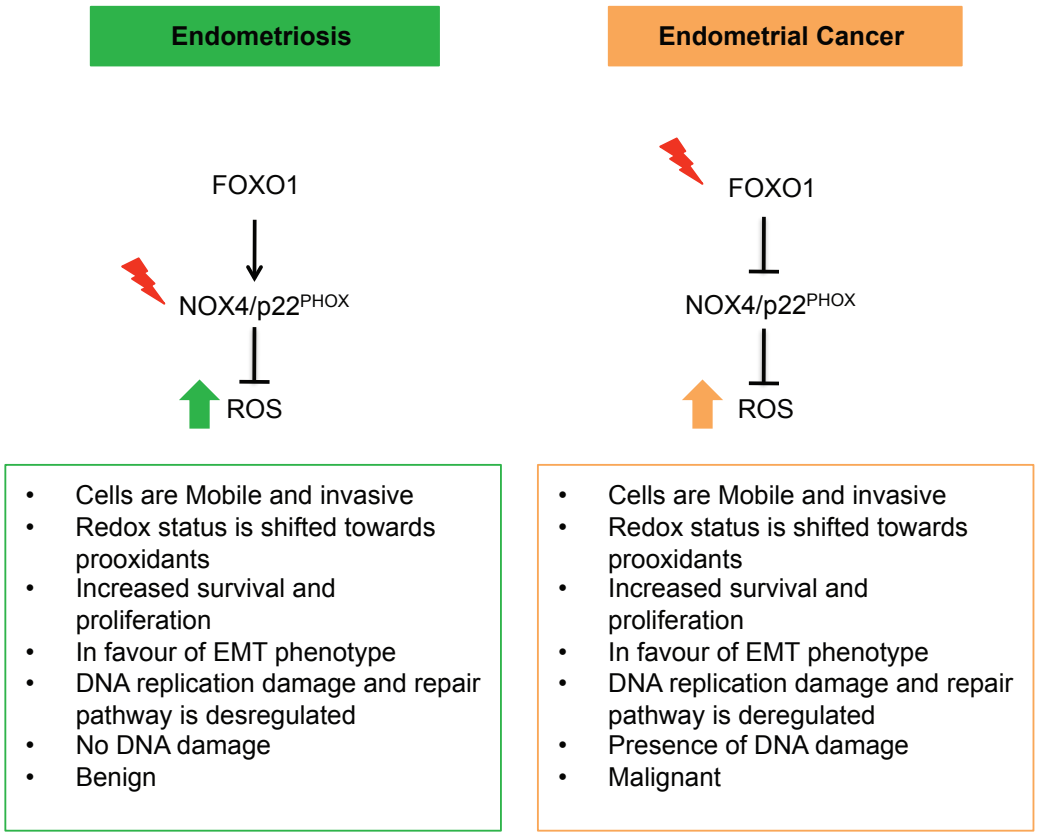


Fig 6.1 Similarities between endometriosis and endometrial cancer. The diagram illustrates the similarities and differences between the two clinical conditions. The lightening bolts indicate perturbations FOXO1 appears to be deregulated in endometrial cancer but not in endometriosis.

Appendices

Appendix 1

RTQ-PCR primer pairs

Gene	Forward Primer	Reverse Primer
BIRC5	GGACCACCGCATCTCTACAT	GTCTGGCTCGTTCTCAGTGG
BRCA2	TGGTATGTGGGAGTTTGTTTCA	ATCAGGATCCACCTCAGCTC
COLEC10	TCCAGGAGAAGAGGGAAAGC	CTTGCCAATATTGCCCTGAT
FOXO1	TGGACATGCTCAGCAGACATC	TTGGGTCAGGCGGTTCA
GPx3	GAAGTAACTGAAGGCCGTCTCATC	CACGGATTTCTTCCTGAACAAAG
IGFBP1	CGAAGGCTCTCCATGTCACCA	TGTCTCCTGTGCCTTGGCTAAAC
L19	GCGGAAGGGTACAGCCAA	GCAGCCGGCGCAAA
NOX4	AGCAACATTTGGGGTTCATC	GGCAGAATTTCGGAGTCTTG
PRL	AAGCTGTAGAGATTGAGGAGCAAAC	TCAGGATGAACCTGGCTGACTA
$P22^{PHOX}$	ATGACCGCCGTGGTGAAG	GGCACCGAGAGCAGGAGA
RAC1	TGCAGACACTTGCTCTCCTATGTAG	GAGTTCAATGGCAACGCTTCA
SOD2	AATTGCTGCTTGTCCAAATCAG	TCCCCAGCAGTGGAATAAGG
TXN	TGTGGATGACTGTCAGGATGTTG	TGTCCCTTCTTAAAAAACTGGAATG

Appendix 2

NOX4/p22^{PHOX}-repressed genes

Gene Name	Description	Fold-Change
BIRC5*	baculoviral IAP repeat-containing 5	4.22
CENPF*	centromere protein F, 350/400ka (mitosin)	3.66
NCAPG	non-SMC condensin I complex, subunit G	3.36
ANLN*	anillin, actin binding protein	3.16
TYMS*	thymidylate synthetase	3.15
ASPM*	asp (abnormal spindle) homolog, microcephaly associated	3.09
DLGAP5	discs, large (Drosophila) homolog-associated protein 5	3.07
CEP55	centrosomal protein 55kDa	2.95
HMMR*	hyaluronan-mediated motility receptor (RHAMM)	2.95
NUSAP1*	nucleolar and spindle associated protein 1	2.87
NDC80	NDC80 homolog, kinetochore complex component	2.86
MLF1IP*	MLF1 interacting protein	2.82
TOP2A*	topoisomerase (DNA) II alpha	2.80
PRC1*	protein regulator of cytokinesis 1	2.70
DTL	denticleless homolog)	2.67
KIF11*	kinesin family member 11	2.65
MKI67	antigen identified by monoclonal antibody Ki-67	2.62
NUF2	NUF2, NDC80 kinetochore complex component, homolog	2.58
KIAA0101*	KIAA0101	2.56
EBF1	early B-cell factor 1	2.47
AOX1	aldehyde oxidase 1	2.45
TPX2*	TPX2, microtubule-associated, homolog (Xenopus laevis)	2.45
ATAD2	ATPase family, AAA domain containing 2	2.43
CASC5	cancer susceptibility candidate 5	2.42
BUB1B*	budding uninhibited by benzimidazoles 1 homolog beta	2.37
KIF20A*	kinesin family member 20A	2.36
MELK*	maternal embryonic leucine zipper kinase	2.34
REV3L	REV3-like, catalytic subunit of DNA polymerase zeta	2.32
SORBS1	sorbin and SH3 domain containing 1	2.30
CLSPN	claspin homolog (Xenopus laevis)	2.20
CCNB1*	cyclin B1	2.18
CCNB2*	cyclin B2	2.18
RRM2	ribonucleotide reductase M2	2.18
BTN3A3*	butyrophilin, subfamily 3, member A3	2.16
KIF4A*	kinesin family member 4A	2.16

MELTTL7A	methyltransferase like 7A	2.16
NEK2*	NIMA (never in mitosis gene a)-related kinase 2	2.14
SHCBP1	SHC SH2-domain binding protein 1	2.14
CENPE*	centromere protein E, 312kDa	2.13
CYP1B1	cytochrome P450, family 1, subfamily B, polypeptide 1	2.12
NFIA*	nuclear factor I/A	2.10
THNSL1*	threonine synthase-like 1	2.09
KIF18A	kinesin family member 18A	2.07
SPC25	SPC25, NDC80 kinetochore complex component, homolog	2.07
SNORD21	small nucleolar RNA, C/D box 21	2.05
BUB1*	budding uninhibited by benzimidazoles 1 homolog (yeast)	2.03
CKAP2L	cytoskeleton associated protein 2-like	2.02
FAM111B	family with sequence similarity 111, member B	2.02
KIF20B	kinesin family member 20B	2.02
ITGA6*	integrin, alpha 6	1.99
RACGAP1*	Rac GTPase activating protein 1	1.97
CENPK	CENPK // centromere protein K	1.96
JAZF1*	JAZF zinc finger 1	1.96
BARD1*	BRCA1 associated RING domain 1	1.94
MLLT6	myeloid/lymphoid or mixed-lineage leukemia	1.94
CCNE2	cyclin E2	1.93
HSD17B6	hydroxysteroid (17-beta) dehydrogenase 6 homolog	1.93
PRKG1	protein kinase, cGMP-dependent, type I	1.93
P2RY1	purinergic receptor P2Y, G-protein coupled, 1	1.92
FAM72D	family with sequence similarity 72, member D	1.91
MAD2L1*	MAD2 mitotic arrest deficient-like 1 (yeast)	1.89
LRRC4C	leucine rich repeat containing 4C	1.88
RAD51AP1*	RAD51 associated protein 1	1.88
SNORD61	small nucleolar RNA, C/D box 61	1.88
PLK4	polo-like kinase 4	1.86
C14orf143	chromosome 14 open reading frame 143	1.85
SNORD30	small nucleolar RNA, C/D box 30	1.84
PRIM1	primase, DNA, polypeptide 1 (49kDa)	1.83
CACNB2	calcium channel, voltage-dependent, beta 2 subunit	1.79
DEPDC1*	DEP domain containing 1	1.79
TSHZ1	teashirt zinc finger homeobox 1	1.79
TTK*	TTK protein kinase	1.79
CD109*	CD109 molecule	1.78
IRAK3	interleukin-1 receptor-associated kinase 3	1.78
NRXN3*	neurexin 3	1.78
TXNRD3IT1	thioredoxin reductase 3 intronic transcript 1	1.78

TAF7L	TAF7-like RNA polymerase II, TATA box binding protein	1.77
ELMO1	engulfment and cell motility 1	1.76
ACE2	angiotensin I converting enzyme (peptidyl-dipeptidase A)	1.75
CNR1	cannabinoid receptor 1 (brain)	1.74
FAM65B	family with sequence similarity 65, member B	1.74
FGGY	FGGY carbohydrate kinase domain containing	1.74
CDC2*	cell division cycle 2, G1 to S and G2 to M	1.73
TRAF5	TNF receptor-associated factor 5	1.73
C8orf79	chromosome 8 open reading frame 79	1.72
ALDH1L2	aldehyde dehydrogenase 1 family, member L2	1.70
SLC39A8*	solute carrier family 39 (zinc transporter), member 8	1.70
TRPC4	transient receptor potential cation channel, subfamily C,	1.69
ALS2CR8	amyotrophic lateral sclerosis 2 (juvenile) chromosome region candidate 8	1.68
DCLRE1B	DNA cross-link repair 1B	1.68
FBXO5*	F-box protein 5	1.68
NRIP3	nuclear receptor interacting protein 3	1.68
SKA3	spindle and kinetochore associated complex subunit 3	1.68
DHFR*	dihydrofolate reductase	1.67
PRR11	proline rich 11	1.67
LDB2*	LIM domain binding 2	1.65
PCDH19*	protocadherin 19	1.65
CCNA2*	cyclin A2	1.64
HSPB1	heat shock 27kDa protein 1	1.64
PSMB9*	proteasome (prosome, macropain) subunit, beta type, 9	1.64
PTTG1*	pituitary tumor-transforming 1	1.64
NUP37	nucleoporin 37kDa	1.63
SGOL1	shugoshin-like 1 (S. pombe)	1.63
SP110	SP110 nuclear body protein	1.63
ARHGEF6	Rac/Cdc42 guanine nucleotide exchange factor (GEF) 6	1.62
FABP5	fatty acid binding protein 5 (psoriasis-associated)	1.62
PLK1	polo-like kinase 1 (Drosophila)	1.62
RNASEH2A*	ribonuclease H2, subunit A	1.62
DHFR*	dihydrofolate reductase	1.59
NPAS2	neuronal PAS domain protein 2	1.59
SNAI2	snail homolog 2 (Drosophila)	1.59
C6orf173*	chromosome 6 open reading frame 173	1.58
KIAA1524	KIAA1524	1.58
PLXNA4	plexin A4	1.57
UBE2C*	ubiquitin-conjugating enzyme E2C	1.57
ADAM32	ADAM metallopeptidase domain 32	1.56

ALG6	asparagine-linked glycosylation 6, alpha-1,3-glucosyltransf	1.56
ANKRD13B	ankyrin repeat domain 13B	1.56
RGS2	regulator of G-protein signalling 2, 24kDa	1.56
BRIP1*	BRCA1 interacting protein C-terminal helicase 1	1.55
DNA2	DNA replication helicase 2 homolog (yeast)	1.55
KIF15	kinesin family member 15	1.55
MARVELD2	MARVEL domain containing 2	1.55
MSL3L2	male-specific lethal 3-like 2	1.55
DRAM1	DNA-damage regulated autophagy modulator 1	1.54
KIF14*	kinesin family member 14	1.54
LASS6	LAG1 homolog, ceramide synthase 6	1.54
BCAT1	branched chain aminotransferase 1, cytosolic	1.53
EBPL	emopamil binding protein-like	1.53
LOC100289612	arsenic transactivated protein 1	1.53
ZNF311	ZNF311 // zinc finger protein 311	1.52
ACSS2	acyl-CoA synthetase short-chain family member 2	1.51
C15orf41	chromosome 15 open reading frame 41	1.51
APOBEC3F	apolipoprotein B mRNA editing enzyme, catalytic polypep	1.50
C6orf192*	chromosome 6 open reading frame 192	1.50
NRCAM*	neuronal cell adhesion molecule	1.50
POLH*	polymerase (DNA directed), eta	1.50
SCARNA9L	small Cajal body-specific RNA 9-like (retrotransposed)	1.50
C11orf1	chromosome 11 open reading frame 1	1.49
DPH5	DPH5 homolog	1.49
S100A4	S100 calcium binding protein A4	1.49
TCF19	transcription factor 19	1.49
HOXA13	homeobox A13	1.48
MPHOSPH9*	M-phase phosphoprotein 9	1.48
NBN	nibrin	1.48
S100A10*	S100 calcium binding protein A10	1.48
SNORA14B	small nucleolar RNA, H/ACA box 14B	1.48
SPRY2	sprouty homolog 2 (Drosophila)	1.48
AHCY*	adenosylhomocysteinase	1.47
APOBEC3C*	apolipoprotein B mRNA editing enzyme, catalytic polypep	1.47
FOXM1*	forkhead box M1	1.47
NCAPD2	non-SMC condensin I complex, subunit D2	1.47
NSUN6*	NOL1/NOP2/Sun domain family, member 6	1.47
PMCH	pro-melanin-concentrating hormone	1.47
RNF39	ring finger protein 39	1.47
SAMD13	sterile alpha motif domain containing 13	1.47

VGLL3	vestigial like 3	1.47
SMC2*	structural maintenance of chromosomes 2	1.47
STXBP6*	syntaxin binding protein 6 (amisyn)	1.47
CADPS2*	Ca++-dependent secretion activator 2	1.46
MOSC2	MOCO sulphurase C-terminal domain containing 2	1.46
PIK3C2B	phosphoinositide-3-kinase, class 2, beta polypeptide	1.46
XRCC6BP1	XRCC6 binding protein 1	1.46
DENND2C	DENN/MADD domain containing 2C	1.45
MTHFD1	methylenetetrahydrofolate dehydrogenase (NADP+ dependent)	1.45
ACLY*	ATP citrate lyase	1.44
CHCHD6	coiled-coil-helix-coiled-coil-helix domain containing 6	1.44
OBFC1	oligonucleotide/oligosaccharide-binding fold containing 1	1.44
PARG	poly (ADP-ribose) glycohydrolase	1.44
SIAE	sialic acid acetylesterase	1.44
SNORA7B	small nucleolar RNA, H/ACA box 7B	1.44
TCEANC	transcription elongation factor A (SII) N-terminal	1.44
VAMP5	vesicle-associated membrane protein 5 (myobrevin)	1.44
ZNF470	zinc finger protein 470	1.44
CCDC111	coiled-coil domain containing 111	1.43
LRIG3	leucine-rich repeats and immunoglobulin-like domains 3	1.43
SLC25A37	solute carrier family 25, member 37	1.43
CKAP2*	cytoskeleton associated protein 2	1.42
DISP1	dispatched homolog 1 (Drosophila)	1.42
PRIM2	primase, DNA, polypeptide 2 (58kDa)	1.42
SAMD4A	sterile alpha motif domain containing 4A	1.42
STK39*	serine threonine kinase 39	1.42
TNIP2	TNFAIP3 interacting protein 2	1.42
ALDH18A1*	aldehyde dehydrogenase 18 family, member A1	1.41
FIGNL1*	fidgetin-like 1	1.41
GBP1	guanylate binding protein 1, interferon-inducible, 67kDa	1.41
HARBI1	harbinger transposase derived 1	1.41
KLF7	Kruppel-like factor 7 (ubiquitous)	1.41
LOC644714	hypothetical protein LOC644714	1.41
NEFL	neurofilament, light polypeptide	1.41
NUP85	nucleoporin 85kDa	1.41
PTCD2*	pentatricopeptide repeat domain 2	1.41
ZNF876P	zinc finger protein 876 (pseudogene)	1.41
C4orf21	chromosome 4 open reading frame 21	1.40
GYG1	glycogenin 1	1.40
MYC	v-myc myelocytomatosis viral oncogene homolog (avian)	1.40

TMEM194B	transmembrane protein 194B	1.40
BIRC5*	baculoviral IAP repeat-containing 5	1.39
STIL	SCL/TAL1 interrupting locus	1.39
IMPDH2	IMP (inosine monophosphate) dehydrogenase 2	1.38
KDELR3*	KDEL (Lys-Asp-Glu-Leu) endoplasmic reticulum protein	1.38
NEIL3	nei endonuclease VIII-like 3	1.38
BLM	Bloom syndrome, RecQ helicase-like	1.37
HTRA2	HtrA serine peptidase 2	1.37
INPP1	inositol polyphosphate-1-phosphatase	1.37
OR2A9P	olfactory receptor, family 2, subfamily A, member 9	1.37
CDCA2*	cell division cycle associated 2	1.36
HRSP12	heat-responsive protein 12	1.36
INTS3	integrator complex subunit 3	1.36
LASP1	LIM and SH3 protein 1	1.36
SATB2	SATB homeobox 2	1.36
TRIP13*	thyroid hormone receptor interactor 13	1.36
TUBG2	tubulin, gamma 2	1.36
ZNF471	zinc finger protein 471	1.36
CDC42EP4	CDC42 effector protein (Rho GTPase binding) 4	1.35
DCAF11	DDB1 and CUL4 associated factor 11	1.35
FANCI	Fanconi anemia, complementation group I	1.35
HSPA4L	heat shock 70kDa protein 4-like	1.35
MTBP	Mdm2, transformed 3T3 cell double minute 2, p53 binding protein	1.35
RBM43	RNA binding motif protein 43	1.35
SDR39U1	short chain dehydrogenase/reductase family 39U, member 1	1.35
RMI1	RMI1, RecQ mediated genome instability 1, homolog	1.35
SPAG5*	sperm associated antigen 5	1.35
TARSL2	threonyl-tRNA synthetase-like 2	1.35
ACTN1*	actinin, alpha 1	1.34
C15orf42	chromosome 15 open reading frame 42	1.34
C3orf31	chromosome 3 open reading frame 31	1.34
TMEM216	transmembrane protein 216	1.34
ZNF383	zinc finger protein 383	1.34
ZNF518A	zinc finger protein 518A	1.34
CCDC99	coiled-coil domain containing 99	1.33
FOXN2	forkhead box N2	1.33
MCM10	minichromosome maintenance complex component 10	1.33
MTHFD2	methylenetetrahydrofolate dehydrogenase (NADP+ dependent)	1.33
NDRG3	NDRG family member 3	1.33

PHKA2	phosphorylase kinase, alpha 2 (liver)	1.33
POLA1	polymerase (DNA directed), alpha 1, catalytic subunit	1.33
PPIL3*	peptidylprolyl isomerase (cyclophilin)-like 3	1.33
RPL39L	ribosomal protein L39-like	1.33
RPP40	ribonuclease P/MRP 40kDa subunit	1.33
SGOL2	shugoshin-like 2 (S. pombe)	1.33
VCL*	vinculin	1.33
AASS	aminoadipate-semialdehyde synthase	1.32
ARL9	ADP-ribosylation factor-like 9	1.32
APAF1	apoptotic peptidase activating factor 1	1.32
BIVM*	basic, immunoglobulin-like variable motif containing	1.32
BTN3A1	butyrophilin, subfamily 3, member A1	1.32
CCDC6	coiled-coil domain containing 6	1.32
E2F4	E2F transcription factor 4, p107	1.32
MLLT10	myeloid/lymphoid or mixed-lineage leukemia	1.32
PSTK	phosphoseryl-tRNA kinase	1.32
PTPLA	protein tyrosine phosphatase-like	1.32
PTTG3P	pituitary tumor-transforming 3	1.32
QARS	glutaminyl-tRNA synthetase	1.32
SGMS1	sphingomyelin synthase 1	1.32
SHMT2	serine hydroxymethyltransferase 2 (mitochondrial)	1.32
TRERF1*	transcriptional regulating factor 1	1.32
WDR5B	WDR5B	1.32
ATP8B4	ATPase, class I, type 8B, member 4	1.31
BRCA2	breast cancer 2, early onset	1.31
C14orf43	chromosome 14 open reading frame 43	1.31
CDH13	cadherin 13, H-cadherin (heart)	1.31
GPR88	G protein-coupled receptor 88	1.31
HIST1H2AM	histone cluster 1, H2am	1.31
HMGB1	high-mobility group box 1	1.31
KCNMB4	potassium large conductance calcium-activated channel	1.31
KDM4C	lysine (K)-specific demethylase 4C	1.31
LRRC9	leucine rich repeat containing 9	1.31
NUDT10	nudix (nucleoside diphosphate linked moiety X)-type motif	1.31
PLP2	proteolipid protein 2 (colonic epithelium-enriched)	1.31
PRDM8	PR domain containing 8	1.31
RNF39	RNF39 // ring finger protein 39	1.31
RPS27L	ribosomal protein S27-like	1.31
TDRD3	tudor domain containing 3	1.31
ZCCHC7*	zinc finger, CCHC domain containing 7	1.31
ZNF30*	zinc finger protein 30	1.31

MYO9A	myosin IXA	1.30
NUP205	nucleoporin 205kDa	1.30
OIP5*	Opa interacting protein 5	1.30
OR5K2	olfactory receptor, family 5, subfamily K, member 2	1.30
SF3A2	splicing factor 3a, subunit 2, 66kDa	1.30

Key:

Red: Decidual-induced genes
Blue: Decidual-repressed genes
Italics: FOXO1-induced
***: Genes identified by Talbi et al (2006) to be repressed during the secretory phase of the menstrual cycle**

Appendix 3

NOX4/p22^{PHOX}-induced genes

Gene Name	Description	Fold-Change
MYO15B	myosin XVB pseudogene	-1.30
PAPOLG*	poly(A) polymerase gamma	-1.30
CNTN4*	contactin 4	-1.31
GAN	gigaxonin	-1.31
IGF1R*	insulin-like growth factor 1 receptor	-1.31
NR1D2	nuclear receptor subfamily 1, group D, member 2	-1.31
WDSUB1	WD repeat, sterile alpha motif and U-box domain	-1.31
ZNF441	zinc finger protein 441	-1.31
CSNK1E	casein kinase 1, epsilon	-1.32
CYTH2	cytohesin 2	-1.32
ELF4	E74-like factor 4 (ets domain transcription factor)	-1.32
TTLL7	tubulin tyrosine ligase-like family, member 7	-1.32
ZBTB38	zinc finger and BTB domain containing 38	-1.32
CCL22	chemokine (C-C motif) ligand 22	-1.33
PHF16*	PHD finger protein 16	-1.33
POM121L9P	POM121 membrane glycoprotein-like 9 (rat) pseudogene	-1.33
RHBDD2	rhomboid domain containing 2	-1.33
TNFRSF21*	tumor necrosis factor receptor superfamily member 21	-1.33
ZNF708	zinc finger protein 708	-1.33
EML5	echinoderm microtubule associated protein like 5	-1.34
HS3ST3B1*	heparan sulfate (glucosamine) 3-O-sulfotransferase 3B1	-1.34
RHBDD1	family with sequence similarity 100, member B	-1.34
BEX1	brain expressed, X-linked 1	-1.35
CD46	CD46 molecule, complement regulatory protein	-1.35
IFNAR2*	interferon (alpha, beta and omega) receptor 2	-1.35
LRRC37B	leucine rich repeat containing 37B	-1.35
PARP9	poly (ADP-ribose) polymerase family, member 9	-1.35
PDCD6IP	programmed cell death 6 interacting protein	-1.35
RBBP6*	retinoblastoma binding protein 6	-1.35
NAG18	NAG18 mRNA	-1.36
PLK3	polo-like kinase 3 (Drosophila)	-1.36
ZBTB34*	zinc finger and BTB domain containing 34	-1.36
ARHGDIA*	Rho GDP dissociation inhibitor (GDI) alpha	-1.37
C110RF61	chromosome 11 open reading frame 61	-1.37
DUSP22	dual specificity phosphatase 22	-1.37
FOSL2*	FOS-like antigen 2	-1.37
MEX3B	mex-3 homolog B	-1.37
SLC7A11	solute carrier family 7	-1.37
UBE2D1*	ubiquitin-conjugating enzyme E2D 1	-1.37
ACPP*	acid phosphatase, prostate	-1.37
ARL6IP1	ADP-ribosylation factor-like 6 interacting protein 1	-1.38
SIK1	salt-inducible kinase 1	-1.38

E2F6	E2F transcription factor 6	-1.39
EYA1	eyes absent homolog 1	-1.39
NETO1	neuropilin (NRP) and tolloid (TLL)-like 1	-1.39
TTC7B*	tetratricopeptide repeat domain 7B	-1.39
ZNF720	zinc finger protein 720	-1.39
COL24A1	collagen, type XXIV, alpha 1	-1.40
KLF3*	Kruppel-like factor 3 (basic)	-1.40
KU-MEL-3	KU-MEL-3	-1.40
SNCAIP*	synuclein, alpha interacting protein	-1.40
SOX4*	SRY (sex determining region Y)-box 4	-1.40
MAML3	mastermind-like 3 (Drosophila)	-1.41
GPR137B	G protein-coupled receptor 137B	-1.41
CUL4B	cullin 4B	-1.42
SLC20A1*	solute carrier family 20 (phosphate transporter)	-1.42
AGPAT9	1-acylglycerol-3-phosphate O-acyltransferase 9	-1.43
DDX60L	DEAD (Asp-Glu-Ala-Asp) box polypeptide 60-like	-1.43
LRRC8A	leucine rich repeat containing 8 family, member A	-1.43
RAB30	RAB30, member RAS oncogene family	-1.43
RFK*	riboflavin kinase	-1.43
ATXN7L1	ataxin 7-like 1	-1.45
IFITM1*	interferon induced transmembrane protein 1 (9-27)	-1.45
WHAMML1	WAS protein homolog associated with actin, golgi membran	-1.45
MYO10	myosin X	-1.45
CDKN2B*	NM_078487 cyclin-dependent kinase inhibitor 2B	-1.46
EMP2	epithelial membrane protein 2	-1.46
CPEB4*	cytoplasmic polyadenylation element binding protein 4	-1.49
RHOH*	ras homolog gene family, member H	-1.49
C10orf58*	chromosome 10 open reading frame 58	-1.50
DDI2	DDI1, DNA-damage inducible 1, homolog 2	-1.50
AGPAT5	1-acylglycerol-3-phosphate O-acyltransferase 5	-1.52
CD68	CD68 molecule	-1.53
ZDHHC2	zinc finger, DHHC-type containing 2	-1.53
ABCC9	ATP-binding cassette, sub-family C (CFTR/MRP), member 9	-1.54
HTRA3	HtrA serine peptidase 3	-1.54
DYNC1I2	dynein, cytoplasmic 1, intermediate chain 2	-1.55
NTRK2	neurotrophic tyrosine kinase, receptor, type 2	-1.56
SNCA	synuclein, alpha	-1.56
SYT11*	synaptotagmin XI	-1.56
BAMBI*	BMP and activin membrane-bound inhibitor homolog	-1.57
CEP135	centrosomal protein 135kDa	-1.57
PARP4	poly (ADP-ribose) polymerase family, member 4	-1.57
ZNF704	zinc finger protein 704	-1.57
AKD1	adenylate kinase domain containing 1	-1.58
PHACTR2*	phosphatase and actin regulator 2	-1.60
TCF4*	transcription factor 4	-1.61
ASPN	asporin	-1.62
LIMCH1	LIM and calponin homology domains 1	-1.63
SMAP2	small ArfGAP2	-1.63
FOXP1*	forkhead box P1	-1.64

SNX30	sorting nexin family member 30	-1.64
ADAM22	ADAM metallopeptidase domain 22	-1.65
ARSE*	arylsulfatase E (chondrodysplasia punctata 1)	-1.65
RGL1	ral guanine nucleotide dissociation stimulator-like 1	-1.67
TMEM35*	transmembrane protein 35	-1.69
ZSWIM5	zinc finger, SWIM-type containing 5	-1.69
SLC2A12	solute carrier family 2	-1.70
VLDLR	very low density lipoprotein receptor 4	-1.70
TREM1	triggering receptor expressed on myeloid cells 1	-1.72
RAPH1*	Ras association (RalGDS/AF-6) and pleckstrin homology doma	-1.74
EPHA7	EPH receptor A7	-1.76
NID2*	nidogen 2 (osteonidogen)	-1.76
PLSCR1*	phospholipid scramblase 1	-1.77
TOX	thymocyte selection-associated high mobility group box	-1.77
MAP2	microtubule-associated protein 2	-1.78
F13A1	coagulation factor XIII, A1 polypeptide	-1.81
ITGA11	integrin, alpha 11	-1.82
RFTN1	raftlin, lipid raft linker 1	-1.82
HAP1*	huntingtin-associated protein 1	-1.83
ZNF217	zinc finger protein 217	-1.83
OLFML2B*	olfactomedin-like 2B	-1.86
CNKSR2*	connector enhancer of kinase suppressor of Ras 2	-1.88
TNFAIP6	tumor necrosis factor, alpha-induced protein 6	-1.89
MYO5A*	myosin VA (heavy chain 12, myoxin)	-1.90
PLAGL1*	pleiomorphic adenoma gene-like 1	-1.91
PRRG4*	proline rich Gla (G-carboxyglutamic acid) 4	-1.91
SCARA3*	scavenger receptor class A, member 3	-1.92
CLU*	clusterin	-1.98
ATRNL1	attractin-like 1	-2.05
CAPNS2	calpain, small subunit 2	-2.10
STMN2	stathmin-like 2	-2.15
ERBB3*	v-erb-b2 erythroblastic leukemia viral oncogene homolog 3	-2.36
RARB	retinoic acid receptor, beta	-2.37
LRIG1	leucine-rich repeats and immunoglobulin-like domains 1	-2.40
EFTUD1	elongation factor Tu GTP binding domain containing 1	-2.43
VIT	vitrin	-2.62
SERPINB2	serpin peptidase inhibitor, clade B (ovalbumin)	-2.71
ABI3BP	ABI family, member 3 (NESH) binding protein	-2.93
ATP8A1*	ATPase, aminophospholipid transporter (APLT), class I	-3.22
TMEM154	transmembrane protein 154	-3.29
COLEC10	collectin sub-family member 10	-4.17

Key:

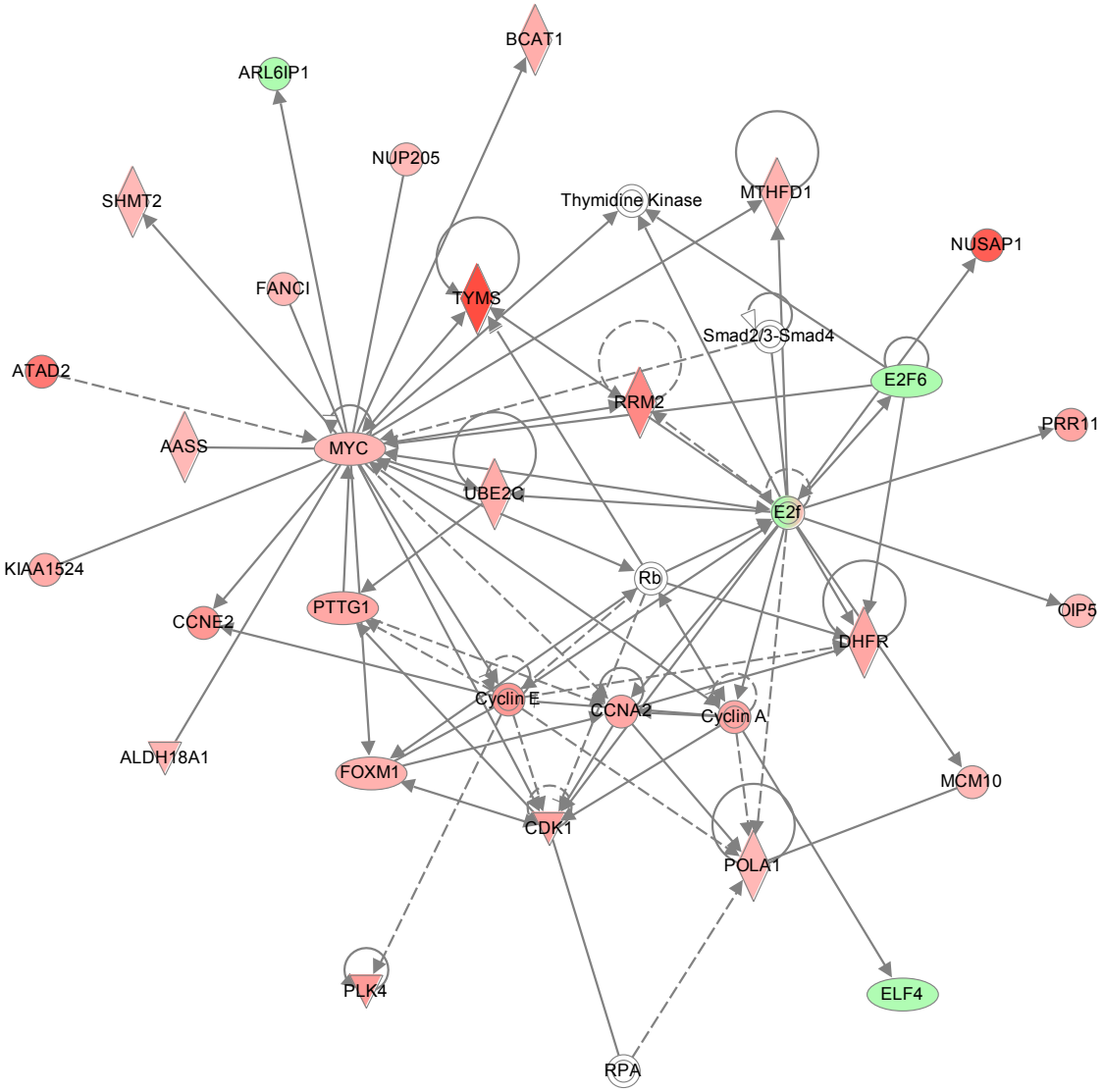
Red: Decidual-induced genes
Blue: Decidual-repressed genes
Italics: FOXO1-induced
***: Genes identified by Talbi et al (2006) to be induced during the secretory phase of the menstrual cycle**

Appendix 4

The top five associated networks resulted from the *in silico* analysis of the NOX4/p22^{PHOX}-dependent genes.

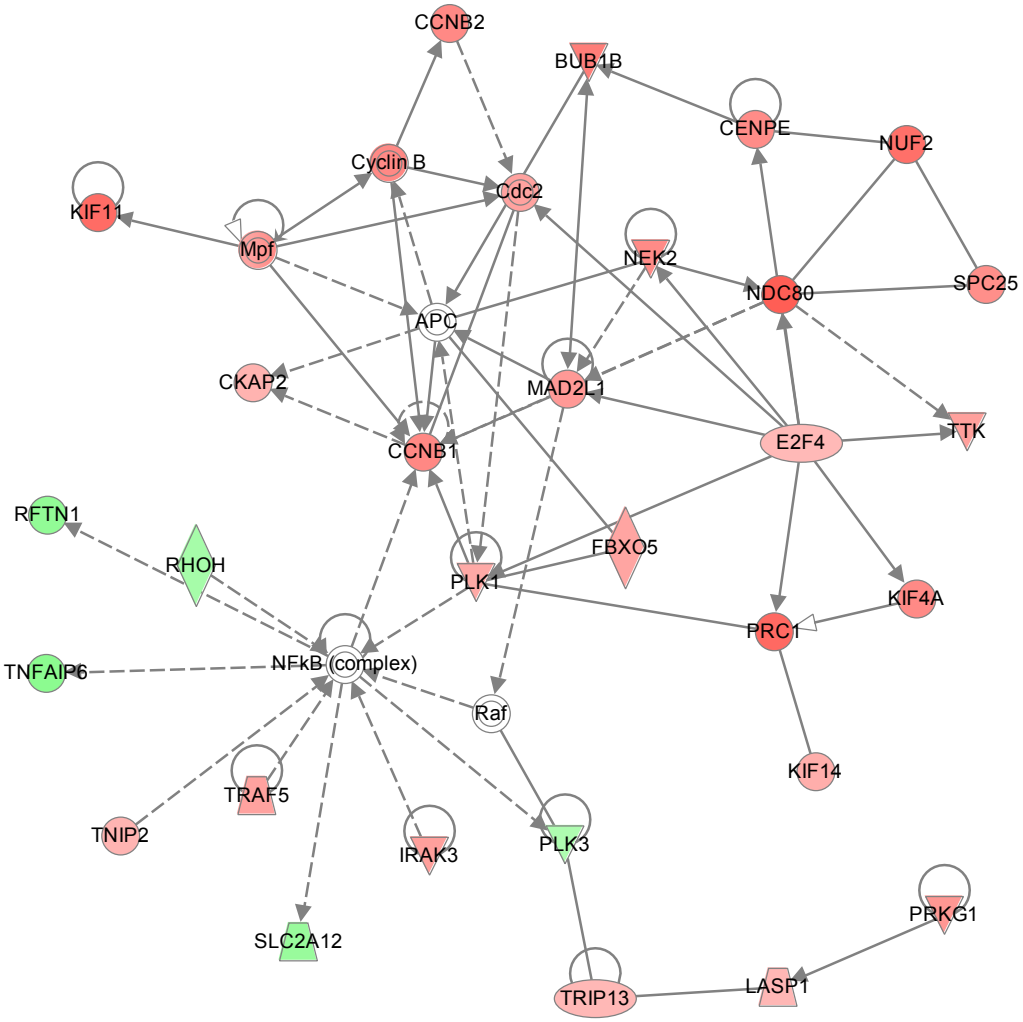
The genes shaded in green were downregulated upon knockdown of NOX4 and p22^{PHOX}, whereas the molecules shaded in red were upregulated upon the knockdown.

Network 1: Cell Cycle, Cancer, Skeletal and Muscular Disorders



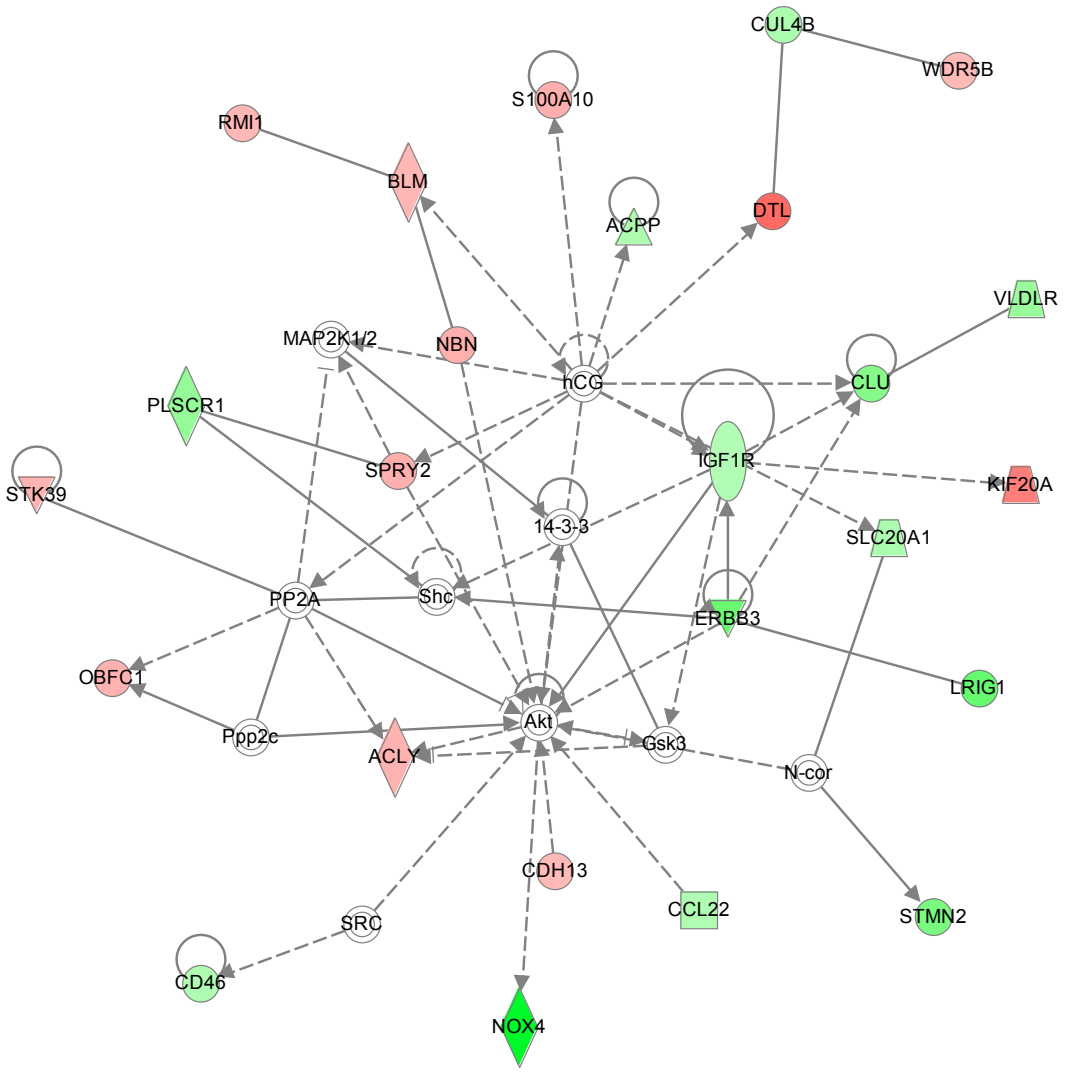
Source: Ingenuity® Systems

Network 2: Cell Cycle, Cellular Assembly and Organization, DNA Replication, Recombination, and Repair



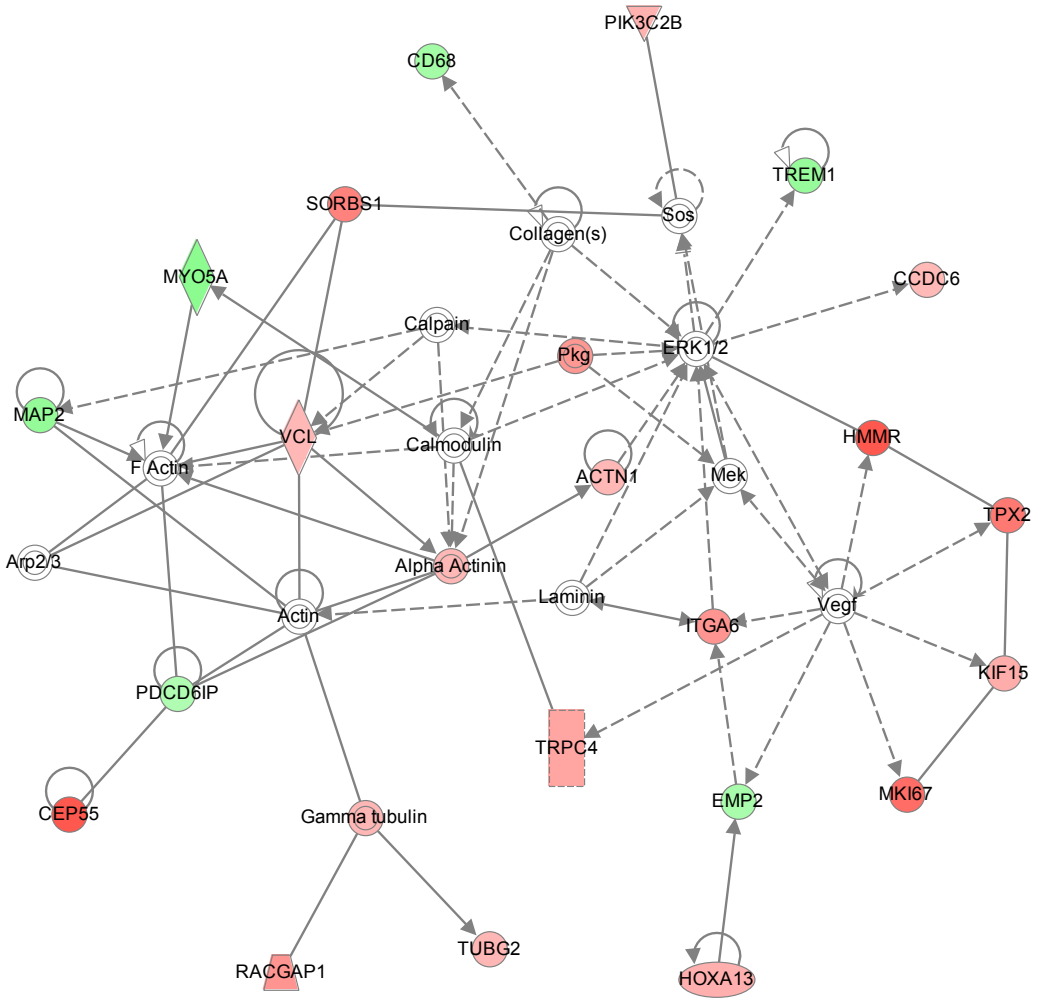
Source: Ingenuity® Systems

Network 3: Cell-To-Cell Signalling and Interaction, Cell Cycle, DNA Replication, Recombination, and Repair



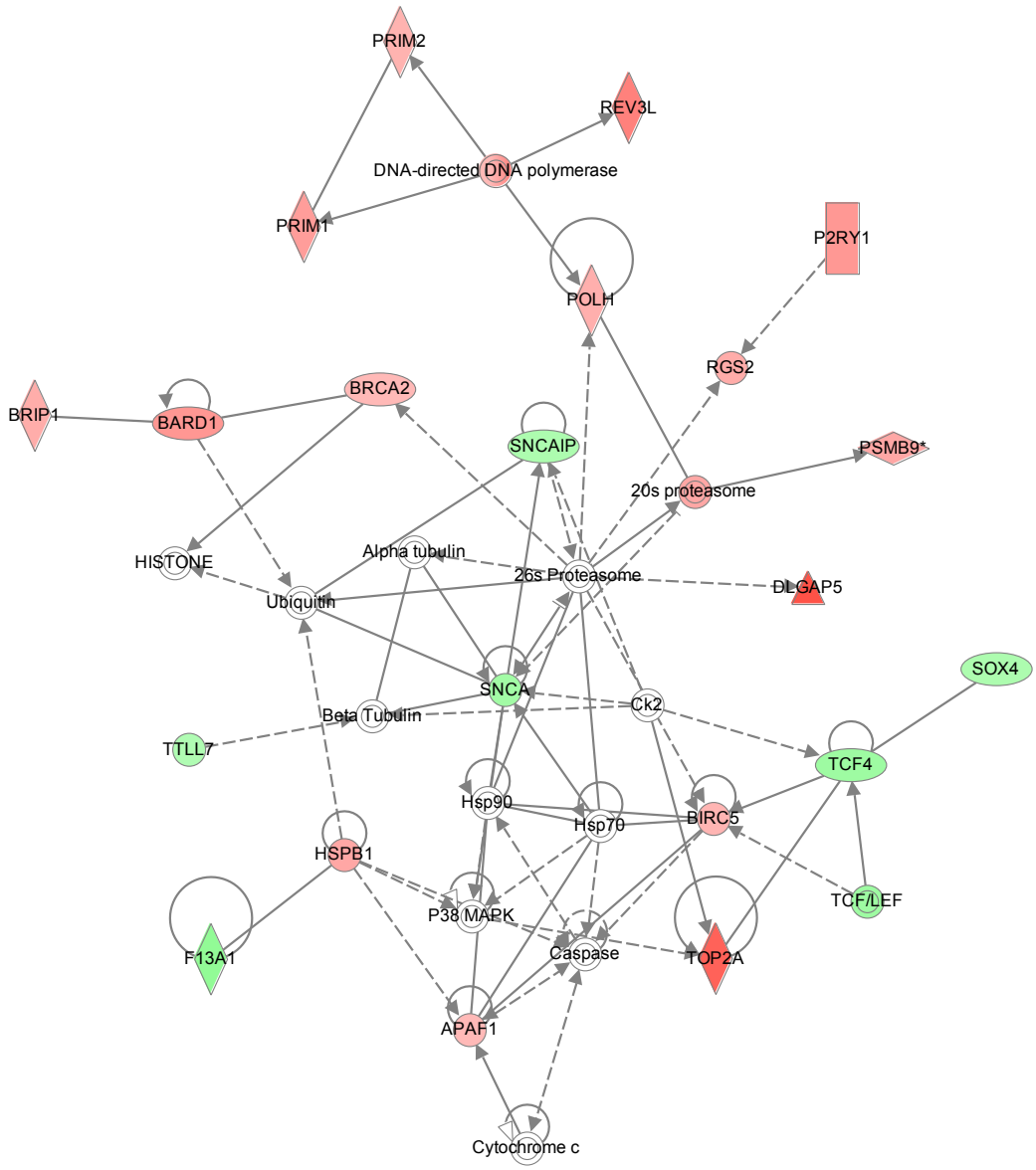
Source: Ingenuity® Systems

Network 4: Cellular Assembly and Organization, Cellular Growth and Proliferation, Haematological Disease



Source: Ingenuity® Systems

Network 5: DNA Replication, Recombination, and Repair, Gene Expression, Cell Cycle



Source: Ingenuity® Systems

References

Refrences

1. **Brosens JJ, Pijnenborg R, Brosens IA** 2002 The myometrial junctional zone spiral arteries in normal and abnormal pregnancies: a review of the literature. Am J Obstet Gynecol 187:1416-1423

2. **Maruyama T, Masuda H, Ono M, Kajitani T, Yoshimura Y** 2010 Human uterine stem/progenitor cells: their possible role in uterine physiology and pathology. Reproduction 140:11-22

3. **Masuda H, Matsuzaki Y, Hiratsu E, Ono M, Nagashima T, Kajitani T, Arase T, Oda H, Uchida H, Asada H, Ito M, Yoshimura Y, Maruyama T, Okano H** 2010 Stem cell-like properties of the endometrial side population: implication in endometrial regeneration. PLoS One 5:e10387

4. **Gargett CE, Chan RW, Schwab KE** 2008 Hormone and growth factor signaling in endometrial renewal: role of stem/progenitor cells. Mol Cell Endocrinol 288:22-29

5. **Brosens JJ, Gellersen B** 2006 Death or survival--progesterone-dependent cell fate decisions in the human endometrial stroma. J Mol Endocrinol 36:389-398

6. **Talbi S, Hamilton AE, Vo KC, Tulac S, Overgaard MT, Dosiou C, Le Shay N, Nezhat CN, Kempson R, Lessey BA, Nayak NR, Giudice LC** 2006 Molecular phenotyping of human endometrium distinguishes menstrual cycle phases and underlying biological processes in normo-ovulatory women. Endocrinology 147:1097-1121

7. **Gellersen B, Brosens J** 2003 Cyclic AMP and progesterone receptor cross-talk in human endometrium: a decidualizing affair. J Endocrinol 178:357-372

8. **Gellersen B, Brosens IA, Brosens JJ** 2007 Decidualization of the human endometrium: mechanisms, functions, and clinical perspectives. Semin Reprod Med 25:445-453

9. **Kliman HJ** 2000 Uteroplacental blood flow. The story of decidualization, menstruation, and trophoblast invasion. Am J Pathol 157:1759-1768

10. **Gellersen B, Brosens B** eds. 2008 The Endometrium: Signalling and transcription factor networks in the human endometrial stroma. second Edition ed: Informa

11. **Wynn RM** 1974 Ultrastructural development of the human decidua. Am J Obstet Gynecol 118:652-670

12. **Kao LC, Tulac S, Lobo S, Imani B, Yang JP, Germeyer A, Osteen K, Taylor RN, Lessey BA, Giudice LC** 2002 Global gene profiling in human endometrium during the window of implantation. Endocrinology 143:2119-2138

13. **Horcajadas JA, Riesewijk A, Martin J, Cervero A, Mosselman S, Pellicer A, Simon C** 2004 Global gene expression profiling of human endometrial receptivity. J Reprod Immunol 63:41-49

14. **Riesewijk A, Martin J, van Os R, Horcajadas JA, Polman J, Pellicer A, Mosselman S, Simon C** 2003 Gene expression profiling of human endometrial receptivity on days LH+2 versus LH+7 by microarray technology. Mol Hum Reprod 9:253-264

15. **Carson DD, Lagow E, Thathiah A, Al-Shami R, Farach-Carson MC, Vernon M, Yuan L, Fritz MA, Lessey B** 2002 Changes in gene expression during the early to mid-luteal (receptive phase) transition in human endometrium detected by high-density microarray screening. Mol Hum Reprod 8:871-879

16. **Mirkin S, Arslan M, Churikov D, Corica A, Diaz JI, Williams S, Bocca S, Oehninger S** 2005 In search of candidate genes critically expressed in the human endometrium during the window of implantation. Hum Reprod 20:2104-2117

17. **Borthwick JM, Charnock-Jones DS, Tom BD, Hull ML, Teirney R, Phillips SC, Smith SK** 2003 Determination of the transcript profile of human endometrium. Mol Hum Reprod 9:19-33

18. **Takano M, Lu Z, Goto T, Fusi L, Higham J, Francis J, Withey A, Hardt J, Cloke B, Stavropoulou AV, Ishihara O, Lam EW, Unterman TG, Brosens JJ, Kim JJ** 2007 Transcriptional cross talk between the forkhead transcription factor forkhead box O1A and the progesterone receptor coordinates cell cycle regulation and differentiation in human endometrial stromal cells. Mol Endocrinol 21:2334-2349

19. **Popovici RM, Kao LC, Giudice LC** 2000 Discovery of new inducible genes in in vitro decidualized human endometrial stromal cells using microarray technology. Endocrinology 141:3510-3513

20. **Giudice LC** 2004 Microarray expression profiling reveals candidate genes for human uterine receptivity. Am J Pharmacogenomics 4:299-312

21. **Oliver C, Montes MJ, Galindo JA, Ruiz C, Olivares EG** 1999 Human decidual stromal cells express alpha-smooth muscle actin and show ultrastructural similarities with myofibroblasts. Hum Reprod 14:1599-1605

22. **Christian M, Marangos P, Mak I, McVey J, Barker F, White J, Brosens JJ** 2001 Interferon-gamma modulates prolactin and tissue factor expression in differentiating human endometrial stromal cells. Endocrinology 142:3142-3151

23. **Tseng L, Gao JG, Chen R, Zhu HH, Mazella J, Powell DR** 1992 Effect of progestin, antiprogestin, and relaxin on the accumulation of prolactin and insulin-like growth factor-binding protein-1 messenger ribonucleic acid in human endometrial stromal cells. Biol Reprod 47:441-450

24. **Christensen S, Verhage HG, Nowak G, de Lanerolle P, Fleming S, Bell SC, Fazleabas AT, Hild-Petito S** 1995 Smooth muscle myosin II and alpha smooth muscle actin expression in the baboon (Papio anubis) uterus is

associated with glandular secretory activity and stromal cell transformation. Biol Reprod 53:598-608

25. **Tang B, Guller S, Gurpide E** 1993 Mechanisms involved in the decidualization of human endometrial stromal cells. Acta Eur Fertil 24:221-223

26. **Tang B, Guller S, Gurpide E** 1993 Cyclic adenosine 3',5'-monophosphate induces prolactin expression in stromal cells isolated from human proliferative endometrium. Endocrinology 133:2197-2203

27. **Chaffer CL, Thompson EW, Williams ED** 2007 Mesenchymal to epithelial transition in development and disease. Cells Tissues Organs 185:7-19

28. **Chaffer CL, Brennan JP, Slavin JL, Blick T, Thompson EW, Williams ED** 2006 Mesenchymal-to-epithelial transition facilitates bladder cancer metastasis: role of fibroblast growth factor receptor-2. Cancer Res 66:11271-11278

29. **Micalizzi DS, Farabaugh SM, Ford HL** 2010 Epithelial-mesenchymal transition in cancer: parallels between normal development and tumor progression. J Mammary Gland Biol Neoplasia 15:117-134

30. **Shook D, Keller R** 2003 Mechanisms, mechanics and function of epithelial-mesenchymal transitions in early development. Mech Dev 120:1351-1383

31. **Choi SS, Diehl AM** 2009 Epithelial-to-mesenchymal transitions in the liver. Hepatology 50:2007-2013

32. **Hay ED** 2005 The mesenchymal cell, its role in the embryo, and the remarkable signaling mechanisms that create it. Dev Dyn 233:706-720

33. **Li R, Liang J, Ni S, Zhou T, Qing X, Li H, He W, Chen J, Li F, Zhuang Q, Qin B, Xu J, Li W, Yang J, Gan Y, Qin D, Feng S, Song H, Yang D, Zhang B, Zeng L, Lai L, Esteban MA, Pei D** 2010 A mesenchymal-to-epithelial transition initiates and is required for the nuclear reprogramming of mouse fibroblasts. Cell Stem Cell 7:51-63

34. **Cloke B, Fusi L, Brosens J** eds. 2010 Decidualization: Cambridge University Press

35. **Kajihara T, Jones M, Fusi L, Takano M, Feroze-Zaidi F, Pirianov G, Mehmet H, Ishihara O, Higham JM, Lam EW, Brosens JJ** 2006 Differential expression of FOXO1 and FOXO3a confers resistance to oxidative cell death upon endometrial decidualization. Mol Endocrinol 20:2444-2455

36. **Kim JJ, Taylor HS, Lu Z, Ladhani O, Hastings JM, Jackson KS, Wu Y, Guo SW, Fazleabas AT** 2007 Altered expression of HOXA10 in endometriosis: potential role in decidualization. Mol Hum Reprod 13:323-332

37. **Lee B, Du H, Taylor HS** 2009 Experimental murine endometriosis induces DNA methylation and altered gene expression in eutopic endometrium. Biol Reprod 80:79-85

38. **Kunz G, Herbertz M, Beil D, Huppert P, Leyendecker G** 2007 Adenomyosis as a disorder of the early and late human reproductive period. Reprod Biomed Online 15:681-685

39. **Teklenburg G, Salker M, Heijnen C, Macklon NS, Brosens JJ** 2010 The molecular basis of recurrent pregnancy loss: impaired natural embryo selection. Mol Hum Reprod 16:886-895

40. **Salker M, Teklenburg G, Molokhia M, Lavery S, Trew G, Aojanepong T, Mardon HJ, Lokugamage AU, Rai R, Landles C, Roelen BA, Quenby S, Kuijk EW, Kavelaars A, Heijnen CJ, Regan L, Macklon NS, Brosens JJ** 2010 Natural selection of human embryos: impaired decidualization of endometrium disables embryo-maternal interactions and causes recurrent pregnancy loss. PLoS One 5:e10287

41. **Teklenburg G, Salker M, Molokhia M, Lavery S, Trew G, Aojanepong T, Mardon HJ, Lokugamage AU, Rai R, Landles C, Roelen BA, Quenby S, Kuijk EW, Kavelaars A, Heijnen CJ, Regan L, Brosens JJ, Macklon NS** 2010 Natural selection of human embryos: decidualizing endometrial stromal cells serve as sensors of embryo quality upon implantation. PLoS One 5:e10258

42. **Fazleabas AT, Kim JJ, Strakova Z** 2004 Implantation: embryonic signals and the modulation of the uterine environment--a review. Placenta 25 Suppl A:S26-31

43. **Graham CH, Lala PK** 1991 Mechanism of control of trophoblast invasion in situ. J Cell Physiol 148:228-234

44. **Lyall F** 2006 Mechanisms regulating cytotrophoblast invasion in normal pregnancy and pre-eclampsia. Aust N Z J Obstet Gynaecol 46:266-273

45. **Lockwood CJ, Krikun G, Schatz F** 2001 Decidual cell-expressed tissue factor maintains hemostasis in human endometrium. Ann N Y Acad Sci 943:77-88

46. **Lockwood CJ, Krikun G, Hickey M, Huang SJ, Schatz F** 2009 Decidualized human endometrial stromal cells mediate hemostasis, angiogenesis, and abnormal uterine bleeding. Reprod Sci 16:162-170

47. **Dietl J, Honig A, Kammerer U, Rieger L** 2006 Natural killer cells and dendritic cells at the human feto-maternal interface: an effective cooperation? Placenta 27:341-347

48. **King A** 2000 Uterine leukocytes and decidualization. Hum Reprod Update 6:28-36

49. **Koopman LA, Kopcow HD, Rybalov B, Boyson JE, Orange JS, Schatz F, Masch R, Lockwood CJ, Schachter AD, Park PJ, Strominger JL** 2003 Human decidual natural killer cells are a unique NK cell subset with immunomodulatory potential. J Exp Med 198:1201-1212

50. **Ledee N, Chaouat G, Serazin V, Lombroso R, Dubanchet S, Oger P, Louafi N, Ville Y** 2008 Endometrial vascularity by three-dimensional power

Doppler ultrasound and cytokines: a complementary approach to assess uterine receptivity. J Reprod Immunol 77:57-62

51. **Kitaya K, Yamaguchi T, Honjo H** 2005 Central role of interleukin-15 in postovulatory recruitment of peripheral blood CD16(-) natural killer cells into human endometrium. J Clin Endocrinol Metab 90:2932-2940

52. **Mellor AL, Chandler P, Lee GK, Johnson T, Keskin DB, Lee J, Munn DH** 2002 Indoleamine 2,3-dioxygenase, immunosuppression and pregnancy. J Reprod Immunol 57:143-150

53. **Mellor AL, Keskin DB, Johnson T, Chandler P, Munn DH** 2002 Cells expressing indoleamine 2,3-dioxygenase inhibit T cell responses. J Immunol 168:3771-3776

54. **Munn DH, Shafizadeh E, Attwood JT, Bondarev I, Pashine A, Mellor AL** 1999 Inhibition of T cell proliferation by macrophage tryptophan catabolism. J Exp Med 189:1363-1372

55. **Munn DH, Zhou M, Attwood JT, Bondarev I, Conway SJ, Marshall B, Brown C, Mellor AL** 1998 Prevention of allogeneic fetal rejection by tryptophan catabolism. Science 281:1191-1193

56. **Harirah HM, Donia SE, Parkash V, Jones DC, Hsu CD** 2002 Localization of the Fas-Fas ligand system in human fetal membranes. J Reprod Med 47:611-616

57. **Burton GJ, Jauniaux E** 2004 Placental oxidative stress: from miscarriage to preeclampsia. J Soc Gynecol Investig 11:342-352

58. **Burton GJ, Jauniaux E, Watson AL** 1999 Maternal arterial connections to the placental intervillous space during the first trimester of human pregnancy: the Boyd collection revisited. Am J Obstet Gynecol 181:718-724

59. **Jauniaux E, Poston L, Burton GJ** 2006 Placental-related diseases of pregnancy: Involvement of oxidative stress and implications in human evolution. Hum Reprod Update 12:747-755

60. **Jauniaux E, Watson AL, Hempstock J, Bao YP, Skepper JN, Burton GJ** 2000 Onset of maternal arterial blood flow and placental oxidative stress. A possible factor in human early pregnancy failure. Am J Pathol 157:2111-2122

61. **Storz G, Imlay JA** 1999 Oxidative stress. Curr Opin Microbiol 2:188-194

62. **Thannickal VJ, Fanburg BL** 2000 Reactive oxygen species in cell signaling. Am J Physiol Lung Cell Mol Physiol 279:L1005-1028

63. **Maruyama T, Kitaoka Y, Sachi Y, Nakanoin K, Hirota K, Shiozawa T, Yoshimura Y, Fujii S, Yodoi J** 1997 Thioredoxin expression in the human endometrium during the menstrual cycle. Mol Hum Reprod 3:989-993

64. **Maruyama T, Sachi Y, Furuke K, Kitaoka Y, Kanzaki H, Yoshimura Y, Yodoi J** 1999 Induction of thioredoxin, a redox-active protein, by ovarian steroid hormones during growth and differentiation of endometrial stromal cells in vitro. Endocrinology 140:365-372

65. **Leitao B, Jones MC, Fusi L, Higham J, Lee Y, Takano M, Goto T, Christian M, Lam EW, Brosens JJ** 2010 Silencing of the JNK pathway maintains progesterone receptor activity in decidualizing human endometrial stromal cells exposed to oxidative stress signals. FASEB J 24:1541-1551

66. **Thyss R, Virolle V, Imbert V, Peyron JF, Aberdam D, Virolle T** 2005 NF-kappaB/Egr-1/Gadd45 are sequentially activated upon UVB irradiation to mediate epidermal cell death. EMBO J 24:128-137

67. **Zerbini LF, Libermann TA** 2005 Life and death in cancer. GADD45 alpha and gamma are critical regulators of NF-kappaB mediated escape from programmed cell death. Cell Cycle 4:18-20

68. **Sarno JL, Schatz F, Lockwood CJ, Huang ST, Taylor HS** 2006 Thrombin and interleukin-1beta regulate HOXA10 expression in human term decidual cells: implications for preterm labor. J Clin Endocrinol Metab 91:2366-2372

69. **Brosens JJ, Hayashi N, White JO** 1999 Progesterone receptor regulates decidual prolactin expression in differentiating human endometrial stromal cells. Endocrinology 140:4809-4820

70. **Jones MC, Fusi L, Higham JH, Abdel-Hafiz H, Horwitz KB, Lam EW, Brosens JJ** 2006 Regulation of the SUMO pathway sensitizes differentiating human endometrial stromal cells to progesterone. Proc Natl Acad Sci U S A 103:16272-16277

71. **Brar AK, Frank GR, Kessler CA, Cedars MI, Handwerger S** 1997 Progesterone-dependent decidualization of the human endometrium is mediated by cAMP. Endocrine 6:301-307

72. **Gao J, Mazella J, Suwanichkul A, Powell DR, Tseng L** 1999 Activation of the insulin-like growth factor binding protein-1 promoter by progesterone receptor in decidualized human endometrial stromal cells. Mol Cell Endocrinol 153:11-17

73. **Telgmann R, Gellersen B** 1998 Marker genes of decidualization: activation of the decidual prolactin gene. Hum Reprod Update 4:472-479

74. **Telgmann R, Maronde E, Tasken K, Gellersen B** 1997 Activated protein kinase A is required for differentiation-dependent transcription of the decidual prolactin gene in human endometrial stromal cells. Endocrinology 138:929-937

75. **Dessauer CW, Posner BA, Gilman AG** 1996 Visualizing signal transduction: receptors, G-proteins, and adenylate cyclases. Clin Sci (Lond) 91:527-537

76. **Tanaka N, Miyazaki K, Tashiro H, Mizutani H, Okamura H** 1993 Changes in adenylyl cyclase activity in human endometrium during the menstrual cycle and in human decidua during pregnancy. J Reprod Fertil 98:33-39

77. **Reem GH, Ray DW, Davis JR** 1999 The human prolactin gene upstream promoter is regulated in lymphoid cells by activators of T-cells and by cAMP. J Mol Endocrinol 22:285-292

78. **Gao JG, Mazella J, Tseng L** 1994 Activation of the human IGFBP-1 gene promoter by progestin and relaxin in primary culture of human endometrial stromal cells. Mol Cell Endocrinol 104:39-46

79. **Palejwala S, Tseng L, Wojtczuk A, Weiss G, Goldsmith LT** 2002 Relaxin gene and protein expression and its regulation of procollagenase and vascular endothelial growth factor in human endometrial cells. Biol Reprod 66:1743-1748

80. **Milne SA, Perchick GB, Boddy SC, Jabbour HN** 2001 Expression, localization, and signaling of PGE(2) and EP2/EP4 receptors in human nonpregnant endometrium across the menstrual cycle. J Clin Endocrinol Metab 86:4453-4459

81. **Ivell R, Balvers M, Pohnke Y, Telgmann R, Bartsch O, Milde-Langosch K, Bamberger AM, Einspanier A** 2003 Immunoexpression of the relaxin receptor LGR7 in breast and uterine tissues of humans and primates. Reprod Biol Endocrinol 1:114

82. **Hsu SY, Nakabayashi K, Nishi S, Kumagai J, Kudo M, Sherwood OD, Hsueh AJ** 2002 Activation of orphan receptors by the hormone relaxin. Science 295:671-674

83. **Bartsch O, Bartlick B, Ivell R** 2001 Relaxin signalling links tyrosine phosphorylation to phosphodiesterase and adenylyl cyclase activity. Mol Hum Reprod 7:799-809

84. **Bartsch O, Bartlick B, Ivell R** 2004 Phosphodiesterase 4 inhibition synergizes with relaxin signaling to promote decidualization of human endometrial stromal cells. J Clin Endocrinol Metab 89:324-334

85. **Tang M, Mazella J, Zhu HH, Tseng L** 2005 Ligand activated relaxin receptor increases the transcription of IGFBP-1 and prolactin in human decidual and endometrial stromal cells. Mol Hum Reprod 11:237-243

86. **Tang B, Gurpide E** 1993 Direct effect of gonadotropins on decidualization of human endometrial stroma cells. J Steroid Biochem Mol Biol 47:115-121

87. **Gellersen B, Kempf R, Telgmann R** 1997 Human endometrial stromal cells express novel isoforms of the transcriptional modulator CREM and up-regulate ICER in the course of decidualization. Mol Endocrinol 11:97-113

88. **Lamas M, Molina C, Foulkes NS, Jansen E, Sassone-Corsi P** 1997 Ectopic ICER expression in pituitary corticotroph AtT20 cells: effects on morphology, cell cycle, and hormonal production. Mol Endocrinol 11:1425-1434

89. **Molina CA, Foulkes NS, Lalli E, Sassone-Corsi P** 1993 Inducibility and negative autoregulation of CREM: an alternative promoter directs the expression of ICER, an early response repressor. Cell 75:875-886

90. **Stehle JH, Foulkes NS, Molina CA, Simonneaux V, Pevet P, Sassone-Corsi P** 1993 Adrenergic signals direct rhythmic expression of transcriptional repressor CREM in the pineal gland. Nature 365:314-320

91. **Servillo G, Della Fazia MA, Sassone-Corsi P** 2002 Coupling cAMP signaling to transcription in the liver: pivotal role of CREB and CREM. Exp Cell Res 275:143-154

92. **Gellersen B, Kempf R, Telgmann R, DiMattia GE** 1994 Nonpituitary human prolactin gene transcription is independent of Pit-1 and differentially controlled in lymphocytes and in endometrial stroma. Mol Endocrinol 8:356-373

93. **Berwaer M, Martial JA, Davis JR** 1994 Characterization of an up-stream promoter directing extrapituitary expression of the human prolactin gene. Mol Endocrinol 8:635-642

94. **Kastner P, Krust A, Turcotte B, Stropp U, Tora L, Gronemeyer H, Chambon P** 1990 Two distinct estrogen-regulated promoters generate transcripts encoding the two functionally different human progesterone receptor forms A and B. EMBO J 9:1603-1614

95. **Vegeto E, Shahbaz MM, Wen DX, Goldman ME, O'Malley BW, McDonnell DP** 1993 Human progesterone receptor A form is a cell- and promoter-specific repressor of human progesterone receptor B function. Mol Endocrinol 7:1244-1255

96. **Ismail PM, Amato P, Soyal SM, DeMayo FJ, Conneely OM, O'Malley BW, Lydon JP** 2003 Progesterone involvement in breast development and tumorigenesis--as revealed by progesterone receptor "knockout" and "knockin" mouse models. Steroids 68:779-787

97. **Li X, O'Malley BW** 2003 Unfolding the action of progesterone receptors. J Biol Chem 278:39261-39264

98. **Mulac-Jericevic B, Conneely OM** 2004 Reproductive tissue selective actions of progesterone receptors. Reproduction 128:139-146

99. **Gellersen B, Fernandes MS, Brosens JJ** 2009 Non-genomic progesterone actions in female reproduction. Hum Reprod Update 15:119-138

100. **Rider V** 2002 Progesterone and the control of uterine cell proliferation and differentiation. Front Biosci 7:d1545-1555

101. **Lydon JP, DeMayo FJ, Funk CR, Mani SK, Hughes AR, Montgomery CA, Jr., Shyamala G, Conneely OM, O'Malley BW** 1995 Mice lacking progesterone receptor exhibit pleiotropic reproductive abnormalities. Genes Dev 9:2266-2278

102. **Tsai MJ, O'Malley BW** 1994 Molecular mechanisms of action of steroid/thyroid receptor superfamily members. Annu Rev Biochem 63:451-486

103. **Mulac-Jericevic B, Mullinax RA, DeMayo FJ, Lydon JP, Conneely OM** 2000 Subgroup of reproductive functions of progesterone mediated by progesterone receptor-B isoform. Science 289:1751-1754

104. **Wen DX, Xu YF, Mais DE, Goldman ME, McDonnell DP** 1994 The A and B isoforms of the human progesterone receptor operate through distinct signaling pathways within target cells. Mol Cell Biol 14:8356-8364

105. **McDonnell DP, Shahbaz MM, Vegeto E, Goldman ME** 1994 The human progesterone receptor A-form functions as a transcriptional modulator of mineralocorticoid receptor transcriptional activity. J Steroid Biochem Mol Biol 48:425-432

106. **Conneely OM, Lydon JP** 2000 Progesterone receptors in reproduction: functional impact of the A and B isoforms. Steroids 65:571-577

107. **Conneely OM, Mulac-Jericevic B, Lydon JP, De Mayo FJ** 2001 Reproductive functions of the progesterone receptor isoforms: lessons from knock-out mice. Mol Cell Endocrinol 179:97-103

108. **Mote PA, Balleine RL, McGowan EM, Clarke CL** 1999 Colocalization of progesterone receptors A and B by dual immunofluorescent histochemistry in human endometrium during the menstrual cycle. J Clin Endocrinol Metab 84:2963-2971

109. **Chen D, Ma H, Hong H, Koh SS, Huang SM, Schurter BT, Aswad DW, Stallcup MR** 1999 Regulation of transcription by a protein methyltransferase. Science 284:2174-2177

110. **Chen H, Lin RJ, Xie W, Wilpitz D, Evans RM** 1999 Regulation of hormone-induced histone hyperacetylation and gene activation via acetylation of an acetylase. Cell 98:675-686

111. **Wardell SE, Boonyaratanakornkit V, Adelman JS, Aronheim A, Edwards DP** 2002 Jun dimerization protein 2 functions as a progesterone receptor N-terminal domain coactivator. Mol Cell Biol 22:5451-5466

112. **Li X, Lonard DM, O'Malley BW** 2004 A contemporary understanding of progesterone receptor function. Mech Ageing Dev 125:669-678

113. **Abdel-Hafiz H, Takimoto GS, Tung L, Horwitz KB** 2002 The inhibitory function in human progesterone receptor N termini binds SUMO-1 protein to regulate autoinhibition and transrepression. J Biol Chem 277:33950-33956

114. **Lange CA, Shen T, Horwitz KB** 2000 Phosphorylation of human progesterone receptors at serine-294 by mitogen-activated protein kinase signals their degradation by the 26S proteasome. Proc Natl Acad Sci U S A 97:1032-1037

115. **Weigel NL** 1996 Steroid hormone receptors and their regulation by phosphorylation. Biochem J 319 (Pt 3):657-667

116. **Heine GF, Parvin JD** 2007 BRCA1 control of steroid receptor ubiquitination. Sci STKE 2007:pe34

117. **Faus H, Haendler B** 2006 Post-translational modifications of steroid receptors. Biomed Pharmacother 60:520-528

118. **Melchior F, Schergaut M, Pichler A** 2003 SUMO: ligases, isopeptidases and nuclear pores. Trends Biochem Sci 28:612-618

119. **Hochstrasser M** 2001 SP-RING for SUMO: new functions bloom for a ubiquitin-like protein. Cell 107:5-8

120. **Muller S, Hoege C, Pyrowolakis G, Jentsch S** 2001 SUMO, ubiquitin's mysterious cousin. Nat Rev Mol Cell Biol 2:202-210

121. **Christian M, Zhang X, Schneider-Merck T, Unterman TG, Gellersen B, White JO, Brosens JJ** 2002 Cyclic AMP-induced forkhead transcription factor, FKHR, cooperates with CCAAT/enhancer-binding protein beta in differentiating human endometrial stromal cells. J Biol Chem 277:20825-20832

122. **Kim JJ, Buzzio OL, Li S, Lu Z** 2005 Role of FOXO1A in the regulation of insulin-like growth factor-binding protein-1 in human endometrial cells: interaction with progesterone receptor. Biol Reprod 73:833-839

123. **Kim JJ, Taylor HS, Akbas GE, Foucher I, Trembleau A, Jaffe RC, Fazleabas AT, Unterman TG** 2003 Regulation of insulin-like growth factor binding protein-1 promoter activity by FKHR and HOXA10 in primate endometrial cells. Biol Reprod 68:24-30

124. **Jabbour HN, Critchley HO, Boddy SC** 1998 Expression of functional prolactin receptors in nonpregnant human endometrium: janus kinase-2, signal transducer and activator of transcription-1 (STAT1), and STAT5 proteins are phosphorylated after stimulation with prolactin. J Clin Endocrinol Metab 83:2545-2553

125. **Mak IY, Brosens JJ, Christian M, Hills FA, Chamley L, Regan L, White JO** 2002 Regulated expression of signal transducer and activator of transcription, Stat5, and its enhancement of PRL expression in human endometrial stromal cells in vitro. J Clin Endocrinol Metab 87:2581-2588

126. **Pohnke Y, Kempf R, Gellersen B** 1999 CCAAT/enhancer-binding proteins are mediators in the protein kinase A-dependent activation of the decidual prolactin promoter. J Biol Chem 274:24808-24818

127. **Watanabe K, Kessler CA, Bachurski CJ, Kanda Y, Richardson BD, Stanek J, Handwerger S, Brar AK** 2001 Identification of a decidua-specific enhancer on the human prolactin gene with two critical activator protein 1 (AP-1) binding sites. Mol Endocrinol 15:638-653

128. **Brar AK, Kessler CA, Handwerger S** 2002 An Ets motif in the proximal decidual prolactin promoter is essential for basal gene expression. J Mol Endocrinol 29:99-112

129. **Krikun G, Lockwood CJ** 2002 Steroid hormones, endometrial gene regulation and the Sp1 family of proteins. J Soc Gynecol Investig 9:329-334

130. **Krikun G, Schatz F, Mackman N, Guller S, Demopoulos R, Lockwood CJ** 2000 Regulation of tissue factor gene expression in human endometrium by transcription factors Sp1 and Sp3. Mol Endocrinol 14:393-400

131. **Pohnke Y, Schneider-Merck T, Fahnenstich J, Kempf R, Christian M, Milde-Langosch K, Brosens JJ, Gellersen B** 2004 Wild-type p53 protein is up-regulated upon cyclic adenosine monophosphate-induced differentiation of human endometrial stromal cells. J Clin Endocrinol Metab 89:5233-5244

132. **Satokata I, Benson G, Maas R** 1995 Sexually dimorphic sterility phenotypes in Hoxa10-deficient mice. Nature 374:460-463

133. **Hsieh-Li HM, Witte DP, Weinstein M, Branford W, Li H, Small K, Potter SS** 1995 Hoxa 11 structure, extensive antisense transcription, and function in male and female fertility. Development 121:1373-1385

134. **Gendron RL, Paradis H, Hsieh-Li HM, Lee DW, Potter SS, Markoff E** 1997 Abnormal uterine stromal and glandular function associated with maternal reproductive defects in Hoxa-11 null mice. Biol Reprod 56:1097-1105

135. **Lim H, Ma L, Ma WG, Maas RL, Dey SK** 1999 Hoxa-10 regulates uterine stromal cell responsiveness to progesterone during implantation and decidualization in the mouse. Mol Endocrinol 13:1005-1017

136. **Christian M, Pohnke Y, Kempf R, Gellersen B, Brosens JJ** 2002 Functional association of PR and CCAAT/enhancer-binding protein beta isoforms: promoter-dependent cooperation between PR-B and liver-enriched inhibitory protein, or liver-enriched activatory protein and PR-A in human endometrial stromal cells. Mol Endocrinol 16:141-154

137. **Richer JK, Lange CA, Manning NG, Owen G, Powell R, Horwitz KB** 1998 Convergence of progesterone with growth factor and cytokine signaling in breast cancer. Progesterone receptors regulate signal transducers and activators of transcription expression and activity. J Biol Chem 273:31317-31326

138. **Carter ME, Brunet A** 2007 FOXO transcription factors. Curr Biol 17:R113-114

139. **Burgering BM, Medema RH** 2003 Decisions on life and death: FOXO Forkhead transcription factors are in command when PKB/Akt is off duty. J Leukoc Biol 73:689-701

140. **Brunet A, Bonni A, Zigmond MJ, Lin MZ, Juo P, Hu LS, Anderson MJ, Arden KC, Blenis J, Greenberg ME** 1999 Akt promotes cell survival by phosphorylating and inhibiting a Forkhead transcription factor. Cell 96:857-868

141. **Biggs WH, 3rd, Meisenhelder J, Hunter T, Cavenee WK, Arden KC** 1999 Protein kinase B/Akt-mediated phosphorylation promotes nuclear exclusion of the winged helix transcription factor FKHR1. Proc Natl Acad Sci U S A 96:7421-7426

142. **Wagner BL, Norris JD, Knotts TA, Weigel NL, McDonnell DP** 1998 The nuclear corepressors NCoR and SMRT are key regulators of both ligand- and 8-bromo-cyclic AMP-dependent transcriptional activity of the human progesterone receptor. Mol Cell Biol 18:1369-1378

143. **Rowan BG, Garrison N, Weigel NL, O'Malley BW** 2000 8-Bromo-cyclic AMP induces phosphorylation of two sites in SRC-1 that facilitate ligand-independent activation of the chicken progesterone receptor and are critical for functional cooperation between SRC-1 and CREB binding protein. Mol Cell Biol 20:8720-8730

144. **Owen GI, Richer JK, Tung L, Takimoto G, Horwitz KB** 1998 Progesterone regulates transcription of the p21(WAF1) cyclin- dependent kinase inhibitor gene through Sp1 and CBP/p300. J Biol Chem 273:10696-10701

145. **Schatz F, Krikun G, Caze R, Rahman M, Lockwood CJ** 2003 Progestin-regulated expression of tissue factor in decidual cells: implications in endometrial hemostasis, menstruation and angiogenesis. Steroids 68:849-860

146. **Hancock JT, Desikan R, Neill SJ** 2001 Role of reactive oxygen species in cell signalling pathways. Biochem Soc Trans 29:345-350

147. **Bedard K, Krause KH** 2007 The NOX family of ROS-generating NADPH oxidases: physiology and pathophysiology. Physiol Rev 87:245-313

148. **Kovacic P, Jacintho JD** 2001 Mechanisms of carcinogenesis: focus on oxidative stress and electron transfer. Curr Med Chem 8:773-796

149. **Droge W** 2002 Free radicals in the physiological control of cell function. Physiol Rev 82:47-95

150. **Harman D** 1956 Aging: a theory based on free radical and radiation chemistry. J Gerontol 11:298-300

151. **Harman D** 1981 The aging process. Proc Natl Acad Sci U S A 78:7124-7128

152. **Harman D** 2009 Origin and evolution of the free radical theory of aging: a brief personal history, 1954-2009. Biogerontology 10:773-781

153. **Valko M, Leibfritz D, Moncol J, Cronin MT, Mazur M, Telser J** 2007 Free radicals and antioxidants in normal physiological functions and human disease. Int J Biochem Cell Biol 39:44-84

154. **Valko M, Rhodes CJ, Moncol J, Izakovic M, Mazur M** 2006 Free radicals, metals and antioxidants in oxidative stress-induced cancer. Chem Biol Interact 160:1-40

155. **Abid MR, Kachra Z, Spokes KC, Aird WC** 2000 NADPH oxidase activity is required for endothelial cell proliferation and migration. FEBS Lett 486:252-256

156. **Ushio-Fukai M, Alexander RW** 2004 Reactive oxygen species as mediators of angiogenesis signaling: role of NAD(P)H oxidase. Mol Cell Biochem 264:85-97

157. **Veal EA, Day AM, Morgan BA** 2007 Hydrogen peroxide sensing and signaling. Mol Cell 26:1-14

158. **Martin KR, Barrett JC** 2002 Reactive oxygen species as double-edged swords in cellular processes: low-dose cell signaling versus high-dose toxicity. Hum Exp Toxicol 21:71-75

159. **Finkel T, Holbrook NJ** 2000 Oxidants, oxidative stress and the biology of ageing. Nature 408:239-247

160. **Sies H** 1993 Strategies of antioxidant defense. Eur J Biochem 215:213-219

161. **Sies H** 1997 Oxidative stress: oxidants and antioxidants. Exp Physiol 82:291-295

162. **Kaneto H, Katakami N, Matsuhisa M, Matsuoka TA** 2010 Role of reactive oxygen species in the progression of type 2 diabetes and atherosclerosis. Mediators Inflamm 2010:453892

163. **Adiga IK, Nair RR** 2008 Multiple signaling pathways coordinately mediate reactive oxygen species dependent cardiomyocyte hypertrophy. Cell Biochem Funct 26:346-351

164. **Houstis N, Rosen ED, Lander ES** 2006 Reactive oxygen species have a causal role in multiple forms of insulin resistance. Nature 440:944-948

165. **Furukawa S, Fujita T, Shimabukuro M, Iwaki M, Yamada Y, Nakajima Y, Nakayama O, Makishima M, Matsuda M, Shimomura I** 2004 Increased oxidative stress in obesity and its impact on metabolic syndrome. J Clin Invest 114:1752-1761

166. **Kuroda J, Ago T, Matsushima S, Zhai P, Schneider MD, Sadoshima J** 2010 NADPH oxidase 4 (Nox4) is a major source of oxidative stress in the failing heart. Proc Natl Acad Sci U S A 107:15565-15570

167. **Valko M, Izakovic M, Mazur M, Rhodes CJ, Telser J** 2004 Role of oxygen radicals in DNA damage and cancer incidence. Mol Cell Biochem 266:37-56

168. **Lambeth JD** 2007 Nox enzymes, ROS, and chronic disease: an example of antagonistic pleiotropy. Free Radic Biol Med 43:332-347

169. **Chrissobolis S, Faraci FM** 2008 The role of oxidative stress and NADPH oxidase in cerebrovascular disease. Trends Mol Med 14:495-502

170. **Liou GY, Storz P** 2010 Reactive oxygen species in cancer. Free Radic Res 44:479-496

171. **Liu H, Colavitti R, Rovira, II, Finkel T** 2005 Redox-dependent transcriptional regulation. Circ Res 97:967-974

172. **Ngo C, Chereau C, Nicco C, Weill B, Chapron C, Batteux F** 2009 Reactive oxygen species controls endometriosis progression. Am J Pathol 175:225-234

173. **Rumbold AR, Crowther CA, Haslam RR, Dekker GA, Robinson JS** 2006 Vitamins C and E and the risks of preeclampsia and perinatal complications. N Engl J Med 354:1796-1806

174. **Cui XL, Brockman D, Campos B, Myatt L** 2006 Expression of NADPH oxidase isoform 1 (Nox1) in human placenta: involvement in preeclampsia. Placenta 27:422-431

175. **Poston L, Briley AL, Seed PT, Kelly FJ, Shennan AH** 2006 Vitamin C and vitamin E in pregnant women at risk for pre-eclampsia (VIP trial): randomised placebo-controlled trial. Lancet 367:1145-1154

176. **Colavitti R, Finkel T** 2005 Reactive oxygen species as mediators of cellular senescence. IUBMB Life 57:277-281

177. **Boonstra J, Post JA** 2004 Molecular events associated with reactive oxygen species and cell cycle progression in mammalian cells. Gene 337:1-13

178. **Giorgio M, Trinei M, Migliaccio E, Pelicci PG** 2007 Hydrogen peroxide: a metabolic by-product or a common mediator of ageing signals? Nat Rev Mol Cell Biol 8:722-728

179. **Rhee SG** 2006 Cell signaling. H2O2, a necessary evil for cell signaling. Science 312:1882-1883

180. **Rhee SG, Bae YS, Lee SR, Kwon J** 2000 Hydrogen peroxide: a key messenger that modulates protein phosphorylation through cysteine oxidation. Sci STKE 2000:pe1

181. **Colavitti R, Pani G, Bedogni B, Anzevino R, Borrello S, Waltenberger J, Galeotti T** 2002 Reactive oxygen species as downstream mediators of angiogenic signaling by vascular endothelial growth factor receptor-2/KDR. J Biol Chem 277:3101-3108

182. **Gorlach A, Kietzmann T, Hess J** 2002 Redox signaling through NADPH oxidases: involvement in vascular proliferation and coagulation. Ann N Y Acad Sci 973:505-507

183. **Vladimirov YA, Proskurnina EV** 2009 Free radicals and cell chemiluminescence. Biochemistry (Mosc) 74:1545-1566

184. **Karakoyun B, Uslu U, Ercan F, Aydin MS, Yuksel M, Ogunc AV, Alican I** 2011 The effect of phosphodiesterase-5 inhibition by sildenafil citrate on inflammation and apoptosis in rat experimental colitis. Life Sci 89:402-407

185. **Griendling KK, Sorescu D, Ushio-Fukai M** 2000 NAD(P)H oxidase: role in cardiovascular biology and disease. Circ Res 86:494-501

186. **Ohara Y, Peterson TE, Harrison DG** 1993 Hypercholesterolemia increases endothelial superoxide anion production. J Clin Invest 91:2546-2551

187. **Griendling KK, Minieri CA, Ollerenshaw JD, Alexander RW** 1994 Angiotensin II stimulates NADH and NADPH oxidase activity in cultured vascular smooth muscle cells. Circ Res 74:1141-1148

188. **Rossary A, Arab K, Steghens JP** 2007 Polyunsaturated fatty acids modulate NOX 4 anion superoxide production in human fibroblasts. Biochem J 406:77-83

189. **Qin Y, Lu M, Gong X** 2008 Dihydrorhodamine 123 is superior to 2,7-dichlorodihydrofluorescein diacetate and dihydrorhodamine 6G in detecting intracellular hydrogen peroxide in tumor cells. Cell Biol Int 32:224-228

190. **Henderson LM, Chappell JB** 1993 Dihydrorhodamine 123: a fluorescent probe for superoxide generation? Eur J Biochem 217:973-980

191. **Colston JT, de la Rosa SD, Strader JR, Anderson MA, Freeman GL** 2005 H2O2 activates Nox4 through PLA2-dependent arachidonic acid production in adult cardiac fibroblasts. FEBS Lett 579:2533-2540

192. **Rhee SG, Chang TS, Jeong W, Kang D** Methods for detection and measurement of hydrogen peroxide inside and outside of cells. Mol Cells 29:539-549

193. **Kovacic P, Osuna JA, Jr.** 2000 Mechanisms of anti-cancer agents: emphasis on oxidative stress and electron transfer. Curr Pharm Des 6:277-309

194. **Bokoch GM, Knaus UG** 2003 NADPH oxidases: not just for leukocytes anymore! Trends Biochem Sci 28:502-508

195. **Wink DA, Hines HB, Cheng RY, Switzer CH, Flores-Santana W, Vitek MP, Ridnour LA, Colton CA** Nitric oxide and redox mechanisms in the immune response. J Leukoc Biol 89:873-891

196. **Nishino T, Okamoto K, Eger BT, Pai EF** 2008 Mammalian xanthine oxidoreductase - mechanism of transition from xanthine dehydrogenase to xanthine oxidase. FEBS J 275:3278-3289

197. **Schroder K, Wandzioch K, Helmcke I, Brandes RP** 2009 Nox4 acts as a switch between differentiation and proliferation in preadipocytes. Arterioscler Thromb Vasc Biol 29:239-245

198. **Clempus RE, Sorescu D, Dikalova AE, Pounkova L, Jo P, Sorescu GP, Schmidt HH, Lassegue B, Griendling KK** 2007 Nox4 is required for maintenance of the differentiated vascular smooth muscle cell phenotype. Arterioscler Thromb Vasc Biol 27:42-48

199. **Bertolotti M, Yim SH, Masciarelli S, Kim YJ, Garcia-Manteiga JM, Vene R, Iuchi Y, Kang MH, Fujii J, Rubartelli A, Rhee SG, Sitia R** 2010 B to plasma cell terminal differentiation entails oxidative stress and profound reshaping of the antioxidant responses. Antioxid Redox Signal 13:1133-1144

200. **Sasaki H, Yamamoto H, Tominaga K, Masuda K, Kawai T, Teshima-Kondo S, Rokutan K** 2009 NADPH oxidase-derived reactive oxygen species are essential for differentiation of a mouse macrophage cell line (RAW264.7) into osteoclasts. J Med Invest 56:33-41

201. **Buggisch M, Ateghang B, Ruhe C, Strobel C, Lange S, Wartenberg M, Sauer H** 2007 Stimulation of ES-cell-derived cardiomyogenesis and neonatal cardiac cell proliferation by reactive oxygen species and NADPH oxidase. J Cell Sci 120:885-894

202. **Sardina JL, Lopez-Ruano G, Sanchez-Abarca LI, Perez-Simon JA, Gaztelumendi A, Trigueros C, Llanillo M, Sanchez-Yague J, Hernandez-Hernandez A** 2010 p22(phox)-dependent NADPH oxidase activity is required for megakaryocytic differentiation. Cell Death Differ 17:1842-54

203. **Babior BM** 1999 NADPH oxidase: an update. Blood 93:1464-1476

204. **Babior BM** 2004 NADPH oxidase. Curr Opin Immunol 16:42-47

205. **Babior BM** 2002 The leukocyte NADPH oxidase. Isr Med Assoc J 4:1023-1024

206. **Lambeth JD** 2000 Regulation of the phagocytic respiratory burst oxidase by protein interaction. Journal of Biochemistry and Molecular Biology 33:427-439

207. **Lambeth JD** 2004 NOX enzymes and the biology of reactive oxygen. Nat Rev Immunol 4:181-189

208. **Alom-Ruiz SP, Anilkumar N, Shah AM** 2008 Reactive oxygen species and endothelial activation. Antioxid Redox Signal 10:1089-1100

209. **Jessaitis AJ, Buescher ES, Harrison D, Quinn MT, Parkos CA, Livesey S, Linner J** 1990 Ultrastructural localization of cytochrome b in the membranes of resting and phagocytosing human granulocytes. J Clin Invest 85:821-835

210. **Ambasta RK, Kumar P, Griendling KK, Schmidt HH, Busse R, Brandes RP** 2004 Direct interaction of the novel Nox proteins with p22phox is required for the formation of a functionally active NADPH oxidase. J Biol Chem 279:45935-45941

211. **Edderkaoui M, Nitsche C, Zheng L, Pandol SJ, Gukovsky I, Gukovskaya AS** NADPH oxidase activation in pancreatic cancer cells is mediated through Akt-dependent up-regulation of p22phox. J Biol Chem 286:7779-7787

212. **Babior BM** 2000 The NADPH oxidase of endothelial cells. IUBMB Life 50:267-269

213. **Quinn MT, Evans T, Loetterle LR, Jesaitis AJ, Bokoch GM** 1993 Translocation of Rac correlates with NADPH oxidase activation. Evidence for equimolar translocation of oxidase components. J Biol Chem 268:20983-20987

214. **Babior BM, Lambeth JD, Nauseef W** 2002 The neutrophil NADPH oxidase. Arch Biochem Biophys 397:342-344

215. **Cheng G, Cao Z, Xu X, van Meir EG, Lambeth JD** 2001 Homologs of gp91phox: cloning and tissue expression of Nox3, Nox4, and Nox5. Gene 269:131-140

216. **Brandes RP, Schroder K** 2008 Differential vascular functions of Nox family NADPH oxidases. Curr Opin Lipidol 19:513-518

217. **Brandes RP, Schroder K** 2008 Composition and functions of vascular nicotinamide adenine dinucleotide phosphate oxidases. Trends Cardiovasc Med 18:15-19

218. **Cave A** 2009 Selective targeting of NADPH oxidase for cardiovascular protection. Curr Opin Pharmacol 9:208-213

219. **Dworakowski R, Alom-Ruiz SP, Shah AM** 2008 NADPH oxidase-derived reactive oxygen species in the regulation of endothelial phenotype. Pharmacol Rep 60:21-28

220. **Martyn KD, Frederick LM, von Loehneysen K, Dinauer MC, Knaus UG** 2006 Functional analysis of Nox4 reveals unique characteristics compared to other NADPH oxidases. Cell Signal 18:69-82

221. **Anilkumar N, Weber R, Zhang M, Brewer A, Shah AM** 2008 Nox4 and nox2 NADPH oxidases mediate distinct cellular redox signaling responses to agonist stimulation. Arterioscler Thromb Vasc Biol 28:1347-1354

222. **Hilenski LL, Clempus RE, Quinn MT, Lambeth JD, Griendling KK** 2004 Distinct subcellular localizations of Nox1 and Nox4 in vascular smooth muscle cells. Arterioscler Thromb Vasc Biol 24:677-683

223. **Ziegler WH, Liddington RC, Critchley DR** 2006 The structure and regulation of vinculin. Trends Cell Biol 16:453-460

224. **Chen K, Kirber MT, Xiao H, Yang Y, Keaney JF, Jr.** 2008 Regulation of ROS signal transduction by NADPH oxidase 4 localization. J Cell Biol 181:1129-1139

225. **Wolin MS** 2004 Subcellular localization of Nox-containing oxidases provides unique insight into their role in vascular oxidant signaling. Arterioscler Thromb Vasc Biol 24:625-627

226. **Li JM, Shah AM** 2002 Intracellular localization and preassembly of the NADPH oxidase complex in cultured endothelial cells. J Biol Chem 277:19952-19960

227. **Pagano PJ, Chanock SJ, Siwik DA, Colucci WS, Clark JK** 1998 Angiotensin II induces p67phox mRNA expression and NADPH oxidase superoxide generation in rabbit aortic adventitial fibroblasts. Hypertension 32:331-337

228. **Jaquet V, Scapozza L, Clark RA, Krause KH, Lambeth JD** 2009 Small-molecule NOX inhibitors: ROS-generating NADPH oxidases as therapeutic targets. Antioxid Redox Signal 11:2535-2552

229. **Li Y, Trush MA** 1998 Diphenyleneiodonium, an NAD(P)H oxidase inhibitor, also potently inhibits mitochondrial reactive oxygen species production. Biochem Biophys Res Commun 253:295-299

230. **Riganti C, Costamagna C, Bosia A, Ghigo D** 2006 The NADPH oxidase inhibitor apocynin (acetovanillone) induces oxidative stress. Toxicol Appl Pharmacol 212:179-187

231. **Stefanska J, Pawliczak R** 2008 Apocynin: molecular aptitudes. Mediators Inflamm 2008:106507

232. **Johnson DK, Schillinger KJ, Kwait DM, Hughes CV, McNamara EJ, Ishmael F, O'Donnell RW, Chang MM, Hogg MG, Dordick JS, Santhanam L, Ziegler LM, Holland JA** 2002 Inhibition of NADPH oxidase activation in endothelial cells by ortho-methoxy-substituted catechols. Endothelium 9:191-203

233. **Vejrazka M, Micek R, Stipek S** 2005 Apocynin inhibits NADPH oxidase in phagocytes but stimulates ROS production in non-phagocytic cells. Biochim Biophys Acta 1722:143-147

234. **Stolk J, Hiltermann TJ, Dijkman JH, Verhoeven AJ** 1994 Characteristics of the inhibition of NADPH oxidase activation in neutrophils by apocynin, a methoxy-substituted catechol. Am J Respir Cell Mol Biol 11:95-102

235. **Harrison DG** 1997 Cellular and molecular mechanisms of endothelial cell dysfunction. J Clin Invest 100:2153-2157

236. **Bulun SE** 2009 Endometriosis. N Engl J Med 360:268-279

237. **Giudice LC, Kao LC** 2004 Endometriosis. Lancet 364:1789-1799

238. **Aghajanova L, Horcajadas JA, Weeks JL, Esteban FJ, Nezhat CN, Conti M, Giudice LC** 2010 The protein kinase A pathway-regulated transcriptome of endometrial stromal fibroblasts reveals compromised differentiation and persistent proliferative potential in endometriosis. Endocrinology 151:1341-1355

239. **Brosens I, Benagiano G** 2011 Endometriosis, a modern syndrome. Indian J Med Res 133:581-593

240. **Bellelis P, Podgaec S, Abrao MS** 2011 Environmental factors and endometriosis. Rev Assoc Med Bras 57:456-461

241. **Cakmak H, Guzeloglu-Kayisli O, Kayisli UA, Arici A** 2009 Immune-endocrine interactions in endometriosis. Front Biosci (Elite Ed) 1:429-443

242. **Herington JL, Bruner-Tran KL, Lucas JA, Osteen KG** 2011 Immune interactions in endometriosis. Expert Rev Clin Immunol 7:611-626

243. **Sampson JA** 1927 Peritoneal endometriosis due to the menstrual dissemination of endometrial tissue into the peritoneal cavity. Am J Obstet Gynecol 14:422

244. **Vinatier D, Dufour P, Oosterlynck D** 1996 Immunological aspects of endometriosis. Hum Reprod Update 2:371-384

245. **Painter JN, Anderson CA, Nyholt DR, Macgregor S, Lin J, Lee SH, Lambert A, Zhao ZZ, Roseman F, Guo Q, Gordon SD, Wallace L, Henders AK, Visscher PM, Kraft P, Martin NG, Morris AP, Treloar SA, Kennedy SH, Missmer SA, Montgomery GW, Zondervan KT** 2011 Genome-wide association study identifies a locus at 7p15.2 associated with endometriosis. Nat Genet 43:51-54

246. **Uno S, Zembutsu H, Hirasawa A, Takahashi A, Kubo M, Akahane T, Aoki D, Kamatani N, Hirata K, Nakamura Y** 2010 A genome-wide association study identifies genetic variants in the CDKN2BAS locus associated with endometriosis in Japanese. Nat Genet 42:707-710

247. **Aghajanova L, Giudice LC** 2011 Molecular evidence for differences in endometrium in severe versus mild endometriosis. Reprod Sci 18:229-251

248. **Nasu K, Kawano Y, Tsukamoto Y, Takano M, Takai N, Li H, Furukawa Y, Abe W, Moriyama M, Narahara H** 2011 Aberrant DNA methylation status of endometriosis: Epigenetics as the pathogenesis, biomarker and therapeutic target. J Obstet Gynaecol Res 37:683-695

249. **Lebovic DI, Mueller MD, Taylor RN** 2001 Immunobiology of endometriosis. Fertil Steril 75:1-10

250. **Tseng JF, Ryan IP, Milam TD, Murai JT, Schriock ED, Landers DV, Taylor RN** 1996 Interleukin-6 secretion in vitro is up-regulated in ectopic and eutopic endometrial stromal cells from women with endometriosis. J Clin Endocrinol Metab 81:1118-1122

251. **Noble LS, Takayama K, Zeitoun KM, Putman JM, Johns DA, Hinshelwood MM, Agarwal VR, Zhao Y, Carr BR, Bulun SE** 1997 Prostaglandin E2 stimulates aromatase expression in endometriosis-derived stromal cells. J Clin Endocrinol Metab 82:600-606

252. **Noble LS, Simpson ER, Johns A, Bulun SE** 1996 Aromatase expression in endometriosis. J Clin Endocrinol Metab 81:174-179

253. **Wu Y, Strawn E, Basir Z, Halverson G, Guo SW** 2007 Aberrant expression of deoxyribonucleic acid methyltransferases DNMT1, DNMT3A, and DNMT3B in women with endometriosis. Fertil Steril 87:24-32

254. **Oosterlynck DJ, Cornillie FJ, Waer M, Vandeputte M, Koninckx PR** 1991 Women with endometriosis show a defect in natural killer activity resulting in a decreased cytotoxicity to autologous endometrium. Fertil Steril 56:45-51

255. **Oosterlynck DJ, Meuleman C, Waer M, Vandeputte M, Koninckx PR** 1992 The natural killer activity of peritoneal fluid lymphocytes is decreased in women with endometriosis. Fertil Steril 58:290-295

256. **Oosterlynck DJ, Meuleman C, Waer M, Koninckx PR, Vandeputte M** 1993 Immunosuppressive activity of peritoneal fluid in women with endometriosis. Obstet Gynecol 82:206-212

257. **Burney RO, Talbi S, Hamilton AE, Vo KC, Nyegaard M, Nezhat CR, Lessey BA, Giudice LC** 2007 Gene expression analysis of endometrium reveals progesterone resistance and candidate susceptibility genes in women with endometriosis. Endocrinology 148:3814-3826

258. **Kao LC, Germeyer A, Tulac S, Lobo S, Yang JP, Taylor RN, Osteen K, Lessey BA, Giudice LC** 2003 Expression profiling of endometrium from women with endometriosis reveals candidate genes for disease-based implantation failure and infertility. Endocrinology 144:2870-2881

259. **Aghajanova L, Tatsumi K, Horcajadas JA, Zamah AM, Esteban FJ, Herndon CN, Conti M, Giudice LC** 2011 Unique transcriptome, pathways, and networks in the human endometrial fibroblast response to progesterone in endometriosis. Biol Reprod 84:801-815

260. **Seo SK, Yang HI, Lee KE, Kim HY, Cho S, Choi YS, Lee BS** 2010 The roles of thioredoxin and thioredoxin-binding protein-2 in endometriosis. Hum Reprod 25:1251-1258

261. **Jackson LW, Schisterman EF, Dey-Rao R, Browne R, Armstrong D** 2005 Oxidative stress and endometriosis. Hum Reprod 20:2014-2020

262. **Portz DM, Elkins TE, White R, Warren J, Adadevoh S, Randolph J** 1991 Oxygen free radicals and pelvic adhesion formation: I. Blocking oxygen free radical toxicity to prevent adhesion formation in an endometriosis model. Int J Fertil 36:39-42

263. **Murphy AA, Palinski W, Rankin S, Morales AJ, Parthasarathy S** 1998 Evidence for oxidatively modified lipid-protein complexes in endometrium and endometriosis. Fertil Steril 69:1092-1094

264. **Agarwal A, Gupta S, Sikka S** 2006 The role of free radicals and antioxidants in reproduction. Curr Opin Obstet Gynecol 18:325-332

265. **Halme J, Becker S, Hammond MG, Raj MH, Raj S** 1983 Increased activation of pelvic macrophages in infertile women with mild endometriosis. Am J Obstet Gynecol 145:333-337

266. **Van Langendonckt A, Casanas-Roux F, Donnez J** 2002 Oxidative stress and peritoneal endometriosis. Fertil Steril 77:861-870

267. **Ho HN, Wu MY, Chen SU, Chao KH, Chen CD, Yang YS** 1997 Total antioxidant status and nitric oxide do not increase in peritoneal fluids from women with endometriosis. Hum Reprod 12:2810-2815

268. **Lambrinoudaki IV, Augoulea A, Christodoulakos GE, Economou EV, Kaparos G, Kontoravdis A, Papadias C, Creatsas G** 2009 Measurable serum markers of oxidative stress response in women with endometriosis. Fertil Steril 91:46-50

269. **Sakurada H, Koizumi H, Ohkawara A, Ueda T, Kamo N** 1992 Use of dihydrorhodamine 123 for detecting intracellular generation of peroxides upon UV irradiation in epidermal keratinocytes. Arch Dermatol Res 284:114-116

270. **Cloke B, Huhtinen K, Fusi L, Kajihara T, Yliheikkila M, Ho KK, Teklenburg G, Lavery S, Jones MC, Trew G, Kim JJ, Lam EW, Cartwright JE, Poutanen M, Brosens JJ** 2008 The androgen and progesterone receptors regulate distinct gene networks and cellular functions in decidualizing endometrium. Endocrinology 149:4462-4474

271. **Grewal S, Carver JG, Ridley AJ, Mardon HJ** 2008 Implantation of the human embryo requires Rac1-dependent endometrial stromal cell migration. Proc Natl Acad Sci U S A 105:16189-16194

272. **Nagashima T, Maruyama T, Uchida H, Kajitani T, Arase T, Ono M, Oda H, Kagami M, Masuda H, Nishikawa S, Asada H, Yoshimura Y** 2008 Activation of SRC kinase and phosphorylation of signal transducer and activator of transcription-5 are required for decidual transformation of human endometrial stromal cells. Endocrinology 149:1227-1234

273. **Aghajanova L, Velarde MC, Giudice LC** Altered gene expression profiling in endometrium: evidence for progesterone resistance. Semin Reprod Med 28:51-58

274. **Shazand K, Baban S, Prive C, Malette B, Croteau P, Lagace M, Racine JB, Hugo P** 2004 FOXO1 and c-jun transcription factors mRNA are modulated in endometriosis. Mol Hum Reprod 10:871-877

275. **Christian M, Lam EW, Wilson MS, Brosens JJ** 2011 FOXO transcription factors and their role in disorders of the female reproductive tract. Curr Drug Targets 12:1291-1302

276. **Brosens JJ, Parker MG, McIndoe A, Pijnenborg R, Brosens IA** 2009 A role for menstruation in preconditioning the uterus for successful pregnancy. Am J Obstet Gynecol 200:615 e611-616

277. **Mansouri-Attia N, Sandra O, Aubert J, Degrelle S, Everts RE, Giraud-Delville C, Heyman Y, Galio L, Hue I, Yang X, Tian XC, Lewin HA, Renard JP** 2009 Endometrium as an early sensor of in vitro embryo manipulation technologies. Proc Natl Acad Sci U S A 106:5687-5692

278. **Gellersen B, Reimann K, Samalecos A, Aupers S, Bamberger AM** 2010 Invasiveness of human endometrial stromal cells is promoted by decidualization and by trophoblast-derived signals. Hum Reprod 25:862-873

279. **Gravanis A, Stournaras C, Margioris AN** 1999 Paracrinology of endometrial neuropeptides: corticotropin-releasing hormone and opioids. Semin Reprod Endocrinol 17:29-38

280. **Kasahara K, Takakura K, Takebayashi K, Kimura F, Nakanishi K, Noda Y** 2001 The role of human chorionic gonadotropin on decidualization of endometrial stromal cells in vitro. J Clin Endocrinol Metab 86:1281-1286

281. **DiMattia GE, Gellersen B, Duckworth ML, Friesen HG** 1990 Human prolactin gene expression. The use of an alternative noncoding exon in decidua and the IM-9-P3 lymphoblast cell line. J Biol Chem 265:16412-16421

282. **Lynch VJ, Tanzer A, Wang Y, Leung FC, Gellersen B, Emera D, Wagner GP** 2008 Adaptive changes in the transcription factor HoxA-11 are essential for the evolution of pregnancy in mammals. Proc Natl Acad Sci U S A 105:14928-14933

283. **Wagner GP, Lynch VJ** 2010 Evolutionary novelties. Curr Biol 20:R48-52

284. **Lynch VJ, Brayer K, Gellersen B, Wagner GP** 2009 HoxA-11 and FOXO1A cooperate to regulate decidual prolactin expression: towards inferring the core transcriptional regulators of decidual genes. PLoS One 4:e6845

285. **Seshiah PN, Weber DS, Rocic P, Valppu L, Taniyama Y, Griendling KK** 2002 Angiotensin II stimulation of NAD(P)H oxidase activity: upstream mediators. Circ Res 91:406-413

286. **Wang W, Li Q, Bagchi IC, Bagchi MK** 2010 The CCAAT/Enhancer Binding Protein {beta} Is a Critical Regulator of Steroid-Induced Mitotic Expansion of Uterine Stromal Cells during Decidualization. 151:3929-40 Endocrinology

287. **Kannan A, Fazleabas AT, Bagchi IC, Bagchi MK** 2010 The transcription factor C/EBPbeta is a marker of uterine receptivity and expressed at the implantation site in the primate. Reprod Sci 17:434-443

288. **Schneider-Merck T, Pohnke Y, Kempf R, Christian M, Brosens JJ, Gellersen B** 2006 Physical interaction and mutual transrepression between CCAAT/enhancer-binding protein beta and the p53 tumor suppressor. J Biol Chem 281:269-278

289. **Lee H, Lee YJ, Choi H, Ko EH, Kim JW** 2009 Reactive oxygen species facilitate adipocyte differentiation by accelerating mitotic clonal expansion. J Biol Chem 284:10601-10609

290. **Salmeen A, Park BO, Meyer T** 2010 The NADPH oxidases NOX4 and DUOX2 regulate cell cycle entry via a p53-dependent pathway. Oncogene 29:4473-4484

291. **Kamata H, Honda S, Maeda S, Chang L, Hirata H, Karin M** 2005 Reactive oxygen species promote TNFalpha-induced death and sustained JNK activation by inhibiting MAP kinase phosphatases. Cell 120:649-661

292. **Storz P** 2011 Forkhead homeobox type O transcription factors in the responses to oxidative stress. Antioxid Redox Signal 14:593-605

293. **Erol A** 2007 Insulin resistance is an evolutionarily conserved physiological mechanism at the cellular level for protection against increased oxidative stress. Bioessays 29:811-818

294. **Greer EL, Brunet A** 2005 FOXO transcription factors at the interface between longevity and tumor suppression. Oncogene 24:7410-7425

295. **Kousteni S** 2011 FoxO1: A molecule for all seasons. J Bone Miner Res

296. **Lehtinen MK, Yuan Z, Boag PR, Yang Y, Villen J, Becker EB, DiBacco S, de la Iglesia N, Gygi S, Blackwell TK, Bonni A** 2006 A conserved MST-FOXO signaling pathway mediates oxidative-stress responses and extends life span. Cell 125:987-1001

297. **Kops GJ, Dansen TB, Polderman PE, Saarloos I, Wirtz KW, Coffer PJ, Huang TT, Bos JL, Medema RH, Burgering BM** 2002 Forkhead transcription factor FOXO3a protects quiescent cells from oxidative stress. Nature 419:316-321

298. **Brunet A, Sweeney LB, Sturgill JF, Chua KF, Greer PL, Lin Y, Tran H, Ross SE, Mostoslavsky R, Cohen HY, Hu LS, Cheng HL, Jedrychowski MP, Gygi SP, Sinclair DA, Alt FW, Greenberg ME** 2004 Stress-dependent regulation of FOXO transcription factors by the SIRT1 deacetylase. Science 303:2011-2015

299. **Rached MT, Kode A, Xu L, Yoshikawa Y, Paik JH, Depinho RA, Kousteni S** 2010 FoxO1 is a positive regulator of bone formation by favoring protein synthesis and resistance to oxidative stress in osteoblasts. Cell Metab 11:147-160

300. **Teixeira CC, Liu Y, Thant LM, Pang J, Palmer G, Alikhani M** 2010 Foxo1, a novel regulator of osteoblast differentiation and skeletogenesis. J Biol Chem 285:31055-31065

301. **Siqueira MF, Flowers S, Bhattacharya R, Faibish D, Behl Y, Kotton DN, Gerstenfeld L, Moran E, Graves DT** 2011 FOXO1 modulates osteoblast differentiation. Bone 48:1043-1051

302. **Adachi M, Osawa Y, Uchinami H, Kitamura T, Accili D, Brenner DA** 2007 The forkhead transcription factor FoxO1 regulates proliferation and transdifferentiation of hepatic stellate cells. Gastroenterology 132:1434-1446

303. **Yuan Y, Shi XE, Liu YG, Yang GS** 2011 FoxO1 regulates muscle fiber-type specification and inhibits calcineurin signaling during C2C12 myoblast differentiation. Mol Cell Biochem 348:77-87

304. **Erol A** 2007 JNK/FOXO may be key mechanistic pathway for the hormetic anti-aging. Med Hypotheses 68:923-924

305. **Arumugam TV, Gleichmann M, Tang SC, Mattson MP** 2006 Hormesis/preconditioning mechanisms, the nervous system and aging. Ageing Res Rev 5:165-178

306. **Bauer CE, Elsen S, Bird TH** 1999 Mechanisms for redox control of gene expression. Annu Rev Microbiol 53:495-523

307. **Farr SB, Kogoma T** 1991 Oxidative stress responses in Escherichia coli and Salmonella typhimurium. Microbiol Rev 55:561-585

308. **Wu J, Dunham WR, Weiss B** 1995 Overproduction and physical characterization of SoxR, a [2Fe-2S] protein that governs an oxidative response regulon in Escherichia coli. J Biol Chem 270:10323-10327

309. **Aslund F, Zheng M, Beckwith J, Storz G** 1999 Regulation of the OxyR transcription factor by hydrogen peroxide and the cellular thiol-disulfide status. Proc Natl Acad Sci U S A 96:6161-6165

310. **Storz G, Tartaglia LA, Ames BN** 1990 Transcriptional regulator of oxidative stress-inducible genes: direct activation by oxidation. Science 248:189-194

311. **Godon C, Lagniel G, Lee J, Buhler JM, Kieffer S, Perrot M, Boucherie H, Toledano MB, Labarre J** 1998 The H2O2 stimulon in Saccharomyces cerevisiae. J Biol Chem 273:22480-22489

312. **Kuge S, Jones N, Nomoto A** 1997 Regulation of yAP-1 nuclear localization in response to oxidative stress. EMBO J 16:1710-1720

313. **Yates C** 2011 Prostate tumor cell plasticity: a consequence of the microenvironment. Adv Exp Med Biol 720:81-90

314. **Wang Y, Zhou BP** 2011 Epithelial-mesenchymal transition in breast cancer progression and metastasis. Chin J Cancer 30:603-611

315. **Wells A, Yates C, Shepard CR** 2008 E-cadherin as an indicator of mesenchymal to epithelial reverting transitions during the metastatic seeding of disseminated carcinomas. Clin Exp Metastasis 25:621-628

316. **Cannito S, Novo E, di Bonzo LV, Busletta C, Colombatto S, Parola M** 2010 Epithelial-mesenchymal transition: from molecular mechanisms, redox

regulation to implications in human health and disease. Antioxid Redox Signal 12:1383-1430

317. **Sugawara T, Noshita N, Lewen A, Kim GW, Chan PH** 2001 Neuronal expression of the DNA repair protein Ku 70 after ischemic preconditioning corresponds to tolerance to global cerebral ischemia. Stroke 32:2388-2393

318. **Rattan SI** 2008 Hormesis in aging. Ageing Res Rev 7:63-78

319. **Masoro EJ** 1998 Influence of caloric intake on aging and on the response to stressors. J Toxicol Environ Health B Crit Rev 1:243-257

320. **Masoro EJ** 1998 Hormesis and the antiaging action of dietary restriction. Exp Gerontol 33:61-66

321. **Masoro EJ** 2007 The role of hormesis in life extension by dietary restriction. Interdiscip Top Gerontol 35:1-17

322. **Ristow M, Schmeisser S** 2011 Extending life span by increasing oxidative stress. Free Radic Biol Med 51:327-336

323. **Cypser JR, Johnson TE** 2002 Multiple stressors in Caenorhabditis elegans induce stress hormesis and extended longevity. J Gerontol A Biol Sci Med Sci 57:B109-114

324. **Schulz TJ, Zarse K, Voigt A, Urban N, Birringer M, Ristow M** 2007 Glucose restriction extends Caenorhabditis elegans life span by inducing mitochondrial respiration and increasing oxidative stress. Cell Metab 6:280-293

325. **Kemnitz JW** 2011 Calorie restriction and aging in nonhuman primates. ILAR J 52:66-77

326. **Ohlsson Teague EM, Van der Hoek KH, Van der Hoek MB, Perry N, Wagaarachchi P, Robertson SA, Print CG, Hull LM** 2009 MicroRNA-regulated pathways associated with endometriosis. Mol Endocrinol 23:265-275

327. **Hawkins SM, Creighton CJ, Han DY, Zariff A, Anderson ML, Gunaratne PH, Matzuk MM** 2011 Functional microRNA involved in endometriosis. Mol Endocrinol 25:821-832

328. **Myatt SS, Wang J, Monteiro LJ, Christian M, Ho KK, Fusi L, Dina RE, Brosens JJ, Ghaem-Maghami S, Lam EW** 2010 Definition of microRNAs that repress expression of the tumor suppressor gene FOXO1 in endometrial cancer. Cancer Res 70:367-377

329. **Ward EC, Hoekstra AV, Blok LJ, Hanifi-Moghaddam P, Lurain JR, Singh DK, Buttin BM, Schink JC, Kim JJ** 2008 The regulation and function of the forkhead transcription factor, Forkhead box O1, is dependent on the progesterone receptor in endometrial carcinoma. Endocrinology 149:1942-1950

330. **Pani G, Giannoni E, Galeotti T, Chiarugi P** 2009 Redox-based escape mechanism from death: the cancer lesson. Antioxid Redox Signal 11:2791-2806

331. **Hapangama DK, Turner MA, Drury JA, Quenby S, Saretzki G, Martin-Ruiz C, Von Zglinicki T** 2008 Endometriosis is associated with aberrant endometrial expression of telomerase and increased telomere length. Hum Reprod 23:1511-1519

Publications

Publications

Al Sabbagh M, Fusi L, Higham J, Lee Y, Lei K, Hanyaloglu AC, Lam W-F, Christian M, Brosens J. 2011 NADPH oxidase-derived reactive oxygen species mediate decidualization of human endometrial stromal cells in response to cyclic AMP signalling. Endocrinology 152:730-740

Salker MS, Christian M, Steel JH, Nautiyal J, Lavery S, Trew G, Webster Z, Al Sabbagh M, Puchchakayala G, Föller M, Landles C, Sharkey AM, Quenby S, Aplin JD, Regan L, Lang F, Brosens JJ. Deregulation of the serum- and glucocorticoid-inducible kinase SGK1 in the endometrium causes reproductive failure. Nat Med 17:1509-1513

Khanjani S, Al Sabbagh M, Fusi L, Brosens J. Role of steroid hormones: Progesterone signalling. Endometriosis: Science and Practice. (Wiley-Blackwell, 2012)

Al Sabbagh M, Lam W-F, Brosens J. Mechanisms of endometrial progesterone resistance. Mol Cell Endocrinol. Epub: 2011 Nov 9